

N O T I C E

THIS DOCUMENT HAS BEEN REPRODUCED FROM
MICROFICHE. ALTHOUGH IT IS RECOGNIZED THAT
CERTAIN PORTIONS ARE ILLEGIBLE, IT IS BEING RELEASED
IN THE INTEREST OF MAKING AVAILABLE AS MUCH
INFORMATION AS POSSIBLE

1
DOE/NASA/0139-1
NASA CR-159872
AESD-TME-3064

Sept

DISK MHD GENERATOR STUDY

F. D. Retallick
Advanced Energy Systems Division
Westinghouse Electric Corporation

October 1980

Prepared for
NATIONAL AERONAUTICS AND
SPACE ADMINISTRATION
Lewis Research Center
Under Contract DEN 3-139



for
U.S. DEPARTMENT OF ENERGY
Office of Magnetohydrodynamics

(NASA-CR-159872) DISK MHD GENERATOR STUDY
Final Report (Westinghouse Electric Corp.)
424 p HC A18/MF A01 CSCL 10A

N81-18491

G3/44
Unclas
16557

DOE/NASA/0139-1
NASA CR-159872
AESD-TME-3064

DISK MHD GENERATOR STUDY

**F. D. Retallick
Advanced Energy Systems Division
Westinghouse Electric Corporation
Pittsburgh, Pa 15236**

October 1980

**Prepared for
National Aeronautics and Space Administration
Lewis Research Center
Cleveland, Ohio 44135
Under Contract DEN 3-139**

**for
U.S. DEPARTMENT OF ENERGY
Office of Magnetohydrodynamics
Washington, D.C. 20545
Under Interagency Agreement DEAI01-77ET10769**

TABLE i.1
DISK MHD GENERATOR STUDY
FINAL REPORT AUTHORS

Westinghouse Electric Corporation

AESD

F. D. Retallick - Project Manager
R. R. Holman
C-L. Lu
F. R. Spurrier
M. E. Stella

R&D Center

S. J. Schneider
P. Wood

Consultant

W. D. Jackson

Massachusetts Institute of Technology

Energy Laboratory

J. F. Louis - Program Director
W. J. Loubsky
B. Misra
J. Nash-Webber
J. D. Teare

Francis Bitter National Magnet Laboratory

H. Becker
P. Marston

Burns and Roe

A. W. Carlson

FluidDyne Engineering

D. G. De Coursin
L. R. White

TABLE OF CONTENTS

<u>Section</u>		<u>Page</u>
1	INTRODUCTION	1-1
	1.1 Background	1-1
	1.2 Objectives of the Study	1-2
	1.3 Systems Study Status	1-3
2	SUMMARY AND CONCLUSIONS	2-1
	2.1 Open Cycle Disk MHD Studies	2-1
	2.2 Closed Cycle Disk MHD Studies	2-17
3	BASIS FOR STUDY	3-1
	3.1 Experimental and Analytical Studies of Disk Generators	3-1
	3.2 Approach to the Study	3-3
4	DISK MHD SYSTEM DESIGN BASIS	4-1
	4.1 Disk System Configurations	4-1
	4.2 Fuel Characteristics	4-13
	4.3 Emissions Standards and Emissions Control	4-13
	4.4 Plant Performance and Heat Sink Design Conditions	4-17
5	OPEN CYCLE DISK SYSTEMS STUDIES	5-1
	5.1 Open Cycle Disk Generator Modeling	5-1
	5.2 Open Cycle Systems Modeling	5-21
	5.3 Disk Generator Suboptimization	5-25
	5.4 Open Cycle Disk Systems Analysis	5-58

TABLE OF CONTENTS (Continued)

<u>Section</u>		<u>Page</u>
6	OPEN CYCLE DISK SYSTEMS: MAJOR COMPONENT AND SUBSYSTEM DESIGN	6-1
	6.1 Disk Generator, Nozzle, and Diffuser Design	6-1
	6.2 Coal Combustor	6-21
	6.3 Magnet Subsystem	6-42
	6.4 Disk Generator Power Management System	6-64
	6.5 Radiant Furnace Design	6-82
	6.6 Air Heater Systems	6-102
	6.7 OCD Systems Power Train Layout Representations and Furnace Duct Design	6-116
7	COSTING OF MAJOR OPEN CYCLE COMPONENTS	7-1
	7.1 Cost Basis	7-1
	7.2 Major Component Costs	7-5
	7.3 Comparison of Disk and Linear MHD Component Costs	7-9
8	CLOSED CYCLE DISK SYSTEMS STUDIES	8-1
	8.1 Closed Cycle Disk Generator Modeling	8-1
	8.2 Closed Cycle Disk MHD Systems Modeling	8-9
	8.3 Closed Cycle Disk Systems Performance	8-18
	8.4 Heaters for Closed Cycle MHD	8-34
9	SUMMARY OF CCD COMPONENT COSTS AND COMPARISON TO OCD COMPONENT COSTS	9-1
	9.1 Discussion of Reference Case CCD System	9-1
	9.2 Relative Cost Assessments	9-2
10	REFERENCES	10-1

TABLE OF CONTENTS (Continued)

<u>Section</u>		<u>Page</u>
Appendix A	Estimation of Relative Heat Losses for Combustor/Nozzle of Outflow and Inflow Disk Generators	A-1
Appendix B	Closed Cycle Disk Equations and Solutions	B-1
Appendix C	Natural Resource Requirements and Emissions Levels for OCD Plants	C-1
Appendix D	NO _x Control in 1920 K Directly-Fired Disk Generator System	D-1
Appendix E	Component Dimensions and Weights for Reference 500 MW Disk Generator Power Management System	E-1

DISK MHD GENERATOR STUDY LIST OF FIGURES

<u>Figure Number</u>		<u>Page</u>
2-1-1	OCD MHD/Steam Power System Generator Arrangement of MHD Power Train for 1000 MWe Directly-Fired Plant	2-10
2-1-2	Disk Generator Structural Concept	2-13
2-1-3	Effect of Radial Field Component in Solenoidal Single Coil Magnet	2-14
2-2-1	CCD Power System Flow Diagram	2-19
2-2-2	1000 MWe Closed Cycle Disk Generator Conceptual Design	2-23
3-1-1	Enthalpy Extraction Correlation for Disk Generator Experiments	3-2
3-2-1	Disk MHD Generator Study Simplified Logic Diagram	3-8
4-1-1	Direct Fired Open Cycle Disk Generator System Flow Diagram	4-3
4-1-2	Indirect Fired Open Cycle Disk Generator System Flow Diagram	4-6
4-1-3	Open Cycle Disk Generator System Flow Diagram (Integrated Oxygen Plant and Metallic Air Preheater)	4-8
4-1-4	Closed Cycle Disk Generator System Flow Diagram (Direct Coal-Combustor-Fired Regenerator)	4-9
4-1-5	Closed Cycle Disk Generator System Flow Diagram (Gasifier - Fired Noble Gas Regenerator)	4-12
5-1-1	Disk Generator Geometry	5-2
5-1-2	Optimized Local Electrical Efficiency for Disk Generator with Swirl	5-6
5-1-3	Plasma Temperature Versus Flow Length for Supersonic Combustion Gas Generators of Various Sizes (Approach to Equilibrium Conditions)	5-16
5-1-4	Electron Concentration in Combustion Gas Plasma Versus Flow Length in Supersonic Generators of Various Sizes	5-17

LIST OF FIGURES (Continued)

<u>Figure Number</u>		<u>Page</u>
5-3-1	Schematic Enthalpy - Entropy Diagram of Channel Expansion	5-30
5-3-2	Enthalpy Extraction Length as Function of Mach Number and Swirl	5-31
5-3-3	Enthalpy Extraction Length as Function of Mach Number and Swirl with Electrical Efficiency Contours	5-32
5-3-4	Variation of Disk Generator Characteristics with Inlet Stagnation Pressure	5-34
5-3-5	Variation of Gross Power with Exit Radius and Mach Number	5-36
5-3-6	Electrical Characteristics of Single-Load Disk Generators	5-39
5-3-7	V-I Characteristic for Front 3.116 Meters of Reference Channel	5-41
5-3-8	Variation of Radial Electric Field Distribution for Reference Channel	5-42
5-3-9	Off-Design Electrical Performance of Segmented Disk Generator	5-44
5-3-10	Off-Design Electrical Performance of Segmented Disk Generator	5-45
5-3-11	Electrical Loading Parameters Within Segmented Generator	5-51
5-3-12	Electrical and Fluid Parameters Within Segmented Generator	5-52
5-3-13	Open Cycle Disk Generator Performance Sensitivity to Design Constraint and Conductivity	5-57
5-4-1	OCD Power Output Variation with Oxygen Enrichment Level and Combustor Pressure	5-74
5-4-2	OCD Generator System Performance Variation with Oxygen Enrichment Level at Fixed Combustor Pressure	5-76

LIST OF FIGURES (Continued)

<u>Figure Number</u>		<u>Page</u>
5-4-3	Optimized Steam System Design for Open Cycle Disk Generator System Case 1A (Direct Firing with 1920 K Preheat)	5-82
5-4-4	Directly Fired OCD MHD/Steam System - Statepoint Stations for Optimized Design Cases 1A and 1B	5-84
5-4-5	Separately Fired OCD MHD/Steam System - Statepoint Stations for Optimized Design Case 2	5-86
5-4-6	Oxygen-Augmented OCD MHD/Steam System with Metallic Oxidant Preheater - Statepoint Stations for Optimized Design Case 3	5-89
6-1-1	Disk Generator Structural Concept	6-2
6-2-1	Disk Combustor Outline Drawing (Elevation)	6-22
6-2-2	Disk Combustor Wall Design Concept	6-31
6-3-1	Single Coil Disk Magnet General Configuration and Structural Details (Coil Region A)	6-45
6-3-2	Single Coil Disk Magnet Structural Details of Dewar and Coil Region B	6-46
6-3-3	Data for Direct Fired MHD Disk Generator Magnet	6-50
6-3-4	Block Diagram for MHD Magnet Cryogenic System	6-53
6-3-5	Power Supply and Discharge Subsystem for MHD Magnet	6-57
6-3-6	Effect of Radial Field Component in Solenoidal Single Coil Magnet	6-65
6-4-1	500 MW Disk Power System Elemental Converter Conditioning Schematic	6-69
6-4-2	Single Line Diagram for AC Interface of 500 MW Disk Power System	6-70
6-4-3	Open Cycle Disk Generator MHD/Steam Power Plant 500 MW Power Conditioning System Overall Yard Layout	6-73
6-4-4	Open Cycle Disk Generator MHD/Steam Power Plant 500 MW Power Conditioning System Valve Hall and Control Building Layout	6-74

LIST OF FIGURES (Continued)

<u>Figure Number</u>		<u>Page</u>
6-5-1	Disk Generator Diffuser and Radiant Furnace Interface with Outlet Scroll Collector	6-86
6-5-2	Disk Generator Diffuser and Radiant Furnace Interface with Annular Furnace Design	6-87
6-5-3	Disk Generator Diffuser and Radiant Furnace Interface with Silo-Type Furnaces	6-90
6-5-4	Open Cycle Disk Generator System Radiant Furnace Arrangement	6-99
6-7-1	General Arrangement for OCD Directly-Fired System MHD Power Train	6-119
6-7-2	Isometric Arrangement Drawing for OCD Directly-Fired System MHD Power Train	6-120
6-7-3	General Arrangement for OCD Directly-Fired System MHD Power Train with Revised Radiant Furnace Exhaust Ducting to Provide Easy Access to Generator Magnet and Combustor	6-123
7-1-1	Sample Disk Generator Study Cost Estimate	7-4
8-1-1	Maximum Electrical Efficiency Versus Mach Number for CCD Generator	8-3
8-1-2	Electron Density and Enthalpy Extraction Length Versus Mach Number for CCD Generator	8-4
8-1-3	Effective Hall Parameter Versus Mach Number for CCD Generator	8-5
8-2-1	CCD Generator System Model for Performance Studies	8-11
8-3-1	Example Closed Cycle Disk Generator Design (Case #22)	8-24
8-3-2	Electrical and Effective Transport Properties for Case 22 Generator	8-25
8-3-3	Profiles of Fluid Properties for Case #22 Disk Generator	8-26
8-3-4	Example CCD Generator Designs for High Plasma Turbulence	8-27

LIST OF FIGURES (Continued)

<u>Figure Number</u>		<u>Page</u>
8-3-5	Electrical and Effective Transport Properties for the High Turbulence Disk Generator (Case #31)	8-28
8-3-6	Profiles of the Fluid Properties for the High Turbulence Disk Generator (Case #31)	8-29
8-3-7	Enthalpy Extraction Vs. Turbine Efficiency of Generator and Diffuser for Disk and Linear Closed Cycle Systems	8-31
8-3-8	Pressure Ratio Versus Isentropic Efficiency Comparison of Disk and Linear Generators	8-32
8-3-9	Estimated CCD System Performance with Match Point Operation and Atmospheric Combustion	8-33
A-1	Inflow Geometry for Disk Generator Combustors	A-2
A-2	Outflow Geometry for Disk Generator Combustors	A-3
B-1	Load Map for Closed Cycle Disk Generator	B-6

DISK MHD GENERATOR STUDY

LIST OF TABLES

<u>Number</u>		<u>Page</u>
2.1.1	Base Parameters for the Near-Optimum-Performance Open Cycle Disk Generator Systems	2-2
2.1.2	Performance Summary for the Near-Optimum-Performance Open Cycle Disk Generator Systems	2-3
2.1.3	OCD Power System Sensitivity Study Results	2-5
2.1.4	Major Subsystem Cost Estimates for Disk Generator Power Plants of 1000 MWe Capacity	2-8
2.2.1	Closed Cycle Disk Generator System Performance Survey	2-20
4.2.1	Coal and Ash Analyses of Selected Coals for Disk MHD Generator Study	4-14
4.2.2	Emissions Standards for Disk Generator Study	4-16
5.1.1	Combustor Losses for Disk Generators	5-10
5.2.1	Assumptions for Parametric Analyses of OCD Systems	5-26
5.3.1	Off-Design-Point Impedance Characteristics of Single-Load Open Cycle Disk Generator	5-38
5.3.2	Disk Generator Performance Survey Effect of Load Factor Control in Segmented Disks	5-49
5.3.3	Disk Generator Performance Survey Sensitivity to Magnetic Field and Conductivity Variations	5-54
5.4.1	Parametric Variations for OCD Direct-Fired HTAH	5-60
5.4.2	Summary of Power Generation and Consumption, OCD Direct-Fired Preheater	5-65
5.4.3	Parametric Variations for OCD Separately-Fired Preheater Systems	5-67
5.4.4	Summary of Power Generation and Consumption, OCD Separately-Fired Preheater Systems	5-70
5.4.5	Parameters for OCD with Metallic Preheater and Oxygen Augmentation	5-72

LIST OF TABLES (Continued)

<u>Number</u>		<u>Page</u>
5.4.6	Summary of Power Generation and Consumption, OCD with Metallic Air Preheater and Oxygen Enrichment	5-77
5.4.7	Base Parameters for the Final Selected OCD Systems	5-81
5.4.8	Gas and Air Side Statepoints 1920 K Directly-Fired OCD (Case 1A)	5-83
5.4.9	Gas and Air Side Statepoints 1650 K Directly-Fired OCD (Case 1B)	5-85
5.4.10	Gas and Air Side Statepoints 1920 K Separately-Fired OCD (Case 2)	5-87
5.4.11	Gas and Air Side Statepoints 922 K OCD with Oxygen Augmentation (Case 3)	5-90
5.4.12	Performance Summary for Optimized OCD Systems	5-91
6.1.1	Nozzle and Disk Generator Design Data, OCD Power System	
	6.1.1A (Case 1A, 1920 K Directly-Fired)	6-3
	6.1.1B (Case 1B, 1650 K Directly-Fired)	6-4
	6.1.1C (Case 2, 1920 K Separately-Fired)	6-5
	6.1.1D (Case 3, 922 K Oxygen-Augmented)	6-6
6.1.2	Open Cycle Disk System Data	6-11
6.2.1	MHD Coal Combustor Design Data For OCD Power Systems	
	6.2.1A (Case 1A, 1920 K Directly-Fired)	6-33
	6.2.1B (Case 1B, 1650 K Directly-Fired)	6-35
	6.2.1C (Case 2, 1920 K Separately-Fired)	6-37
	6.2.1D (Case 3, 922 K Oxygen-Augmented)	6-40
6.2.2	Open Cycle Disk Generator System Coal Combustor Dimensional Data	6-41
6.3.1	OCD Systems - Major Magnet Design Parameters	6-48
6.3.2	Evaluation of Safety Factors for Major Structural Components of Disk Magnets	6-52
6.3.3	Summary of Estimated Heat Loads for Magnet Cryogenic System	6-55
6.3.4	Design Data for Superconducting Magnet Power Supply Subsystem	6-58

LIST OF TABLES (Continued)

<u>Number</u>		<u>Page</u>
6.4.1	Design Point Electrical Data for Reference OCD MHD Power Management System	6-67
6.4.2	Component List for 500 MW Disk Converter	6-71
6.4.3	Losses for 527.3 MW Disk Generator Power Management Equipment	6-78
6.4.4	Cost Estimates for 527.3 MW Disk Generator Power Management System	6-79
6.4.5	Disk Power Management System Design Data - Disk/ Converter Interface	6-81
6.5.1	OCD Radiant Furnace Subsystem Heat Transfer Data	6-94
6.5.2	OCD Radiant Furnace Dimensions and Weights	6-101
6.6.1	Size and Operating Conditions for 1000 MWe OCD Directly-Fired HTAH	6-105
6.6.2	Refractory Materials for 1000 MWe OCD Directly- Fired HTAH	6-107
6.6.3	Estimated Heater System Cost for 1000 MWe OCD Directly-Fired HTAH	6-108
6.6.4	Size and Operating Conditions for 1000 MWe OCD Indirectly-Fired HTAH	6-113
6.6.5	Refractory Materials for 1000 MWe OCD Indirectly- Fired HTAH	6-114
6.6.6	Estimated Heater Cost Without Ancillaries for 1000 MWe OCD Indirectly-Fired HTAH	6-115
6.7.1	Radiant Furnace Exhaust Duct Design Conditions	6-124
6.7.2	Refractory Materials Data for OCD Radiant Furnace Exhaust Duct Insulation	6-126
6.7.3	Thicknesses of Insulation Layers for OCD Radiant Furnace Exhaust Ducts	6-127
6.7.4	Parameters for Determining OCD Furnace Duct Steel Wall Thickness	6-128

LIST OF TABLES (Continued)

<u>Number</u>		<u>Page</u>
7.2.1	Cost Estimate for Disk Magnet of Case 1A (1920 K OCD Directly-Fired System)	7-7
7.2.2	Cost Estimate for Major Components, OCD Case 1A	7-10
7.2.3	Cost Estimate for Major Components, OCD Case 1B	7-11
7.2.4	Cost Estimate for Major Components, OCD Case 2	7-12
7.2.5	Cost Estimate for Major Components, OCD Case 3	7-13
7.3.1	AVCO/PSPEC Comparison Cases for Disk/Linear Component Costs	7-16
7.3.2	GE/PSPEC Comparison Cases for Disk/Linear Component Costs	7-17
7.3.3	Comparison of OCD Power System Costs for Disk and Linear Generator Cases	7-18
8.2.1	Summary of System Parameters for Closed Cycle Disk System Model	8-16
8.3.1	Closed Cycle Disk Generator System Performance Survey	8-20
8.3.2	Estimated Plant Parasitic Loads for 1000 MWe CCD System	8-21
9.2.1	Cost Estimate for Case 22 CCD Power System MHD Power Management Equipment	9-5

1.0 INTRODUCTION

1.1 BACKGROUND

This report contains the information developed during the Disk MHD Generator Study carried out under NASA Contract DEN3-139. The study was conducted by a contract team composed of the Westinghouse Advanced Energy Systems Division (AESD); the Energy Laboratory of the Massachusetts Institute of Technology; Burns and Roe, Incorporated; Fluidyne Engineering; and the Westinghouse Research and Development Center. Westinghouse AESD served as prime contractor for NASA on the program.

The study was motivated by the various theoretical and experimental investigations of disk-shaped MHD channels carried out over the past decade and a half. These studies indicated that the disk geometry had potential to provide equivalent performance to the more commonly studied linear MHD channels but with the potential for certain geometrical, electrical, and cost advantages.

The configurations envisioned for the disk MHD generator and its magnet offer promise of substantial generator cost reductions in comparison with linear channels and magnets designed to produce equivalent MHD power. The radial flow disk generator is a Hall device; with swirl it can be considered to be the cylindrically configured analogue of the linear diagonal MHD generator. The advantageous geometry of the disk permits the closure of the Faraday current entirely within the plasma. The simple configurations realizable for disk generator system components indicate the possibility for use of higher design specification values for the performance-critical parameters of magnetic induction and allowable electric field intensity, thus implying a potential for achieving an enhanced performance from the disk generator in comparison to that provided by the more complicated Faraday or diagonal linear MHD generators. The simple disk generator configurations possible also hold promise of enhanced reliability in comparison to the more complicated linear MHD channels.

The major effort of the Disk MHD Generator Study was a parametric power plant systems analysis comprised of three basic subtasks:

- Modeling of disk generator power systems;
- Analysis of disk generator power system performance, and subsequent optimization of this performance through selection of optimum values for critical parameters;
- Conceptual design and cost estimating for the major components of open cycle disk generator power systems.

1.2 OBJECTIVES OF THE STUDY

The key objective of the Disk MHD Generator Study was established initially to be the development of information on the expected performance, potential benefits, and development possibilities for both combustion gas and inert gas MHD generators, when these are considered as part of appropriately configured coal-fired MHD/steam electrical power generating systems.

Four "reference plant" configurations were specified by NASA, which are thought to be representative of possible disk generator MHD/steam power system configurations. These four configurations formed a basis from which detailed information on generator and system parameters was to be developed through analysis. The expected performance of near-term and longer-term disk generator MHD power systems was to be established, with reference to the four representative configurations.

For the major components of open-cycle disk MHD power systems, estimates of costs were to be made. The estimates then were to be utilized in a cost comparison between disk MHD system components and their analogous linear MHD system components (as represented by the costs obtained for such components in the parallel NASA "Parametric Study of Potential Early Commercial MHD Power Plants (PSPEC).")

As the study progressed, it became clear that some comparisons of the disk generator systems study performance results would be made with the parallel linear MHD systems study results. The disk generator power systems were reconfigured where possible to more closely match the systems designs assumed for linear MHD power systems in the parallel studies.

1.3 SYSTEMS STUDY STATUS

It is emphasized that this study represents a first major attempt to relate the disk generator into a complete system. As compared to linear systems which have been the subject of repeated studies with ever increasing refinement, it should therefore be considered a preliminary attempt. Design detail of the MHD components was carried only to the extent necessary to obtain reasonable cost estimates. No cost estimating was performed outside of the MHD disk related components.

Due to the lack of previous effort on disk generators in a complete system, much of the effort had to be expended on determining the level and sensitivity of parameters to desired overall plant performance. During the course of the study several refinements for improvement became apparent. Continued study of these refinements as well as more detailed design investigations could be pursued in an attempt to better the performance and give greater confidence in its comparison to linear systems.

2.0 SUMMARY AND CONCLUSIONS

2.1 OPEN CYCLE DISK MHD STUDIES

2.1.1 SYSTEM STUDIES

Studies have been performed for directly-fired, separately-fired, and oxygen-augmented MHD power plants incorporating a disk geometry for the MHD generator. As a result of these studies, base parameters for four near-optimum-performance MHD/steam power systems of various types have been defined. The base parameters for the selected systems and a performance summary for each are presented in Table 2.1.1 and 2.1.2 respectively. The finally selected systems consisted of two directly-fired cases, one at 1920 K (2996°F) preheat and the other at 1650 K (2500°F) preheat; a separately-fired case where the air is preheated to the same level as the higher temperature directly-fired case; and an oxygen-augmented case with the same generator inlet temperature of 2839 K (4650°F) as the high temperature directly-fired and the separately-fired cases. Supersonic Mach numbers at the generator inlet, gas inlet swirl and constant Hall field operation were specified based on disk generator optimization conducted as part of the study. System pressures were based on optimization of MHD net power. Supercritical reheat steam plants were used in all cases.

System Performance

The resulting power plant efficiencies shown on Table 2.1.2 are found to be in the range of similar studies on linear systems. As expected, a large difference of 6.5 percentage points in efficiency exists for the directly- and separately-fired cases at the same preheat temperature level. The separately-fired case studied used a pressurized coal gasifier to fire the preheaters and a gas turbine energy recovery system driven by the preheater exhaust. The efficiency of the oxygen-augmented system is found to be slightly higher (1.5 percentage points) than the separately-fired case with the same generator inlet temperature. Thus, previous conclusions on the performance competitiveness of oxygen-enriched systems for linear generators also hold true for the disk systems.

TABLE 2.1.1 BASE PARAMETERS FOR THE NEAR OPTIMUM-PERFORMANCE OPEN CYCLE DISK GENERATOR SYSTEMS

	<u>DIRECTLY-FIRED 1920K PREHEAT</u>	<u>DIRECTLY-FIRED 1650K PREHEAT</u>	<u>SEPARATELY-FIRED 1920K PREHEAT</u>	<u>O₂ ENRICHED</u>
Plant Size, MWe	1000 Nominal	1000 Nominal	1000 Nominal	1000 Nominal
Oxidant	Air	Air	Air	O ₂ Enriched
Air				
Oxidant Preheat Temperature, K	1920	1650	1920	922
Oxidant Preheater Type	Direct- Fired HTAH	Direct- Fired HTAH	Indirect- Fired HTAH	Metallic Heaters
Generator Inlet Mach Number	1.9	1.7	1.9	1.9
Generator Inlet Swirl	0.5	0.5	0.5	0.5
Generator Design Mode	Constant Hall Field	Constant Hall Field	Constant Hall Field	Constant Hall Field
Maximum Hall Field, kV/m	12	12	12	12
Diffuser Pressure Recovery Factor	0.6	0.6	0.6	0.6
Magnetic Induction, T	7	7	7	7
Steam Bottoming Plant	3500/1000/ 1000	3500/1000/ 1000	3500/1000/ 1000	3500/1000/ 1000
	Extraction Type	Extraction Type	Extraction Type	Extraction Type
NO _x Scrubbing System	NH ₃ Scrubber	None Required	None Required	None Required

TABLE 2.1.2 PERFORMANCE SUMMARY FOR THE NEAR-OPTIMUM-PERFORMANCE
OPEN CYCLE DISK GENERATOR SYSTEMS

	DIRECTLY-FIRED 1920 K PREHEAT	DIRECTLY-FIRED 1650 K PREHEAT	SEPARATELY-FIRED 1920 K PREHEAT	O ₂ ENRICHED
Coal Input to Plant, MW _t				
MHD Combustor	2077.1	2284.8	1453.9	2367.8
Gasifier	-	-	1039.4	-
Seed Regeneration	41.5	45.7	29.1	47.4
Total	2118.6	2330.5	2522.4	2415.2
Gross Power Out, MW _e				
MHD (dc)	595.9	522.3	407.4	450.6
Steam	627.4	738.6	727.9	810.2
Gas Turbine	-	-	131.0	-
Total	1223.3	1260.9	1266.3	1260.8
Power Consumption, MW _e				
Cycle Air Compressor	154.4	146.5	108.1	124.1
Boiler Feed Pumps	21.6	25.1	24.8	27.7
Oxygen Plant	-	-	-	71.9
NO _x Scrubber	12.2	-	-	-
Other	72.1	77.3	149.6	59.1
Total	260.3	248.9	282.5	282.8
Generator Inlet Pressure - Atm.	6.15	4.97	6.15	8.13
Generator Mass Flow - kg/s	736.0	809.6	515.2	542.8
Generator Inlet Temperature - K	2839	2731	2829	2839
Disk Inlet Radius (m)	1.26	1.31	1.05	0.92
Disk Outlet Radius (m)	5.21	5.18	4.91	5.35
Radial E - field (kv/m)	12	12	12	12
Voltage (kV)	47.4	46.5	46.3	53.1
Total Enthalpy in (MW)	3102.5	3174.8	2171.8	2466.0
Enthalpy Extraction (%)	19.2	16.5	18.8	18.3
Generator Isentropic eff. (%)	69.9	66.9	68.3	62.5
Plant Net Power Out, MW _e	963.0	1012.0	983.8	978.0
Plant Efficiency, %	45.5	43.4	39.0	40.5

In the case of the directly-fired system with a preheat level of 1920 K (2996°F), it was found that the temperatures out of the radiant boiler to the preheater had to be at such a high level as to preclude attaining the desired low level of NO_x in the furnace exhaust gas. Thus, for that case an NO_x scrubber was specified.

Performance Sensitivity Studies

The results of sensitivity studies on plant efficiency for the directly- and separately-fired cases are presented in Table 2.1.3.

A review of this table results in some interesting observations. First, it is to be noted that over the range of 500 MWe to 2000 MWe the overall plant efficiency is affected approximately 1%. This is less than is found for comparable studies on linear generator systems.

System performance does not require inlet swirl above 0.5 and performance is not overly sensitive to swirl below this level. Thus, assuming combustors can introduce swirl in the range of 0.5, extraordinary measures to introduce swirl are not required in the generator. This is further reinforced by the low efficiency decrement of 0.2 points which results from a doubling of the total combustor pressure loss from 8% to 16%. Thus, some pressure loss can be traded for achieving combustor induced swirl.

For this study the design Hall field was initially selected to be 12 kV/m. This value was somewhat arbitrarily assigned, recognizing that the disk should be theoretically capable of a much higher value than a linear generator, but with a desire to remain on the conservative side. The study results indicate that no significant performance improvement is achieved with reasonable increases above this value. The size of the disk, however, can be decreased with higher values of Hall field and thus the tradeoff can be between cost and risk without performance penalty.

Performance sensitivity to a B field increase from 7 T to 8 T and 12 T was evaluated. Based on the recommended configuration for the disk and magnet (see

2.2 below) increased tesla design conditions appear to be more easily attained for the disk than for the linear system. In the single coil disk magnet design the major structural limitations encountered in the design of linear system magnets with high tesla fields are not expected to be evident. An efficiency increase of 1.2 percentage points was calculated for the increase of magnetic induction from 7 T to 12 T.

The diffuser recovery coefficient is reasonably influential on overall performance, with 0.5 points of efficiency gained by increasing the assumed recovery factor from 0.45 to 0.60. For a well-integrated generator, diffuser, and radiant furnace design, the higher values of recovery factor can be more easily achieved in disk generator systems, since boundary layer blockage at the diffuser entry is expected to be minimal, and the hot wall design of the disk generator and diffuser minimize density and velocity differences in the flow cross-section at any radius.

For detailed information on the basis for the study and systems design, the reader is referred to Section 3.0 and 4.0. Details of the systems analysis itself will be found in Section 5.0.

Plasma Conductivity

In performing and reviewing this study, it was found that differences in calculated plasma conductivities exist when compared to companion linear generator studies. Specifically the PSPEC study performed by AVCO[1] uses higher conductivities and the PSPEC study performed by General Electric[2] uses lower conductivity values. High plasma conductivity is important for the open cycle disk generator configuration, which optimizes from a performance standpoint at supersonic inlet velocities. The uncertainty in conductivity differs from the other parameters studied in this program, because it is not a design parameter, except insofar as it is affected by the selection of a seeding level. Its importance lies primarily in assuring consistency between the results of various studies from which conclusions are to be drawn. Although the evaluation of the effects of a gross percentage change in conductivity is felt to be an extreme simplification (since the actual conductivity changes are

derived from species included, rate constants, ionization potential, calculational methods, etc.), two cases, one each for an "across-the-board" increase and decrease in conductivity, were calculated and are included in Table 2.1.3. As expected, the performance of the disk generator and thus the overall power system is sensitive to conductivity variations, though not unduly so. Variations in plasma conductivity affect the division of power generation capability between the topping cycle and the bottoming plant, more so than they cause significant changes in overall plant power output. The most significant effect of conductivity is the change in extraction length required to maintain equivalent performance from the generator. Variations in generator size have a great effect upon disk and magnet sizes, and therefore, costs. A direct and truly valid comparison of the overall performance and costing results obtained in this study with other studies can only be made following a review and careful consideration of the differences in methods and assumptions used in the studies.

Disk MHD Component Costs

This study called for an estimate of the costs of the major components in OGD MHD plants that can differ significantly in design from their linear counterparts. A summary of this data is presented in Table 2.1.4. A review of the cost of these disk-related components against their counterparts in the most recent linear studies (PSPEC)[1,2] indicates a potential cost reduction from 24-56% for the disk components, or in absolute dollars a value of $\$23 \times 10^6$ to $\$103 \times 10^6$ (Mid-1978 basis) for the 1000 MWe plants investigated. The large range results from major differences in the estimated cost of the generator and the magnet for the comparison linear systems. It was found that the combustor system will be of similar cost to that for linear systems. The MHD generator consisting of the nozzle, channel and diffuser, the magnet, and the channel power management system will all have significantly lower costs than for a linear system of similar size. The radiant furnace, as conceived for this study, is slightly higher in cost than for a linear system. Based on observations of the physical design differences, and based on the National Magnet Laboratory assessment of magnet costs, the potential for cost savings is heavily biased toward the upper end of the 23-103 million dollar range indicated above. Verification of this conclusion is dependent on

Table 2.1.4 MAJOR SUBSYSTEM COST ESTIMATES FOR DISK GENERATOR POWER PLANTS
OF 1000 MWe CAPACITY

<u>SUBSYSTEM</u>	<u>COST - DOLLARS, MID-1978 BASIS</u>			
	<u>DIRECTLY-FIRED</u> <u>1920 K PREHEAT</u>	<u>DIRECTLY-FIRED</u> <u>1650 K PREHEAT</u>	<u>SEPARATELY-FIRED</u> <u>1920 K PREHEAT</u>	<u>OXYGEN</u> <u>AUGMENTED</u>
COMBUSTOR	\$ 917,000	\$ 883,000	\$ 805,000	\$ 601,000
NOZZLE AND CHANNEL	1,892,000	1,869,000	1,720,000	1,996,000
DIFFUSER	2,919,000	2,765,000	2,881,000	2,529,000
MAGNET	49,302,000	50,198,000	47,112,000	52,219,000
DISK POWER MANAGEMENT	25,045,000	21,833,000	17,414,000	19,249,000
RADIANT FURNACE	25,089,000	30,837,000	20,248,000	22,460,000

resolution of the large differences presently existing in studies of the linear system components. For further information on the data generated in support of the above cost conclusions see Section 7.0.

2.1.2 OPEN CYCLE DISK POWER TRAIN ARRANGEMENT

A selection study was performed to arrive at a candidate plant arrangement. Figure 2-1-1 is a general arrangement drawing of the MHD portion of the directly-fired disk generator plant selected for layout. An attempt has been made to utilize the natural features of the disk to provide significant advantages in cost, operation and maintenance. A simple single solenoid coil magnet is used and is positioned below the radial outflow disk at ground level. This allows for an easily supported permanent magnet installation with rapid access from above to the channel for maintenance and replacement. The combustor is in a natural vertical orientation for slagging and fires upward through the central hole in the magnet into the center of the disk. Tunnel access is provided to the combustor for servicing and removal, and for routing of feed lines.

The outflow of the disk undergoes sonic transition and is radially diffused at the disk periphery, where it is fed to three upright cylindrical radiant boiler sections. The flow from these three radiant boiler sections is collected by means of insulated ducting and manifolding and directed to a single train of heat and seed recovery equipment with configurations virtually identical to equipment used in linear systems.

The overall arrangement of the channel and combustor is especially encouraging from serviceability, support and structures considerations. The diffuser design, and that of the radiant boilers and ducting, is straightforward and feasible; yet it appears that considerable work must be done in this area to combine the functions of these three elements and optimize their performance as integrated portions of the heat recovery and gas dynamic systems.

There are several features of the disk power train which when combined could result in major operating systems advantage. These can be in the form of

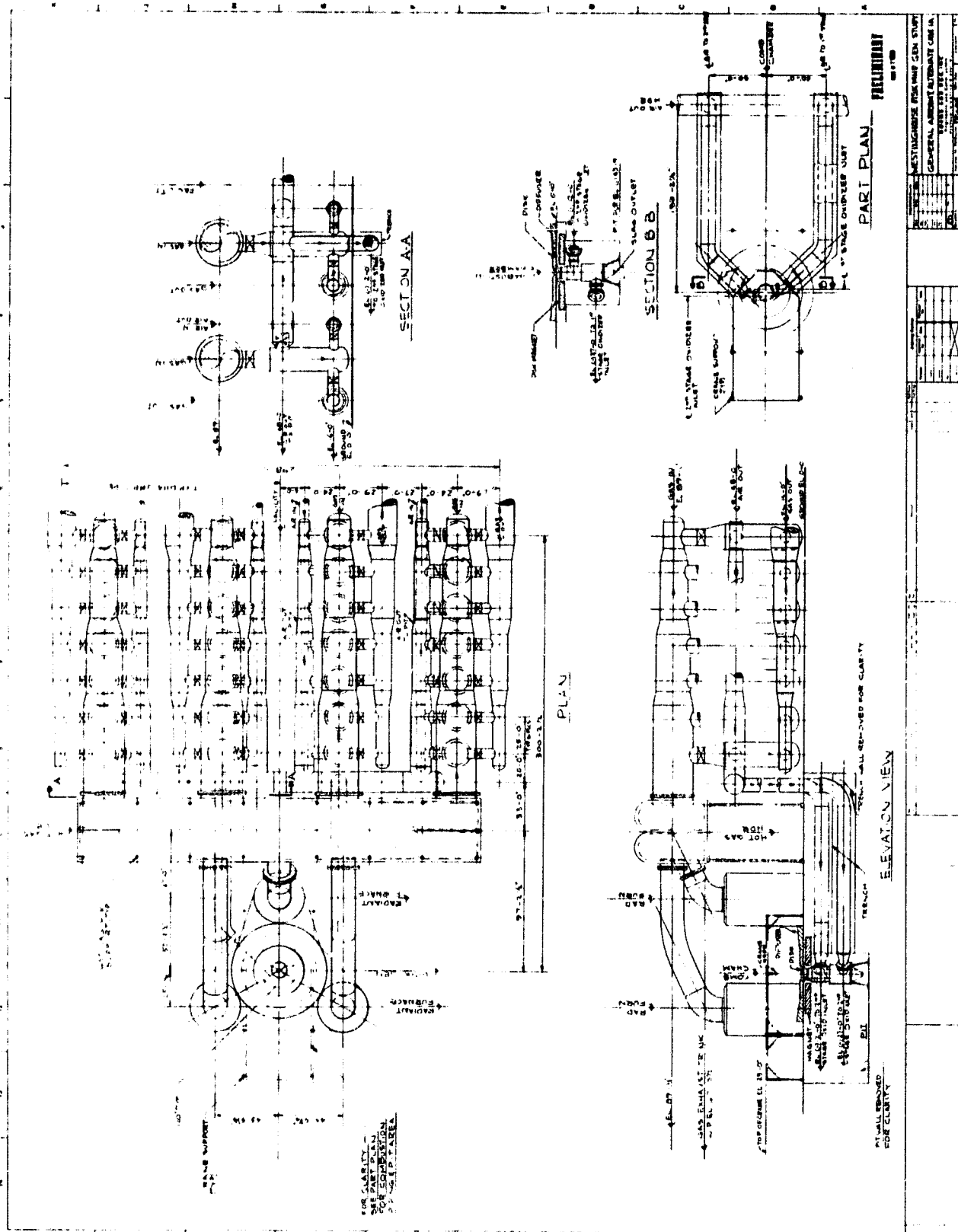


Figure 2-1-1. OCD MHD/Steam Power System General Arrangement of MHD Power Train for 1000 MWe Directly - Fired Plant

ORIGINAL PAGE IS
OF POOR QUALITY

power plant availability advantages or power plant integration advantages. It is believed that the selected simplified arrangement of the disk and magnet could result in major time advantages for removal and or repair of the disk. Likewise the disk itself with many fewer parts and electrical interconnections may well prove to be considerably more rugged than linear units. The quantification of such features in terms of plant availability is very difficult without operating experience, yet if even 1-2% availability difference can be attributed to these features it can overcome a sizable plant efficiency difference when viewed from the standpoint of cost of electricity. In terms of plant integration the much lower heat loss from the walls of the disk channel as compared to the linear makes the combining of the turbine plant feedwater train with the channel cooling load an easier task. The use of stainless steel cooling passages in the disk, as designed herein, assures compatibility of water chemistry, requirements with the bottoming plant. The incompatibility of copper passages, as presently used in linear systems, has been avoided.

More specific information on the power train arrangement can be found in Section 6.7.

2.1.3 OPEN CYCLE DISK COMPONENT CONCLUSIONS

Combustor - The combustor envisioned is a vertically upfiring unit with slag tapping at the bottom, incorporating two stages of combustion. Its characteristics are not unlike those for linear system combustors with the exception that swirl is desired at the inlet to the disk. This swirl is introduced by tangential inflow of the oxidant to both stages. Swirls up to 0.5, which improve the system performance, are conceived as being possible from the combustor alone, thus eliminating the need for swirl vanes in the disk generator inlet. Preliminary calculations of the losses that would be encountered with combustion systems to provide radial swirling inflow were sufficient to indicate the desirability for a radial outflow configuration.

The combustor effort on this study is more fully covered in Section 6.2.

Disk Generator - As previously discussed under the systems description, the selected configuration of the disk and magnet was a flat disk generator with a single coil superconducting magnet beneath it. Optimization studies of the disk performance, with accounting for swirl vane losses, indicated desirable swirls of approximately 0.5. It was assumed for the study that the combustor alone could produce values of this magnitude. This eliminated the need for swirl vanes at the generator inlet. The conclusion that such devices may not be necessary is an important one, and considerably enhances the engineering feasibility of the disk generator.

Particular emphasis was placed on determining electrical constraints and is explained in Section 5.3. A constant radial E-field was found to provide the best generator performance. Although single load (two-terminal) disk generators can be designed on the basis of this constraint, the maintenance of acceptable performance under off-design conditions requires that the radial voltage gradient be controlled. Accordingly, a small number (3-5) of intermediate electrode rings are required. Control of the radial voltage gradient is achieved by the inverters between adjacent electrode rings.

The selection of a disk geometry brings about important simplification in the specification of channel wall requirements. Basically the walls of a disk generator have only to (1) support the Hall field and (2) provide power take-off points which as explained above can be few in number. It is to be noted that the Faraday Current closes on itself within the gas and thus it is not necessary to provide external closure paths as in a linear diagonal machine, nor to accommodate multiple loading as in the linear segmented Faraday case. This also has important simplifying implications for the magnet and the power management subsystem as discussed below.

Figure 2-1-2 indicates the conceptual design of the disk generator and its radial diffuser as developed in this study. The disk consists of two pierced fiberglass walls to which are joined water-cooled ceramic walls operating at high temperature. The electrodes are water-cooled copper rings separated from the refractory walls at their inner and outer radii by appropriate insulating

materials. A typical diameter of 5.2 meters is shown for the active channel for a 1000 MWe plant. Two points of design importance for the disk are (1) the walls are much simplified from those of the linear systems with their complex and intricate multiple electrodes and (2) the mechanical design should be easily scaled from small size prototypes; a characteristic that is not obvious for linear systems.

Details on the performance optimization studies of the disk generator can be found in Section 5.1 and 5.2. Design studies of the disk generator are contained in Section 6.1.

Magnet - The choice in magnet configuration is between; (1) a pair of coils to provide a substantially uniform axial field with radius, but having difficult support requirements (penetration of the disk for upper coil support) thus making it difficult to maintain and replace the disk; and (2) a single coil below the disk generator with a substantial radial field that increases with radius as depicted in Figure 2-1-3. The advantages of (2) were considered so overwhelming that it was adopted for all aspects of the study with the simplifying assumption of flat disk geometry. Analysis of the resultant field for the axial and radial components indicates that flow streams shaped as shown on the bottom half of Figure 2-1-3 will place the flow normal to the magnetic field at all radii. A further beneficial optimization of disk generator performance is to be expected if this approach is adopted, and it is recommended for future investigations.

A study effort in defining the magnet is contained in Section 6.3.

Channel Power Management - The channel power management system consists of the equipment necessary for consolidation, conversion and conditioning of the MHD generated power to make it acceptable for transmission.

An initial review of the voltage-current relationship of the disk generator in a two-terminal configuration showed significant sensitivity at design point to current changes. For example, variations in front-end load current of less

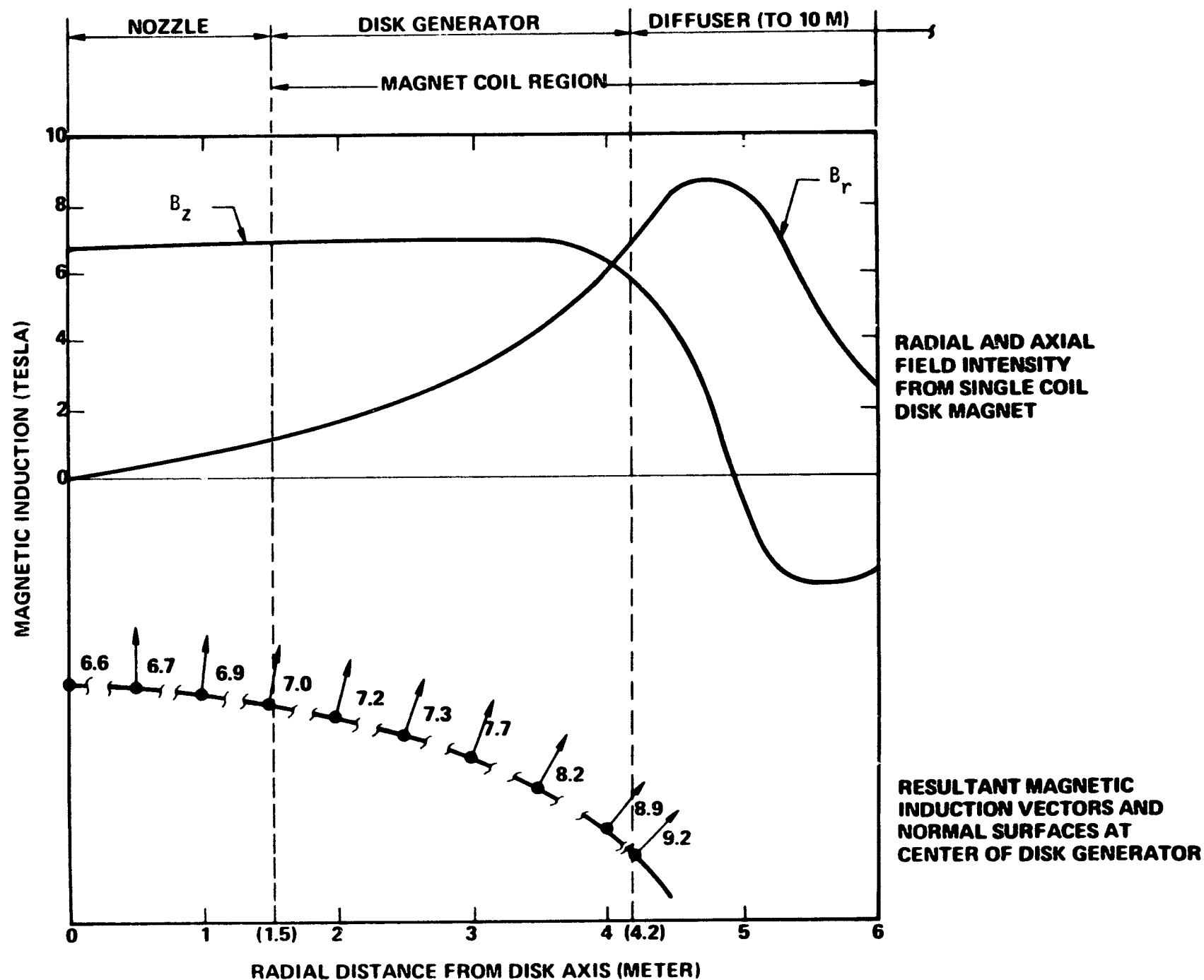


Figure 2-1-3. Effect of Radial Field Component in Solenoidal Single Coil Magnet

than 0.33% resulted in a 55% change in Mach number. This indicates that successful operation of the channel would require adjustment of the back-end electrical loading to maintain compatibility with gas dynamic conditions. This was accomplished by segmenting the channel into four parts by providing intermediate current take-off electrode rings which typically decrease in radial spacing from inlet to outlet. Although the feasibility of radial field control has been established in this study, future effort will be beneficial in defining more precisely the power take-off electrode requirements, and their location, as well as defining potential regulator circuits applicable to the task. A discussion of the analysis performed to arrive at the above conclusions can be found in Section 5.3.4.

The multiple electrode disk generator requires that inverter units of appropriate rating be connected in series across adjacent electrodes. The current levels required by the intermediate and outer electrodes are compatible with direct connection, to an inverter. Electrode current density considerations will probably require multiple (2-4) collecting electrodes, and an accompanying consolidation scheme. As this will be located in the fringing field of the coil, the voltage will be low as in the end connection of a linear diagonal machine.

The closure of the Faraday current within the plasma should eliminate the need for local current control as in the frame current control of linear diagonal generators. The simplification of consolidation circuitry and dispensing with current control greatly simplifies the overall power management subsystem and provides the disk configuration with a key electrical advantage that translates into reduced cost and increased reliability. The costs of such a disk conversion system have been estimated to be approximately 3% of the cost of that for a linear generator MHD powerplant, with the savings coming from the simplification described in more detail in Section 6.4.

Diffuser and Radiant Furnace - Figure 2-1-1 indicated the general arrangement of the MHD power train and Figure 2-1-2 indicated the conceptual design of the diffuser. As previously indicated, arrangement studies showed the highly

desirable effects of locating the disk in a horizontal plane above the magnet. Likewise, the conceptual design of the disk generator indicated the desirability of a section of radial diffuser at the periphery of the disk generator through which struts could be built thus allowing it to serve as a structural member for supporting the disk walls. The additional desire to have an area of access over the disk for maintenance and removal resulted in the selection of a concept using discrete silo-type radiant boilers located around the periphery of the radial diffuser. This appears to be a rather straightforward, low risk approach. Extensive insulated ducting and manifolding is required to collect the effluent from the three radiant boilers and direct it to air preheaters or to a common train of downstream heat and seed recovery equipment.

Refractory water wall construction has been assumed for the diffuser and radiant boilers, and refractory-insulated exhaust ducting has been proposed. Costing estimates are consistent with that performed on similar studies for linear systems. Based on the costing information developed and on the best interpretations of linear MHD power plant data, the radiant boiler system was found to be approximately 40% higher in cost in the separately fired case and 20% higher in the oxygen-augmented case.

The arrangement and design of the combined diffuser, radiant boiler and ducting is not a feasibility problem, but it does appear that this area could benefit from additional conceptual effort at combining functions to minimize cost and complexity, and to optimize aerodynamic and heat recovery performance.

Conceptual design information on the radiant boiler system design can be found in Section 6.5.

2.2 CLOSED CYCLE DISK MHD STUDIES

The study of closed cycle disk systems required extensive effort in defining acceptable analytical representations for the disk generator and its integration into systems models. As a result, the primary effort in this study was concentrated on determining the general characteristics of the disk

generator and on predicting the level of system performance with emphasis on overall plant efficiency. Conceptual design and costing were given only a cursory evaluation.

2.2.1 CLOSED CYCLE DISK SYSTEM STUDIES

The powerplant configuration which was investigated consisted of regenerative refractory heaters fired directly with coal combustion products, and heating an argon closed cycle fluid seeded as necessary with cesium. On the basis of previous studies, and early exploration in this study, the energy derived from a supercritical steam bottoming plant was matched to the pump work required in the cycle, and electrical power output of the plant was totally derived from the disk generator. Figure 2-2-1 is a schematic diagram of the cycle investigated.

Thirty-three system performance cases are presented in the body of this report covering a range of disk generator variables. All calculations were performed with a 1920 K (2996°F) inlet temperature to the channel and a magnetic field of 6 T. Optimization of the closed cycle disk is complicated by the fact that the electron population of the plasma is not in thermal equilibrium with the surrounding gas and electron temperature becomes an additional variable. Thus, plasma turbulence level and impurity level are parameters which must be considered in addition to swirl, Mach number, and seeding level.

The systems analyzed covered a range of power levels, mass flow rates, inlet pressure levels, inlet swirls, inlet Mach numbers and seed ratios; with selected investigation of turbulence level and impurities content. A summary of the performance survey results is presented in Table 2.2.1. These cases have generally been optimized on system efficiency within the constraints of an effective Hall parameter limit, an exit Mach number of 1.0-1.1, and the required matching of steam power and pumping power. Several observations can be made from reviewing the information contained in this table.

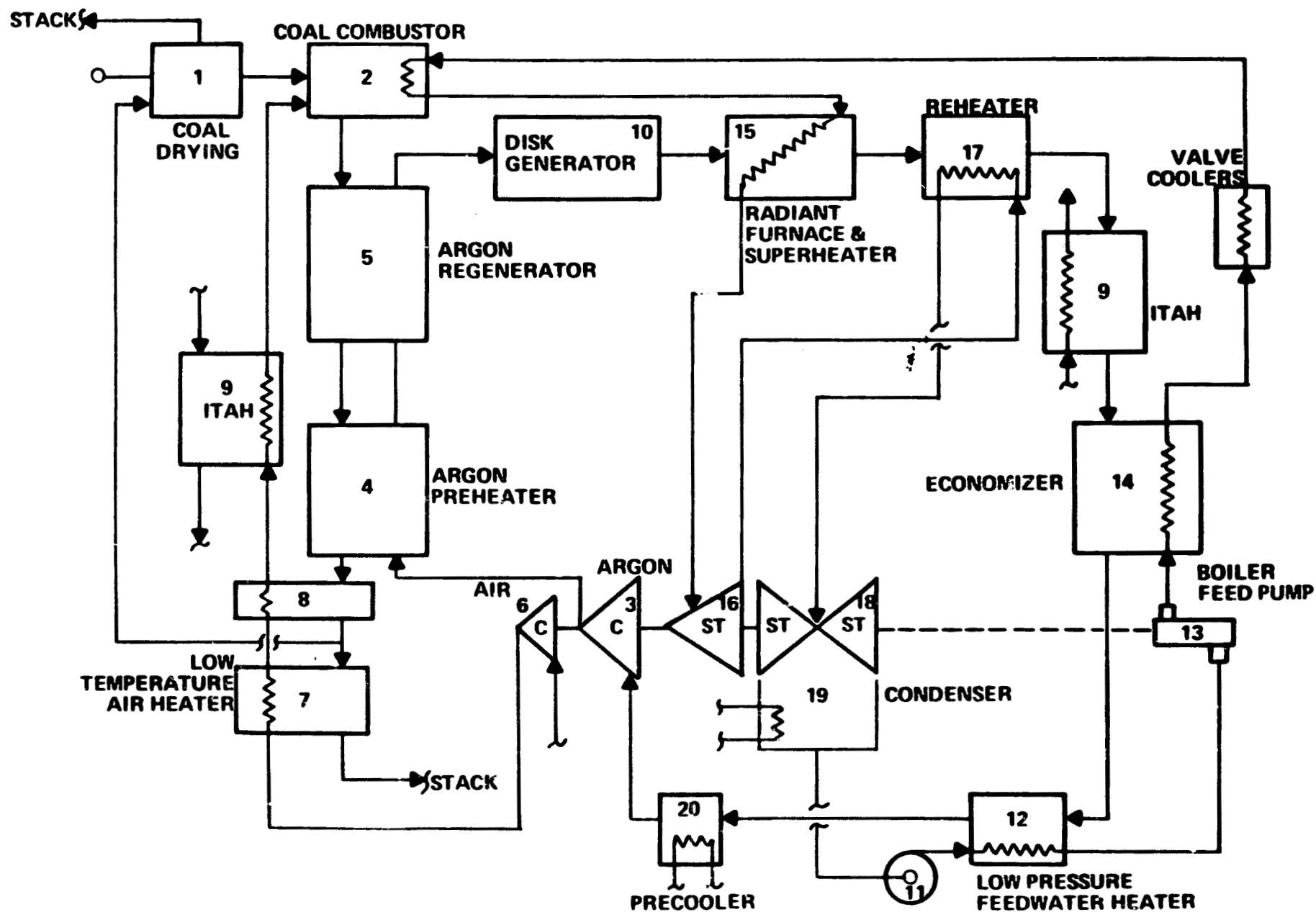


Figure 2-2-1. CCD Power System Flow Diagram

TABLE 2.2.1 CLOSED CYCLE DISK GENERATOR SYSTEM PERFORMANCE SURVEY
(INLET CHANNEL HEIGHT = 0.5 METER)

100 ppm Impurities; Turbulence Level 0.2

CASE NO.	ARGON FLOW kg/s	INLET SWIRL	INLET MACH NO.	INLET PRESSURE ATM.	SEED FRACTION %	CHANNEL INLET RADIUS METERS	CHANNEL LENGTH METERS	POWER GENERATED MWe	SYSTEM EFFICIENCY %
1	1060	2.0	2.02	4	.135	2.5	.29	376	46.2
2	1294	2.0	2.00	4	.405	3.0	.28	459	46.0
3	1171	2.0	2.22	6	.135	2.1	.45	416	45.7
4	2196	2.0	2.25	8	.405	3.0	.86	763	45.1
5	1922	2.0	2.50	10	.100	2.5	.92	674	44.9
6	1196	1.5	2.00	6	.035	1.5	.36	420	45.1
7	1136	1.5	2.08	6	.015	1.5	.43	396	45.0
8	2059	1.5	1.95	6	.045	2.5	.36	712	45.2
9	1980	1.5	2.01	6	.015	2.5	.51	703	45.4
10	1344	1.5	2.26	8	.007	1.5	.80	467	44.5
11	3089	1.5	2.05	8	.035	3.0	.61	1085	45.1
12	2989	1.5	2.10	8	.015	3.0	.77	1057	45.1
13	1749	1.5	2.20	10	.045	1.5	.67	608	44.4
14	3054	1.5	2.13	10	.045	2.5	.82	1069	44.7
15	1963	1.5	2.30	12	.045	1.5	.84	677	44.0
16	2978	1.5	2.25	12	.045	2.2	.96	1027	44.3
17	3476	1.5	2.21	12	.045	2.5	1.11	1206	44.4
18	2098	1.0	1.95	8	.005	1.5	.84	715	43.5
19	2550	1.0	1.93	8	.005	1.8	.86	875	43.7
20	3155	1.0	1.91	8	.005	2.2	.88	1085	43.8
21	2460	1.0	2.05	10	.005	1.5	.90	833	43.2
22	3048	1.0	2.00	10	.005	1.8	.98	1039	43.4
23	3387	1.0	2.00	10	.005	2.0	.96	1146	43.4
24	3774	1.0	1.98	10	.005	2.2	1.00	1284	43.5
25	4234	1.0	2.00	10	.005	2.5	.96	1449	43.6
26	2857	1.0	2.10	12	.005	1.5	1.06	962	42.8
27	5016	1.0	2.02	12	.005	2.5	1.24	1703	43.3

100 ppm Impurities; Turbulence Level 0.5

28	463	4.0	2.35	4	.300	2.5	.42	162	45.2
29	556	4.0	2.35	4	.300	3.0	.42	197	45.3
30	318	4.0	2.75	6	.300	1.5	.43	104	43.7
31	369	4.0	2.95	8	.100	1.5	.61	125	43.2
32	734	4.0	3.02	10	.100	2.5	.95	246	42.8

200 ppm Impurities; Turbulence Level 0.2

33	1545	2.0	2.50	8	.405	2.5	1.13	531	44.5
----	------	-----	------	---	------	-----	------	-----	------

- (1) The level of optimum system efficiency for all the cases investigated lies within a relatively narrow band centered around 44% and is of a level comparable to that observed for linear closed cycle investigations;
- (2) The system efficiency does not deteriorate with power level, making the closed cycle disk potentially attractive for small size plants;
- (3) For the optimized cases investigated a change in the impurities from 100 to 200 PPM did not cause a significant degradation in performance. The impact of impurities on a given design needs further investigation.
- (4) High turbulence levels force a requirement for high swirl and high inlet Mach numbers, and as investigated herein resulted in power plants that attained maximum efficiency at relatively low power levels (162 - 246 MWe).
- (5) The seeding ratio declines with swirl, for example to 0.005% at a swirl of 1.0 and thus implies limitations from the control viewpoint. However the performance benefits afforded by the reduced plasma turbulence resulting from full ionization of the seed have not been investigated. Higher coefficients should be allowable which would increase the system efficiency. Better control of the generator operation is implied since the electron density is proportional to the gas pressure in the fully ionized limit.

The closed cycle disk generator was found to be a compact high interaction unit. Swirl is much more beneficial to the performance of the closed cycle disk than it is to the open cycle disk, with the potential for a one-half to one percentage point gain in plant efficiency for a swirl increase of $\Delta S = 0.5$ at a given power level. The compact arrangement minimizes the heat and friction

losses in the generator and minimizes boundary layer thickness flowing to the diffuser. Within the constraints of the one dimensional modeling of the closed cycle disk used in this study, its turbine efficiency appears to be approximately four points higher than an equivalent closed cycle linear Faraday generator for the same enthalpy extraction.

The study has established that the MHD closed cycle disk generator achieves levels of systems efficiency which are comparable with or exceed those published in previous linear closed cycle investigations (GE 102, 102A studies). This comparison is based on using compatible assumptions for the generator and diffuser in each case, together with less optimistic assumptions about losses throughout the remainder of the disk system than were used in the linear system studies. The study was not carried to the point where it was possible to determine cost or design concept relationships to the many variables. The use of a disk generator does not alter the demanding requirements on the regenerative argon heater defined in previous studies. Closed cycle systems using direct combustion of coal for the reheat gas source to the heaters will also require scrubbers for SO_x and NO_x , since seed is not contained in the combustion gas stream to provide a means of sulfur removal, and no comparable system to the radiant boiler exists for reduction of the NO_x .

Detailed reporting on the closed cycle disk generator systems study may be found in Section 8.0.

2.2.2 CLOSED CYCLE DISK GENERATOR DESCRIPTION AND COST RELATIONS

Figure 2-2-2 is a schematic arrangement of the closed cycle disk generator where the aerodynamic configuration is drawn to scale. As a result of high interaction, the generator is relatively short ($L/D < 2.0$) and two-dimensional electrical and gasdynamic effects can be expected to be of some significance. For a representative 1000 MWe power plant (Case 22 of Table 2.2.1 has been selected as representative), the channel inlet radius is 1.8 meters, the exit radius is 2.78 meters and the inlet channel height is 0.5 meters.



Figure 2-2-2. 1000 MWe Closed Cycle Disk Generator Conceptual Design

Due to the compactness of the generator and its high current, low voltage characteristics, surface provisions within current density limits for the cathode and anode are best provided outside of the interaction length. The practical aspects of this requirement are evident in the selected case by the fact that nearly the entire wetted surface area available within the channel itself would have to be used as electrode surface area if current densities not exceeding $30\text{--}50 \text{ kA/m}^2$ are to be used. To ease this situation the anode in the sketch of Figure 2-2-2 is envisioned as consisting of the walls at the disk inlet and the cathode as a series of collector rings installed in the exit gas stream. Electrode consolidation circuits would therefore be required for cathode connection.

A simplified cost evaluation of closed cycle disk components was performed by relating them to corresponding elements in the open cycle part of this study. Case 22 in Table 2.2.1 was again selected as typical for a 1000 MWe closed cycle disk configuration. Details of this cost evaluation are to be found in Section 9.0.

The operating conditions of the closed cycle disk which have a bearing on structural design of the disk itself are not markedly different. Therefore, the structural design could be assumed similar to that of the open cycle disk and cost relations as a function of radius developed; such an approach indicates the closed cycle disk structure can be expected to have a cost in the range of 30-50% of that for the open cycle case. The complications of introducing electrodes with the large surface areas presumably required is expected to substantially affect design complexity and cost, which may offset this advantage to a large degree.

A similar approach was used on the magnet in applying cost scaling relationships derived during the open cycle work. This indicated that the closed cycle magnet could be expected to have a substantially lower cost than for comparable open cycle generator cases.

Three major considerations enter into the cost of the power management system for the closed cycle disk. First, since all power generated for transmission comes from MHD, the amount of power to be converted and conditioned is greater than twice that for the same size open cycle plant. Secondly, without a steam turbine generator as part of the system, VAR compensation must be provided by added components, which may be either static or rotating. Thirdly, the high current, low voltage characteristic of the disk requires a large number of converter bridges to stay within accepted amperage limitations per bridge.

Taking these items into consideration, the cost of the power management system for the closed cycle disk is expected to be 115% greater than the open cycle plant of similar net electrical power output.

3.0 BASIS FOR STUDY

3.1 EXPERIMENTAL AND ANALYTICAL STUDIES OF DISK GENERATORS

The disk configuration was initially used to provide a convenient experimental environment for fundamental studies of plasma properties, nonequilibrium ionization, and interaction with a magnetic field [1-2]. A pebble bed heater with blowdown capability was the initial source of plasma; later the well established shock-tube/shock-tunnel technology for production of high enthalpy gas flows became the natural partner of the disk geometry. Both cesium-seeded argon and cesium-seeded molecular gas mixtures were used, with some of the channels inducing inlet swirl, and the steady progression of improvements in enthalpy extraction [3-8] is well-illustrated in Figure 3-1-1, taken from Reference [9]. The abscissa is a normalized enthalpy extraction length, being the ratio of device size to an idealized rate of enthalpy extraction under the channel inlet conditions (see 5.1).

These experiments have clearly established the potential of the disk as an MHD generator. They have been accompanied by a substantial body of theoretical work, ranging from the original descriptive paper [10] to several assessments of the commercial power generation potential [9, 11, 12]. The associated theoretical work also includes studies of the effects of nonuniformities [13-17], the most critical potential problem area for any disk configuration relying on high swirl induced by inlet guide vanes. These previous experimental and theoretical analyses have built a foundation on which the present systems study could be based. For both open-cycle and closed-cycle applications there is a reasonable data base to aid in the selection of the ranges of parameters and operating modes.

Parameter choices include the plasma conditions, stagnation levels, expansion conditions to generator inlet, electrical loading, electrical stress levels (i.e., Hall field limitations) and exit conditions from the generator channel to the diffuser. All of these choices are systematically examined in Sections 5.0 and 8.0 where the rationale for the present systems study is laid out.

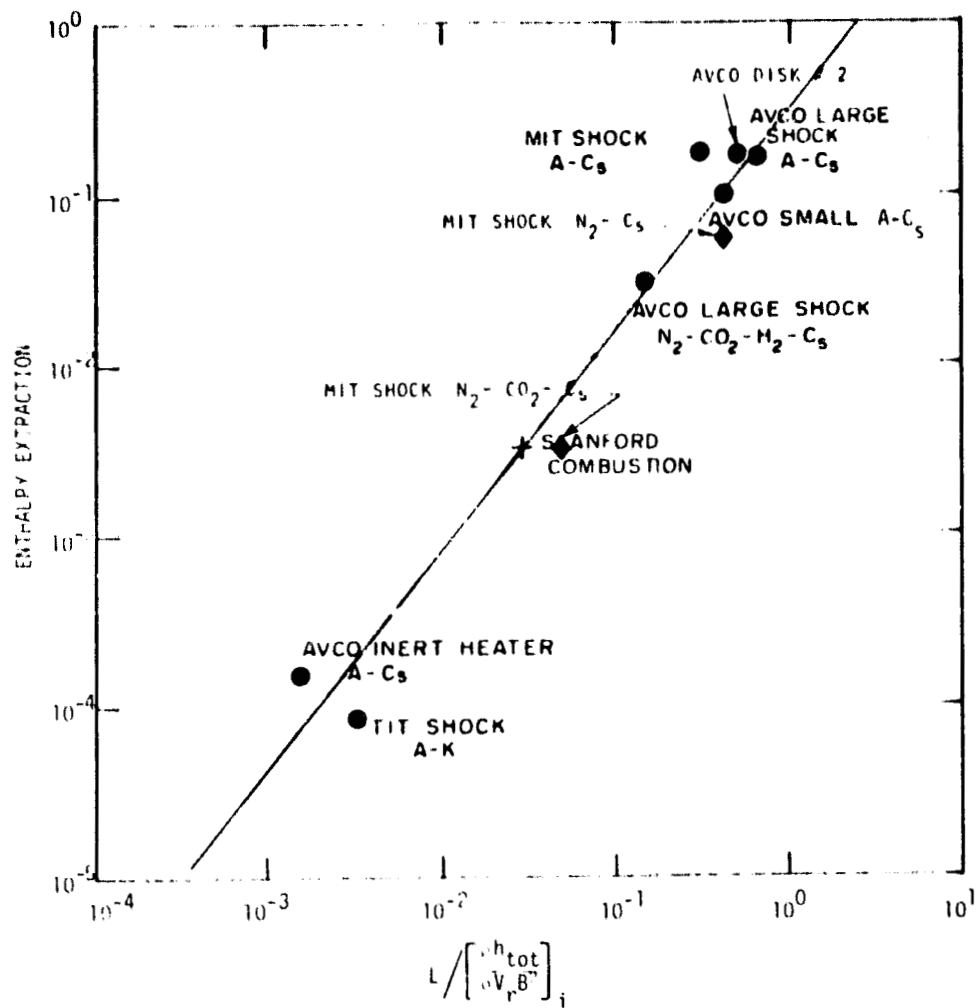


Figure 3-1-1. Enthalpy Extraction Correlation for Disk Experiments

It was expected that various ongoing DOE experimental programs would impact the present study and permit refinement of some of the assumptions which were least solidly based. In one case the experimental evidence is indeed encouraging; hot wall disk experiments at Stanford have established that electric fields of up to 9 kV/m pose no problem with respect to breakdown and there is no indication that 9 kV/m is in any sense a threshold [18]. Refinements to the combustor assumptions have not been forthcoming, however; and the progress reports on the 20 MW_t combustor development programs have so far yielded no helpful details on slag rejection or heat loss.

3.2 APPROACH TO THE STUDY

3.2.1 GUIDELINES AND REQUIREMENTS

In the initial contract documents and in succeeding communications, at the beginning of the study, NASA provided certain guidelines and requirements which applied to the performance of the Disk MHD Generator Study. These are summarized below:

- The study was to be conducted through parametric analysis of four specified MHD/steam power plant configurations incorporating the disk generator.
- The four "Base Case" reference plant configurations defined by NASA were
 - (1) Open cycle disk with directly-fired high temperature air heaters.
 - (2) Open cycle disk with clean fuel gas-fired high temperature air heaters.
 - (3) Closed cycle disk with noble gas regenerators reheated with combustion gas from a coal-fired combustor.
 - (4) Closed cycle disk with noble gas regenerators reheated with combustion gas derived from burning clean fuel gas.

Clean fuel gas for systems (2) and (4) was assumed to be provided by a pressurized advanced technology gasifier.

- All plants were to utilize a recuperative metallic heat exchanger to reheat air or fuel from the combustion gas stream.
- Disk generators with pure radial flow and with swirl were to be investigated.
- Impulse and mixed modes of the disk operation were to be investigated.
- Coal types were specified: Illinois #6 and Montana Rosebud.
- The steam bottoming plant to be used in all cases was specified to be a supercritical single-reheat type.
- Emission limits for particulates, SO_2 , and NO_x were specified.
- Plant design life and capacity factors were specified.
- All plant designs were to be developed with emphasis upon base-load operation.
- Oxygen enrichment of the combustion air could be considered, if desired by the contractor.
- Cost estimates for the major disk-related components of the open-cycle disk generator MHD/steam power systems were to be prepared. These major components were defined to be:
 - MHD Combustor and Nozzle
 - MHD Generator and Diffuser
 - MHD Magnet and Dewar
 - DC/AC Inverter and Control System
 - Radiant Furnace
- Expected differences in cost between open-cycle disk generator major components were to be discussed, if any significant differences in detail were involved.

Section 4.0 of this report contains the specifics of the guidelines and requirements as applied to the study.

As the study progressed, modifications to the initial requirements and assumptions were made. Major changes from the original study guidelines, and additional requirements proposed by NASA and accepted by Westinghouse during the term of the study, are given below.

- For the final performance calculations for each disk generator reference system, NASA requested that a direct cooling system be assumed for the MHD components, i.e., cooling water was to be bottoming plant working fluid. There were two reasons for adopting such a system design:
 - (1) Higher overall plant thermal efficiency could be obtained.
 - (2) The disk systems would be configured in a manner consistent with the PSPEC systems, against which their performance was to be compared.
- NASA requested that the steam bottoming plants for the disk generator systems be evaluated with extraction feedwater heating included. This was agreed upon for the calculation of final overall performance figures.
- NASA agreed to permit the introduction of a fifth "Base Case" reference plant design, in lieu of the performance of parametric analyses for certain open cycle disk cases proposed in the initial technical plan submitted by Westinghouse. These open cycle disk cases were determined to be redundant and/or infeasible in practice after the detailed analysis work had begun. The fifth "Base Case" reference plant to be evaluated was an open cycle disk system with no high temperature air heaters, but with combustor stagnation temperature maintained by using oxygen augmentation of the combustor oxidant. A recuperative metallic heat exchanger was the final preheating module for combustor oxidant. NASA specified that the Lotepro (Linde A.G.) high efficiency oxygen plant was to be used as an oxygen source; full integration with the MHD plant was assumed. The details of oxygen plant modeling and the listing of parametric cases for the open-cycle disk analyses supplanted by the consideration of a fifth reference design are contained in Section 5.0 of this report.
- For the closed cycle disk, the generator modeling effort was found to be more extensive than originally planned. NASA agreed to permit the replacement of the specified parametric analyses by a performance assessment of closed cycle disk generator systems over a range of power levels, and by a sensitivity study to define the generator performance variations caused by perturbations to certain critical generator parameters. These substitute studies were carried out only for closed cycle disk systems with noble gas regenerators reheated with combustion gas from an atmospheric coal combustor.

3.2.2 LOGIC OF THE STUDY

A set of base case parameters thought to be characteristic of the optimum-performance disk systems for each base case reference plant investigated was defined, along with the specific plant configuration.

System and Disk Model Development

Models for the disk generator types themselves, and for the overall disk generator systems were defined, together with the assumed values for each independent variable or limit in the model. Where possible, values for assumed parameters such as heat losses or draft losses were reviewed by members of the project team with the most expertise and experience in the areas of interest.

Disk and System Parametric Analyses

A suboptimization of each open cycle disk generator type was performed leading to the specification of a design constraint and a set of inlet conditions considered likely to provide the maximum disk generator performance (i.e., maximize disk performance given predefined constraints on the geometric, electrical magnetic, thermal, or mechanical parameters critical to the analysis). With the OCD generator model and appropriate design constraint(s) specified, the systems analyses were performed for each parametric case proposed in order to identify possible approaches to disk generator system performance improvement.

In the case of the closed-cycle disk, the generator suboptimization itself required direct integration of the disk and systems model. The imposed systems constraint of matching compressor (and feed pump) work to the steam plant output strongly affects the optimal generator parameters and partially determines the generator length. In addition, this systems constraint partially dictates the generator design constraint. Parametric studies were carried out for power levels in the range 100 MWe to 1700 MWe. The critical generator parameters studied were turbulence level, impurity level, seed fraction, pressure, inlet swirl and inlet Mach number.

Delineation of Optimum System Configurations

For the three distinct open cycle reference configurations (directly-fired, separately-fired, and oxygen-augmented combustion gas disk generator systems) the development of a detailed generator/system integrated model made it possible to delineate a final set of parameters for potential commercial-scale disk generator MHD/steam power systems. The parameters were representative of those required to provide optimum system performance.

For the direct-fired closed-cycle case generator and system performance was defined for a range of base-load power levels for a given plant configuration.

Development of Conceptual Designs for Open Cycle Disk System Components

For parameters representative of these optimum cases, conceptual designs for the major components were determined. Investigation of various alternative design possibilities for disk generators, nozzles, diffusers, power management equipment, magnets, radiant furnaces, and combustors was carried out, and general configurations for each were selected with reference to the interface requirements, design life, and reliability requirements for the systems, as specified by NASA (Section 4.0 of this report). The materials, transportation, construction, and erection costs for each set of major components were determined, to provide a comparison basis for equivalent linear MHD systems cost analyses, and in particular, for the analogous linear MHD system component costs developed in the parallel PSPEC studies by other NASA contractors.

A key element in the selection of designs for disk system components was the concern that each design should consider and provide means to extend the conceptual simplicity of the disk generator geometry. In most cases, it was found to be possible to define a simple component design which offered the potential for providing reasonable service life and minimum design complexity, within the preferred guidelines. Attention was also given to providing for ease of replacement of the disk channel itself, under the assumption that the lifetime of the aerothermodynamic and electrical surfaces of the disk generator interior could not be made compatible with a 30-year plant design life and a 65 percent capacity factor.

Figure 3-2-1 displays a simplified block diagram of the Disk MHD Generator Study logic.

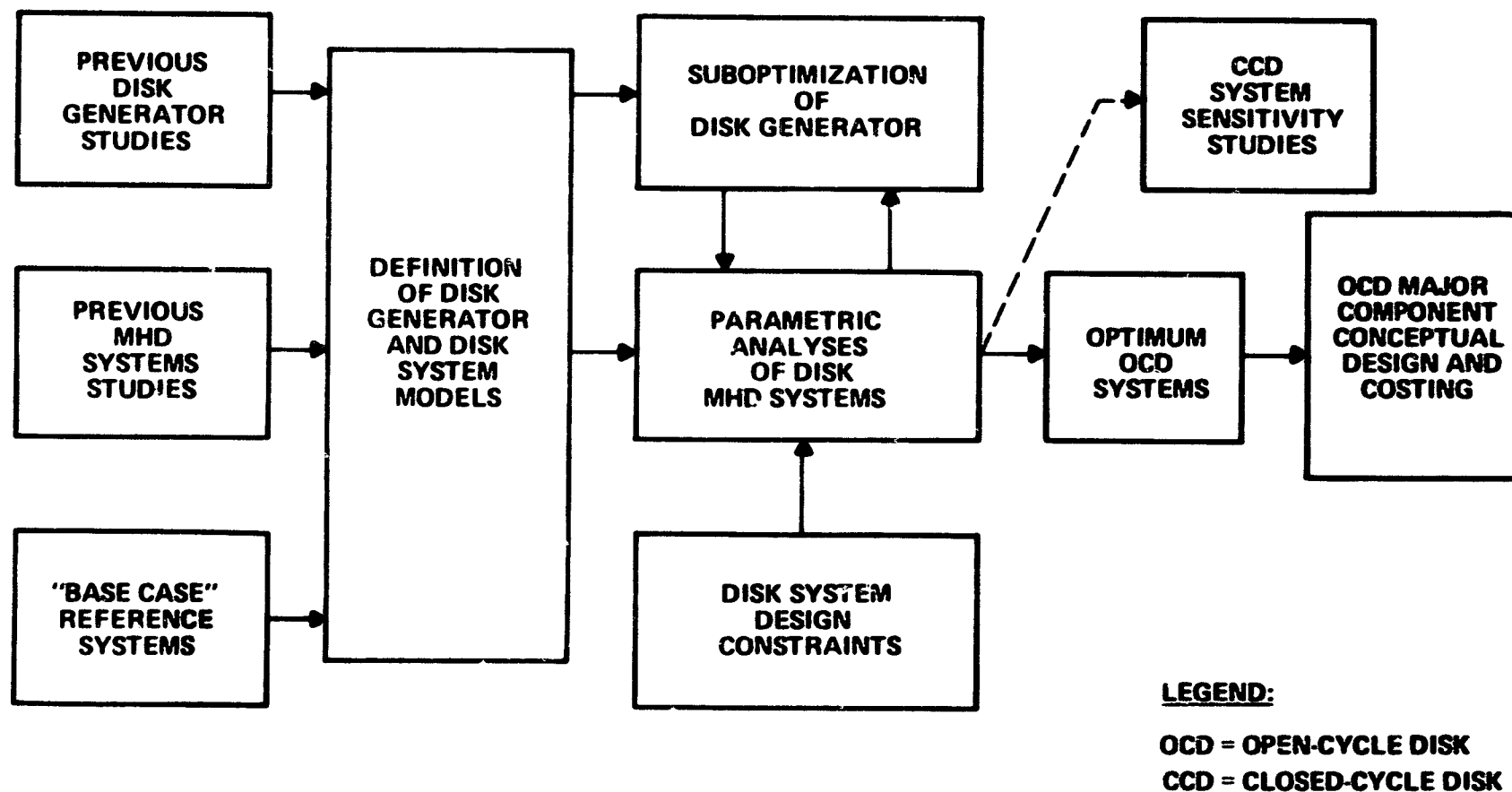


Figure 3-2-1. Disk MHD Generator Study Simplified Logic Diagram

4.0 DISK MHD SYSTEM DESIGN BASIS

4.1 DISK SYSTEM CONFIGURATIONS

Three open cycle disk (OCD) MHD systems and two closed cycle disk (CCD) MHD systems were to be considered in the study. These included:

1. OCD with directly-fired high temperature air heaters (HTAH), where the regenerative HTAH is assumed to be fired directly with hot combustion gases exhausting from the MHD power train;
2. OCD with separately-fired high temperature air heaters, where the HTAH is fired by a clean fuel gas produced in an on-site coal gasification plant;
3. OCD with metallic air heater and oxygen augmentation of combustor oxidant, where the desired high combustion temperature is attained by enriching the combustion air with oxygen produced in an on-site air separation plant;
4. CCD with noble gas regenerators fired directly from a coal-burning combustor with high slag rejection;
5. CCD with noble gas regenerators fired by a clean fuel gas produced in an on-site coal gasification plant.

The basic configuration of each of the five disk MHD systems is shown in Figures 4-1-1 through 4-1-5. As described in Section 3.2.1, the investigation of CCD systems was amended, and the performance studies for the closed cycle systems were restricted to the directly-fired atmospheric combustion case.

4.1.1 OCD SYSTEM DESCRIPTIONS

As is the case in a linear MHD system, the directly-fired OCD system offers the potential for the highest plant thermal efficiency among the three systems to be considered, since maximum utilization is made of the coal thermal energy in MHD power extraction. Preheating of the combustion air with slag- and seed-laden gases to the requisite temperatures (up to 1920 K) in a directly-fired HTAH represents a significant extrapolation from current blast furnace stove

technology. A substantial advance in HTAH technology will therefore be required for successful development of the directly-fired MHD system. The separately-fired HTAH system provides relatively clean combustion gases which mitigate potential materials corrosion problems, but only at the expense of efficiency penalties. Similarly, the oxygen augmentation system obviates the necessity to provide an HTAH system altogether, but with accompanying plant economic and performance trade-offs. Thus, while the latter two systems represent the more likely candidates for early MHD plants, a mature MHD plant will most probably incorporate a directly-fired HTAH system to achieve the maximum obtainable plant efficiency.

OCD Directly-Fired System

A schematic diagram for a representative system of this type is given in Figure 4-1-1.

Pulverized coal is burned with preheated air in a cyclone combustor. The resulting combustion gases are mixed with a small amount of seed to enhance their bulk conductivity, and accelerated through a nozzle to a high Mach number. Upon leaving the nozzle, these conductive gases pass through the magnetized region of the generator. With the magnetic field aligned perpendicular to the direction of flow of the gases, dc power is generated and extracted by placing electrode surfaces in contact with the gas. The combustion gas and seed mixture then passes through a diffuser where it is further decelerated and diffused to a pressure slightly above ambient pressure, to prepare it for use in the downstream heat recovery components.

Gases leaving the diffuser pass in sequence through a radiant furnace, a set of high temperature air heaters, a reheater, superheater, and high temperature economizer. At the exit of the high temperature economizer, an electrostatic precipitator is provided to remove seed and flyash from the gas stream.

Induced draft fans are provided to maintain a balanced draft in the gas system downstream of the diffuser. Some of the gases leaving the precipitator are utilized to dry the coal for the combustor, and the remainder of the gas stream

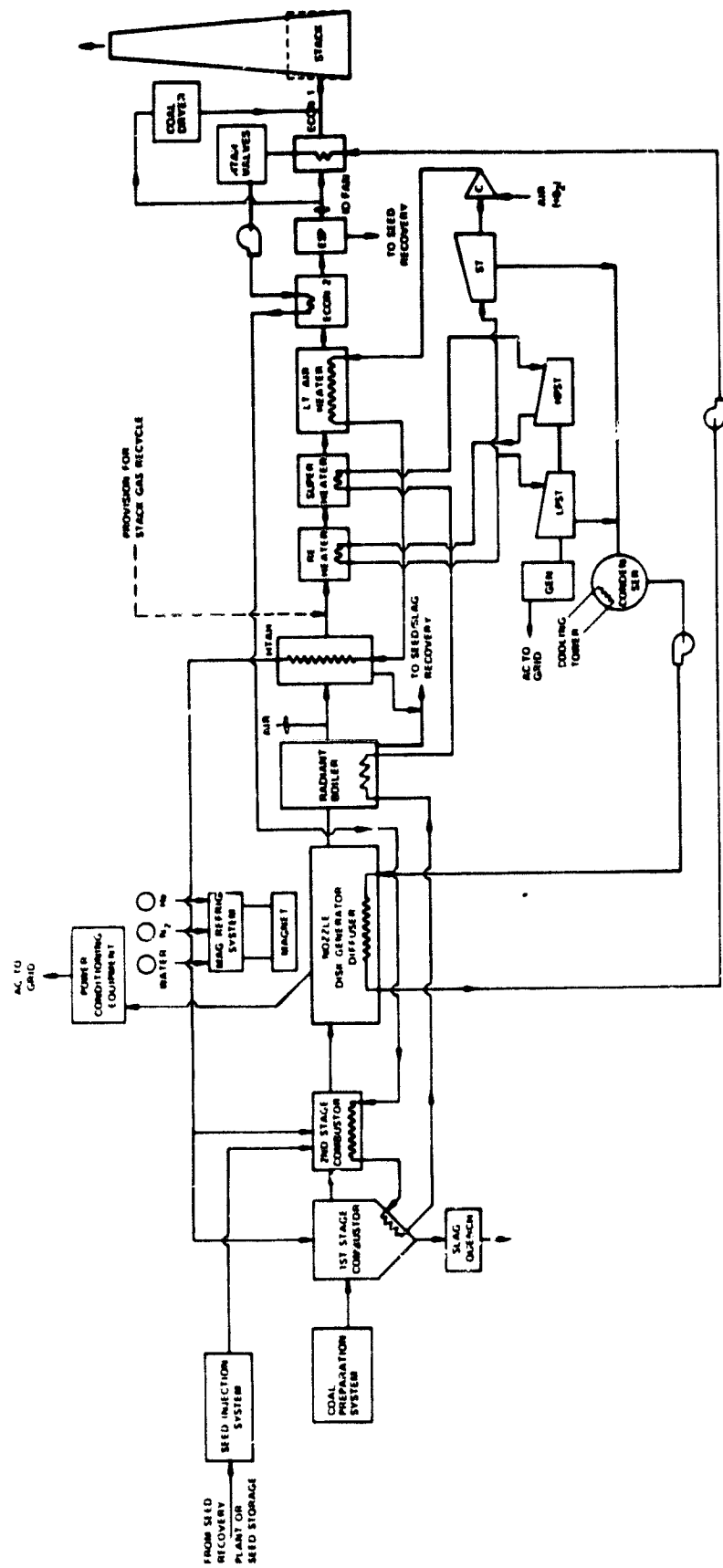


FIGURE 4-1

Figure 4-1-1. Direct Fired Open Cycle Disk Generator System Flow Diagram

is cooled further through a low temperature economizer to the specified stack temperature before being exhausted to the atmosphere.

To minimize NO_x formation in the combustion process, the coal combustor is operated under fuel-rich conditions. Complete combustion is attained by injecting secondary air into the gas stream at a location just upstream of the high temperature air heater system.

The MHD components (combustor, nozzle, disk generator, and diffuser) may be cooled either by an isolated low temperature, low pressure loop, or by a loop which connects directly with the steam bottoming plant cycle.

As previously stated, waste heat in the gases exhausted from the MHD power train components is utilized to generate steam in the bottoming plant. Condensate from the steam plant condenser picks up heat from the MHD component cooling system, passes through the low temperature economizer, HTAH valve cooling system, high temperature economizer, radiant boiler and superheater before entering the high pressure turbine steam chest. After leaving the high pressure turbine, the steam is reheated by combustion gases in the reheater and is directed to the low pressure turbines, one for MHD cycle compressor drive and another for electrical power generation. High-pressure feedwater pumps are also driven by bottoming plant steam. All turbines exhaust to the main condenser.

The dc power extracted from the disk generator is converted to ac power suitable for supply to the local grid by conditioning through a series of inverter bridges, filter systems and transformers. The ac power generated by the steam bottoming plant power turbines is also supplied to the grid through a power transformer. Plant auxiliary loads are provided by plant startup and auxiliary transformers which can take power from the grid (with the plant shut down) or directly from the plant output busses (during plant operation).

OCD Separately-Fired System

The separately-fired disk generator system is shown schematically in Figure 4-1-2. The main gas flow train is similar to that provided for the OCD directly-fired system, with the exception that the HTAH is removed from the MHD exhaust train. The separate HTAH is fired with a clean fuel gas produced in an integrated coal gasification plant. Heated air is directed to the combustor supplying the main MHD gas flow stream from the HTAH. An intermediate air preheat level is still obtained by first passing the air leaving the MHD cycle compressor through a metallic air preheater which is in the direct gas flow stream from the MHD power train. The gasifier design selected for modeling was the Westinghouse pressurized type with hot gas cleanup capability. Low-BTU gas from the gasifier is cleaned to remove sulfur and particulates and then burned with preheated air in a separate combustor. The resultant combustion gases then enter the regenerative HTAH for MHD cycle air preheating.

The gasifier operating pressure is selected to provide a balance between cycle air and reheat gas pressure, in order to minimize losses from gas leakage between systems and to eliminate the cyclic pressurization and depressurization of the HTAH vessels which would otherwise be required.

The pressure of the reheat gas leaving the HTAH system is recovered by expanding the combustion products through a compressor drive gas turbine and a generator drive gas turbine. Gas exhausting from these turbines is mixed with the MHD cycle exhaust gas, then passes subsequently through the low temperature economizer of the steam bottoming plant before exhausting to the stack.

The compressor drive turbine driven by the HTAH reheat exhaust gas powers an air compressor which provides air for the gasifier and HTAH burner. That portion of the air required for HTAH combustion is preheated in a metallic heat exchanger located directly in the MHD hot gas exhaust train.

The steam bottoming plant and MHD component cooling water systems for the separately-fired OCD plant are configured identically to those provided for the directly-fired OCD plant.

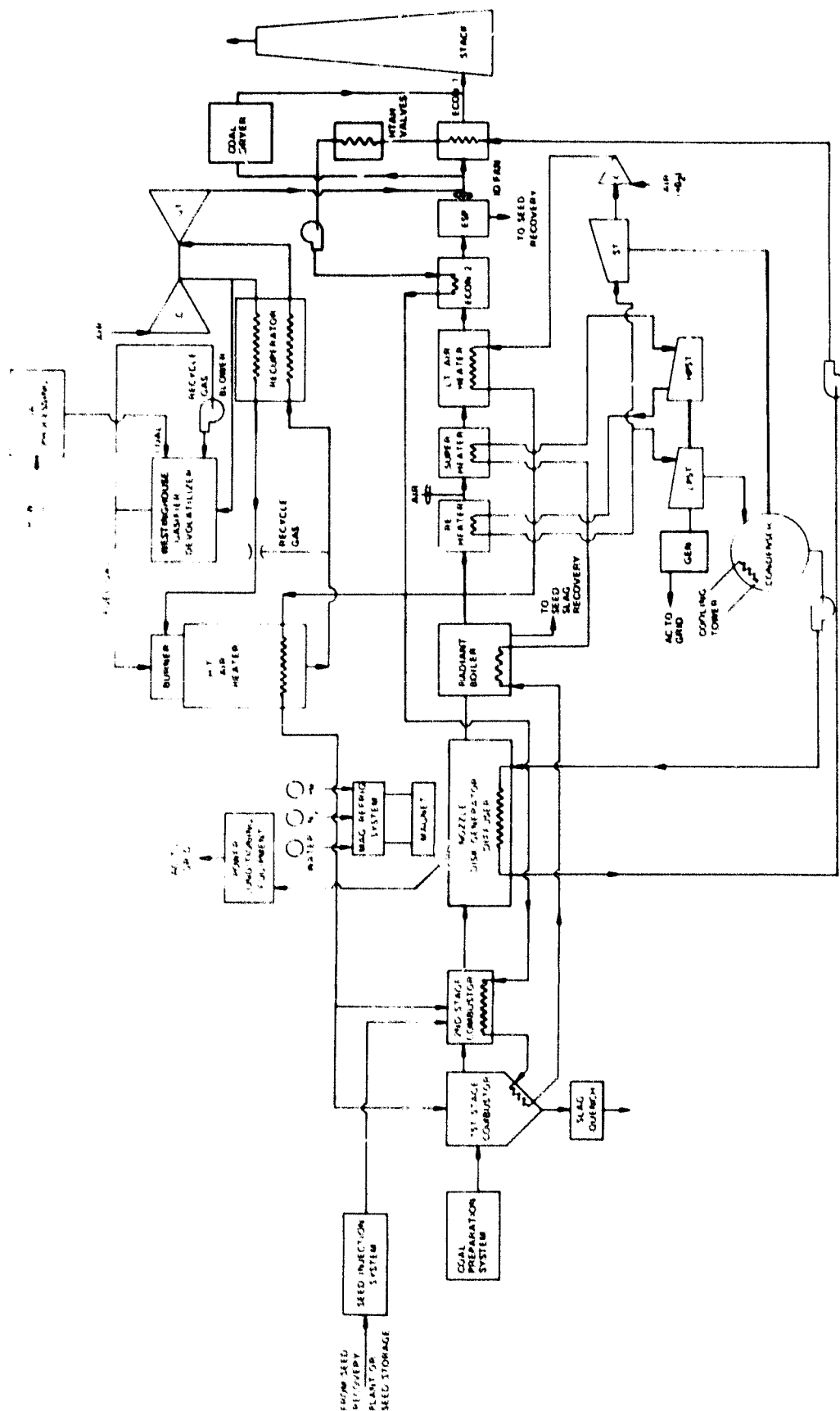


Figure 4-1-2. Indirect Fired Open Cycle Disk Generator System Flow Diagram

OCD with Metallic Air Heater and Oxygen Augmentation

In this configuration the HTAH is deleted from the system altogether. The oxidizer supplied to the MHD combustor is preheated in a metallic recuperative heat exchanger only. The enrichment level of the oxidant is adjusted to provide the desired combustor temperature. The gas flow train is otherwise similar to that for the OCD directly-fired system, as illustrated in Figure 4-1-3.

Oxygen required for augmentation of the normal oxygen level in air is produced by an on-site separation plant. This plant is shown in a simplified integration scheme, with the oxygen plant pre-compressor placed on the same shaft as the turbine-driven MHD cycle air compressor. The steam turbine drive for the dual compressor arrangement must be sized accordingly. The steam bottoming plant is identical in overall specification to that for the OCD directly-fired case.

4.1.2 CCD SYSTEM DESCRIPTIONS

Two potential system configurations for the CCD systems were originally proposed as subjects for detailed parametric studies; however, as noted in Section 3.2.1, NASA agreed to the substitution of CCD studies which were confined to systems in which the noble gas regenerators were reheated with combustion gas from an atmospheric coal combustor.

Figures 4-1-4 and 4-1-5 are provided in order to delineate, at the first level of detail, the major differences between the gasifier-fired CCD system and that which has a regenerator reheated directly with coal combustor combustion products.

CCD - Regenerator Fired Directly by Coal Combustor

As illustrated in Figure 4-1-4, the basic combustion subsystem for the coal combustor-fired regenerator CCD system uses both a combustion air preheater and intermediate temperature air heater (ITAH) to preheat the combustor oxidant. Pulverized coal is supplied to the unpressurized combustor. The combustion products are then used to regeneratively reheat the ceramic checker beds of the

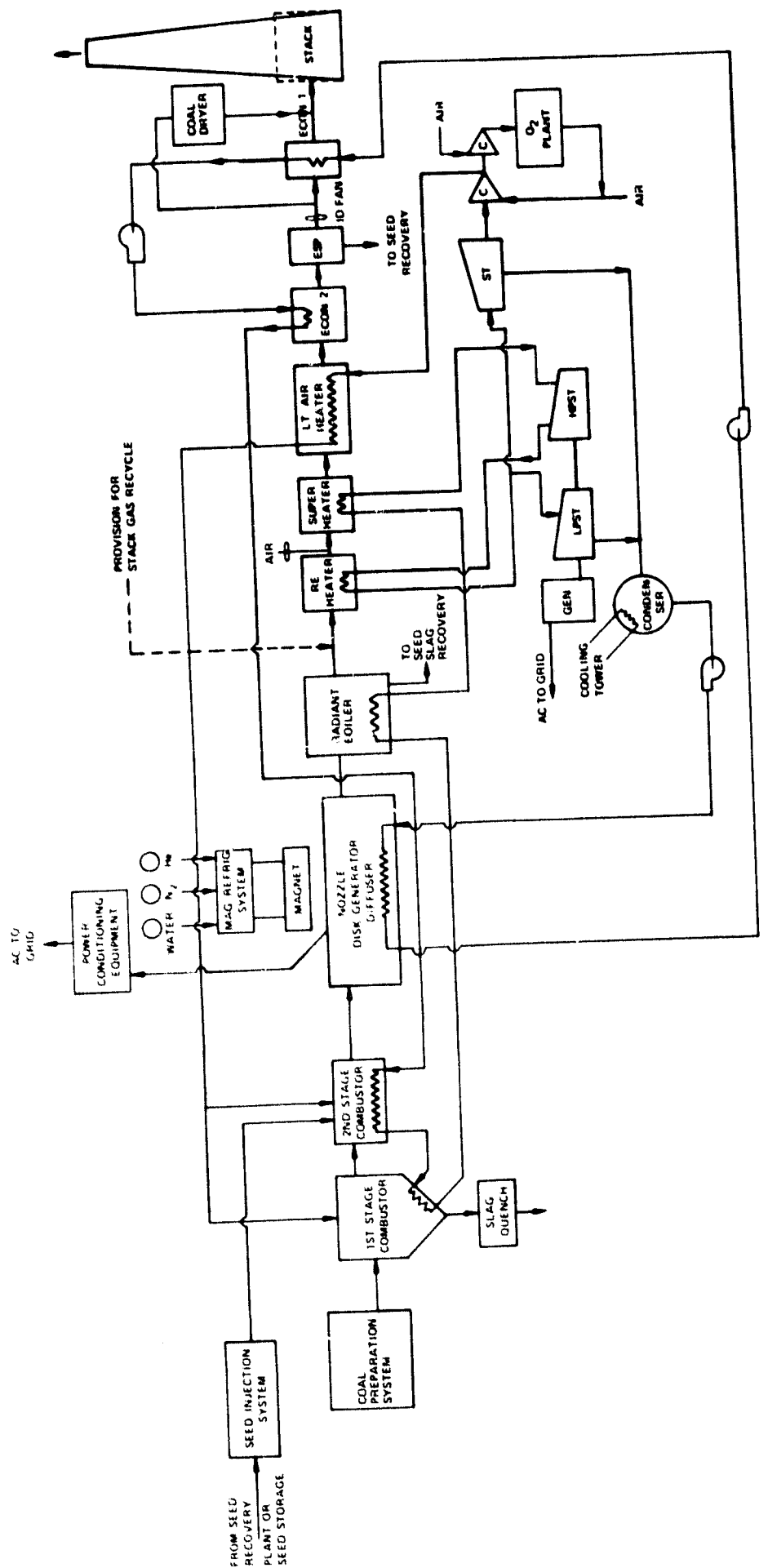
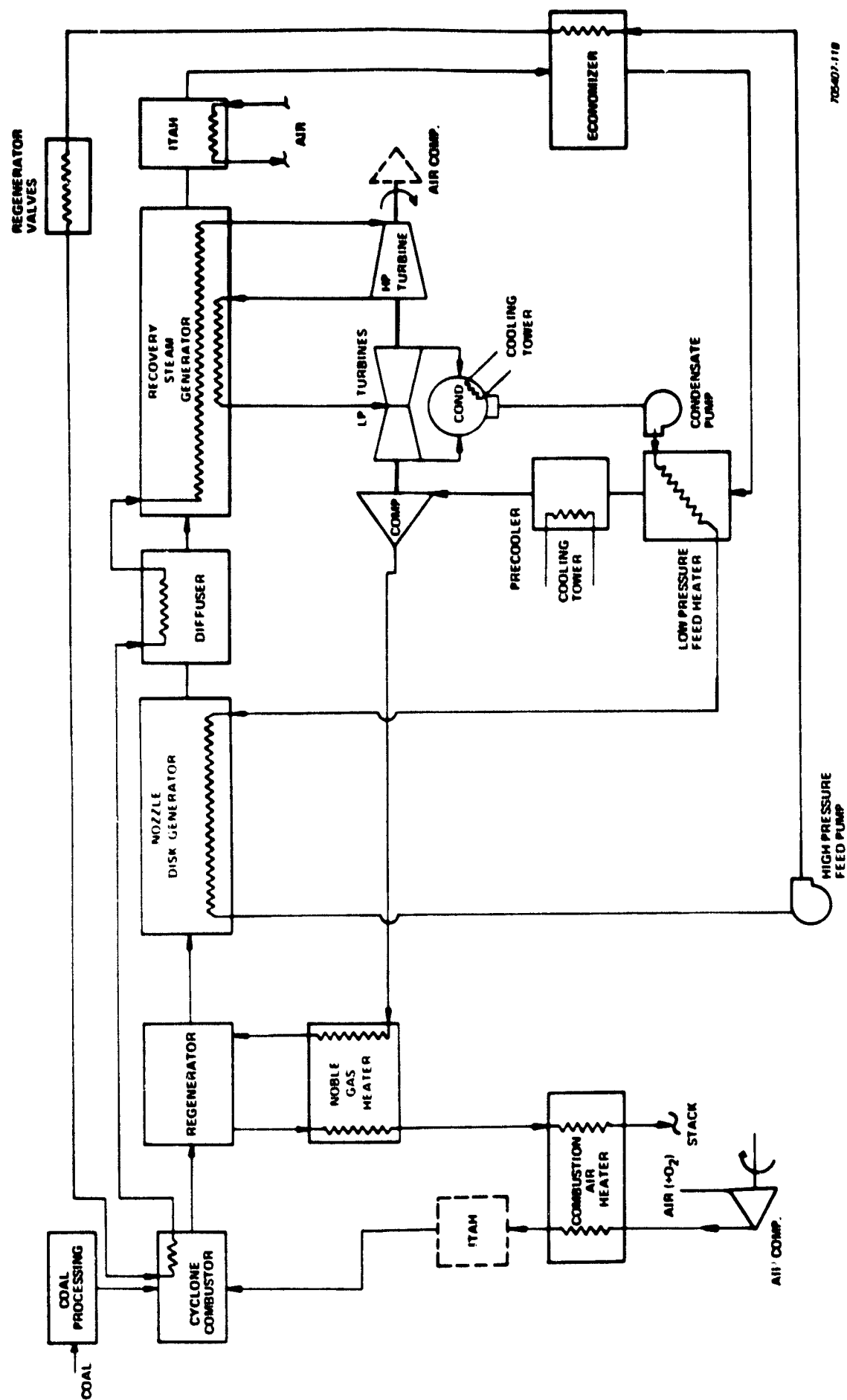


Figure 4-1-3. Open Cycle Disk Generator System Flow Diagram Integrated Oxygen Plant and Metallic Air Preheater



705407-118

Figure 4-1-4. Closed Cycle Disk Generator System Flow Diagram
(Regenerator Directly Fired by Coal Combustor)

Figure 4-1-5. Closed Cycle Disk Generator System Flow Diagram
(Gasifier-Fired Noble Gas Regenerator)

noble gas regenerator. Cooled reheat gas then is directed through a recuperative metal heat exchanger (the combustion air preheater) which provides a portion of the required preheating for the combustion air. The exhaust gases must then be treated to remove sulfur dioxide and the remaining particulates, prior to release through the plant stack. For SO_2 removal, a lime scrubber has been assumed to be required.

The MHD cycle is based upon the use of a cesium-seeded noble gas (argon) to provide the conductive working fluid for the MHD generator. Low temperature argon is compressed by a compressor driven by bottoming plant steam turbines, and directed through a recuperative metallic heat exchanger to increase its temperature by heat exchange with the reheat combustion gases leaving the regenerators. The argon is then heated to the required stagnation conditions by passing it over the hot ceramic checker beds of the noble gas regenerators. Cesium seed is injected into the hot high pressure argon prior to its acceleration to a high Mach number through a nozzle with guide vanes. After passing through the power extraction region of the disk generator, the seeded argon is then diffused to a pressure and velocity condition suitable for use in the heat recovery steam generator. Further cooling through the intermediate temperature air heater and economizer sections reduces argon temperature to the point where the cesium seed may be fully condensed and removed from the noble gas stream, purified, and returned to the injection point prior to the generator inlet nozzle.

A low pressure feed heater reduces the temperature of the noble gas further, to recover the maximum amount of heat from the argon for use in the bottoming plant. To prevent excessively high compressor discharge temperatures and to minimize the required argon compressor power, the argon may be further cooled to near the ultimate heat sink temperature by passing it through a precooler prior to its return to the cycle compressor inlet.

The bottoming plant steam cycle provides supercritical steam to drive the MHD cycle compressor, combustion air compressor, and high pressure boiler feed pumps. The turbines exhaust to the plant main condenser. Condensate is pumped

through the low pressure feed heater where it performs the final recoverable cooling on the MHD cycle noble gas stream. The condensate is then passed through the MHD component cooling lines (for disk generator and nozzle) if necessary before being taken to high pressure through the steam turbine driven boiler feed pumps. Further regenerative heat recovery occurs in the economizer and the noble gas regenerator valve cooling system, the coal combustor, and the splitter vane and wall of the diffuser before the supercritical fluid enters the recovery steam generator. In the recovery steam generator, the bottoming plant working fluid is raised to the required temperature for admission to the HP turbine. Following reheat in the steam generator section, the steam drives the LP turbines and feed pump turbines as it exhausts to the main condenser again.

The bottoming plant is designed to operate with the MHD topping cycle at the "match point"; that is, the amount of steam generated is just enough to drive the noble gas and air compressors and the feed pump turbines. No turbo-generator is provided. All electrical power is generated as dc output of the MHD channel.

CCD - Gasifier Fired Regenerator

Figure 4-1-5 illustrates the configuration for this type of system. In the coal combustor fired CCD system, the combustor must be designed to provide the highest possible slag rejection, in order to minimize the buildup of ash and slag constituents on the heat exchange surfaces of the regenerator matrices, and in the flow passages provided. The use of an advanced technology gasifier which removes sulfur and all potential particulates or condensed vapors from the combustion gas used for reheat of the noble gas in the regenerator system simplifies system design to some extent. The high pressure gases leaving the regenerators on reheat are utilized to turn a combustion gas turbine which drives the gasifier/burner air compressor. After leaving the turbine, the heated combustion gases are passed through a metallic heat exchanger to provide initial preheat for the MHD cycle argon working fluid, and then are used to preheat the regenerator combustion air before exhausting at the stack conditions. The combustion air is further heated by passing it through an argon/air

metallic heat exchanger (ITAH) before it is introduced into the regenerator burners. Use of high moisture Montana Rosebud coal in the gasifier eliminates the need for an additional steam supply to the unit.

The MHD topping cycle is identical to that described for the coal combustor fired regenerator CCD system. The steam bottoming plant for the gasifier-fired system is similar in design as well. With the pressurized gasifier providing clean fuel gas to the regenerator burners, it is possible to attain higher flame temperatures and potentially higher performance for this system, when compared to the atmospheric coal combustor-fired CCD system. As with the combustor-fired CCD system, all electrical power is generated by the MHD cycle.

4.2 FUEL CHARACTERISTICS

NASA specified that both a high moisture, low sulfur coal (Montana Rosebud) and a high heat value, high sulfur coal (Illinois #6) were to be considered in the Disk MHD Generator Study. The specifications for these two coals are given in Table 4.2.1, and were provided by NASA at the study's inception.

4.3 EMISSIONS STANDARDS AND EMISSIONS CONTROL

In the initial contract work statement for the Disk MHD Generator Study, NASA provided the emissions standards to be used as a basis for evaluation of the performance of disk generator systems. These original standards were the EPA New Source Performance Standards (NSPS) proposed for August 1978 enactment. On June 11, 1979, the EPA issued revised emissions standards for electrical power plants, and these were subsequently identified as being applicable to the Disk MHD Generator Study by NASA.

The revised emissions standards are shown in Table 4.2.2 as they apply specifically to the two coals of interest for the study.

Estimates of Environmental Intrusion

The initial contract documents required that estimates of the environmental intrusion resulting from the operation of proposed power plant designs be prepared for each point in the study.

TABLE 4.2.1

COAL AND ASH ANALYSES OF SELECTED COALS
FOR DISK MHD GENERATOR STUDY

<u>Ash Analysis, %</u>	<u>Illinois #6</u>	<u>Montana (Rosebud)</u>
SiO ₂	41.4 ± 5.4	37.6
Al ₂ O ₃	19.3 ± 6.8	17.3
Fe ₂ O ₃	22.3 ± 6.8	5.1
TiO ₂	0.9	0.7
P ₂ O ₅	0.12	0.4
CaO	5.4 ± 3.3	11.0
MgO	1.7 ± 1.3	4.0
Na ₂ O	0.6 ± 0.2	3.1
K ₂ O	2.1 ± 0.4	0.5
SO ₃	7.5 ± 0.6	17.5
Initial Deformation		
Temp. °F	1960 ± 70	2190 ± 230
Softening Temp °F	2030 ± 70	2230 ± 240
Fluid Temp °F	2260 ± 200	2280 ± 240
<u>Proximate Analysis, Coal as rec'd, %</u>		
Moisture	8.9	22.7
Volatile Matter	38.0	29.4
Fixed Carbon	41.7	39.2
Ash	11.4	8.7
<u>Ultimate Analysis, %</u>		
Hydrogen	5.4	6.0
Carbon	62.4	52.1
Nitrogen	1.2	.79

TABLE 4.2.1 (Continued)

<u>Ultimate Analysis, %</u>	<u>Illinois #6</u>	<u>Montana (Rosebud)</u>
Oxygen	16.3	31.5
Sulfur	3.3	0.85
Heating value, Wet, Btu/lbm	11265	8920
Heating value, Dry, Btu/lbm	12370	11560
Coal Rank	BVCB	Subbit B

TABLE 4.2.2

EMISSIONS STANDARDS FOR DISK GENERATOR STUDY

- I. SO_2 Standard
 - a) Illinois #6 coal: 260 ng/J (0.60 lbm/MBTU) of heat input, which is equivalent to 0.90 removal of sulfur.
 - b) Montana Rosebud Coal: 247 ng/J (0.57 lbm/MBTU) of heat input, which is equivalent to 0.70 removal of sulfur.
- II. NO_x Standard
 - a) Illinois #6 coal:
 - i) Direct firing - 260 ng/J (0.60 lbm/MBTU) heat input.
 - ii) Gasification - 210 ng/J (0.50 lbm/MBTU) heat input.
 - b) Montana Rosebud Coal:
 - i) Direct firing and gasification - 210 ng/J (0.50 lbm/MBTU) heat input.
- III. Particulate Matter Standard
 - a) Emissions: 13 ng/J (.03 lbm/MBTU) heat input.
 - b) Opacity of emissions: 0.20 (6 minute average).

Items to be considered in this area were SO_2 , NO_x , CO, CO_2 , unburned hydrocarbons, particulates, wastes, and thermal pollution.

Since the intent of the Disk MHD Generator Study was to provide estimates of potential disk generator power system performance, and detail differences between disk generator systems and comparable linear generator systems, the modeling of the overall plant was carried out only to the detail necessary to permit such evaluations. It was therefore not possible in general to realistically evaluate the performance of all plant features provided to mitigate or eliminate the release of chemical or thermal pollutants, as noted in the list above.

In most instances, the disk generator MHD systems are no different in performance or in design features to address pollutant removal or reduction from analogous linear MHD systems. For NO_x control, the use of a separate flue gas scrubber with a high preheat level directly-fired disk system seems to be required, at least for the supersonic near-impulse mode of operation selected as the optimum mode for combustion gas disk systems. A lower preheat level will permit NO_x reduction through use of radiant furnace residence time control in the OCD directly-fired units, although at a performance penalty with respect to similar preheat level linear MHD systems. Performance and design details for these OCD directly-fired disk systems, and the delineation of features required for NO_x control in them, are discussed further in Sections 5.0 and 6.0.

4.4 PLANT PERFORMANCE AND HEAT SINK DESIGN CONDITIONS

For performance evaluation and cooling tower design calculations the following ultimate heat sink design conditions were specified.

Heat Rejection System

All configurations used mechanical draft wet cooling towers, sized for the 5 percent summer environmental conditions. These included:

- Air temperature (wet bulb) - 77°F
- Relative humidity - 60 percent
- Ambient pressure - 1 atmosphere

The plant performance calculations were based on "average day" conditions of 59°F.

5.0 OPEN CYCLE DISK SYSTEMS STUDIES

5.1 OPEN CYCLE DISK GENERATOR MODELING

5.1.1 DISK CHANNEL

A disk channel is axially symmetric, with the magnetic field aligned parallel to the axis of symmetry, as in Figure 5-1-1. The usual analysis, equivalent to the quasi-one-dimensional treatment of linear generator channels, treats all variables as functions of radial position only, so that the velocity vector has components u_r and u_θ , with the swirl parameter defined as $S = u_\theta/u_r$. The load current flows in the r direction, while the equivalent Faraday current, j_θ , flows in closed loops and thus does not interact with any solid surfaces. In the case of an outward-flow channel, the anode is close to the axis of symmetry and the cathode is at the exit radius. If the swirl parameter is initially zero the $\underline{j} \times \underline{B}$ body force tends to induce a u_θ component; the published disk analyses have shown that there are substantial advantages to be gained from introducing inlet swirl in the direction opposing the induced swirl. The $u_\theta \times B$ induced field supplements the radial current produced by the Hall effect, and the net result is an increase in efficiency and performance. From conservation of angular momentum, the magnitude of the swirl will decrease as the gas flows outward; for this reason consideration has also been given to radial-inflow channels, in which conservation of angular momentum helps to maintain a u_θ component in the desired direction.

The fluid-dynamical behavior of the channel is governed by the usual conservation equations relating the velocity components with the gas pressure, density and enthalpy (p , ρ and h , respectively). Friction and heat loss effects from interaction with the channel walls are included in the governing equations, along with the electrodynamic effects on momentum (due to body forces) and on energy conservation (due to electrical power extraction).

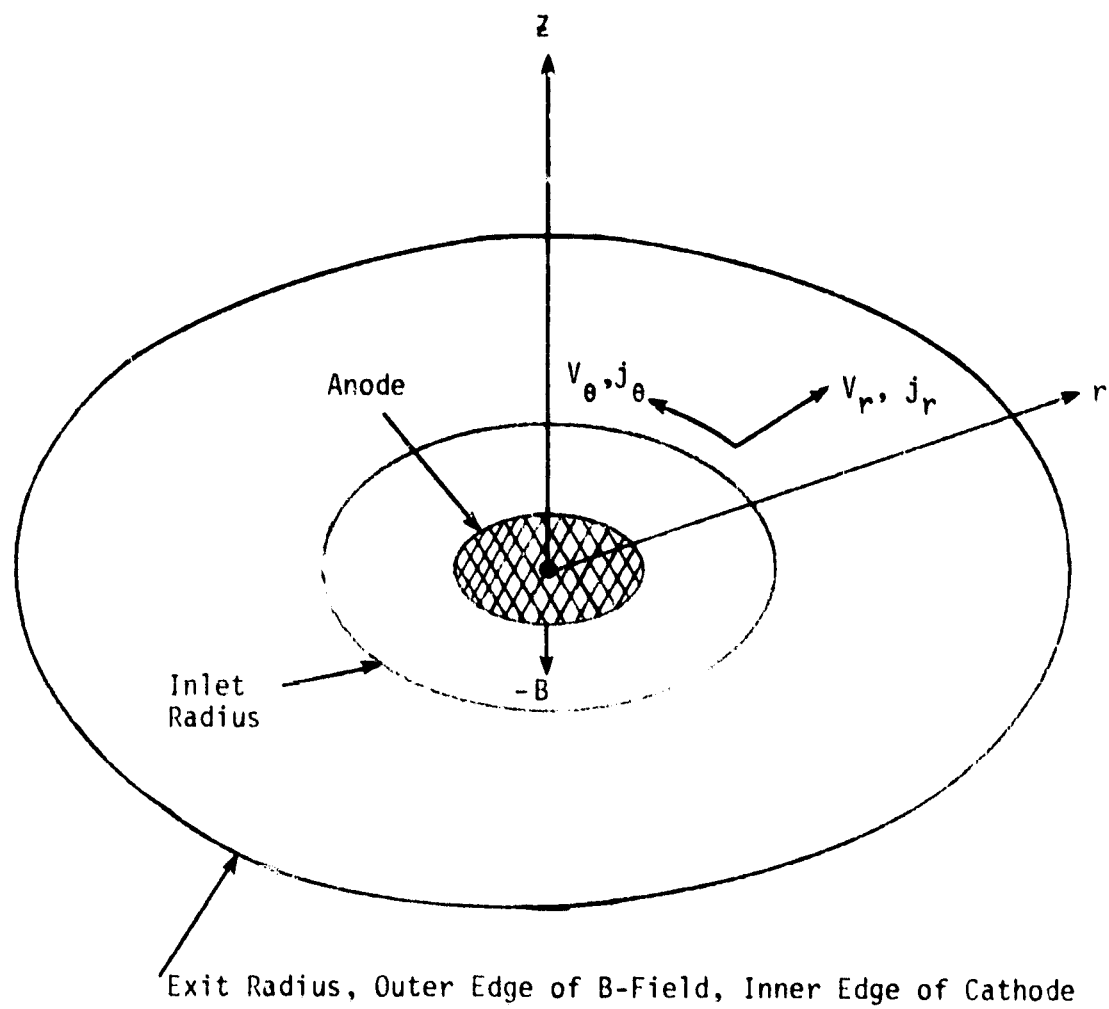


Figure 5-1-1. Disk Generator Geometry

Conservation of radial momentum, angular momentum and total energy, respectively, can then be expressed as follows:

$$\rho u_r \frac{du_r}{dr} + \frac{dp}{dr} = \frac{\rho u_\theta^2}{r} + j_\theta B - \frac{u u_r f}{z} \quad (1)$$

$$\rho u_r \frac{du_\theta}{dr} = - \frac{u_r u_\theta}{r} - j_r B - \frac{\rho u u_\theta f}{z} \quad (2)$$

$$\rho u_r \frac{d}{dr} \left(h + \frac{u_r^2 + u_\theta^2}{2} \right) = j_r E + \frac{2}{z} \dot{Q} \quad (3)$$

where the friction coefficient, f , is given in terms of the flow Reynolds number by

$$f = 0.0576 [\text{Re}]^{-0.2},$$

and the wall heat transfer is written in terms of the Stanton number and adiabatic wall enthalpy as

$$\dot{Q} = \rho u [\text{St}](h_{aw} - h_w)$$

with $[\text{St}] = 0.0295 [\text{Re}]^{-0.2} [\text{Pr}]^{-0.4}$

The channel height, z , enters the above equations through the averaging of wall effects occurring for $r_0 \leq r \leq r_0 + \Delta r$ over the entire fluid volume $2\pi r_0 \Delta r$. Channel height also appears in the equations for conservation of mass and radial current:

$$\dot{m} = 2\pi r z \rho u_r \quad (4)$$

and

$$I_{\text{load}} = 2\pi r z j_r \quad (5)$$

Since the circular symmetry ensures that the only component of electric field is radial (in the quasi-one-dimensional approximation), the remaining description of the electrical behavior is derivable by expressing Ohm's law in the form

$$j_r = [E + u_\theta B + \beta u_r B] \sigma / (1 + \beta^2)$$

and

$$j_\theta = [\beta(E + u_\theta B) - u_r B] \sigma / (1 + \beta^2),$$

where β is the effective Hall coefficient ($\beta = \mu B$ for a uniform plasma in which μ is the electron mobility); and σ is the electrical conductivity.

Hence the local short-circuit current density is given by

$$j_{rsc} = \sigma(\beta + S) u_r B / (1 + \beta^2)$$

Using a current load factor, K , in the form $K = j_r / j_{rsc}$, the radial electric field and azimuthal current density become

$$E = -(1 - K)(\beta + S) u_r B$$

and

$$j_\theta = \beta j_r - \sigma u_r B.$$

Local power density, $-\underline{j} \cdot \underline{E}$, or $-j_r E$, has the value

$\sigma u_r^2 B^2 K(1 - K)(\beta + S)^2 / (1 + \beta^2)$, which attains maximum when $K = 0.5$. However, the local electrical efficiency takes the form

$$\eta_L = \frac{j_r E}{\underline{u} \cdot (\underline{j} \times \underline{B})} = \frac{(\beta + S)^2 K(1 - K)}{(1 + \beta^2) - (\beta^2 - S^2)K}$$

Using the notation $S_1^2 = 1 + S^2$ and $\beta_1^2 = 1 + \beta^2$, it is readily established that η_L is maximized when

$$K = K_{opt} = \beta_1 / (\beta_1 + S_1)$$

with

$$\eta_L (\max) = [(\beta + S) / (\beta_1 + S_1)]^2$$

The importance of swirl in the disk configuration can best be illustrated by consideration of the variation of this optimum local electrical efficiency as a function of β and S , as plotted in Figure 5-1-2. Optimal values of K are indicated on the plot. It is clearly seen that high values of η_L for zero swirl require very high values of β , whereas the addition of swirl permits attainment of adequate η_L at more moderate values of β .

When the electrical loading is not at this optimum value, it can be shown that

$$\frac{\eta_L}{\eta_L (\max)} = \frac{K (1 - K)}{K (1 - K) + (K - K_{opt})^2},$$

an expression which is independent of both β and S .

Thus a successful disk generator design is the result of compromise between maximizing the power density ($K = 0.5$) and attaining high electrical efficiency ($K \rightarrow K_{opt}$). The size of the resultant generator is governed by the rate of conversion of enthalpy to usable electric power, usually referred to as the enthalpy extraction rate, and given from Equation (3) by

$$\frac{dh_o}{dr} = \frac{j_r E}{\rho u_r} = \frac{K(1 - K)(S + \beta)^2 \sigma u_r B^2}{\rho (1 + \beta^2)}$$

Total enthalpy extraction is defined as the integrated extraction over the complete radius of the disk as a percentage of the inlet enthalpy.

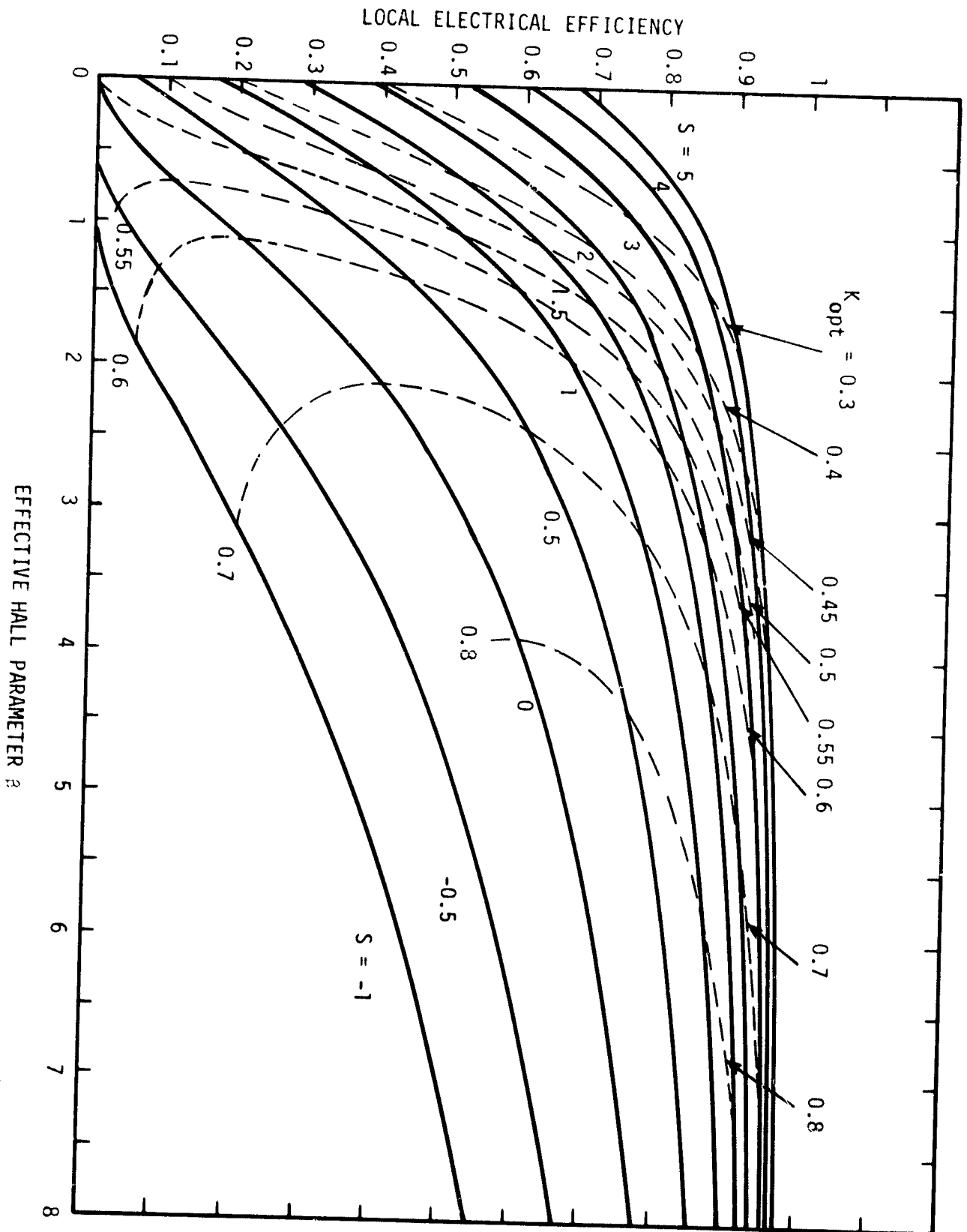


Figure 5-1-2. Optimized Local Electrical Efficiency for Disk Generator with Swirl

Since the disk must be configured to yield an adequate total enthalpy extraction (at least 16% and preferably closer to 20%) and since the diameter of the magnet is a major parameter in the overall system cost, the paramount consideration in the design becomes extraction of enthalpy in as short a radial distance as feasible.

In terms of a target level of enthalpy to the "extracted", Δh_o , an extraction length can be defined by writing

$$\frac{dh_o}{dr} = - \frac{\Delta h_o}{L_{ex}}.$$

$$\text{Then } L_{ex}(K) = \frac{\rho \Delta h_o}{\sigma u_r B^2} \frac{(1 + \beta^2)}{K(1 - K)(S + \beta)^2}$$

$$\text{and } L_{ex}(K_{opt}) = \frac{\rho \Delta h_o}{\sigma u B^2} \frac{\beta_1}{\eta_L(\max)}$$

It should be stressed that the value of Δh_o is entirely arbitrary, with L_{ex} scaling linearly with variation in Δh_o . L_{ex} also clearly scales inversely with conductivity, σ . The extraction length is merely a convenient parameter for use in scaling and in assessment of choice of operating conditions for an MHD generator. It will be discussed further in connection with both OCD and CCD applications. One comment on the functional behavior of $L_{ex}(K)$ should be made at this time. Treating the above expression as a function of S , it may be deduced that L_{ex} is reduced by increasing S only as long as $\beta < 2.8$; for larger values of β (obtainable in the open cycle case) the extraction length is optimized at fairly low values of S , and increases slightly with increasing S .

The equations discussed above form a closed set which can be used for the evaluation of the fluid and electrical properties within a specified channel,

as long as the state of the plasma can be specified. For the coal combustion products plasma encountered in OCD applications it is expected that the electron temperature will not be significantly elevated above the heavy particle temperature, and that the various chemical species present will be in chemical equilibrium (exceptions to the latter condition are discussed in a later section). Thus all plasma properties can be expressed as functions of two variables only, for example, either pressure and temperature, or preferably pressure and enthalpy. With ρ , σ and β all given as functions of p , and h , and with z given as a function of r , then Equations (1) through (4) are sufficient to define the four dependent variables p , h , u_r and u_θ at every point within the channel. The electrical variables are directly calculable from the remaining equations. This type of channel evaluation is carried out by means of a "performance mode" code. Such evaluation should lead to a numerical description of the overall electrical characteristics of the channel (V-I curves, or load-lines), and this aspect receives further treatment below.

In contrast to the above, however, is the "design mode", wherein plasma entrance conditions and initial electrical loading are selected, and then $z(r)$, the channel height, is treated as a dependent variable. This means that an additional equation, usually derived by imposing a "design constraint", is necessary. For example, it is possible to specify that the channel be designed to operate in the impulse mode (constant static energy), reaction mode (large change in static enthalpy, constant kinetic energy), or some intermediate mixed-mode. Constraint selection is more fully discussed in 5.3.1 below.

5.1.2 INLET GUIDE VANES

One final aspect of the numerical modeling of the channel requires introduction at this point. In the suboptimization of the disk channel it is necessary to evaluate the effect of variation on inlet swirl ratio. As discussed above, S values can increase the electrical efficiency of the channel, but high swirl cannot be attained without penalty. Although low values of S might be developed within a combustor (using the swirl to enhance the efficiency of combustion), it is clear that larger swirl must be produced with the

aid of inlet guide vanes (IGVs). Losses due to such IGVs have been rather simplistically modeled by means of the expressions

$$\Delta P_o/P_o = L_{p1} + L_{p2}(S - 0.5)$$

and

$$\Delta h_o/h_{flux} = L_{h1} + L_{h2}(S - 0.5) \text{ whenever } S > 0.5.$$

L_{p1} and L_{h1} are the fractional losses attributable to the specific combustor, independent of any need for IGVs. L_{p2} , in the range 0.025 - 0.04, represents a total pressure loss taken from gas turbine technological data on cascades of turning vanes, while L_{h2} represents the heat lost from the plasma because of the IGVs. Typical values for L_{h2} range from 0.005 for ceramic vanes to 0.01 for watercooled blades. The above expressions imply a ramp-like increase in penalties with increasing swirl, whereas a step increase would be incurred at whatever S value dictates the need for IGVs. However, the model permits a qualitatively satisfactory assessment of the advantages/disadvantages of increased swirl. Using the higher values of the coefficients L_{p2} and L_{h2} , the increased penalties are $0.04P_o$ and $0.01 h_{flux}$ when $S = 1.5$. High swirl cascades for turbines typically yield losses of four percent of the exit dynamic pressure, or three percent of the total pressure for $M = 1.8$. The heat loss in a typical case translate to ~ 30 MW, comparable to the wall losses in the rest of the generator, but consistent with what would be calculated for a set of cooled IGVs.

5.1.3 COMBUSTOR AND NOZZLE

For consistency in the overall systems calculations, estimates were made of heat and total pressure losses, combustion efficiencies, and slag carryover rates believed to be representative of broad classes of combustor/nozzle configuration (see Table 5.1.1). Refined and updated versions of these estimates are used for the definition of particular conceptual designs. The classes considered were:

- i) single-stage cyclone;
- ii) two-stage cyclone;
- iii) two-stage high exit-swirl cyclone.

TABLE 5.1.1. COMBUSTOR LOSSES FOR DISK GENERATORS

Variations	Radial Outflow	Radial Inflow
(i) Single Stage	$\Delta h/H_i = .04$.15
Discrete (4 combustors	$\Delta P_o/P_{oi} = .06$.07
for radial inflow)	$\eta_c = .98$.98
	$\Delta S/S_i = .10 - .20$.10 - .20**
(ii) Two Stage Discrete	.07	.23
(4 combustors for	.08	.09
radial inflow)	.99	.99
	.10	.10
Two Stage Hybrid	NA	.21
(1 first-stage,	NA	.10
4 second stage for	NA	.99
radial inflow)	NA	.10
(iii) Two Stage,	.06	NA
High Exit	.12	NA
Swirl	.99	NA
	.10	NA

Δh = Enthalpy rejected to coolant by combustor(s), ducting and nozzle(s).

H_i = Enthalpy at combustor inlet (chemical, and sensible enthalpy of oxidizer).

ΔP_o = Total pressure lost to friction between secondary oxidizer inlet to combustion system and MHD generator entry station.

η_c = Combustion Efficiency.

ΔS = Slag carryover into MHD channel, total of all phases.

**Approximate formula for slag carryover in single-stage combustors:

$$\frac{\Delta S}{S_i} = 0.1 + 0.2 \left(\frac{T_o}{1000} - 2.5 \right), \quad [T_o > 2500 \text{ K}]$$

These combustors were considered for application to radial inflow and radial outflow generators. Classes (i) and (ii) apply to either type, but (iii) applies only to the outflow type .

For radial inflow generators, the combustor/nozzle system is charged with losses arising in any ducting or plenums required. These tend to provide a very large increase in plasma-wetted area over that encountered in radial outflow configurations. The simplest concept is to use several tangentially-firing single or two-stage combustors discharging into a toroidal plenum/nozzle. Four units is probably a practical minimum, from the point of view of azimuthal uniformity of the generator inlet flow field. Since each combustor must have the same residence time as a single combustor for the entire mass flow, the total wall area will scale as the number of combustors to the $(1/3)$ power. Thus, four combustors have 1.6 times the wall area of a single combustor, for example. To this area one must add the wall area of the plenum/nozzle. Further discussion of the relative heat losses of inflow and outflow configurations may be found in Appendix A.

Another possible configuration would be a "hybrid" having a single first stage and ducting to several tangentially-firing second stages. This is estimated to have marginally lower heat losses, but higher pressure losses than the multiple discrete combustor configurations.

The combustion efficiency estimates are consistent with reported values for first-stage or single-stage residence times on the order of 50 ms, being marginally higher for two-stage combustors.

The fractional slag carryover clearly depends on the plasma final temperature and the details of the combustion process, especially for single stage combustors. The simple relation chosen for the systems calculations is consistent with the most optimistic of the scanty data in the literature, both experimental [1] and theoretical.

5.1.4 DIFFUSER

The attainable pressure rise in a radial diffuser operating at the exit of a swirling radial outflow MHD generator can be estimated only by analogy with the vaneless diffusers of centrifugal compressors. There are no usable experimental data, and there has been no usable reported theoretical treatment of this exceedingly complex flow. For use in systems calculations, a value of C_p in the range 0.45 - 0.60 seems appropriate for all subsonic-entry cases, with C_p defined as the increase in static pressure normalized by inlet kinetic head.

In the case of supersonic entry, there will be a shock system of some sort near the diffuser entrance or in the outer part of the channel. The integrated total pressure loss across this system can be adequately modeled as being equal to that due to a normal shock at the generator exit Mach number. Downstream of the shock system, a further static pressure rise consistent with a subsonic C_p value may be assumed for systems calculations.

In the case of the radial inflow generator, a diffuser having a $C_p \sim 0.5$ is also consistent with the values experimentally obtained for the analogous radial inflow turbines.

In the generator suboptimization work reported in Section 5.3 the diffuser constraint has been applied by requiring a diffuser exit total pressure of 1.068 atm, with C_p values specified (variously) as 0.45, 0.55 and 0.60.

5.1.5 IMPLICIT SIMPLIFICATIONS

The mathematical model of the disk generator flow behavior described in the preceding sections is clearly a vast simplification of the flow in a true three-dimensional channel with curvilinear boundary layers and with magnetic field vectors which are not everywhere perpendicular to the flow direction. The detailed design procedure for a disk channel would certainly not be handled by means of a quasi-one-dimensional code; it would be more appropriate to follow the type of procedure currently used for linear channel design, where an

inviscid core flow is coupled to the boundary-layer flows developing on the channel walls. In the disk case these boundary layers are confined to the insulating walls, so that they are less complex than those on the electrode walls of a linear channel. However, the disk boundary layers are analogous to those on a swept-wing, with different momentum-thickness laws being applied in the radial and azimuthal directions. The detailed solution to such a flow situation, with its attendant electrodynamics complications, presents an interesting problem which is considerably beyond the scope of the present study contract. Fortunately, one may reach the conclusion that the quasi-one-dimensional approach is more valid for the disk geometry than it is for a linear channel, since the effective "aspect ratio" for a typical disk channel is such that there will be very little "inviscid core" region unaffected by the side-wall boundary layers. Thus the "volume-averaging" technique implicit in Equations (1) - (3), Section 5.1.1, is acceptable for the disk systems study, however the friction factor and heat transfer are approximations.

The potential complications arising from magnetic field components which are aligned with the flow direction (or, more specifically, with the r -direction) have not been addressed. Preliminary magnet design concepts discussed elsewhere in this report indicate radial field components approaching 5 - 6 T near the channel exit, and such fields would undoubtedly lead to complexities in the gasdynamic and electrodynamic behavior in the channel. However, it is felt that additional effort on this subject could lead to design of flat magnet-channel combinations for which B_r remained small while B_z increased with radius, which could be perfectly acceptable. Alternatively, it is likely that non-planar magnet-channel configurations could be developed in which the channel direction essentially followed the normal to the field-lines, as indicated in Figure 6-3-6, and as discussed elsewhere. For this reason all B-field components are assumed normal to the velocity vector in the channel calculations reported herein.

5.1.6 REMAINING ASSUMPTIONS

Many of the assumptions implicit in the formulation of Sections 5.1.1 through 5.1.4 have been discussed in context; some minor or some major assumptions still require some assessment.

- (a) Wall conditions. The wall heat transfer correlation requires a wall enthalpy, h_w , and an adiabatic wall enthalpy expressed in terms of free stream conditions by $h_{aw} = [h + (\text{recovery factor}) \times (u^2/2)]$. Most of the calculations reported below have used $T_w = 2000$ K and a recovery factor of 0.9; both these numbers are inputs to the computer program. $T_w = 2000$ K indicates a nonslagging condition; the presence of slag layers would require some code modification.
- (b) Generator inlet radius. Choice of stagnation conditions and of values of M and S at the channel inlet leads to determination of ρ and u_r , and thus to the required inlet area for specified mass flow. In most cases considered for OCP the ratio z/r at inlet has been taken as one third, so that $A_{\text{inlet}} = 2\pi r^2/3$. Again, this inlet z/r ratio is a code input. In all cases one further constraint has been imposed to ensure that a viable geometry is established: if the channel mass flow is considered as being delivered at $M \sim 0.5$ through an axial tube of radius R_0 , then it is required that $r_{\text{inlet}} \geq 1.2 R_0$.
- (c) Uniform plasma conditions. Many studies have been carried out to assess the degradation of performance of MHD generators attributable to non-uniformities in the plasma. For the disk configuration the most likely source of such nonuniformities is the series of wakes generated by an array of IGVs. It is recognized that such wakes would lead to a reduction of the effective Hall parameter, even for equilibrium conditions (see Reference 2, for example). Since most of the disk cases used in the overall systems study have maintained $S \leq 0.5$, no IGVs have been required, and it has not been necessary to study degraded performance. Future studies which use disk configurations optimizing at higher swirl ratios ($S \sim 1.0 - 1.5$) should invoke an appropriate level of degradation.
- (d) Thermodynamic and chemical equilibrium. Rapid expansion to high supersonic Mach number will usually leave the chemical composition of the combustion gas "frozen" at what it was in the plenum; subsequently the gas composition will relax towards equilibrium, which generally entails a conversion of CO to CO₂. The kinetic rates for this relaxation are not well known under the conditions existing in MHD generators.

It has already been established that nonequilibrium chemistry must be included in the analysis of laboratory-scale supersonic combustion experiments. An example of a set of nonequilibrium calculations is shown in Figures 5-1-3 and 5-1-4. Stagnation conditions are typical of OCD applications; from the plenum the gas is expanded to $M = 1.78$, $p = 1.12$ atm, after which it flows adiabatically at constant pressure. No enthalpy extraction is included. This numerical experiment is illustrated for different physical scales; C is approximately CDIF size, B is comparable to the scale of disk generators for base-load application, and A is an order of magnitude larger still. The static temperature of the gas "undershoots" its equilibrium value in the rapid expansion, and then recovers towards equilibrium at a rate controlled by the $\text{CO} + \text{OH} \rightarrow \text{CO}_2 + \text{H}$ reaction. In a sufficiently slow expansion the shifting equilibrium implies continuous conversion of CO to CO_2 ; when the expansion is rapid the CO concentration remains "frozen" and the subsequent temperature recovery is brought about by combustion of the excess CO.

For a 4 m disk operating under the conditions comparable to Figure 5-1-3 it is clear that there is a potential temperature "loss" on the order of 100 K near the generator inlet, and the effect of this on electron concentration (with consequent effect on plasma conductivity) is shown in Figure 5-1-4. If this chemical kinetics effect is real, then it is essential that it be included in the disk analysis procedure. The $\text{CO} + \text{OH}$ rate is well-documented for clean combustion products, but there is very little hard information on the possible catalytic effect of the ash and seed components which would be present in an open cycle disk channel. An order of magnitude increase in $\text{CO}:\text{CO}_2$ conversion rate would permit equilibrium analysis to be used for the OCD case (the commercial size open cycle linear generator, being an order of magnitude larger in physical scale, does not face this need for nonequilibrium analysis procedures). In the present study it has been decided that available equilibrium analytical tools should be used for the parametric cases, but it remains necessary to use nonequilibrium programs to check on the possible effects of departure from equilibrium, especially for those cases which represent minimum physical size.

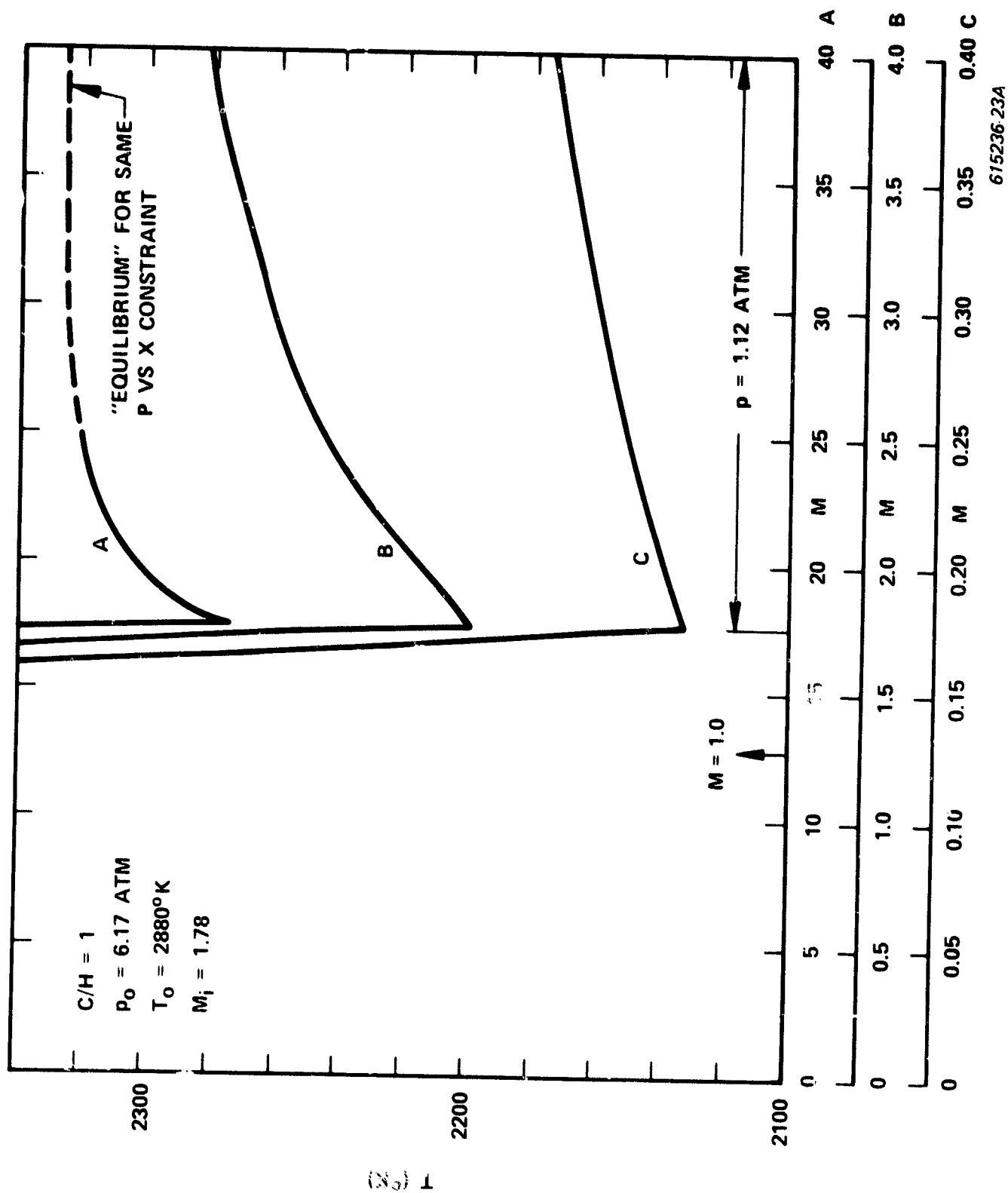
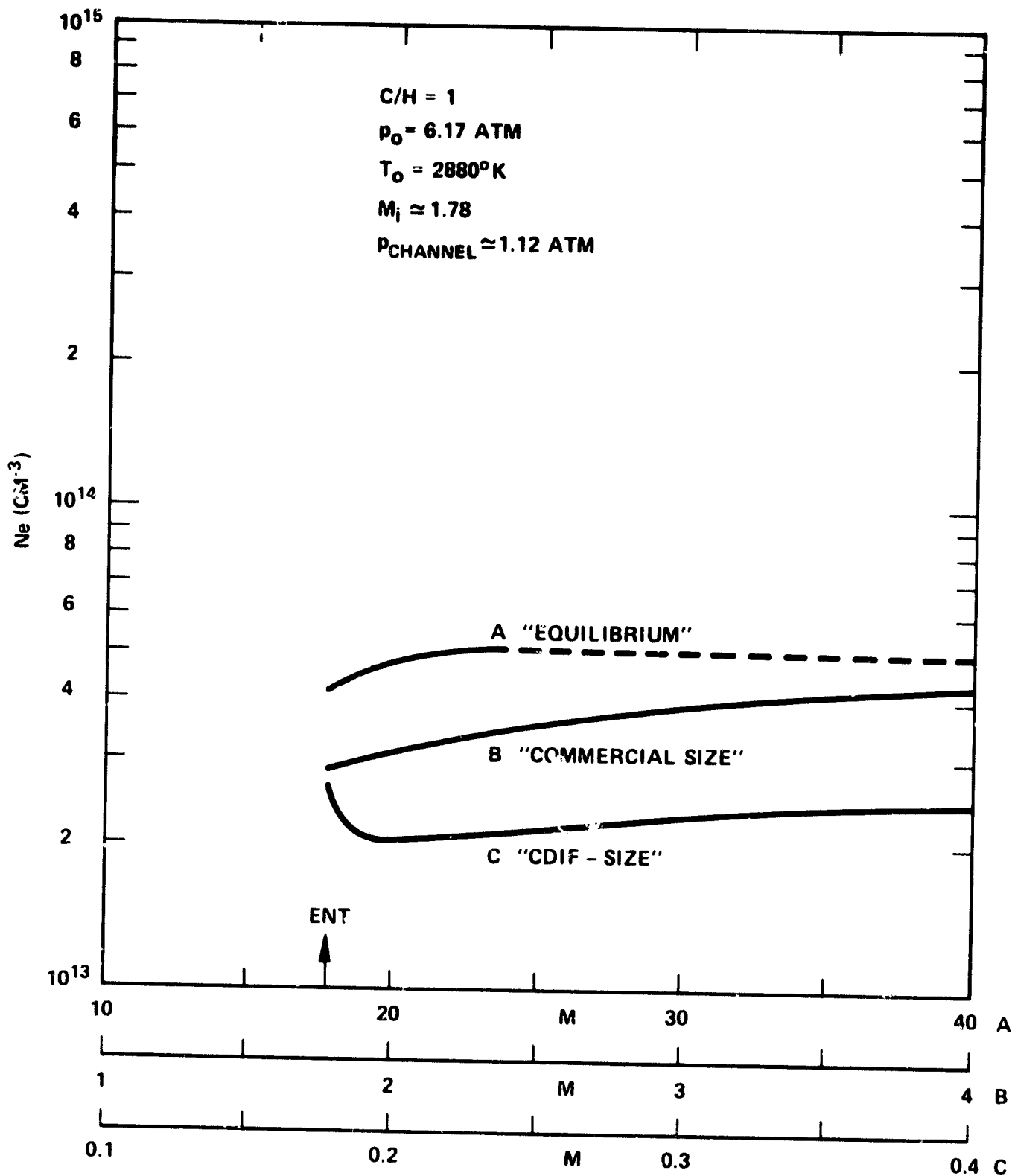


Figure 5-1-3. Plasma Temperature Versus Flow Length for Supersonic Combustion Gas Generators of Various Sizes (Approach to Equilibrium Conditions)



615236-22A

Figure 5-1-4. Electron Concentration in Combustion Gas Plasma Versus Flow Length in Supersonic Generators of Various Sizes

5.1.7 SPECIFICATION OF HALL FIELD CONSTRAINT FOR DISK GENERATORS

A high-performance disk generator must undoubtedly withstand very much higher Hall fields (in the radial direction) than an equivalent linear generator, but the technological problems associated with an insulating wall are quite different from those of electrode wall construction. In MIT shock tube experiments with cold walls, fields in excess of 30 kV/m have been measured without any indication of breakdown. The most recent Stanford experiments [3] have sustained hot-wall electric fields of 9 kV/m with no evidence of breakdown. The 9 kV/m applied field was limited only by the particular experimental configuration and external circuitry. There are no other relevant experimental data for the hot wall situation. In the interest of a conservative design choice for the present systems analysis it was proposed that the base case be restricted to a radial electric field of 12 kV/m, with parametric variations covering the range 8 kV/m to 16 kV/m. As a single exception to this, it was proposed that this constraint be relaxed for one case to permit a design calculation to be carried out for a 12 T magnet. For this case it was considered that the examination of far-term potential should not be unfairly shackled, and that an electric field up to 20 kV/m should be permitted if the optimized design requires it.

The rationale for the choice of the 12 kV/m nominal values is given below. Experience acquired in the operation of large (linear) combustion driven generators has shown that the breakdown potential between adjacent elements of the insulator wall is at least three times that for adjacent elements on the electrode wall. Elements of an insulator wall do not carry current, and are cooled so that they are shielded from the plasma by a relatively cold boundary layer. In contrast, electrodes are designed to be in good contact with the plasma non-uniformities, which include the current concentrations. The breakdown potential between adjacent electrode-wall elements is a function of the voltage between elements, the surface temperature, and the local current density entering the elements. Damage after breakdown is a function of power density and the degree to which a breakdown arc can couple to the bulk of the plasma.

For the open-cycle disk, the problem is more serious since higher fields ($E \sim \beta_{\text{eff}} UB$) are obtained due to the high values of the Hall coefficient ($\beta_{\text{eff}} \approx \beta_{\text{ideal}}$; in the range of 4-8 or higher). In closed-cycle application, $\beta_{\text{eff}} < 2$ as a result of the nonuniformities associated with the ionization instability (unless the seed is fully ionized, for which case β_{eff} values up to ~ 5 have been reported).

Compared to the linear generator (where the field is limited to $E_{\text{max}} = 4 \text{ kV/m}$), relatively little information exists for E_{max} in disks. As mentioned above, the Stanford apparatus with fused MgO walls withstood applied fields of 9 kV/m in the presence of the plasma. In shock tube experiments, also mentioned above, Hall fields up to $E = 38 \text{ kV/m}$ were measured with simulated combustion gases; these experiments, however, were conducted under ideal wall and flow conditions ($T_{\text{wall}} \sim 300 \text{ K}$) without slag. However, in a disk a slag coating is not necessary for good performance since the walls are not current-carrying elements.

In a linear channel the constraint on the Hall field is determined by the field concentration and by the joule dissipation over the interelectrode insulator. Close to such an insulator the geometrical constraint is $y \approx \text{constant}$, and thus the current density vector has components $j_y \approx 0$ and $j_x \approx \sigma E_x$. The initial dissipation, prior to the development of a fault, is therefore given by the product of the Hall field, E_x , and the current density, j_x ; i.e., the dissipation is σE_x^2 . In the case of an insulator wall, the scalar conductivity is replaced by the tensorial conductivity $\sigma/(1 + \beta^2)$, so that the dissipation over the insulator wall is $\sigma E_x^2/(1 + \beta^2) \approx \sigma (E_x/\beta)^2$. An equivalent expression for the disk configuration can be reduced directly from the current density relationships given in paragraph 5.1.1; close to the disk insulating wall, where $u_r \approx u_\theta \approx 0$, these relationships yield $j_r = \sigma E/(1 + \beta^2)$ and $j_\theta = \beta j_r$ whence the dissipation j^2/σ becomes $\sigma E^2/(1 + \beta^2) \approx \sigma (E/\beta)^2$.

If the Hall field is considered a measure of the stress level over the insulator (of the electrode wall or insulator wall), this simple analysis indicates that the

allowable Hall field is larger for the disk insulating wall than it is for the electrode wall of the linear channel, the multiplicative factor being β , the Hall coefficient. This result agrees with the experience obtained in linear generators that the insulator walls appear to be able to bear an electric field three times larger than for the electrode wall (for existing generators which have operated with maximum Hall coefficients of three).

On this basis the parametric upper limit of 16 kV/m would not be prima facie unreasonable for a disk generator with $\beta \sim 4$, and the nominal 12 kV/m is quite conservative. The same rationale justifies the relaxation of this Hall field constraint for the assessment of the potential usefulness of a 12 Tesla magnetic field, since Hall coefficients would then be correspondingly larger.

5.2 OPEN CYCLE SYSTEMS MODELING

5.2.1 SYSTEM PERFORMANCE ANALYSIS CODE

The Westinghouse system performance analysis (SPA) code formed the basic tool for calculating the performance of the open cycle disk systems. It is a versatile systems code capable of analyzing the thermodynamic performance of many general systems, including the OCD MHD systems. The flexibility of the code is gained by taking the approach in which a system is viewed as consisting of a set of interconnected components. The mode of interconnection is dictated by the user through the input data. Thus the user has complete freedom in assembling the components into a system in a fashion that suits his particular problem.

Basically, SPA is composed of two major parts: an executive and a component subroutine package. The executive subroutines handle data input and output, control the information flow among the components, and perform loop closure and convergence checking if feedback loops are encountered. The component subroutine package includes subroutines modeling the individual components and the required auxiliary subroutines. Each type of component present in the system is represented by a subroutine with sets of input and output variables, and a number of parameters. These parameters define the fixed characteristics of the component such as heat exchanger effectiveness or pump efficiency and select the optional mode of computation. By specifying the input variables for each component as the output variables from another, the user establishes the component interconnections to form his system model. For cases where more than one component of a similar type exists, a given subroutine may be called more than once, with appropriate values of the variables supplied for each use.

Each flow stream encountered in the system is associated with an ID number and its properties are needed for system calculations. For streams with fixed compositions such as steam and air, the properties are calculated internally by the code. For combustion gases, however, tables of equilibrium and transport properties as a function of pressure and temperature must be supplied. These tables are then used in the systems code for interpolation to compute the

desired properties at any pressure and temperature. In this study, a modified NASA chemical equilibrium code [1] was used to generate these tables. The computed electrical conductivities agreed well with most published data [2].

5.2.2 COMPONENT AND SUBSYSTEM MODELING

Combustor

The combustor model is represented by heat and mass balances with given pressure and heat losses. The heat balance accounts for the sensible heat of the fuel, oxidizer, and seed streams entering the combustor, the heat of reaction, and the sensible heat of the combustion products and the slag being removed. The gas flow rate and stagnation temperature and pressure at the combustor exit are calculated in the model.

A pressure loss of 0.08 of inlet pressure and heat loss of 0.07 based on the coal thermal input to the combustor are assumed for cases with a swirl ratio of up to 0.5 attainable without inlet guide vanes. For swirl ratios greater than 0.5, inlet guide vanes are required, resulting in additional pressure and heat losses. These additional pressure and heat losses are approximated by $L_p = 0.04 (S - 0.5)$ and $L_h = 0.01 (S - 0.5)$, respectively, where S is the swirl (>0.5).

Nozzle

The nozzle calculation assumes a frictionless nozzle. The heat loss in the nozzle is assumed lumped in the combustor heat loss and therefore the nozzle exit conditions are computed based on isentropic flow equations.

Channel and Diffuser

A one-dimensional, core-flow model has been incorporated in the SPA code to calculate the performance of a disk generator. The flow in the generator is assumed to be cylindrically symmetric and variations of dependent variables in the z -direction (perpendicular to the plane of the disk) are neglected. The combustion gases are assumed to be at equilibrium throughout the channel so

that equilibrium properties are used. Models for friction and heat losses are incorporated in the code. Optional modes of computation include those for constant Hall field, constant static temperature, constant static enthalpy, and constant velocity designs.

The generator calculations start from the inlet of the disk and proceed until the pressure drops to a value such that a specified pressure is obtained at the exit of the diffuser. The diffuser pressure recovery coefficient is used to calculate the total pressure loss from the generator exit to the outlet of the diffuser for subsonic channel flow. The kinetic head at the diffuser outlet is assumed negligible. For supersonic flow in the generator, a pressure loss based on a simplified normal shock model is taken for transition from the supersonic to subsonic regime and the pressure recovery coefficient is then used to compute the total pressure loss in the subsonic regime. The generator code has been checked with that used for the generator suboptimization study and good agreement has been obtained.

Steam Plant

The SPA code also includes component modules for modeling the bottoming plant components, such as heat exchangers, pumps, compressors and steam turbines. Non-extraction type steam systems were modeled using the SPA code by properly assembling all the components and assuming a given turbine efficiency. For extraction type steam systems, however, a more sophisticated code developed by the Westinghouse Steam Turbine Division was used to calculate the steam plant performance.

Gasifier Subsystem

A simplified model was used to calculate the performance of the gasifier-burner system in the indirectly-fired cases. The Westinghouse gasifier, when coupled with a hot-gas clean-up system, is capable of achieving a thermal efficiency of more than 90%. In the modeling, a combined 10% thermal energy loss based on the coal input to the gasifier was assumed for the gasifier-burner system. It represents a non-recoverable energy charge attributable to carbon conversion inefficiency, ash removal, gas clean-up and other losses.

Oxygen Plant

A fixed value of power requirement per unit mass of oxygen produced was used to compute the total power requirement of the oxygen plant. For a high efficiency air separation plant producing 95 mole-percent pure O_2 , this energy requirement was estimated to be 0.814 MJ/kg O_2 (205 kW-hr/ton) [3]. The oxygen leaving the air separation plant was assumed to be at room temperature and pressure and mixed with the main air before going to the MHD compressor. In a more advanced integration scheme, the oxygen would probably be taken from the air separation plant at a higher pressure and lower temperature to minimize the MHD compressor power.

Sulfur Emissions Control and Seed Regeneration

The choice between seed regeneration and flue gas scrubbing for sulfur emissions control depends on coal sulfur level, specific environmental standards, as well as the specific choice of a seed regeneration process. Economics, rather than energy requirements of the process is the determining factor in selecting one particular system over another. For Montana Rosebud coal having a low sulfur content, sulfur removal by seed regeneration is most appropriate. A seeding level of 0.7% potassium by weight, with sufficient potassium carbonate in the seed mixture would provide adequate plasma conductivity, acceptable seed loss, as well as satisfactory desulfurization. However, economic advantages have suggested that high sulfur coals may be best cleaned by flue gas scrubbing [4]. Accordingly, a conventional sulfur scrubbing system was selected for Ill. #6 coal and pure potassium sulfate was used as a seed, with a seeding level increased to 1% potassium by weight.

Because kinetic and thermodynamic data for most proposed seed regeneration processes are incomplete and/or unreliable, performance and economic evaluations and comparisons have been difficult and inconclusive. The issue is further clouded by differences in the stage of development of these candidate processes. In general, chemical seed regeneration using dry processes, such as the PERC process, requires production of reducing gases from coal feedstock and is relatively energy intensive. It can therefore, substantially impact the

overall plant efficiency. Careful integration of the seed regeneration system into the MHD power plant to utilize the available energy from the regeneration process may be required to minimize the net energy requirement of the process. On the other hand, for a wet process, such as the formate process or a conventional lime scrubber, a large portion of the energy required is buried in the cost of purchasing the lime produced off site and is not accounted for in the plant performance analysis. Solid waste disposal also adds additional cost to the wet processes.

For the purpose of this study, the coal requirement for the seed regeneration was assumed to be 2% of the coal thermal input to the MHD combustor. This is in line with the estimation based on the PERC process [4]. For a system employing a flue gas sulfur scrubber, an efficiency debit of 0.9 percentage point was charged to account for the power requirement of the scrubber auxiliaries.

5.2.3 SYSTEMS AND COMPONENT ASSUMPTIONS

Table 5.2.1 summarizes the assumptions made in the systems modeling regarding pressure drops, heat losses, statepoint constraints, and other major system parameters.

5.3 DISK GENERATOR SUBOPTIMIZATION

5.3.1 OCD PERFORMANCE GOALS

The performance goals for the OCD generator are

- (i) maximum possible net enthalpy extraction (after subtraction of compressor work) from the available plasma, with gross extraction level being preferably in the range 20-25%,
- (ii) maximum possible isentropic and electrical efficiencies consistent with electrical stress limitations imposed by the designer
- (iii) compactness of design to minimize heat losses and magnet costs, and
- (iv) generator exit conditions which are compatible with a diffuser ducted to a radiant furnace.

TABLE 5.2.1
ASSUMPTIONS FOR PARAMETRIC ANALYSES OF OCD SYSTEMS

Efficiencies

Combustor - (complete combustion for species determination - any inefficiency included in heat loss)
MHD Power Conversion (dc to grid) - 97.5%
Air compressor - 90%
Fans - 80%
Pumps - 70%
Turbine - 90%
Generator - 98.4%
Transformer - 99%

Assumed Fixed Temperatures

Gas at superheater exit - 1100 K
Gas at ECON 2 exit - 611 K
Gas exhaust to stack - 408 K
Air at LTAH exit - 922 K (1200°F)
Air at HTAH exit - base case = 1920 K (3000°F), variable 1650-1920 K
Feedwater to ECON 1 - 400 K (maximum) (for separate cooling)
Maximum temperature of power train water coolant - 425 K (for separate cooling)
Turbine throttle conditions - 811 K (1000°F)
Ambient - 288 K

Heat Losses

Combustor/nozzle - 7% of HHV of coal feed. (= 140 MW for 2000 MW thermal input, plus 11 MW loss due to slag removal)
Disk generator - calculated from specified wall temperature
Diffuser - assumed an average heat flux of 0.2 MW/m^2 and a surface area of $0.5 \pi R^2$, where R = generator exit radius
High temperature air heater - 4 % of duty (2% to valve cooling)

ASSUMPTIONS FOR OPEN CYCLE MHD DISK GENERATOR STUDY (Cont'd)

Assumed Pressures/Pressure Drops (in terms of inlet pressures)

Combustor - 8% of inlet pressure (for base case)
Diffuser pressure recovery coefficient - 0.45 (for base case)
Radiant boiler - gas side 3%
 steam side 3.5%
HTAH - gas side 4%
 air side 3.5%
Reheater - gas side 1%
 steam side 3%
Superheater - gas side 2%
 steam side 3%
LTAH - gas side 2%
 air side 3%
ECON 2 - gas side 3%
 steam side 3%
ECON 1 - gas side 3%
 steam side 5%
Ambient - 1 atm
Diffuser exit - 1.07 atm (1 psi above ambient)
HP steam turbine - inlet 3500 psia (238.2 atm)
 exit 652 psia (44.4 atm)
LP steam turbine - inlet 587 psia (40.0 atm)
Condenser - 2 in Hg (311.6 K temperature)

Slag carry-over - Two stage combustor - 10% of nominal

As would be expected, design of a satisfactory disk generator requires some compromise between these partially conflicting goals; indeed, attainment of the "best possible" disk is dependent on how it integrates with the rest of the power generation system, and on the criteria by which the resultant combined MHD/steam power system is evaluated. In this section, the focus is on attaining disk configurations which can be included in the overall systems study with the ultimate figure-of-merit being the overall system efficiency.

5.3.2 FACTORS AFFECTING DISK GENERATOR PERFORMANCE

The factors which impact the disk performance per se are (a) the plasma conductivity, dependent on oxidizer preheat, the combustor losses and the seed fraction, (b) the diffuser specifications, (c) the choice of M , S , and P_0 at inlet to the channel, and (d) the "design constraint," and these four items are discussed below.

(a) Plasma conductivity. The base case choices of oxidizer preheat are predicated on successful achievement of an advanced technology HTAH, with exit air temperature of 1920 K. The parametric variations about this case, and the alternative base case using O_2 -enriched oxidizer, all make less stringent demands on the development of advanced refractory regenerative heaters. The choice of seed fraction, 0.7% K by weight, is based on earlier Westinghouse studies which indicate that further addition of seed to the combustion products is not cost effective. However, since a definitive measurement of electrical conductivity for a coal plasma with slag volatiles has not yet been made, a conductivity enhancement factor of 1.5 has been applied in some of the disk suboptimization.

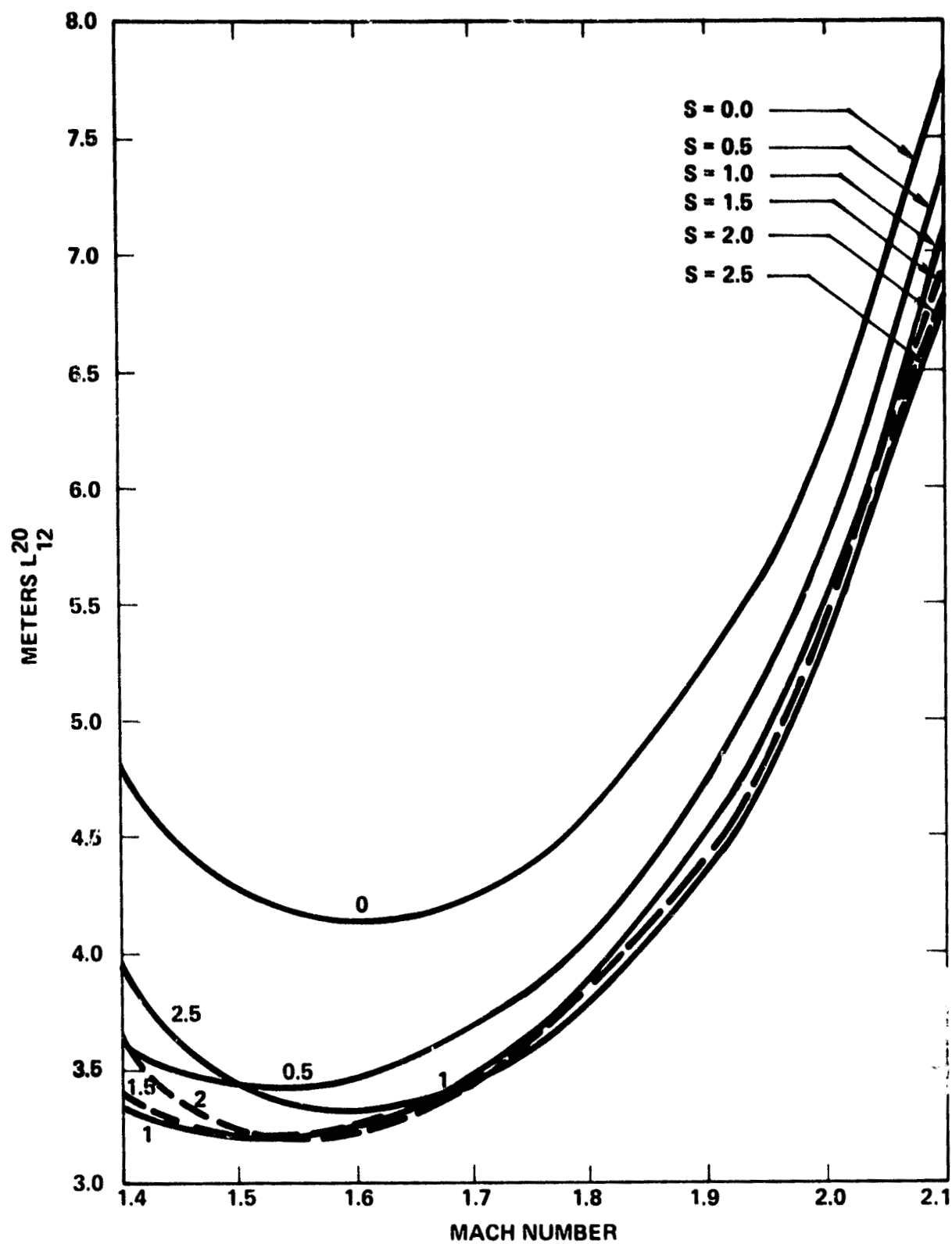
Determination of the temperature or enthalpy of the plasma entering the channel is still necessary before use can be made of the tabulated values of electrical properties. This, in turn, requires insertion of the appropriate combustor and slag rejection losses discussed in 5.1.3.

(b) Diffuser Specifications. All of the generator calculations for the present OCD systems study have used 1.068 atm as the diffuser recovery pressure. Early calculations used a pressure recovery coefficient $C_p \approx 0.55$, but

○ this was later raised to 0.6 for consistency with the linear PSPEC studies. It is conceivable that $C_p = 0.6$ in the radial outflow case could not be achieved without the insertion of struts in the diffuser (to reduce the likelihood of separation); these would impose rapid cooling on some of the gas before it reaches the radiant furnace, and this in turn may have some impact on the level of NO_x production.

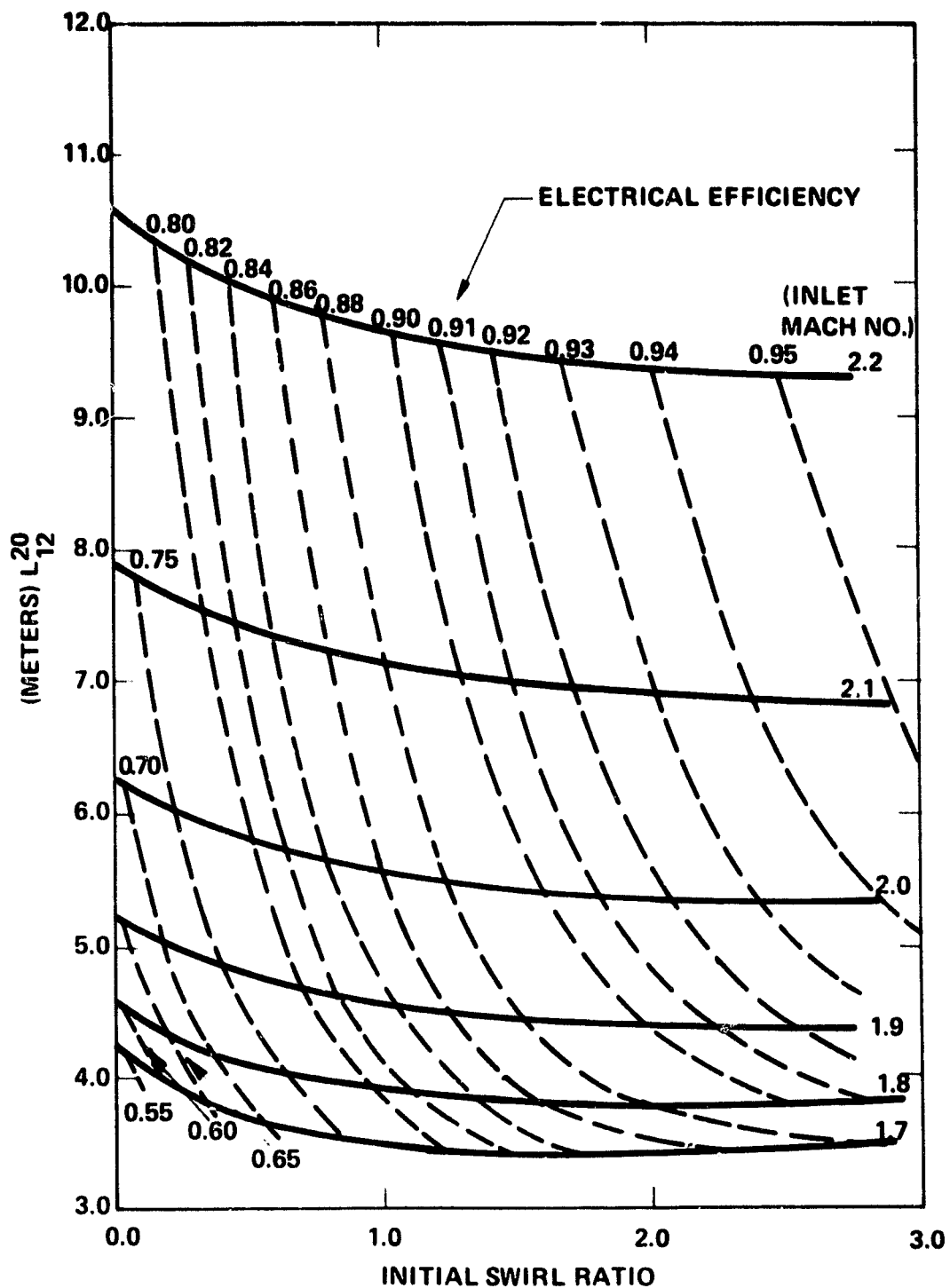
(c) Channel Entry Conditions. Choice of combustor pressure level is ultimately determined by the overall systems optimization procedure, but the factors impacting this choice may be illustrated by means of Figure 5-3-1. It is necessary to make P_0 sufficiently high relative to the diffuser pressure to permit an adequate decrease in enthalpy as the gas flows through the channel. Higher P_0 will, in general, lead to higher enthalpy extraction, but the enthalpy extraction length increases with P_0 , so that the device size must also increase. Eventually, the point is reached at which the added enthalpy extraction fails to exceed the increment in compressor work needed to increase P_0 . For the enthalpy extraction expected in the present study, it can be deduced that the cycle will optimize with P_0 in the range 6-8 atm. Choice of M and S at inlet to the generator can then be made with reference to the enthalpy extraction length L_{ex} . Variation of L_{ex} is displayed in Figures 5-3-2 and 5-3-3; these curves are plotted for $P_0 = 7$ atm, $T_0 = 2844$ K, and for an arbitrary 20% enthalpy extraction. One other parameter which must be selected before L_{ex} can be plotted is the electrical loading, K , and for Figures 5-3-2 and 5-3-3 K is chosen such that the electric field is -12 kV/m, which is the nominal maximum for the design points of the OCD cases. Figure 5-3-2 shows that the minimum with respect to Mach number occurs in the range $1.5 < M < 1.6$ for $0 \leq S \leq 2.5$. There is significant reduction in L_{ex} when S is increased from zero to 0.5, but further increase in S does not appreciably reduce L_{ex} . However, Figure 5-3-3 shows that the electrical efficiency can be increased by increasing S at a given Mach number. To some extent, the low efficiencies in the lower left corner of Figure 5-3-3 are forced by the $E = -12$ kV/m constraint; reduced electric field (or higher K) would bring the loading closer to the local optimum, but at the expense of increase in L_{ex} . The eventual choice of M and S at channel inlet is then

○
c-2



615689-5A

Figure 5-3-2. Enthalpy Extraction Length as Function of M&S at Inlet, for 20% Extraction, Electrical Loading for $E = -12$ kV/m, $P_0 = 7$ Atm, $T_0 = 2844$ K.



615689-6A

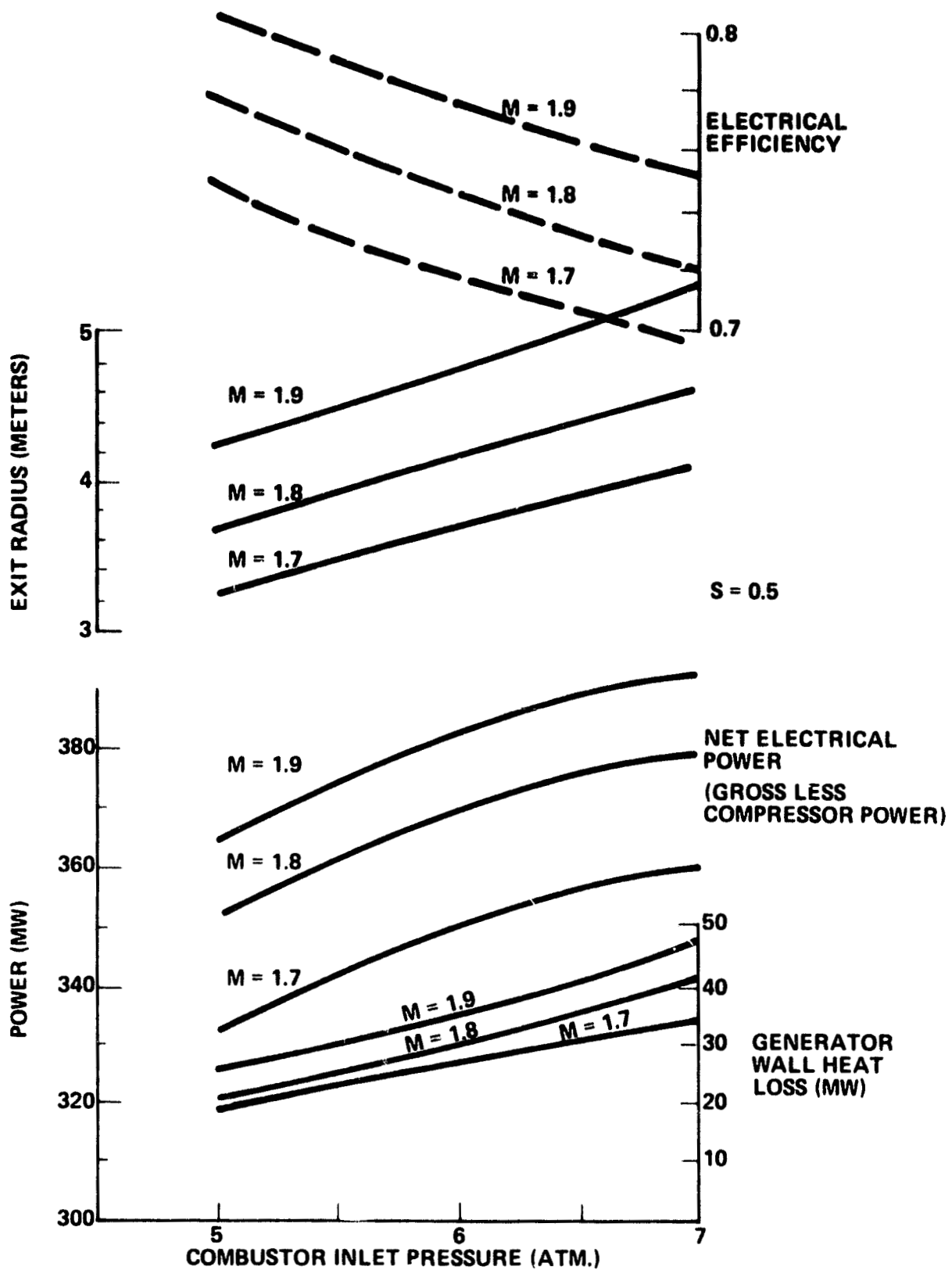
Figure 5-3-3. Enthalpy Extraction Length as Function of M&S at Inlet, for 20% Extraction. Electrical Loading for $E = -12$ kV/m. Local Electrical Efficiency Contours are Shown.

made by parameterizing these two variables and examining the resultant disk performance when the channel is designed with various types of constraint algorithm.

d) Application of the Design Constraint. When all inlet conditions to the generator (mass flow rate, stagnation conditions, Mach number, swirl ratio and load factor) are preselected, it is still necessary to apply one constraint before the fluid and electrical properties throughout the generator can be calculated. In the earlier disk studies this constraint has been applied in several forms, such as by specification of dT/dr , dh/dr or M as a function of radial position. A significant advance came with the recognition that use of the electric-field constraint is an effective way to force a type of suboptimization in the sense that it permits direct comparisons of the results of design calculations for different choices of the inlet values of P_0 , M or S . By choosing the initial load factor, K , to make $E_r = -(1 - K)Bu_r(S + \beta)$ assume the maximum value permitted by the design specification, and by subsequently controlling dh/dr to maintain the radial E-field at this maximum value, it is possible to obtain a generator which is more compact than any other design having the same initial conditions and the same electrical power output. Parametric variations of P_0 , M and S can then be made to provide an optimum choice within the family of constant E-field designs.

5.3.3 OPTIMUM DESIGN CONDITIONS FOR SINGLE-LOAD DISK

The results of the calculations show that a fairly strong argument can be made for selecting $S = 0.5$ for the base case configuration. Figure 5-3-4 shows the results of variation of P_0 for constant swirl ($S = 0.5$) and three values of M . Net electrical power is still increasing at values of P_0 up to 7 atm, but the resulting generator size is also steadily increasing. The figure also shows the rapid increase in heat loss from the generator walls as the size increases; although this heat may be rejected to the steam bottoming cycle, an optimum pressure is reached beyond which the effect of increased heat loss outweighs the benefit of net power gain. In the present case, there is little incentive to operate at $P_0 > 6$ atm as long as $M \geq 1.8$. Operation at lower Mach number may optimize at higher pressure ratio, but only at the expense of



615689-7A

Figure 5-3-4. Variation of Disk Generator Characteristics with Inlet Stagnation Pressure for Constant Swirl Ratio of 0.5

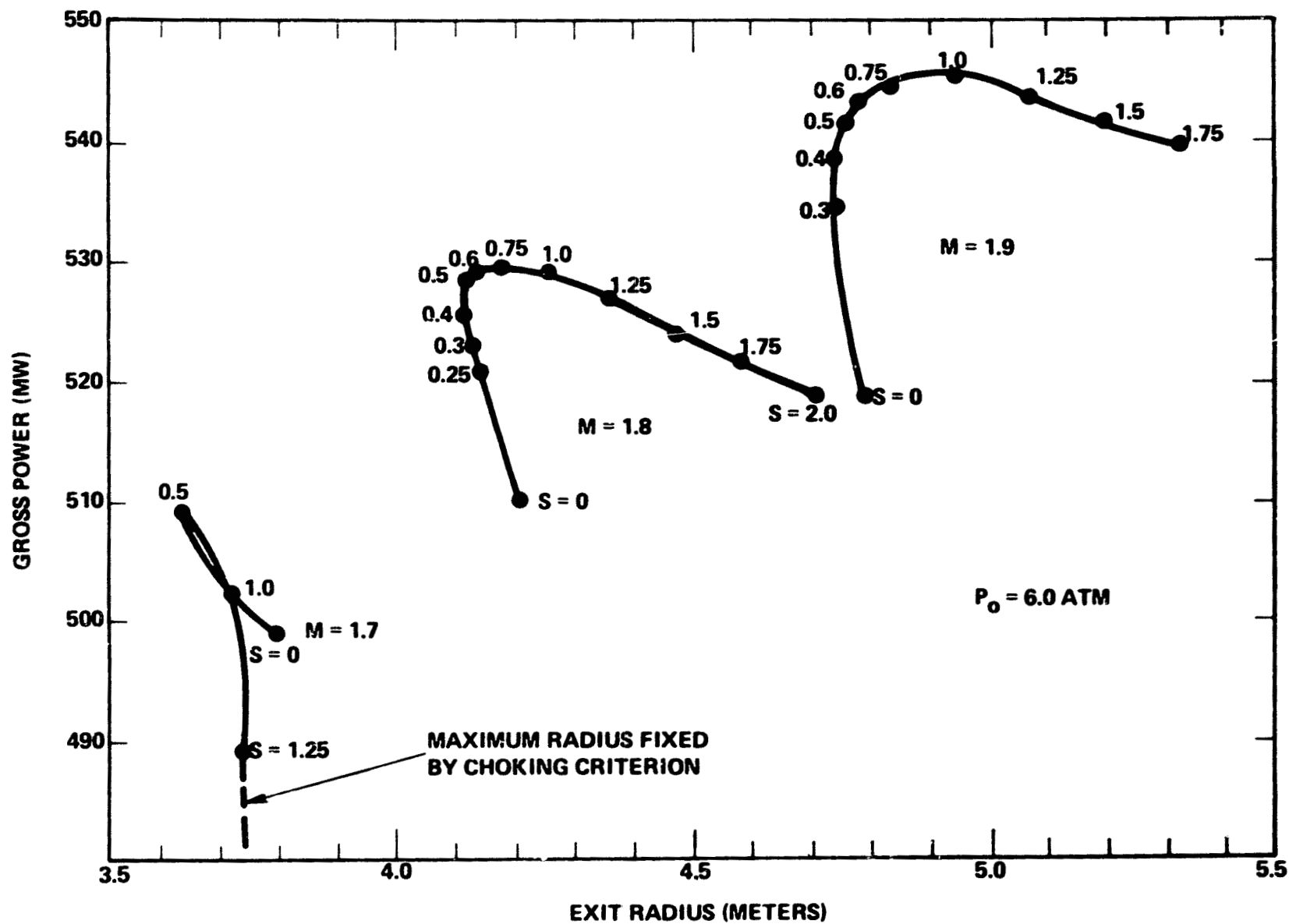
electrical efficiency. Similar sets of curves were obtained for other values of swirl ratio, and the resulting overall variation with S is shown in Figure 5-3-5 for a single inlet pressure, $P_0 = 6$ atm. For $M = 1.7$, there is a sharp optimum at $S = 0.5$, since there is a rapid loss of power at higher swirls caused by choking. At $M = 1.8$ and 1.9 the generator is continued to the radius at which the diffuser can still recover to 1.068 atm after taking a normal shock loss. At $M = 1.8$, the optimum is clearly close to $S = 0.5$, and this gives a configuration with adequate electrical efficiency (Figure 5-3-4). At $M = 1.9$ there is a case to make for examining configurations with $S = 1$, but the three percent increase in gross power achieved by the increase in Mach number is largely offset by the increased heat losses associated with the larger radius (an additional 8 MW for the generator alone, without consideration of the effect of a larger diffuser).

It is possible that other regimes of operation would require higher swirl values for optimal generator configurations, but for the 1920 K preheat case it is clear that $S = 0.5$, achievable without IGVs, provides the most logical choice. For the $M = 1.8$ case, the enthalpy extraction is 18.9 percent of the enthalpy flux to the generator, or 17.8 percent of the enthalpy flux to the combustor.

This optimum occurs at a surprisingly low value of inlet swirl, but this is occasioned by the relatively low pressure (compared to linear generator studies) at which the optimization is achieved. Low pressure leads to high Hall parameter, and the electrical efficiency is then less sensitive to the value of swirl ratio.

5.3.4 OFF-DESIGN OPERATION OF THE DISK GENERATOR

Calculations were carried out to establish the voltage/current characteristics for one of the family of single-load generators designed under the above constant radial E-field constraint. The parameters defining this reference generator are listed in Table 5.3.1; plasma conditions at entry to the channel have stagnation values $P_0 = 5.52$ atm, $T_0 = 2833$ K (after consideration of combustor and nozzle losses), while the static values correspond to $M = 1.8$ and



615689-8A

Figure 5-3-5. Variation of Gross Power with Exit Radius as a Function of Inlet Mach Number and Swirl for Combustion Gas Disk Generator with $P_0 = 6 \text{ atm}$, $T_0 = 2834 \text{ K}$

swirl ratio $S = 0.5$. These parameters established the generator inlet radius and area; the prescribed electric field defines the electrical loading and thus fixes I_L , while the diffuser criteria determine the exit radius of the channel. Table 5.3.1a includes values of channel area, Mach number, swirl ratio, static pressure, electrical conductivity and Hall parameter throughout the generator under the design loading conditions. The area distribution for this channel is such that under zero magnetic field conditions the plasma would expand to $M = 2.46$, exiting at $p = 0.252$ atm with a residual positive swirl ratio, $S = 0.1$ (wall friction and heat losses are included in the $B = 0$ calculation).

The local impedance level at a point within an MHD generator channel can be inferred from the local open-circuit electric field and short-circuit current density. For the disk configuration these local electrical properties are given by $E_{oc} = -(\beta + S)u_r B$ and $j_{rsc} = -\sigma E_{oc} / (1 + \beta^2)$, respectively. The ratio j_{rsc}/E_{oc} implies that the effective conductivity with respect to change of load current is the scalar conductivity divided by the factor $(1 + \beta^2)$. Thus, for a generator behaving in a (mathematically) linear manner, the channel impedance would be calculable as $\int [(1 + \beta^2)/\sigma A] dr$, with the integrand representing the local impedance level in Ω/m . Values of the integrand for the design point loading of the reference channel are given in the right-most column of Table 5.3.1a implying a total impedance on the order of 10 ohms.

Calculation of the channel behavior under off-design operating conditions requires use of a "performance" code rather than the "design-mode" code. Since the channel area is known at every point in the calculation, the set of equations discussed in Section 5.1 is closed, and the "design-mode" constraint is no longer required. Several measures were adopted to achieve understanding of the off-design behavior; one of the first was an investigation of the same channel geometry under much lighter electrical loading, produced by reducing the magnetic field intensity to 2 T. The V-I characteristic obtained with $B = 2$ T is shown in Figure 5-3-6, and values of some of the fluid and electrical properties are given in Table 5.3.1b, for an electrical loading close to the peak power point. Near the peak power conditions the V-I curve has a slope of 4.18Ω ,

TABLE 5.3.1
OFF-DESIGN-POINT IMPEDANCE CHARACTERISTICS OF
SINGLE-LOAD OPEN CYCLE DISK GENERATOR

	R m	A m ²	M	S	P atm	σ mho/m	β	$(1+\beta^2)/\sigma A$ Ω/m
a.								
B = 7T	1.226	3.148	1.800	0.500	1.026	3.086	5.161	2.844
	1.916	3.490	1.667	0.257	0.922	3.172	5.728	3.054
	2.666	4.303	1.523	0.122	0.769	3.195	6.595	3.236
	3.416	5.516	1.365	0.030	0.686	3.211	7.604	3.321
	4.106	7.190	1.252	-0.066	0.586	3.075	8.807	3.553
b.								
B = 2T	1.226	3.148	1.800	0.500	1.026	3.086	1.475	0.245
	1.916	3.490	1.861	0.284	0.824	2.759	1.801	0.441
	2.666	4.303	1.945	0.188	0.614	2.294	2.344	0.658
	3.416	5.516	2.043	0.134	0.443	1.767	3.137	1.112
	4.106	7.190	2.166	0.102	0.309	1.142	4.274	2.346

CHANNEL OPERATING PARAMETERS FOR SINGLE-LOAD GENERATOR

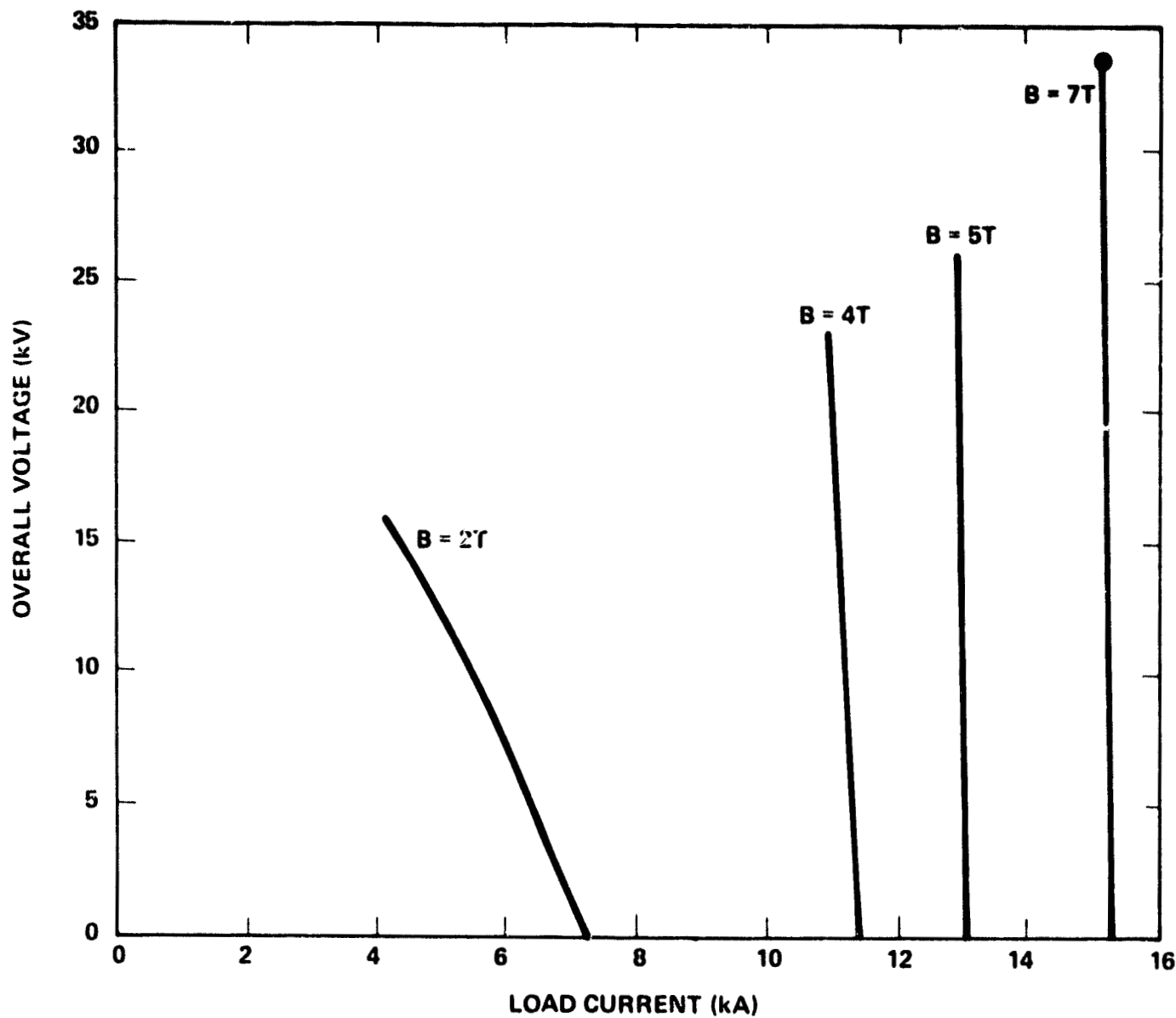
Design constraint - inlet: $P_0 = 5.52$ atm, $T_0 = 2833$ K, $B = 7T$, $E = -12$ kV/m constant
 - exit: diffuser coefficient = 0.45, recovery pressure = 1.068 atm

Electrical loading - a) $B = 7T$ and inlet load factor, $K = 0.783$: $I_L = 15.267$ KA,

$V = 34.56$ KV, $P = 527$ MW

- b) $B = 2T$ and $K_{in} = 0.25$; $I_L = 4.2$ KA, $V = 15.6$ KV,

$P = 65.7$ MW, $E_{max} = -6.5$ KV/m



615689-9A

Figure 5-3-6. Electrical Characteristics of Single-Load Disk Generator with $M = 1.8$, $S = 0.5$, $P_0 = 5.52 \text{ ATM}$

whereas the values of the $(1 + \beta^2)/\sigma A$ integrand listed in Table 5.3.1b yield an "ideal" impedance of 2.9Ω ; thus, even such a lightly loaded channel (2% enthalpy extraction) is beginning to manifest nonlinear behavior. Such nonlinearities become more pronounced as the B-field is increased, as indicated by the "load-lines" for $B = 4$ T, 5 T and 7 T shown in Figure 5-3-6. The essential verticality of these load-lines is a consequence of the single-load operation of the channel, and the insights gained in the understanding of their rather undesirable characteristics at $B = 7$ T are discussed below. In all cases discussed the plasma conditions and mass flow rate at entry to the channel are considered constant, and only the electrical loading is varied.

Figure 5-3-7 shows the V-I characteristic for the reference channel as it would be if the cathode were located at $R = 3.116$ m, or 0.9 m upstream of the exit cathode assumed in the design calculations. The slope of this characteristic near the design point is 158 Ω , considerably higher than the impedance to be expected ($\sim 6\Omega$) from the local impedance values of Table 5.3.1a. Also shown in Figure 5-3-7 is the variation of Mach number at the $R = 3.116$ m station as load current is changed. This shows that a very small decrease in I_L from the design value increases the enthalpy extraction and thus decreases the Mach number at the cathode to a level very close to $M = 1$; further decrease of I_L would induce a shock system and cause subsonic operation of the rear end of the generator. Conversely, very slight increases in I_L from the design point reduce the extraction and allow M to build up, thereby disturbing the electric field distribution and possibly forcing part of the channel into the accelerator mode (i.e., $K > 1$) so that the channel draws power from the external circuit. The decrease of overall voltage to 17 kV in Figure 5-3-7 corresponds to the reconfigured electric field shown in Figure 5-3-8.

Because such small variations in front-end load current result in rather drastic changes in Mach number distribution, it is clear that successful operation of the entire channel is dependent on the back-end electrical loading being adjusted to be compatible with the modified gas dynamic conditions; i.e., the primary load current must be modulated and the single load concept abandoned. Fortunately, it appears that satisfactory broadening of the operating range of the reference channel can be achieved by relatively small perturbations in load current.

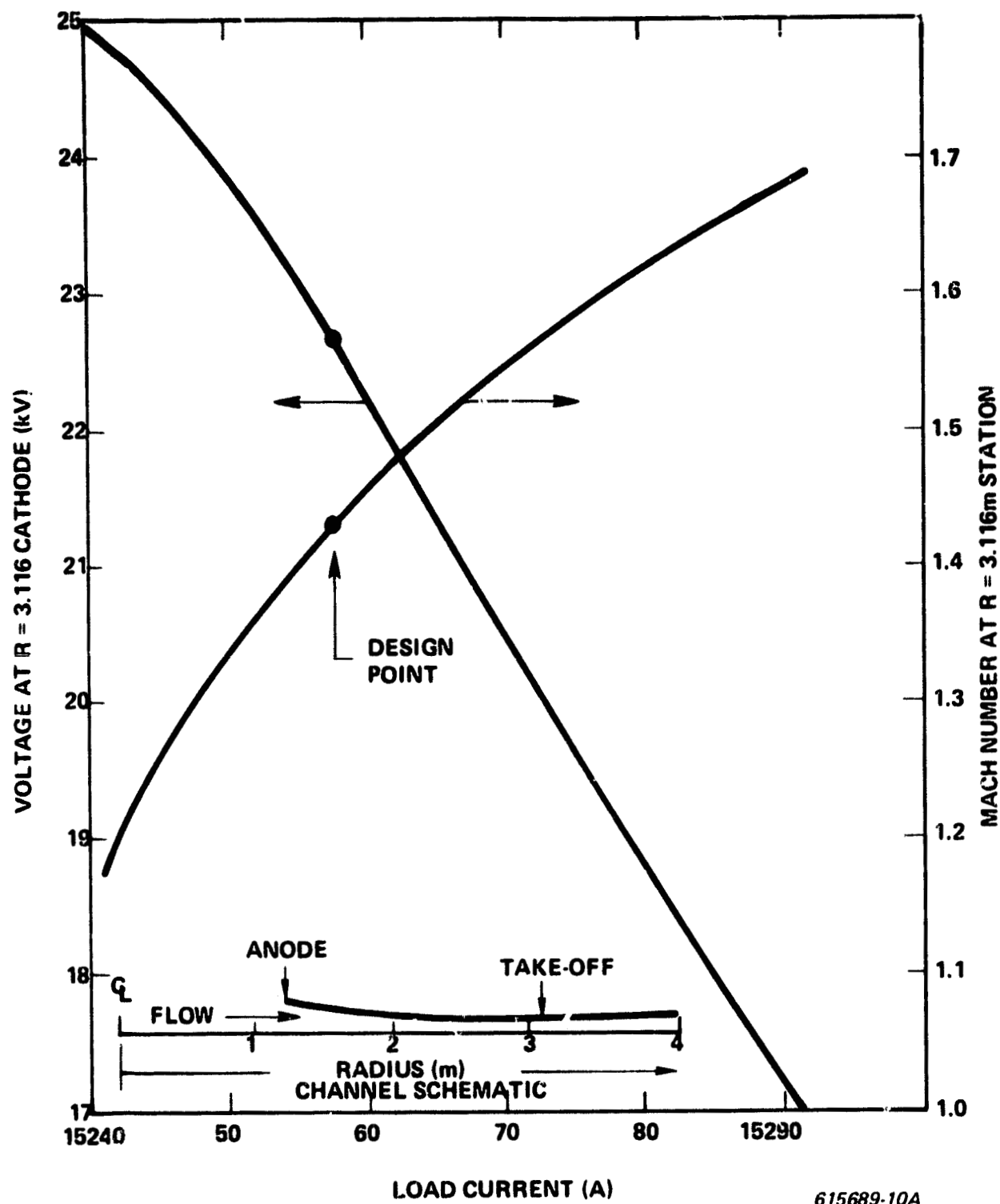
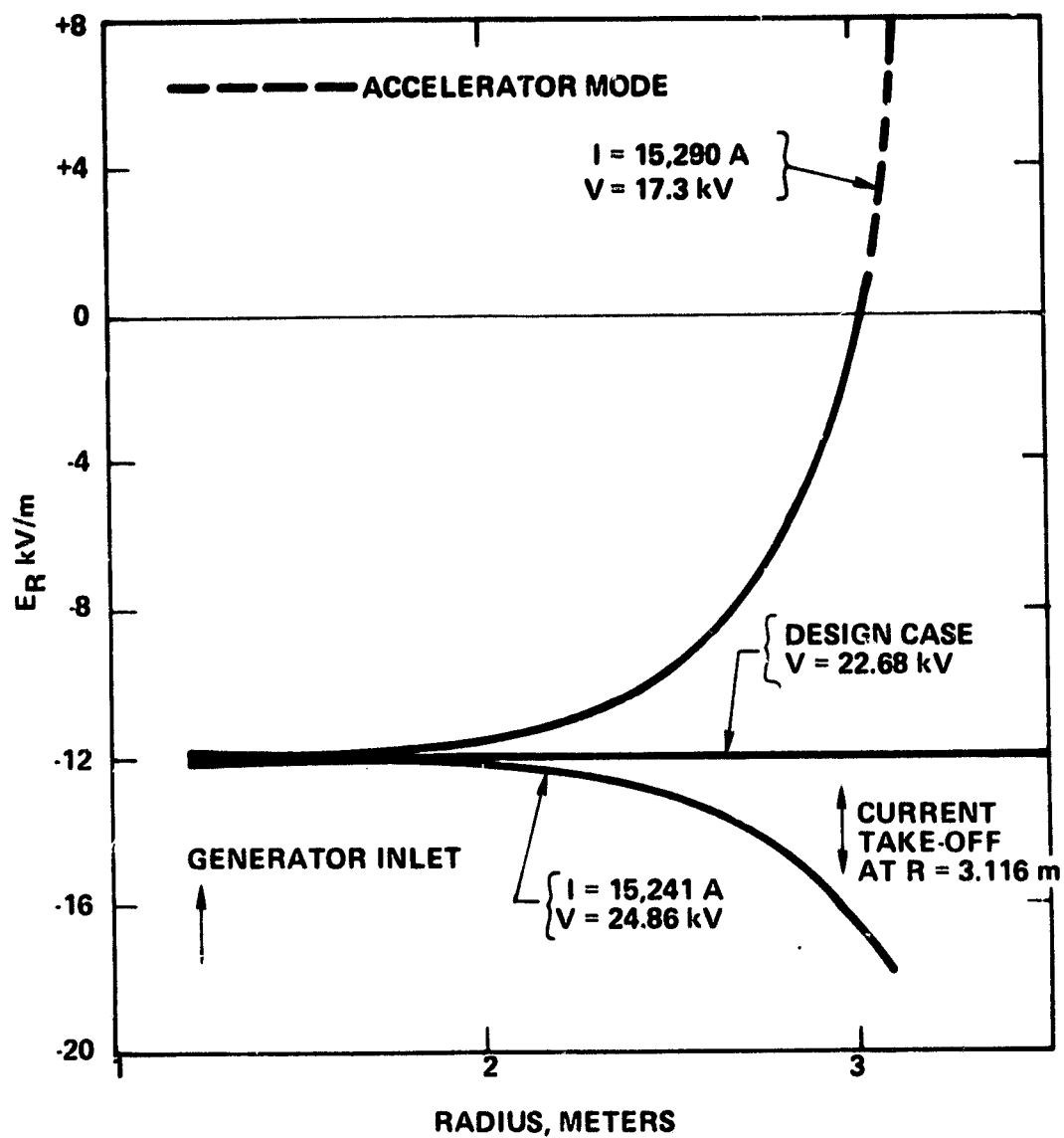


Figure 5-3-7. V-1 Characteristic for Front 3.116m of Reference Channel B = 7T ($M = 1.8$, $S = 0.5$, $P_0 = 5.52$ ATM at Inlet)



615689-11A

Figure 5-3-8. Variation of Radial Electric Field Distribution for Reference Channel (Single Load, Cathode at $R = 3.116$ m)

The sample cases shown below are based on "segmenting" the reference channel design of Tabel 5.3.1 into four parts, with current take-off electrodes in the side-walls at radii 2.216 m, 3.116 m and 3.626 m. Figure 5-3-9 shows two possible operating configurations with a front-end load current of 15,309 A, which is appreciably higher than would be acceptable for a single-load channel. The increments of current which the intermediate electrodes must handle (as percentages of the anode current) are -3.7%, +8.7% and -31.5% for the solid curves, and -3.7%, +4.8% and -20.2% for the dashed curves. The overall channel voltages and power outputs are 25.86 kV and 378.6 MW for the solid curves, and 32.66 kV, 476.4 MW for the dashed curves, respectively. Similar cases for a front-end load current of 15,192 A are shown in Figure 5-3-10; this current would force a shock system to occur in a single-load configuration. Three subcases are plotted in Figure 5-3-10; the intermediate current increments are: + 5%, +2.1%, +1.1% for the solid curves; +5%, +5.2%, -24.8% for the dashed curves; and +5%, +0.5% and +34.3% for the chain-dashed curves. The last of these three subcases is very close to the choking limit for the 4th segment, so that the electrical behavior of this segment exhibits rather high impedance ($\sim 100\Omega$) for load current variation near this critical condition. All the other subcases shown in Figures 5-3-9 and 5-3-10 are well behaved, and analysis of the current voltage relationships over the range examined reveals the following impedance levels:

Segment 1	(1.226 < R < 2.216)	9.7 ± 0.1 ohms
Segment 2	(2.216 < R < 3.116)	14.0 ± 0.3 ohms
Segment 3	(3.116 < R < 3.626)	5.3 ± 0.6 ohms
Segment 4	(3.626 < R < 4.106)	7.5 ± 2.5 ohms

While the control system for such a generator will present a nontrivial design problem, it is clear that segmenting of this nature will permit operation with reasonable impedance levels. Further investigation of this aspect of both disk and linear generator designs is urgently required. The limited study described above indicates that load variation in a disk generator is feasible. One tentative conclusion which may be drawn from the distribution of impedance levels over the four segments: it seems likely that achievement of uniform impedance values along the channel will require a monotonic decrease of segment length from inlet to outlet.

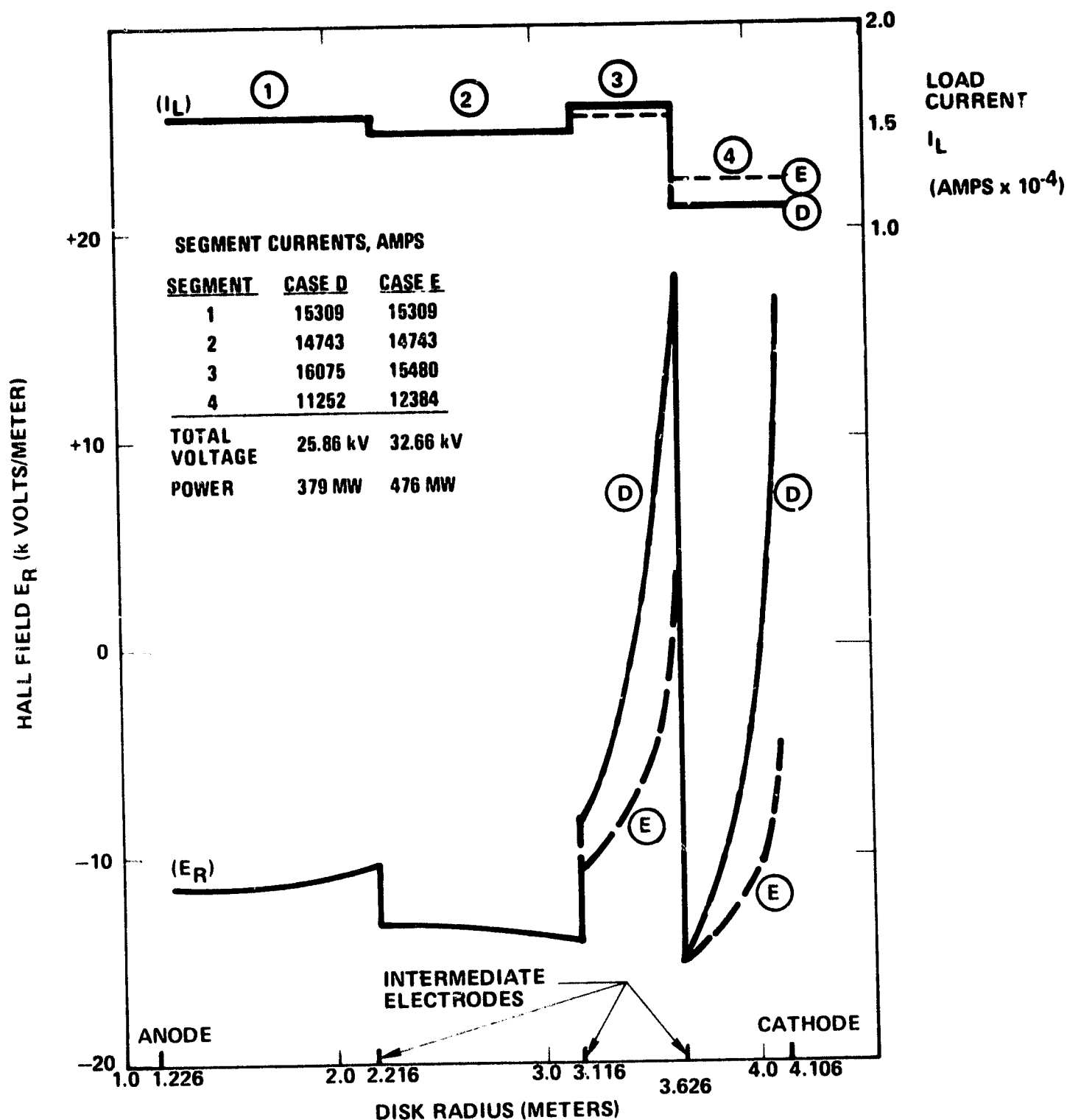


Figure 5-3-9. Off-Design Electrical Performance of Segmented Disk Generator

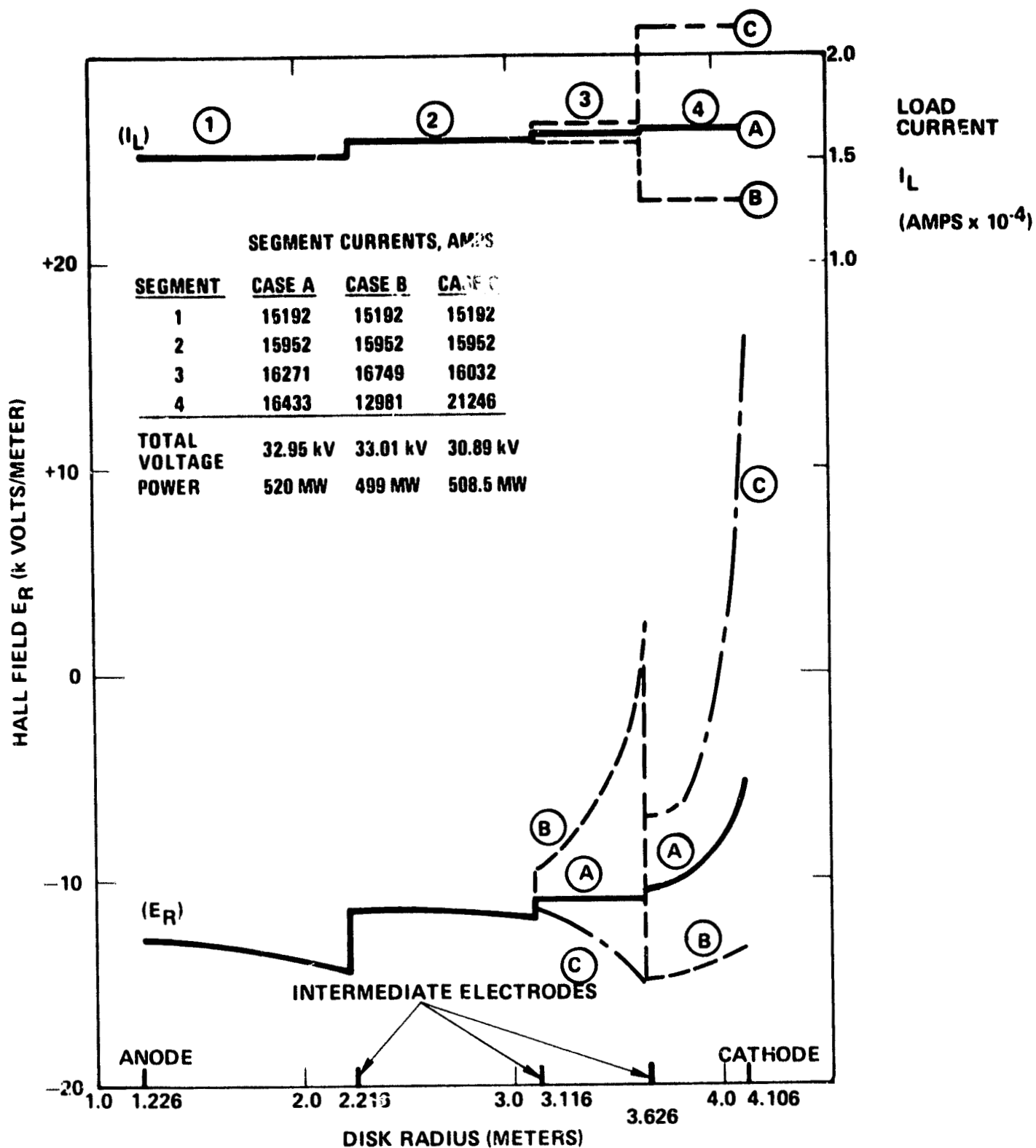


Figure 5-3-10. Off-Design Electrical Performance of Segmented Disk Generator

The above discussion contains no mention of open-circuit voltage across the entire channel. This is because the study was restricted to variations of electrical loading which could be sustained without change of plasma inlet conditions to the channel (although such variations would in general affect the plasma exit conditions, and therefore require eventual adjustment of inlet conditions to attain a new steady-state operating point). Attempts to run open-circuit on any of the four segments of the reference channel immediately indicated that choking would occur, brought about by a 5- to 10-fold increase in the $j_\theta \times B$ braking force which occurs when j_r is reduced to zero. Thus, it will be essential for the overall electrical control system for a disk generator to handle loss of load by prompt reduction of the energy released in the combustor.

5.3.5 ADDITIONAL PARAMETRIC VARIATIONS

The performance of open-cycle disk generators considered in this study has been shown to be "optimized", at least for the single-load disk, by application of the constant radial E-field constraint. The preceding section demonstrated the necessity of providing intermediate electrodes between the anode and cathode of a disk generator, in order to provide for more controllable operation. The presence of intermediate electrodes permits the use of design constraints other than the constant E-field constraint, which could potentially provide enhanced disk performance. Additional disk performance calculations were thus made, in order to explore the differences between single-load and multi-load disks with differing design constraints.

This subsection also contains the results of performance evaluations made with increasing axial magnetic field components from inlet to outlet radius, thus providing some indication of performance potential for the case of an advanced disk generator design similar to that discussed in Sections 6.1.4 and 6.3.5.2. This advanced type of disk generator is configured to utilize the available magnetic field of the single coil disk magnet more efficiently.

One further parametric variation related to the magnetic field was carried out. In this evaluation, a uniform magnetic field intensity of 12 T was assumed, providing a limited assessment of potential performance for fields not presently

attainable with linear magnets of large size, but potentially achievable from single coil disk magnets without substantial reworking of force containment structure design.

As a final parametric case, the results of assuming a higher overall plasma conductivity than that calculated by the properties codes used throughout the remainder of the study were determined. To effect a simple estimation of the effects of higher conductivity, a constant enhancement factor was applied to the normally-calculated values.

5.3.5.1 Evaluation of Disk Generator Load Factor Control with Segmentation

Given the requirement for providing intermediate electrodes in the open-cycle disk generator for off-design operational control purposes, it is relevant to inquire about the potential benefits which could arise from the use of these electrodes to permit load factor control throughout the generator. To provide information bearing upon this subject, a series of disk generator performance calculations were carried out with various design constraint approaches and segmentation lengths assumed. In order to simplify these calculations, it was decided to utilize a fixed segmentation length in each case, rather than vary the segmentation lengths as was shown in Section 5.3.4 to be most appropriate with respect to off-design-point control considerations.

Two slightly different approaches to load factor control were used. In one case, the electrical loading at the beginning of each segment was adjusted to provide:

$$K = 0.9 K_{opt}$$

The load current was then held constant across each segment; at the beginning of the next step the electrical loading was again reset to 90% of optimum, and the resulting load current maintained across this segment. With very fine segmentation chosen (0.03 m) this design mode is analogous to the procedure used in designing segmented linear MHD channels.

A second approach to segmentation of the disk was also considered, using much coarser segmentation which could result in a requirement for many fewer electrodes, thus maintaining a simple disk configuration. The load current in each

segment was established by setting the radial electric field intensity to a preselected maximum value at the inner radius of each segment. In order to calculate the fluid and electrical properties at each radial position in the segment a design constraint was then applied in which the load factor K was progressively forced to approach its optimum value achieving 93 to 95 percent of the optimum at the end of the segment. The load current required to restore the electric field to its previous maximum value was then recalculated and set as the current for the succeeding segment.

Comparison of numerous calculational cases using both the very fine and the much coarser segmentation, with the appropriate constraint on load factor, revealed that the fine segmentation gave very little performance improvement over the coarse segmentation, which in itself represents a more satisfactory configuration from the disk generator engineering standpoint. The addition of interface losses between segments in a very finely segmented disk generator (not considered in these comparison calculations) would most probably result in a clear delineation of the superiority of the coarsely-segmented disk for power system applications.

With this result in mind, the performance survey was redirected to determine the potentialities of the coarsely segmented disk, using plasma properties and diffuser constraints typical of the base case values previously discussed. Table 5.3.2 contains the results of several calculations for OCD designs covering the ranges:

$$1.7 \leq [\text{Mach No}] \leq 1.9$$

$$0.5 \leq [\text{Swirl}] \leq 2.0$$

for selected values of combustor stagnation pressure and segmentation. In each case the magnetic field was held constant at 7 T, with inlet enthalpy at 0.9475 MJ/kg before guide vane losses. The guide vane losses in each case were modeled identically, using the expressions given in Section 5.1.2 with:

$$L_{p2} = 0.025;$$

$$L_{h2} = 0.01.$$

The diffuser exit stagnation pressure was set at 1.068 atmospheres, and the recovery coefficient was taken to be $C_p = 0.6$.

TABLE 5.3.2

DISK GENERATOR PERFORMANCE SURVEY
EFFECT OF LOAD FACTOR CONTROL IN SEGMENTED DISKS

(See Text, Section 5.3.5 for Discussion)

Combustor Exit Enthalpy: 0.9475 MJ/kg before IGV losses

Diffuser Exit Condition: $P_0 = 1.068$ atm with $C_p = 0.6$

Magnetic Induction: 7 Tesla

Design Constraint

for Groups A, B, C: K (segment) approaching 0.95K opt with E_r (initial) = E max

Group A - 0.5m Segmentation, $P_0 = 6$ ATM before IGV losses

PO	INLET S	M	RMAX (M)	NET P (MW)	POWER (MW)	HT. LOSS (MW)	ENTH. EXTR.	ISEN EFFCY	ELEC EFFCY	EMAX (KV/M)	VOLTAGE (KV)	EXIT PO	M
6.00	0.50	1.70	4.306	410.16	553.54	33.98	18.59	67.85	72.02	12.000	36.770	1.068	1.167
6.00	1.00	1.70	4.594	420.42	563.80	37.69	18.94	70.18	74.36	12.003	37.944	1.067	1.129
6.00	1.50	1.70	4.803	420.21	563.59	40.11	18.93	71.17	75.54	12.023	38.585	1.067	1.093
6.00	2.00	1.70	4.981	414.73	558.11	42.15	18.75	71.66	76.11	12.038	38.957	1.067	1.061
6.00	0.50	1.80	5.034	425.91	569.29	40.80	19.12	69.66	75.19	12.000	43.534	1.068	1.257
6.00	1.00	1.80	5.332	434.62	578.00	44.49	19.42	71.51	77.42	12.006	44.780	1.068	1.221
6.00	1.50	1.80	5.571	435.13	578.51	47.29	19.43	72.42	78.69	12.034	45.641	1.068	1.193
6.00	2.00	1.80	5.775	431.21	574.59	49.53	19.30	72.84	79.40	12.059	46.278	1.068	1.148
6.00	0.50	1.90	5.780	428.89	572.27	49.31	19.22	70.03	77.61	12.036	51.773	1.068	1.281
6.00	1.00	1.90	6.190	436.11	578.49	54.32	19.47	71.86	79.99	12.175	53.437	1.068	1.281
6.00	1.50	1.90	6.501	435.41	578.79	57.88	19.44	72.34	81.29	12.954	54.789	1.068	1.281
6.00	2.00	1.90	6.787	431.51	574.69	61.20	19.30	72.81	82.14	12.080	55.890	1.068	1.281

Group B - 0.5m Segmentation, $P_0 = 7$ ATM before IGV losses

PO	INLET S	M	RMAX (M)	NET P (MW)	POWER (MW)	HT. LOSS (MW)	ENTH. EXTR.	ISEN EFFCY	ELEC EFFCY	EMAX (KV/M)	VOLTAGE (KV)	EXIT PO	M
7.00	0.50	1.70	4.654	413.66	573.15	41.79	19.25	64.75	69.76	12.000	42.945	1.068	1.137
7.00	1.00	1.70	5.003	423.49	582.98	46.87	19.58	66.68	71.12	12.002	44.502	1.068	1.111
7.00	1.50	1.70	5.208	422.02	581.51	49.89	19.53	67.45	72.09	12.019	45.121	1.068	1.077
7.00	2.00	1.70	5.365	415.14	574.63	52.36	19.30	67.64	72.44	12.004	45.373	1.068	1.043
7.00	0.50	1.80	5.551	432.21	591.70	51.59	19.88	66.52	72.51	12.000	51.322	1.068	1.233
7.00	1.00	1.80	5.882	439.95	595.44	56.51	20.14	68.11	74.01	12.006	52.805	1.068	1.209
7.00	1.50	1.80	6.124	439.52	595.01	59.87	20.12	68.83	75.70	12.032	53.852	1.068	1.180
7.00	2.00	1.80	6.311	434.81	594.30	62.45	19.86	69.11	76.27	12.056	54.417	1.068	1.154
7.00	0.50	1.90	6.515	435.76	595.25	63.83	20.00	69.81	75.49	14.307	61.397	1.068	1.279
7.00	1.00	1.90	6.922	440.55	600.04	69.86	20.16	69.11	77.53	13.932	63.444	1.068	1.277
7.00	1.50	1.90	7.268	439.17	598.86	74.33	20.11	69.64	78.78	12.807	64.895	1.068	1.279
7.00	2.00	1.90	7.526	434.48	593.97	77.86	19.86	69.78	78.52	12.076	66.070	1.068	1.275

Group C - 1.0m Segmentation, $P_0 = 7$ ATM before IGV losses

PO	INLET S	M	RMAX (M)	NET P (MW)	POWER (MW)	HT. LOSS (MW)	ENTH. EXTR.	ISEN EFFCY	ELEC EFFCY	EMAX (KV/M)	VOLTAGE (KV)	EXIT PO	M
7.00	0.50	1.70	4.656	413.05	572.54	41.96	19.23	64.71	68.73	12.000	42.758	1.068	1.132
7.00	1.00	1.70	4.946	419.59	578.08	46.69	19.45	66.42	70.72	12.002	43.336	1.067	1.084
7.00	1.50	1.70	5.153	417.84	577.33	49.80	19.39	67.21	71.72	12.019	43.868	1.067	1.047
7.00	2.00	1.70	5.317	410.07	569.56	52.15	19.13	67.49	72.21	12.002	44.426	1.062	1.018
7.00	0.50	1.80	5.483	430.08	589.57	51.12	19.81	66.33	72.14	12.000	50.059	1.068	1.209
7.00	1.00	1.80	5.768	436.37	595.86	55.62	20.02	67.84	74.03	12.006	50.876	1.068	1.167
7.00	1.50	1.80	6.002	435.59	595.07	58.98	19.99	68.59	75.15	12.032	51.764	1.067	1.135
7.00	2.00	1.80	6.209	430.84	590.43	61.71	19.83	68.92	75.83	12.056	52.641	1.067	1.110
7.00	0.50	1.90	6.472	435.29	594.78	63.80	19.86	68.86	75.20	12.927	59.428	1.068	1.282
7.00	1.00	1.90	6.803	440.32	599.81	69.69	20.15	69.09	77.05	12.009	60.548	1.068	1.261
7.00	1.50	1.90	7.080	439.01	598.50	72.83	20.10	69.83	78.21	12.036	61.873	1.068	1.237
7.00	2.00	1.90	7.353	434.25	593.74	76.43	19.85	69.80	78.88	12.076	63.314	1.068	1.220

Group D - Constant Radial E-Field Design, $P_0 = 7$ ATM before IGV losses

PO	INLET S	M	RMAX (M)	NET P (MW)	POWER (MW)	HT. LOSS (MW)	ENTH. EXTR.	ISEN EFFCY	ELEC EFFCY	EMAX (KV/M)	VOLTAGE (KV)	EXIT PO	M
7.00	0.50	1.70	4.559	409.61	589.10	40.91	19.12	64.46	68.30	12.000	42.255	1.068	1.110
7.00	1.00	1.70	4.558	401.19	580.87	42.79	19.83	65.22	68.89	12.002	40.615	1.068	1.015
7.00	1.50	1.70	4.582	370.92	530.41	44.56	17.82	65.62	69.69	12.003	38.007	1.177	1.000*
7.00	2.00	1.70	4.717	349.51	509.00	46.78	17.10	66.03	70.64	12.002	38.707	1.253	1.000*
7.00	0.50	1.80	5.104	423.82	583.41	46.68	19.60	65.63	70.96	12.001	48.173	1.068	1.155
7.00	1.00	1.80	5.177	422.88	582.47	49.01	19.57	66.93	72.05	12.003	47.349	1.068	1.071
7.00	1.50	1.80	5.371	417.60	577.09	52.11	19.39	67.52	72.95	12.003	47.667	1.074	1.024
7.00	2.00	1.80	5.618	411.17	570.66	55.38	19.17	67.86	73.75	12.003	48.622	1.075	1.000*
7.00	0.50	1.90	5.891	434.54	594.03	56.16	19.95	66.80	73.94	12.001	56.808	1.068	1.224
7.00	1.00	1.90	6.036	437.18	598.67	59.93	20.04	67.98	75.32	12.003	56.842	1.068	1.157
7.00	1.50	1.90	6.282	434.17	593.66	62.64	19.94	68.53	76.35	12.003	57.697	1.068	1.122
7.00	2.00	1.90	6.571	428.67	586.16	66.01	19.76	68.71	77.17	12.003	58.037	1.068	1.104

* Choked Flow

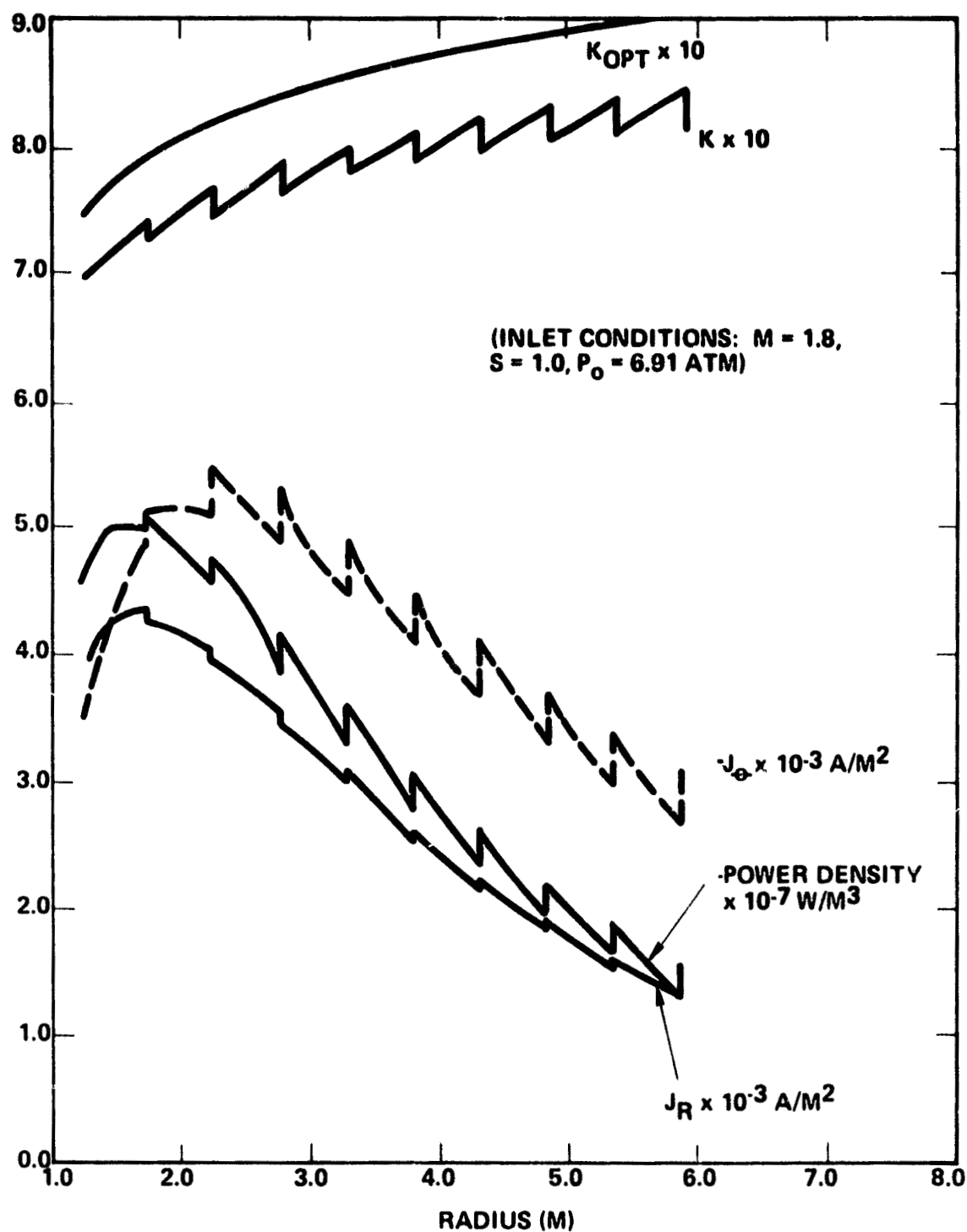
Group A in Table 5.3.2 summarizes the results of calculations for $P_0 = 6$ atmospheres and a segmentation of 0.5 meter, using the design constraint which sets $E_r =$ some maximum value at the inner segment radius. (In most cases, $E_r(\text{max}) = -12 \text{ kV/m}$).

Group B presents the results of an identical set of calculations, made with the higher inlet stagnation pressure $P_0 = 7$ atmospheres. There is less than a 1% net power increase resulting from the change to higher stagnation pressure, but a significant increase in R_{max} (disk outer radius) in each case.

Group C contains the results of calculations for $P_0 = 7$ atmospheres and a segmentation of 1 meter. In comparison to Group B results, there is almost a negligible decrement in net power output with no significant differences in generator size in comparable cases, aside from the higher-swirl comparisons.

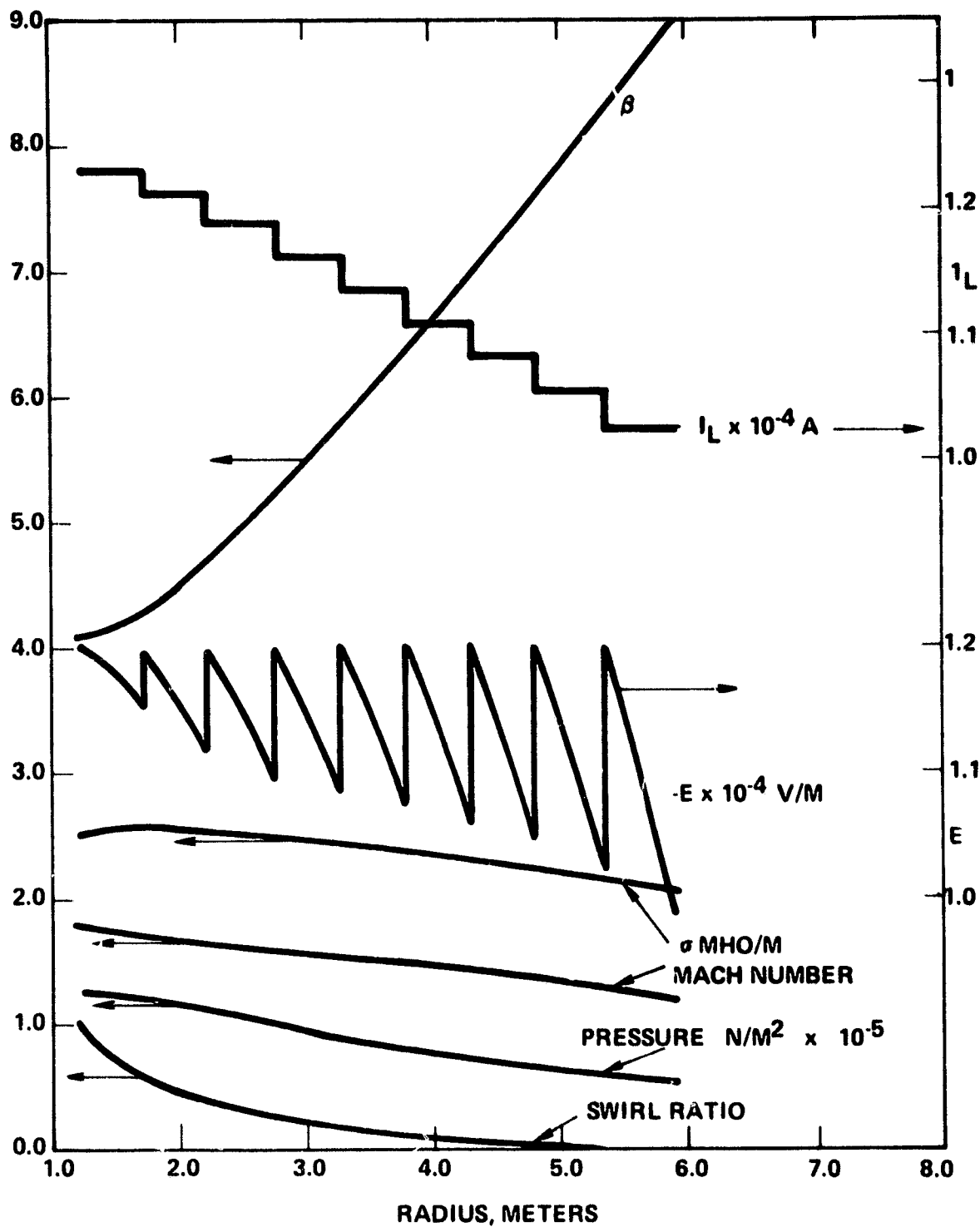
As a control, Group D was prepared to permit direct comparison of the results obtainable with the constant radial E-field constraint applied with no segmentation. In high swirl cases at the lower values of inlet Mach number, choking at the generator exit was predicted. In those cases for which the diffuser constraints were fully met, less than a 1 percent net MHD power decrement with a simultaneous decrease in R_{max} was shown, in comparison to the Group C results. Clearly, the constant E-field constraint can provide a generator design with reasonable power output while minimizing disk generator (and thus magnet) diameter, at least in the case of lower swirl values.

The electrical and fluid properties for a generator with 0.5 meter segmentation are shown in Figures 5-3-11 and 5-3-12, as an example of the load factor control design constraint for the open-cycle disk generator. The load current variation across the disk is from 12.3 kA to 10.2 kA, while the overall voltage is 52.9 kV. For the purposes of the study, it was concluded that no major benefit in either power output or generator down-sizing could accrue from application of the load factor control design constraint, relative to disk generators designed with the constant radial E-field constraint. Therefore, the conceptual design of the disk generators for the "optimized" OCD power



615689-14A

Figure 5-3-11. Electrical Loading Parameters Within Segmented Generator
(Inlet Conditions: $M = 1.8$, $S = 1.0$, $P_0 = 6.91 \text{ atm}$)



615689-15A

Figure 5-3-12. Electrical & Fluid Parameters Within Segmented Generator
(Inlet Conditions: $M = 1.8$, $S = 1.0$, $P_0 = 6.91 \text{ Atm}$)

systems was performed by applying the constant radial E-field constraint. Segmentation was provided, but only for off-design control purposes.

5.3.5.2 MAGNETIC FIELD EFFECTS

Additional parametric variations concerned with specific magnet field intensity/shape changes were also performed in parallel with the investigations of the effects of load factor control. The first represented an attempt to evaluate the performance potential inherent in the more efficient utilization of the disk magnet magnetic field. The flat plate magnet designs discussed in Section 6.3 have resultant field intensities approaching 10 T near the exit of the channel. It is conceivable that a channel configuration could be provided having a curvilinear flow pattern normal to the resultant magnetic field vector of the magnet at all radii, thus providing an increasing magnetic field intensity from inlet to outlet, without significantly increasing the requirement for superconducting material over that for a flat disk magnet. Group A of Table 5.3.3 contains performance calculation results for channel designs having magnetic field variation like Figure 2-1-3. The electric field restriction was modified so that E_r could be allowed to reach values as high as 21 kV/m to take advantage of the increases in field intensity near the channel exit. The actual limiting values were given by:

$$\begin{aligned} E_{\max} &\leq 4 \beta \text{ or} \\ E_{\max} &\sim 20 \text{ kV/m.} \end{aligned}$$

The 4 criterion was discussed in Section 5.1.7.

A segmentation of 0.5 meter was assumed for comparison with Group B of Table 5.3.2. Enthalpy extraction of 22 percent with 74 percent isentropic efficiency is attainable without IGVs in the high Mach number cases, and this without relaxation of any inlet or exit constraints except the 12 kV/m electric field limitation. Significant decreases in R_{\max} (in this case equivalent to the length of the flow path segment normal to the resultant magnetic field) with over a 10 percent increase in MHD net power were obtained. The off-design-point performance of such generators has not been investigated, nor have

TABLE 5.3.3

DISK GENERATOR PERFORMANCE SURVEY
SENSITIVITY OF DISK PERFORMANCE TO MAGNETIC FIELD
AND PLASMA CONDUCTIVITY VARIATIONS

(See Text, Section 5.3.5 for Discussion)

Combustor Inlet Enthalpy: 0.9475 MJ/kg before IGV losses

Diffuser Exit Condition: $P_o = 1.068$ ATM with $C_p = 0.6$

Group A: Efficient Magnetic Field Utilization

B: 7 - 11 Tesla

Segmentation: 0.5m

E max Not to exceed lesser of 48 or 21 kV/m													
PO	INLET S	M	RMAX (M)	NET P (MW)	POWER (MW)	HT. LOSS (MW)	ENTH. EXTR.	ISEN EFFCY	ELEC EFFCY	EMAX (KV/M)	VOLTAGE (KV)	PO	EXIT M
7.00	0.50	1.70	3.915	488.41	642.80	28.25	21.80	72.88	78.18	20.430	53.888	1.068	1.147
7.00	1.00	1.70	4.228	478.00	638.49	33.38	21.48	72.87	78.88	20.306	55.284	1.068	1.135
7.00	1.50	1.70	4.878	478.82	638.31	37.43	21.28	73.88	77.80	20.255	58.123	1.068	1.137
7.00	2.00	1.70	4.813	472.77	632.28	41.08	21.24	73.88	78.70	20.227	61.088	1.068	1.143
7.00	0.50	1.80	4.884	484.01	652.80	32.83	21.88	73.88	78.11	20.381	52.730	1.068	1.208
7.00	1.00	1.80	4.880	488.25	647.74	38.88	21.78	73.88	78.73	20.268	54.485	1.068	1.191
7.00	1.50	1.80	5.021	488.83	643.32	40.88	21.81	73.88	78.81	20.223	57.472	1.068	1.188
7.00	2.00	1.80	5.388	477.88	637.08	44.88	21.40	73.81	80.28	20.203	70.661	1.068	1.184
7.00	0.50	1.90	4.848	488.88	658.48	37.34	22.12	74.01	78.78	20.332	72.135	1.068	1.258
7.00	1.00	1.90	5.188	482.88	652.07	41.72	21.80	74.02	80.44	20.232	75.183	1.068	1.248
7.00	1.50	1.90	5.580	488.03	645.52	48.18	21.88	74.01	81.23	20.188	78.888	1.068	1.252
7.00	2.00	1.90	5.888	477.84	637.33	50.80	21.41	73.81	81.87	20.174	82.788	1.068	1.267

Group B: Enhanced Magnetic Field (B = 12 Tesla)

Segmentation: 0.3m

|E max| Not to exceed 20 kV/m

PO	INLET S	M	RMAX (M)	NET P (MW)	POWER (MW)	HT. LOSS (MW)	ENTH. EXTR.	ISEN EFFCY	ELEC EFFCY	EMAX (KV/M)	VOLTAGE (KV)	PO	EXIT M
7.00	0.50	1.80	2.760	398.33	555.82	18.33	18.87	73.78	78.87	20.000	33.013	1.373	1.000*
7.00	1.00	1.80	3.857	481.42	650.81	28.38	21.88	77.81	80.30	20.000	44.183	1.122	1.000*
7.00	1.50	1.80	4.210	515.88	675.35	31.58	22.88	78.02	82.35	20.000	50.133	1.072	1.021
7.00	2.00	1.80	4.813	517.77	677.28	35.18	22.75	78.88	83.80	20.000	53.888	1.068	1.048

Group C: Enhanced Conductivity (1.5X)

Segmentation: 0.5m

Design Constraint: Same as Table 5.3.2 Groups A, B, C

PO	INLET S	M	RMAX (M)	NET P (MW)	POWER (MW)	HT. LOSS (MW)	ENTH. EXTR.	ISEN EFFCY	ELEC EFFCY	EMAX (KV/M)	VOLTAGE (KV)	PO	EXIT M
7.00	0.50	1.70	3.532	432.38	591.88	24.88	18.88	88.20	88.88	12.000	28.480	1.068	1.130
7.00	1.00	1.70	3.828	445.70	605.18	28.38	20.33	88.34	72.28	12.000	30.481	1.067	1.092
7.00	1.50	1.70	4.034	448.85	608.14	30.72	20.38	70.48	73.82	12.017	31.133	1.067	1.057
7.00	2.00	1.70	4.210	441.51	601.00	32.58	20.18	70.81	74.11	12.010	31.580	1.068	1.027
7.00	0.50	1.80	4.184	454.77	614.28	30.73	20.83	88.08	73.03	12.000	35.185	1.068	1.218
7.00	1.00	1.80	4.483	488.45	625.84	34.01	21.03	71.20	75.41	12.001	38.280	1.068	1.182
7.00	1.50	1.80	4.882	488.38	627.88	38.55	21.08	72.28	78.78	12.024	37.128	1.067	1.148
7.00	2.00	1.80	4.888	485.21	624.70	38.88	20.88	72.83	77.85	12.048	37.823	1.067	1.122
7.00	0.50	1.90	4.828	485.24	624.73	38.40	20.88	70.23	75.84	13.885	42.425	1.068	1.281
7.00	1.00	1.90	5.283	475.88	635.17	42.40	21.34	72.08	78.18	12.004	43.884	1.068	1.274
7.00	1.50	1.90	5.574	477.51	637.00	45.87	21.40	73.01	78.85	12.030	45.147	1.067	1.236
7.00	2.00	1.90	5.824	474.38	633.85	48.43	21.28	73.42	80.41	12.080	48.287	1.068	1.236

* Choked Flow

the implications of the use of this design upon the power conditioning system configuration been considered. The total voltage seen across the generator (50-90 kV) is certainly not outside the range of voltages handled by HVDC converters; however, the design of disk cooling systems will be complicated by the requirement for electrical isolation across such a large voltage difference.

Group B of Table 5.3.3 presents the results of a limited assessment of disk generator performance potential with a uniform magnetic field intensity of 12 T. Again, the disk generators are segmented (with $\Delta R = 0.3$ meter) but the calculations have indicated the need to establish a lower inlet Mach number than for previous cases. The low swirl cases presented cannot be considered optimal, since they choke before making use of all the available stagnation pressure. The extraction of power does not change dramatically with the change to higher magnetic field intensity, but the net MHD power available with $S = 1.5$ exceeds that from comparable cases with a higher Mach number and a much larger exit radius if the electric field limitation is relaxed to 20 kV/meter.

5.3.5.3 Effects of Enhanced Conductivity

While reasonable consensus on the conductivity values characteristic of coal/air combustion products has been obtained throughout the national MHD Community, the fact remains that no reliable measurements of this critical property for the plasma conditions of interest have been made to date. The possibility remains that the "effective" conductivity available in a power-generating device may be substantially different from that calculated by the current property codes. In the case of an actual deviation toward the lower values, it would be necessary to re-evaluate the viability of the supersonic disk MHD channel as an electrical power generating device. In the more desirable event that effective conductivities are found to be higher than predicted, it would be interesting to predict the incremental performance gains possible.

For this purpose, a simple conductivity enhancement factor of 1.5x was applied to the conductivities calculated for each static temperature - pressure combination by the Westinghouse version of the NASA properties code. While the

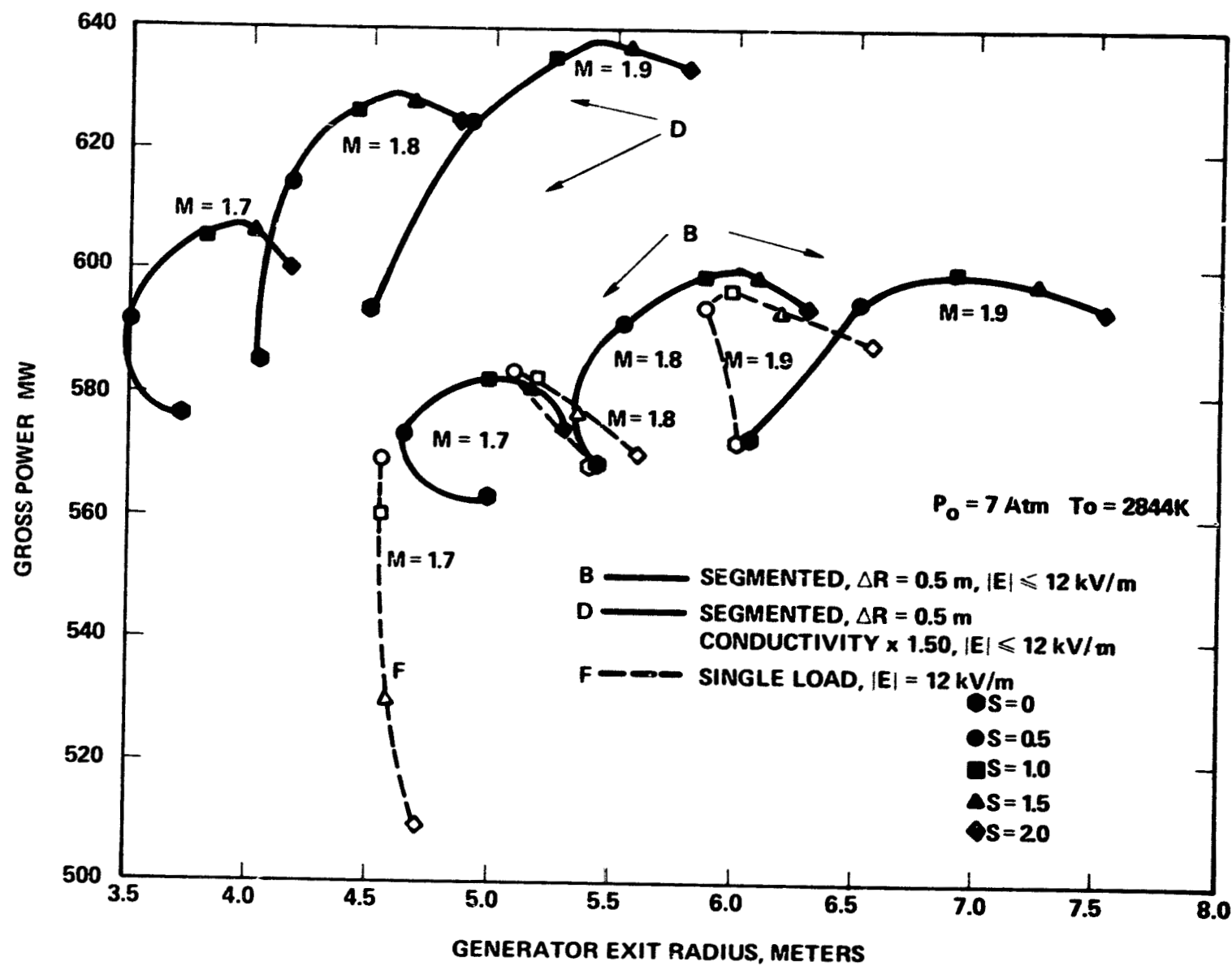
actual factors leading to a potential for higher effective conductivity in seeded coal combustion products would not result in such a universally-applicable incremental relationship, it was felt that this device could permit a quick evaluation of the effect of higher conductivity upon the size and performance relationships of disk generators. Group C of Table 5.3.3 contains the results of calculations performed for open cycle disk generators with the same design constraint as that discussed previously in Section 5.3.5.1. The plasma properties at the generator inlet, and the diffuser/guide vane constraints also remained the same. Comparison of Group B of Table 5.3.2 with Group C of Table 5.3.3 shows that the results of assuming the higher conductivity for the same inlet conditions would be:

- Greater MHD power (5-10% increases);
- Decreased disk exit radius (up to 30% smaller).

Figure 5-3-13 provides a visual summary of the comparisons between the constant radial E-field case (Group D of Table 5.3.2) and either the segmented disk with load factor control ($\Delta R = 0.5$, Group B of Table 5.3.2) or the same disk with enhanced conductivity Group C, (Table 5.3.3). The significant size and performance gains available in the enhanced conductivity cases are obvious. It would be expected that similar results could be obtained for OCD generators designed with the constant radial E-field constraint.

5.4 OPEN CYCLE DISK SYSTEMS ANALYSIS

For the open cycle portion of the Disk MHD Generator Study, it was originally intended to investigate the performance potential of two distinct system configurations, one with a directly-fired oxidant preheater subsystem, and one with a separately-fired oxidant preheater subsystem. During the course of the study, a third combustion gas MHD/steam system configuration was introduced, which was also investigated with respect to its potential performance. This additional OCD system used an oxygen-augmented combustion system with a recuperative metallic heat exchanger for oxidant preheating. The oxygen enrichment level was selected to permit the attainment of a combustor total temperature equal to that obtainable through combustion of coal in 1920 K



615689-16A

Figure 5-3-13. Open Cycle Disk Generator Performance Sensitivity to Design Constraint and Conductivity

preheated air. An advanced high-efficiency oxygen plant was assumed to furnish oxygen for enrichment of the MHD combustor oxidant.

The performance investigation was carried out in similar fashion for each type of OCD MHD/steam system. First, a set of Base Case parameters was defined; these parameters were chosen on the basis of existing information, to represent a plant with the "best" performance attainable. A series of parametric variations about the Base Case parameters for each OCD system type was then proposed. The analyses were carried out using modeling, assumptions, and constraints for OCD generators and systems as described in Sections 5.1, 5.2, and 5.3. From the results of the systems performance analyses for each OCD system type, it was then possible to define a refined set of parameters with which the OCD system was capable of achieving an optimum performance.

The system performance studies for each of the three types of OCD MHD/steam systems were also pursued in an attempt to examine the effects of variations in key system parameters upon the performance of the systems. In principle, the attainment of an optimum system design requires the simultaneous modification of several parameters to obtain a new and better set of performance conditions. For example, an increase in performance may be obtained through an increase in MHD combustor oxidant preheat temperature, but to obtain maximum benefit from this change, it may also be necessary to increase channel inlet total pressure and Mach number at the same time. However, it would be extremely time-consuming to perform numerous system optimization calculations each time a single parameter variation is to be carried out in the system sensitivity studies. It may also be difficult to interpret the impact of each parameter upon overall system performance when several are varied in combination.

In the present study, it was decided to adopt the approach in which selected parameters were singly, perturbed from their Base Case values, as long as the basic disk generator design constraint could remain unaffected, and the system performance was not drastically affected. When a parameter variation clearly required a different design criterion in order to obtain a reasonably

equivalent performance to that of the Base Case, a new design criterion was applied and more than one characteristic or parameter was varied. One example of this latter process is to be found in the evaluation of subsonic disk system performance. While the constant radial Hall field constraint best serves the design of supersonic disk generators, it was determined that a constant velocity or constant Mach number design criterion was more suitable for evaluation of subsonic channel performance.

The details and results of system parametric analyses for each of the stipulated OCD MHD/steam power systems are to be found in Subsection 5.4.1 through 5.4.3, following. Subsection 5.4.4 contains the design details, parameter selections, and calculated performance for optimized OCD system of each type.

5.4.1 OCD DIRECTLY- FIRED SYSTEMS

The basic configuration of the OCD directly-fired MHD/steam power system used in the evaluation of Disk MHD System performance has been described in Section 4.1.1. The salient Base Case system parameters, and the systems parametric analyses performed by variation of specific parameters about the Base Case values, are described in 5.4.1.1 and 5.4.1.2.

5.4.1.1 Delineation of Base Case Conditions

Table 5.4.1 presents the values of all key parameters that define the OCD directly-fired system Base Case (Case 1-1 in the table). A nominal fuel thermal input to the MHD combustor of 2000 MW_t was specified, corresponding to a power level of 900 MW_e (approximately the size of the largest modern coal-fired central power stations). The base fuel was taken to be Montana Rosebud subbituminous coal, dried to 5 percent moisture by weight, pulverized, and burned in air preheated to 1920 K. The combustor has been assumed to be a 2-stage high-exit-swirl slagging type, with 90 percent ash rejection. The combustor operates at a stoichiometric ratio of 0.95 to reduce the production of NO_x in the combustion gas.

TABLE 5.4.1
PARAMETRIC VARIATIONS FOR OGD DIRECT-FIRED HTAH

	1-1 Base Case	1-2	1-3 Half Power Level	1-4 T _w =1600K Coal	1-5 111 #6 Coal	1-6 T _{preheat} = 1810 K	1-7 1650 K + O ₂	1-8 1650 K Mach=0.85	1-9 Swirl=0	1-10 Swirl=1.0	1-11 Diffuser Pressure Recovery Factor=0.6	1-12 Maximum Hall Field = 8 kv/m	1-13 Maximum Hall Field = 16 kv/m	1-14	1-15	1-16 B = 6 Tesla	1-17 B = 8 Tesla	1-18 B = 12 Tesla	1-19 COMBUSTOR ΔP/P in = 0.10	1-20 Joules Power Level
1. Plant Size (MW _e)	2040	-	1020	2040	-	-	-	-	-	-	-	-	-	-	-	2040	-	-	-	-
2. Coal Type	Montana Rosebud Subb.	-	Montana Rosebud Subb.	-	111 #6 HVCB	Montana Rosebud Subb.	-	-	-	-	-	-	-	-	-	-	-	-	-	-
3. MHD Combustor/nozzle Combustor type	2-stage cyclone	-	2-stage cyclone	-	-	-	-	-	-	-	-	-	-	-	-	-	-	-	-	-
Oxidizer	Air	-	Air	-	-	Air	Enriched Air (32.5 wt % O ₂)	Air	-	-	-	-	-	-	-	-	-	-	-	-
Fuel moisture as fired (%)	5	-	5	-	-	-	-	-	-	-	-	-	-	-	-	-	-	-	-	-
Stoichiometric ratio	0.95	-	0.95	-	-	-	-	-	-	-	-	-	-	-	-	-	-	-	-	-
Ash removal (%)	90	-	-	-	-	-	-	-	-	-	-	-	-	-	-	-	-	-	-	-
Seeding level (%)	0.7	-	-	-	1.0	0.7	-	-	-	-	-	-	-	-	-	-	-	-	-	-
Fractional pressure loss, ΔP/P in	0.08	-	-	-	-	-	-	-	0.10	-	0.06	-	-	-	-	-	-	-	0.16	0.46
Fractional heat loss, ΔQ/HHV	0.07	-	-	-	-	-	-	-	0.075	-	0.07	-	-	-	-	-	-	-	-	-
4. MHD Generator/Diffuser generator type	2-terminal radial out flow	-	-	-	-	-	-	-	-	-	-	-	-	-	-	-	-	-	-	-
Mode of generator operation	Constant radial field	-	-	-	-	-	-	Constant Velocity	Constant Radial Field	-	-	-	-	-	-	-	-	-	-	-
Magnetic induction (Tesla)	7	-	-	-	-	-	-	-	-	-	-	-	-	-	-	6	8	12	7	7
Inlet total temp. (K)	2835	-	2835	2835	2833	2797	2950	2740	2835	2825	2835	2835	2835	-	-	2835	2835	2835	2835	2835
Inlet total pressure (atm)	5.73	-	5.73	5.73	5.73	5.73	9.41	5.73	5.73	5.60	5.73	5.73	5.73	-	-	5.73	5.73	5.73	5.73	5.73
Inlet Mach number	1.8	-	-	-	-	-	-	0.85	1.8	-	-	-	-	-	-	-	-	-	-	-
Inlet swirl	0.5	-	-	-	-	-	-	0	1.0	-	0.5	-	-	-	-	-	-	-	-	-
Use of inlet guide vanes	No	-	-	-	-	-	-	-	Yes	-	No	-	-	-	-	-	-	-	-	-
Inlet current loading factor	0.78	-	-	0.78	0.76	0.77	0.70	0.55	0.78	0.74	0.78	0.85	0.70	-	-	0.70	0.83	0.92	0.78	0.78
Maximum Hall field (kv/m)	12	-	-	-	-	-	-	5.6	-	-	-	8	16	-	-	12	-	-	-	-
Generator wall temp (K)	2000	-	-	1600	2000	-	-	-	-	-	-	-	-	-	-	-	-	-	-	-
Diffuser pressure recovery coeff.	0.45	-	-	-	-	-	-	-	-	-	0.6	0.45	-	-	-	-	-	-	-	-
Diffuser exit pressure (atm)	1.07	-	-	-	-	-	-	-	-	-	-	-	-	-	-	-	-	-	-	-
5. MHD Component Cooling	Separate cooling loop	-	-	-	-	-	-	-	-	-	-	-	-	-	-	-	-	-	-	-
6. Oxidizer Preheat HTAH (K)	1920	-	-	-	-	1810	1650	1650	1920	-	-	-	-	-	-	-	-	-	-	-
LTAH (K)	922	-	-	-	-	-	-	-	-	-	-	-	-	-	-	-	-	-	-	-
7. Bottoming Plant Steam conditions	3500 psi/ 1000 F/ 1000 F	-	-	-	-	-	-	-	-	-	-	-	-	-	-	-	-	-	-	-
Steam extractions	none	-	-	-	-	-	-	-	-	-	-	-	-	-	-	-	-	-	-	-
Condenser pressure (in hg absolute)	2.0	-	-	-	-	-	-	-	-	-	-	-	-	-	-	-	-	-	-	-
Final combustion gas stoichiometry	1.05	-	-	-	-	-	-	-	-	-	-	-	-	-	-	-	-	-	-	-
Stack gas temp. (K)	408	-	-	-	-	-	-	-	-	-	-	-	-	-	-	-	-	-	-	-
8. Sulfur Emission Control	Seed re- generation	-	-	-	-	Flue Gas Seed re- Scrubber generation	-	-	-	-	-	-	-	-	-	-	-	-	-	-

The selection of 1920 K preheat temperature represents an optimistic but potentially achievable temperature. Since the disk generator was expected to operate at supersonic flow conditions for optimal performance, the gas static temperature throughout the channel would be appreciably lower than that for a subsonic linear generator. Therefore, a high preheat temperature was selected to attain maximum combustor total temperature so as to explore the disk performance potential. Based on a 7% combustor heat loss and 8% pressure drop, a combustor exit total temperature of 2835 K was calculated at an exit pressure of 5.73 atm which was established from system pre-optimization analyses.

The disk suboptimization study had confirmed that a generator inlet Mach number of 1.8 and swirl of 0.5 would give adequate channel performance with a reasonable disk size. These disk parameters were thus selected for the base case. The channel design was based on a constant Hall field (radial direction) criterion, which was found to yield the best channel performance for a given disk size. A constant Hall field of 12 kV/m was assumed.

The gas flow exhausting from the generator goes through a transition from the supersonic to subsonic regime with an assumed normal shock loss and is then decelerated in a diffuser with a assumed pressure recovery coefficient (C_p) of 0.45. The pressure at the diffuser exit is fixed at 1.07 atm (1 psi above ambient).

In the radiant (slag) furnace, the combustion gases are cooled to 2150 K to permit condensation of slag vapors and their removal from the gas flowstream. Secondary air at ambient conditions is injected at the exit of the radiant furnace to complete the combustion process, with the final stoichiometry being 1.05.

The gases are then cooled to 611 K (640°F) by passing through the HTAH, reheater, superheater, LTAH and high temperature economizer. At this point, an electrostatic precipitator is provided to collect seed and flyash particles, and induced draft fans are used to maintain the required pressure balance. Part of the gas then flows to the coal processing subsystem for coal drying,

and the rest passes through a low temperature economizer. Both streams are exhausted to the stack at 408 K (275°F). Seed is primarily recovered from the combustion gas stream in a radiant heat exchange section (seed furnace) just downstream of the HTAH, which forms part of the reheater heat exchange surface. Additional seed recovery is provided, as noted above, by the downstream precipitator.

For one set of OCD directly-fired systems parametrics, the MHD components were assumed to be cooled with a separate low pressure cooling water loop. The purified cooling water is passed in series through disk, diffuser, and combustor cooling loops. Sufficient cooling water is circulated to limit the maximum fluid temperature to 425 K. Part of the thermal energy rejected by the MHD components can be recovered by the bottoming plant feedwater in a recuperator. The rest is rejected to a cooling tower.

The separate MHD component cooling loop has been recommended previously by Westinghouse for use in potential commercial MHD/steam power system applications. The reasoning for such a recommendation is as follows:

- Use of a separate system which permits limited cooling water temperature and close control of electrical conductivity through water treatment will minimize design and materials problems for the electrical insulation provisions between the MHD components, which operate at high voltage differences from ground, and the grounded portions of the system.
- The use of condensate and feedwater pumping systems to drive flow through the MHD component cooling lines can be expected to exacerbate feedwater control problems, and will increase the number of potential failure modes leading to significant effects on topping cycle components. Failures occurring in bottoming plant components can lead to serious damage in the channel, combustor, or diffuser with an in-line type of component cooling system.
- The compatibility of water chemistry requirements for the bottoming plant heat exchange surfaces and those for the MHD components has not been determined. Incompatibility can lead to accelerated corrosion and failures in either set of equipment.

In order not to unduly penalize the disk generator system performance with respect to linear systems, the majority of which have been studied with an in-line (direct feedwater) MHD component cooling system, it was decided to perform the OCD system parametrics with the in-line MHD component cooling system as well as with the separate cooling system initially proposed.

To recover the maximum amount of useful work from the topping cycle exhaust gases, a bottoming plant using a supercritical single-reheat steam cycle was assumed. For the case of a separate MHD component cooling system, the condensed working fluid first passes through a recuperator to recover most of the thermal energy rejected to the cooling loop, at 400 K. (With an in-line component cooling arrangement, condensate is first used to cool the disk generator and diffuser walls directly.) The heated condensate is then pumped to an intermediate pressure and enters the low temperature economizer and the HTAH valve cooling system for further energy recovery. After being pumped to high pressure, the fluid is heated to 811 K by successively passing through the high temperature economizer, radiant furnace waterwalls, and "superheater" section. (For the direct MHD component cooling case, bottoming plant working fluid leaving the high temperature economizer is passed through the combustor cooling system and the diffuser splitter vanes to effect heat recovery and cooling in each component, before entering the radiant furnace section). After expanding through the ac generator high pressure turbine, the bottoming plant working fluid is reheated to 811 K to condition it to drive the ac generator low pressure turbine and the MHD cycle compressor turbine. Steam is also used to drive the high pressure boiler feed pump turbines. The exhaust from each of the last three turbines is condensed at 2" Hga, and returned to the condenser hotwell.

For each parametric case, an additional coal input equivalent to a 2 percent of the MHD combustor thermal power is charged to the plant performance, representing the power required for the seed regeneration plant.

5.4.1.2 Parametric Analyses and Sensitivity Studies

Table 5.4.1 lists the parametric variations for the OCD directly-fired systems. Case 1-1 represents the Base Case around which parametric variations were made. The parameters varied were considered important ones that could have significant impacts on the system performance. These include power level (Cases 1-3 and 1-20), coal type (Case 1-5), air preheat temperature (Cases 1-6 and 1-7), oxygen level (Case 1-7), magnetic induction (Cases 1-16, 1-17 and 1-18), generator inlet Mach number (Case 1-8), inlet swirl (Cases 1-9 and 1-10), maximum Hall field (Cases 1-12 and 1-13), wall temperature (Case 1-4), combustor pressure loss (Case 1-19), and the diffuser pressure recovery factor (Case 1-11). Cases 1-14 and 1-15 were originally proposed as variations on the generator load factor. Since the channel performance study suggested that the constant Hall field mode of operation would yield satisfactory performance for a supersonic disk, it was selected as the channel design criterion for most of the cases. Once the Hall field is specified in this mode, the inlet load factor is fixed. Consequently, the load factor in the constant Hall field design is not an independent parameter and these two cases are no longer applicable. Further discussion of the variations of disk performance and size with varying design criteria can be found in subsection 5.3.

Case 1-2 was originally proposed to explore the disk potential at maximum combustor temperature by using a high oxygen enrichment level together with HTAH preheating. However, results of channel calculations indicated that, because of reduced total generator mass flow rate, the MHD power was substantially lower than for the Base Case having the same preheat temperature. Thus, it was decided that further systems study was not warranted. Instead, by mutual agreement between NASA and Westinghouse, a separate case was stipulated to focus on the study of oxygen enrichment without HTAH. This case is described in Section 5.4.3, following.

A summary of overall energy balance and system performance for each of the directly-fired cases considered is given in Table 5.4.2. Estimates made for the increased steam power and plant efficiency achieved by configurations incorporating direct MHD component cooling using feedwater are included in this table, in parentheses under the values for the separate cooling loop cases.

TABLE 5.4.2

Base Case	-	Hall Power	Level	Coal = 1810 K T _{Pretreat} = 1600K	+ 0.2 Mach=0.85 1650 K	Swirl=0 1650 K	Swirl=1.0 1650 K	Pressure Hall Maximum	Recovery field = Hall Maximum	field = Hall Maximum	field = Hall Maximum	Level							
1-1	1-2	1-3	1-4	1-5	1-6	1-7	1-8	1-9	1-10	1-11	1-12	1-13	1-14	1-15	1-16	1-17	1-18	1-19	1-20

As might be expected, higher preheat temperature, channel wall temperature, diffuser recovery coefficient, Hall field limit and magnetic field all have beneficial effects on the plant efficiency. A large plant size is also slightly favored from the performance standpoint. Unsurprisingly, higher combustor pressure loss results in lower plant efficiency.

For two-terminal generator design, a subsonic channel yields substantially inferior performance to a supersonic channel, as evidenced by comparison between cases 1-8 and 1-1. Although part of the difference of 183 MW in MHD power between these cases is attributable to the lower preheat temperature (1650 K) for case 1-8, most is due to the subsonic channel design. Indeed, for the same preheat temperature of 1650 K, an MHD power of 465 MW was calculated for a supersonic, constant Hall field channel, as compared with a power level of only 346 MW for the subsonic channel.

The utilization of a direct component cooling system permits the attainment of slightly higher plant overall efficiencies in every case considered. The calculated performance increment is slight, however, and careful design to minimize the possible detrimental effects upon plant safety and reliability of incorporating such a cooling system will be necessary, if a net benefit is to be realizable in an actual power plant.

5.4.2 OCD SEPARATELY-FIRED SYSTEMS

The separately fired combustion gas disk MHD/steam system configuration was fully described in Section 4.1.1. The Base Case system parameters, parametric cases, and resulting performances are delineated in Subsections 5.4.2.1 and 5.4.2.2 below.

5.4.2.1 Delineation of Base Case Conditions

Case 2-1 of Table 5.4.3 contains the listing of Base Case parameters for the separately fired OCD MHD/steam system parametric analyses.

The total coal thermal input to the plant is 2669 MW_t , of which 1537 MW_t is fed to the MHD combustor, 1101 MW_t to the gasifier for producing fuel gas to

TABLE 5.4.3
PARAMETRIC VARIATIONS FOR OCD SEPARATELY-FIRED PREHEATER SYSTEMS

	2-1 Base Case	2-2 -	2-3 Double Power Level	2-4 Half Power Level	2-5 -	2-6 Preheat=1650 K Subsonic	2-7 Swirl = 0	2-8 Higher Comb. Loss
1. Plant Size (MW _t)	2669	-	5339	1335	-	2674	2669	2669
2. Coal Type	Montana Rose- bud Subb.	-	-	-	-	-	-	-
3. MHD Combustor/Nozzle								
Combustor type	2-stage cyclone	-	2-stage cycle	-	-	-	-	-
Oxidizer	Air	-	-	-	-	-	-	-
Fuel moisture as fired (%)	5	-	-	-	-	-	-	-
Stoichiometric ratio	0.95	-	-	-	-	-	-	-
Ash removal (%)	90	-	-	-	-	-	-	-
Seeding level (% K)	0.7	-	-	-	-	-	-	-
Fractional pressure loss, P/P in	0.08	-	-	-	-	-	-	0.10
Fractional heat loss, Q/HHV	0.07	-	-	-	-	-	-	0.08
4. MHD Generator/Diffuser								
Generator type	2-terminal radial outflow	-	-	-	-	-	-	-
Mode of generator operation	Constant radial field	-	-	-	-	Constant Velocity	Constant radial field	-
Magnetic induction (Tesla)	7	-	-	-	-	-	-	-
Inlet total temp. (K)	2835	-	-	-	-	2740	2835	2825
Inlet total pressure (atm)	5.73	-	-	-	-	5.73	5.73	5.60
Inlet Mach number	1.8	-	-	-	-	0.85	1.8	-
Inlet swirl	0.5	-	-	-	-	-	0	1
Use of inlet guide vanes	No	-	-	-	-	-	-	Yes
Inlet current loading factor	0.78	-	-	-	-	0.55	0.78	0.74
Maximum Hall field (kv/m)	12	-	-	-	-	5.3	12	12
Generator wall temp (K)	2000	-	-	-	-	-	-	-
Diffuser pressure recovery coeff.	0.45	-	-	-	-	-	-	-
Diffuser exit pressure (atm)	1.07	-	-	-	-	-	-	-
5. MHD Component Cooling	Separate cooling loop*	-	-	-	-	-	-	-
6. Oxidizer Preheat								
HTAH (K)	1920	-	-	-	-	1650	1920	-
LTAH (K)	922	-	-	-	-	-	-	-
7. Bottoming Plant								
Steam conditions	3500 psi/ 1000 F/1000 F	-	-	-	-	-	-	-
Steam extractions	none*	-	-	-	-	-	-	-
Condenser pressure (in Hg absolute)	2.0	-	-	-	-	-	-	-
Final combustion gas stoichiometry	1.05	-	-	-	-	-	-	-
Stack gas temp. (K)	408	-	-	-	-	-	-	-
8. Sulfur Emission Control	Seed Regeneration	-	-	-	-	-	-	-
9. Gasifier for HTAH								
Type	Pressurized fluidized bed	-	-	-	-	-	-	-
Fuel produced	LBTU	-	-	-	-	-	-	-
Fuel Gas clean-up	Hot	-	-	-	-	-	-	-

* Additional cases with direct cooling by bottoming plant working fluid were also investigated.

fire the HTAH, and 31 MW_t for seed regeneration. Montana Rosebud coal dried to 5% moisture is fired in the main combustor with 1920 K preheated air. The air flow rate is controlled to provide a stoichiometric ratio of 0.95. A mixture of potassium carbonate and potassium sulfate is added at the second stage of the combustor to give a seed level of 0.7 wt % potassium. Only 10% of the coal ash is carried over into the generator and the rest is removed from the combustor. The total temperature and pressure at the combustor exit are 2835 K and 5.73 atm, respectively.

As is the case for the directly-fired Base Case 1-1, the disk generator operates at a constant Hall field of 12 kV/m, with an inlet Mach number of 1.8 and swirl of 0.5. An MHD power of 403 MW is extracted from the combustion gases in the generator for this case. The generator is designed to give a pressure of 1.07 atm at the diffuser exit, with the diffuser pressure recovery coefficient assumed to be 0.45.

The heat recovery systems configuration is quite similar to that used in the directly-fired OCD systems cases. However, the oxidant preheater system is different from that previously described.

As received coal is fed at a rate of 1101 MW_t to a gasifier operating at a pressure of about 6.7 atm. The air to fuel ratio is about 3. The hot, clean fuel gas produced is burned with air preheated to 922 K (1200°F) in a separate combustor to give a final stoichiometry of 1.05. The hot matrix reheat gas passes through a regenerative HTAH system which preheats MHD combustor oxidant to 1920 K; thereafter, the exhausted reheat gas passes through a metallic air recuperator to heat the air for the separate combustor to 922 K, before expanding in gas turbines to generate additional power for air compressors and ac generation. The exhaust gas is then mixed with the MHD gas stream at a location upstream of the low temperature economizer for further heat recovery.

The air for the separate HTAH reheat loop is first compressed to a pressure of 6.82 atm. As noted above a gas turbine is used to drive the compressor. The air stream is then split into two parts, one which provides oxidizer for the

gasifier, the other which is heated to 922 K in a recuperator before being injected into the separate combustor for the regenerative preheater matrix reheat gas.

5.4.2.2 Parametric Analyses and Sensitivity Studies

The parametric variations for the separately-fired cases are presented in Table 5.4.4. Case 2-1 represents the Base Case around which the parametric analyses were made. Power level is varied in Cases 2-3 and 2-4, and swirl ratio in Cases 2-7 and 2-8. A lower preheat temperature with a subsonic channel design is represented by Case 2-6. A higher preheat temperature (2270 K) was originally stipulated for Case 2-5, but was subsequently found unattainable because the reheat gas temperature for the HTAH was calculated to be only about 2108 K.

Parametric analyses for both separate and direct MHD component cooling loops were performed, and results for both appear in Table 5.4.4.

The calculated performances for these separately-fired disk systems are all significantly less than for comparable directly-fired disk systems, as expected. The penalty for providing a clean HTAH reheat gas is sufficient to make such separately-fired systems unattractive, except as early demonstration units, and to prove out the basic coal-fired MHD power train component technology. A more viable option, and one which dispenses altogether with the necessity for operation of large regenerative preheater systems, is the use of enriched air preheated to an intermediate temperature to obtain high combustor total temperatures. This option is discussed, and its performance and parametric sensitivities detailed, in the next section.

5.4.3. OXYGEN-AUGMENTED OCD DISK MHD/STEAM POWER SYSTEMS

The general configuration of these system has been discussed previously in Section 4.1.1. Originally, it was intended to evaluate the effects of oxygen enrichment upon OCD power system performance by evaluating oxygen-enriched parametric cases in the directly-fired and separately-fired system analyses. This proved to be inappropriate, however, for a number of reasons.

TABLE 5.4.4
SUMMARY OF POWER GENERATION AND CONSUMPTION, OCD SEPARATELY-FIRED PREHEATER SYSTEMS

	2-1 Base Case	2-2 -	2-3 Double Power Level	2-4 Half Power Level	2-5 -	2-6 Preheat=1650 K Subsonic	2-7 Swirl = 0	2-8 Higher Comb. Loss
Coal Input (MW)								
MHD Combustor	1537	-	3074	769	-	1740	1537	1537
Gasifier for HTAH	1102	-	2203	551	-	899	1102	1102
Seed Regeneration	31	-	61	15	-	35	31	31
Total	2669	-	5339	1335	-	2674	2669	2669
Power Generation (MW)								
MHD Power	403	-	833	192	-	298	392	403
Steam Power	722 (728)	-	1434 (1444)	364 (367)	-	792 (800)	726 (732)	722 (728)
Gas Turbine Power	135	-	269	67	-	110	135	135
Total	1260 (1266)	-	2536 (2546)	623 (626)	-	1200 (1208)	1253 (1259)	1259 (1265)
Power Consumption (MW)								
Compressor for MHD Loop	110	-	220	55	-	124	110	110
Compressor for Gasifier Loop	89	-	178	44	-	73	89	89
Inverter, Generator & Transformer Losses	28	-	57	14	-	27	28	28
Other Auxiliaries	39	-	79	20	-	41	39	39
Total	267	-	533	133	-	265	266	266
Net Power Output (MW)	993 (999)	-	2003 (2013)	490 (493)	-	935 (943)	987 (993)	992 (998)
Plant Efficiency, (%)	37.2 (37.4)	-	37.5 (37.7)	36.74 (37.0)	-	35.0 (35.3)	37.0 (37.2)	37.2 (37.4)
Deviation of from Base Case 2-1	-	-	+0.3 (+0.3)	-0.5 (-0.5)	-	-2.2 (-2.2)	-0.2 (-0.2)	-0.3 (-0.0)

NOTE: Numbers in parentheses represent estimates for configuration with direct MHD Component cooling

- With 1920 K preheat and enriched air as oxidant, the combustor total temperatures exceeded levels at which materials used in the MHD combustor design could be expected to survive.
- Numerous safety considerations arise when an enriched oxidant is used with the cycling mode of operation typical of regenerative HTAH systems, especially in pressurized heater beds.
- Suitable total temperatures could be achieved by use of oxygen-enriched air preheated to intermediate temperature levels typical of those permissible with recuperative metallic heat exchangers.
- The removal of HTAH systems altogether from the MHD power plant design permits a more reliable system, especially with coal as the selected fuel.

5.4.3.1 Delineation of Base Case Conditions

Table 5.4.5 contains a summary of the Base Case conditions for the oxygen-augmented OCD MHD/steam power system.

The fuel is Montana Rosebud subbituminous coal, as for the previous OCD cases. The enrichment level of the MHD combustor oxidant is selected to provide a combustor total temperature of 2839 K, which is comparable to that obtained in the separately-fired and directly-fired OCD Base Cases with 1920 K air preheat levels. The final oxidant mixture was found to be 38.2% by weight oxygen, with 922 K preheat temperature assumed. For this mixture the ratio $[O_2(\text{added})/O_2(\text{in air})]$ equals 1.07 (i.e. $\alpha = 1.07$).

For the oxygen augmented cases, it was found by parametric evaluations that (as discussed in 5.4.3.2) supersonic OCD performance could be enhanced by increasing the inlet Mach number and total pressure over the values used in previous OCD Base Cases. The maximum net MHD power (that is, MHD VI minus compressor power) was obtained for the Base Case at a stagnation pressure of 8.02 atmospheres with an inlet Mach number of 1.9. The inlet swirl ratio, as in both previous Base Cases, was taken to be 0.5, limited by the maximum value obtainable without guide vanes.

The fuel is dried to 5 percent moisture by weight. In the MHD combustor, the final stoichiometry is 0.95 with 90 percent ash rejection. Again, a seeding

TABLE 5.4.5
PARAMETERS FOR OCD WITH METALLIC PREHEATER AND OXYGEN AUGMENTATION

1. Plant Size (MW_t)	2415 (1000 MW_e nominal)
2. Coal Type	Montana Rosebud
3. MHD Combustor/Nozzle	
Combustor type	2-stage high-swirl
Oxidizer	Enriched Air, $O_{2add}/O_{2air} = 1.07$ (38.2 wt% Oxygen)
Fuel moisture as fired (%)	5
Stoichiometric ratio	0.95
Ash removal (%)	90
Seeding level (% K)	0.7
Fractional pressure loss, $\Delta P/P$	0.08
Fractional heat loss, Q/HHV	0.07
4. MHD Generator/Diffuser	
Generator type	2-terminal radial outflow
Mode of generator operation	Constant radial field (near impulse)
Magnetic induction (Tesla)	7
Inlet total temp. (K)	2839
Inlet total pressure (atm)	8.02
Inlet Mach number	1.9
Inlet swirl	0.5
Use of inlet guide vanes	No
Inlet current loading factor	0.70
Maximum Hall field (kV/m)	12
Generator wall temp (K)	2000
Diffuser pressure recovery coeff.	0.6
Diffuser exit pressure (atm)	1.07
5. MHD Component Cooling	Direct Feedwater Loop
6. Oxidizer Preheat	
LTAH (K)	922
7. Bottoming Plant	
Steam conditions	3500 psia/1000F/1000F
Steam extractions	none
Condenser pressure (in Hg absolute)	2.0
Final combustion gas stoichiometry	1.05
Stack gas temp. (K)	408
8. Sulfur Emission Control	Seed regeneration

level of 0.7 percent K (K_2SO_4 and K_2CO_3) provide adequate plasma conductivity and sulfur emission control. The total thermal input to the combustor for the Base Case was 2368 MW, with an additional 47 MW_t charged to the seed regeneration system. This firing rate was sufficient to permit power generation at the 900 MWe level or above. For the Base Case plant, 450 MW_e is extracted from the disk generator alone.

The heat recovery system and bottoming plant design for the oxygen-augmented OCD system is quite similar to that for the separately-fired OCD system.

However, no analyses of system performance were carried out with a separate MHD component cooling loop assumed. The efficiency decrement expected would be in the 0.1 - 0.3 percentage point range for the separate cooling case, when compared to the results given here.

The oxygen required to attain the 2839 K combustor total temperature is provided by an on-site air separation plant, at 95 percent purity. The oxygen plant compressor is driven by a steam turbine which is supplied with steam from the MHD bottoming plant. As described in Section 5.2, the energy requirement for oxygen production has been based upon a high-efficiency plant. The energy required is debited to plant power output.

5.4.3.2 Parametric Analyses and Sensitivity Studies

A series of parametric cases was investigated for the oxygen-augmented OCD plant, in order to define the optimum pressure level and oxygen enrichment for such a system. As in the Base Case, disk inlet swirl ratio and Mach number were initially fixed at 0.5 and 1.9, respectively. The Hall field design constraint, with $E_r = -12$ kV/m, was used for generator design purposes.

Since overall system performance depends strongly on the combustor stagnation pressure, a first set of parametric evaluations was used to establish the optimal pressure for each oxygen enrichment level. Figure 5-4-1 shows the results of these calculations at selected enrichment levels α ($\alpha = [O_2(\text{added})/O_2(\text{in air})]$). At $\alpha = 0.9$, a clear maximum net MHD power

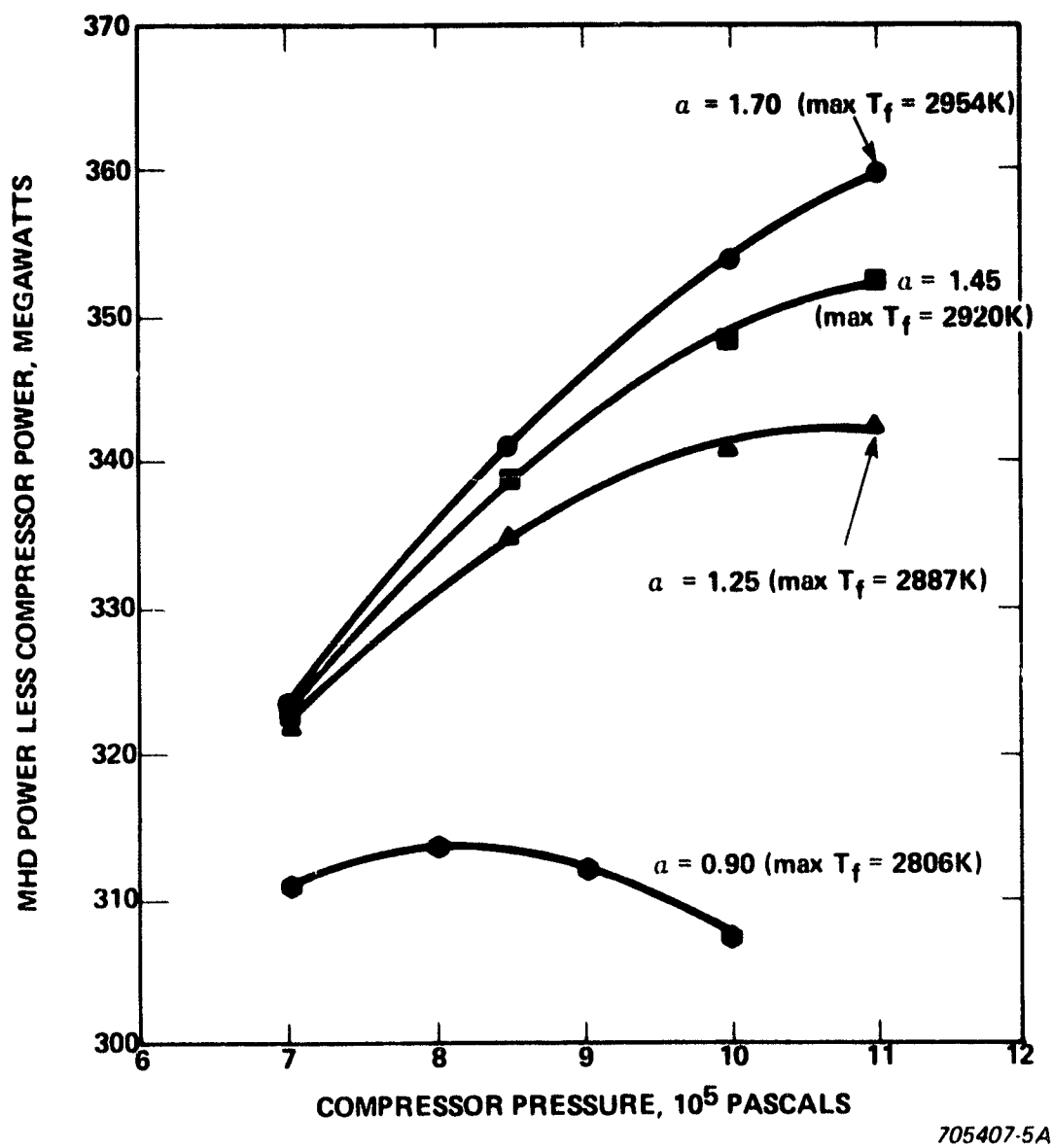
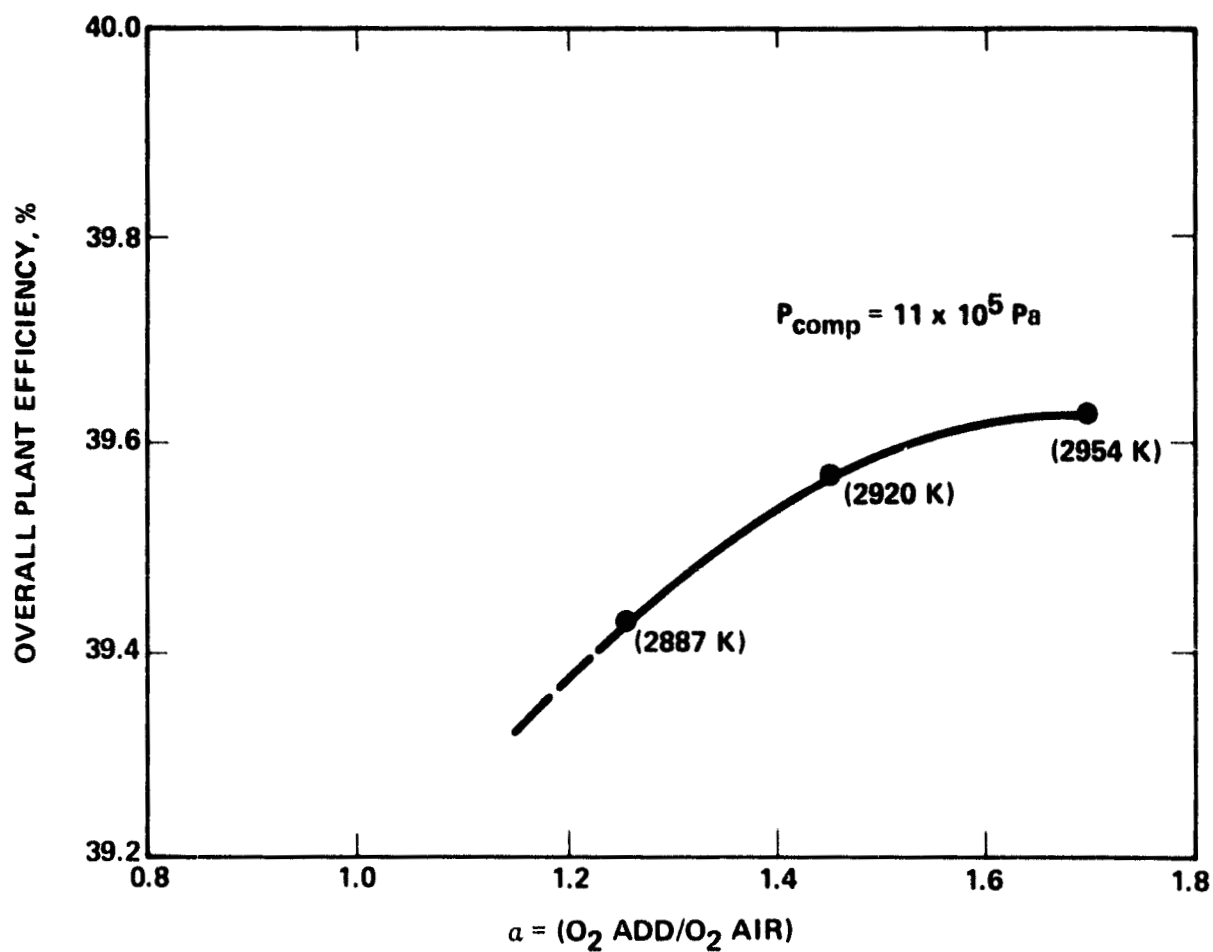


Figure 5-4-1. OCD Power Output Variation With Oxygen Enrichment Level and Combustor Pressure

occurs at a compressor discharge pressure of 8 atm (810 kPa). With increasing α , the location of the pressure maximum shifts toward higher pressures. For this investigation, a limiting pressure of 10.9 atm (1.1 MPa) was assumed as the practical maximum, since little information exists regarding coal-fired combustor operation above this pressure level. Maximum net MHD power for any $\alpha \geq 1.25$ is found to occur at (or above) the limiting pressure level of 10.9 atm.

To establish the optimum oxygen enrichment level, performance calculations were performed for values of $\alpha > 1.25$ at the imposed maximum pressure level of 1.1 atm. Figure 5-4-2 displays the results of the calculations. The total temperature for each is given in parentheses alongside; clearly, the net MHD power output continues to increase (with oxygen plant requirements debited to the gross MHD power output, in addition to the MHD compressor power) with increasing α , to the compressor pressure limit of 10.9 atm (1.1 MPa). The combustor total temperatures are calculated on the basis of identical combustor heat loss assumptions. The total temperature for the $\alpha = 1.70$ case is approaching 3000 K, which is an extremely demanding level for known materials and combustor designs. Plant efficiency calculations, which consider not only the net MHD power increase but also the effect of reduced combustion gas mass flowrate upon bottoming plant performance, show that for the $\alpha = 1.70$, $P_{\text{comp}} = 10.9$ atm case, a 39.6 percent overall efficiency is obtainable. This compares with the calculated 39.2 percent efficiency for the Base Case, using $\alpha = 1.07$ and $P_{\text{comp}} = 9$ atm.

The increased hazard levels and unreliability associated with the use of the high-enrichment, high-pressure case are not directly quantifiable, but it is clear that they will be more than sufficient to offset the minimal performance gain over the Base Case enrichment condition. Therefore, a practical design case (which also permits near-optimal performance) for the oxygen-augmented OCD MHD/steam power system can be considered to be provided by use of the parameters typical of those which give combustor total temperatures equivalent to air with 1920 K preheat. Table 5.4.6 contains a summary of the system performance under these conditions.



705407-6A

Figure 5-4-2. OCD Generator System Performance Variation with Oxygen Enrichment Level at Fixed Combustor Pressure

TABLE 5.4.6

Summary of Power Generation and Consumption, OCD with Metallic
Air Preheater and Oxygen Enrichment, $O_{2\text{add}}/O_{2\text{air}} = 1.07$

Coal Input (MW)	
MHD combustor	2368
Seed Regeneration	47
Total	2415
Power Generation (MW)	
MHD Power	450
Steam Power	758
Total	1207
Power Consumption (MW)	
Compressor	122
Inverter, Generator and Transformer Losses	26
Oxygen Plant	72
Other Auxiliaries	39
Total	259
Net Power Output (MW)	948
Plant Efficiency, η (%)	39.2

5.4.4 SELECTION OF OPTIMUM SYSTEMS

The Base Cases for each of three OCD MHD/Steam power systems were examined in light of the results of systems parametric studies, to determine which features and characteristic parameters of these systems could be modified to further enhance system overall performance. This re-examination included the evaluation and inclusion of specific system design changes, to permit the full performance potential of the disk systems to be delineated.

The OCD MHD/steam system types finally selected included two directly-fired systems, one separately-fired system, and one oxygen-augmented system. The second directly-fired system was selected to be representative of the performance obtainable with supersonic disk generator systems which could provide for NO_x removal from the combustion gas by use of radiant furnace cooling rate control. Since the 1920 K preheat level adopted in the Base Cases precluded the use of radiant furnace design features to reduce NO_x levels in the exhaust gases to meet EPA limits, a lower preheat case (1650 K) was evaluated, for which such NO_x reduction was possible without the use of a separate exhaust gas scrubber. For the 1920 K separately-fired case, and the oxygen-augmented case, substoichiometric combustion and controlled gas cooling in the radiant seed and slag furnaces were considered adequate to reduce NO_x emissions to acceptable levels. No detailed calculations of NO_x removal were performed. For the 1920 K directly-fired case, a separate NO_x scrubbing process was assumed. Estimates of NO_x removal requirements using the EXXON De NO_x process were made, and can be found in Appendix D.

These systems all incorporated a direct cooling system for the MHD power train components using condensate and feedwater as coolant, rather than using a separate cooling loop. The use of the direct cooling system provides full heat recovery capabilities, thus resulting in improved cycle efficiency. However, it was recognized that the full extent of potential problems associated with the operation and safety of such direct cooling systems remain to be determined.

The generator design was based on the constant Hall field constraint, which proved to be a satisfactory design criterion. Except for the 1650 K preheat Case, a generator inlet Mach number of 1.9 was selected. The high initial Mach number allows the hot gas in the generator to expand over a sufficiently long distance before going through sonic transition. For the lower Preheat Case, because of the lower preheat temperature and combustor stagnation temperature, a lower inlet Mach number was selected to prevent the gas static temperature from becoming excessively low.

A diffuser pressure recovery coefficient of 0.6 was adopted for all cases. This recovery efficiency was considered to be near the limit of potentially achievable recovery coefficients for disk/diffuser designs integrated with radiant furnace inlet ducts, as described in Sections 6.1 and 6.5.

A 3500 psia/1000°F/1000°F extraction-type steam bottoming plant was integrated with the MHD cycle. Detailed steam plant modeling and optimization was performed for the 1920 K directly-fired Case. The selected steam plant configuration is shown schematically in Figure 5-4-3. Condensate pump discharge is split into two separate streams, one passing through a feedwater heater train and the other passing through the disk generator cooling system and the low temperature economizer. The heater train contains seven closed heaters and one open heater which serves also as a deaerator. These two streams are then mixed and heated further in a second economizer and subsequent components.

The configuration chosen was found to give an efficiency of 42.4% which is slightly higher steam cycle efficiency than the case where disk cooling and the economizer are in series with the feedwater heater train. In the latter configuration, gas side temperature constraints coupled with the relatively large heat loads of the disk cooling system and the low temperature economizer would require the deletion of some of the lower temperature feedwater heaters, resulting in decreased steam cycle efficiency.

All systems were sized to a nominal net electrical power output of 1000 MWe. This represents a typical central power station size which is widely accepted by larger utilities in terms of capital investment. The 1000 MWe plant also permits adequate load matching for normal power distribution systems, and provides adequate size to realize the benefits of scaling in terms of MHD cycle performance.

Table 5.4.7 summarizes the characteristic parameters for each of the final optimized OCD cases. Gas-side and air-side statepoints for each system are contained in Tables 5.4.8 through 5.4.11. Steam-side statepoints for the supercritical extraction-type system designed specifically for the 1920 K directly-fired case are provided on Figure 5-4-3. Performance for each OCD system is described in Table 5.4.12.

Overall plant efficiencies (coal pile to bus bar) obtained ranged from 39.0 percent for the separately-fired OCD system to 45.5 percent for the 1920 K preheat directly-fired system. The use of separately-fired preheaters or oxygen enrichment to achieve the required combustion temperatures results in substantial performance penalties. The oxygen-augmented system shows a slightly higher performance, and can be considered to provide a higher level of reliability than the separately-fired system with regenerative preheaters.

TABLE 5.4.7 BASE PARAMETERS FOR THE FINAL SELECTED OCD SYSTEMS

	1920 K <u>Direct Fired</u> (CASE 1A)	1650 K <u>Direct Fired</u> (CASE 1B)	Indirect <u>Fired</u> (CASE 2)	O ₂ <u>Enriched</u> (CASE 3)
Plant Size, MWe	1000 Nominal	1000 Nominal	1000 Nominal	1000 Nominal
Oxidant	Air	Air	Air	O ₂ Enriched Air
Oxidant Preheat Temperature, K	1920	1650	1920	922
Oxidant Preheater Type	Direct- Fired HTAH	Direct- Fired HTAH	Indirect- Fired HTAH	Metallic Heaters
Generator Inlet Mach Number	1.9	1.7	1.9	1.9
Generator Inlet Swirl	0.5	0.5	0.5	0.5
Generator Design Mode	Constant Hall Field	Constant Hall Field	Constant Hall Field	Constant Hall Field
Maximum Hall Field, kV/m	12	12	12	12
Diffuser Pressure Recovery Factor	0.6	0.6	0.6	0.6
Magnetic Induction, T	7	7	7	7
MHDS Power Train Component Cooling	Direct Feedwater Cooling	Direct Feedwater Cooling	Direct Feedwater Cooling	Direct Feedwater Cooling
Steam Bottoming Plant	3500/1000/ 1000	3500/1000/ 1000	3500/1000 1000	3500/1000 1000
	Extraction Type	Extraction Type	Extraction Type	Extraction
NO _x Scrubbing System	NH ₃ Scrubber	None Required	None Required	None Required

Figure 5-4-3. Optimized Steam System Design for Open Cycle Disk Generator
System Case 1A (Direct Firing with 1920 K Preheat)

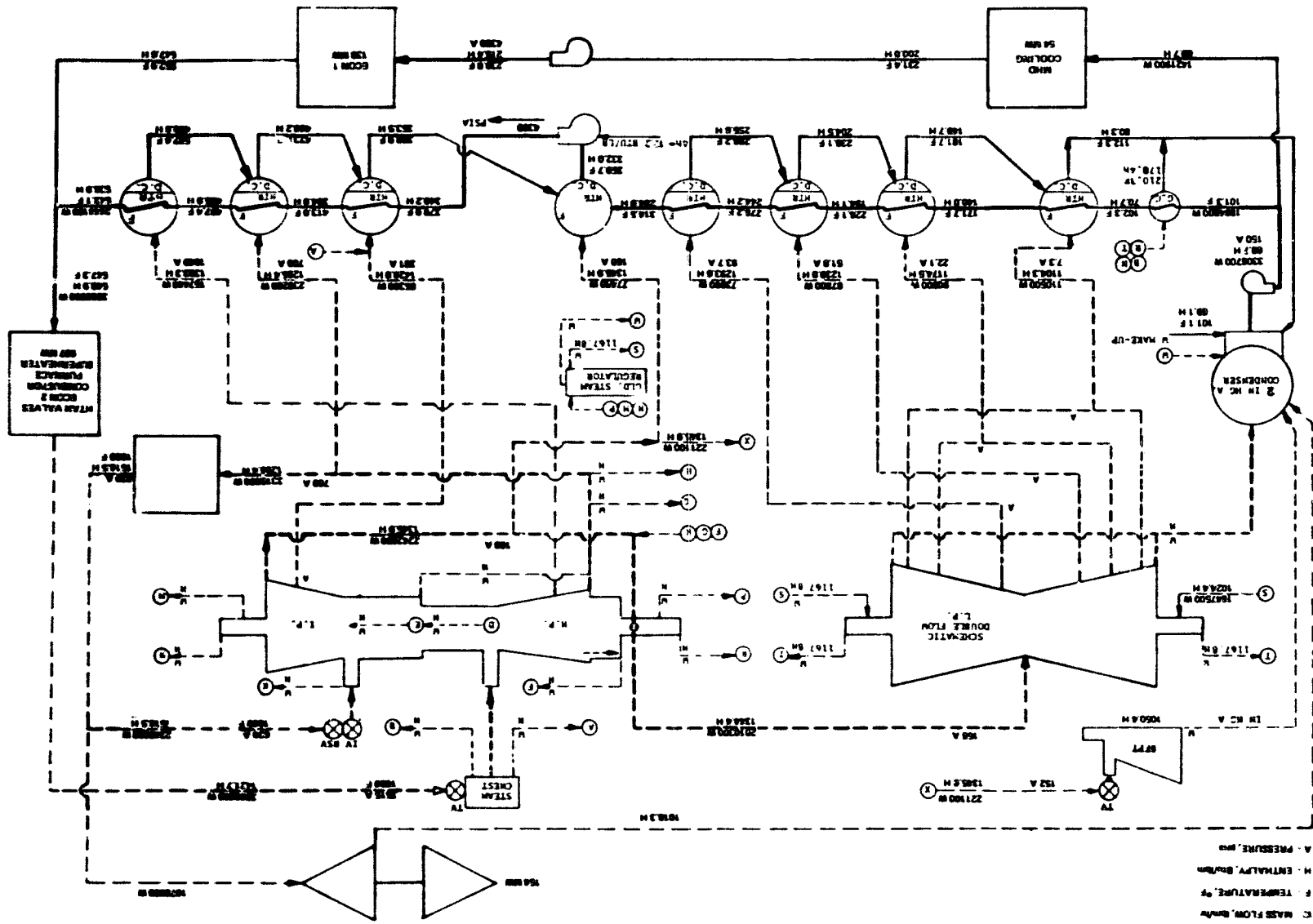
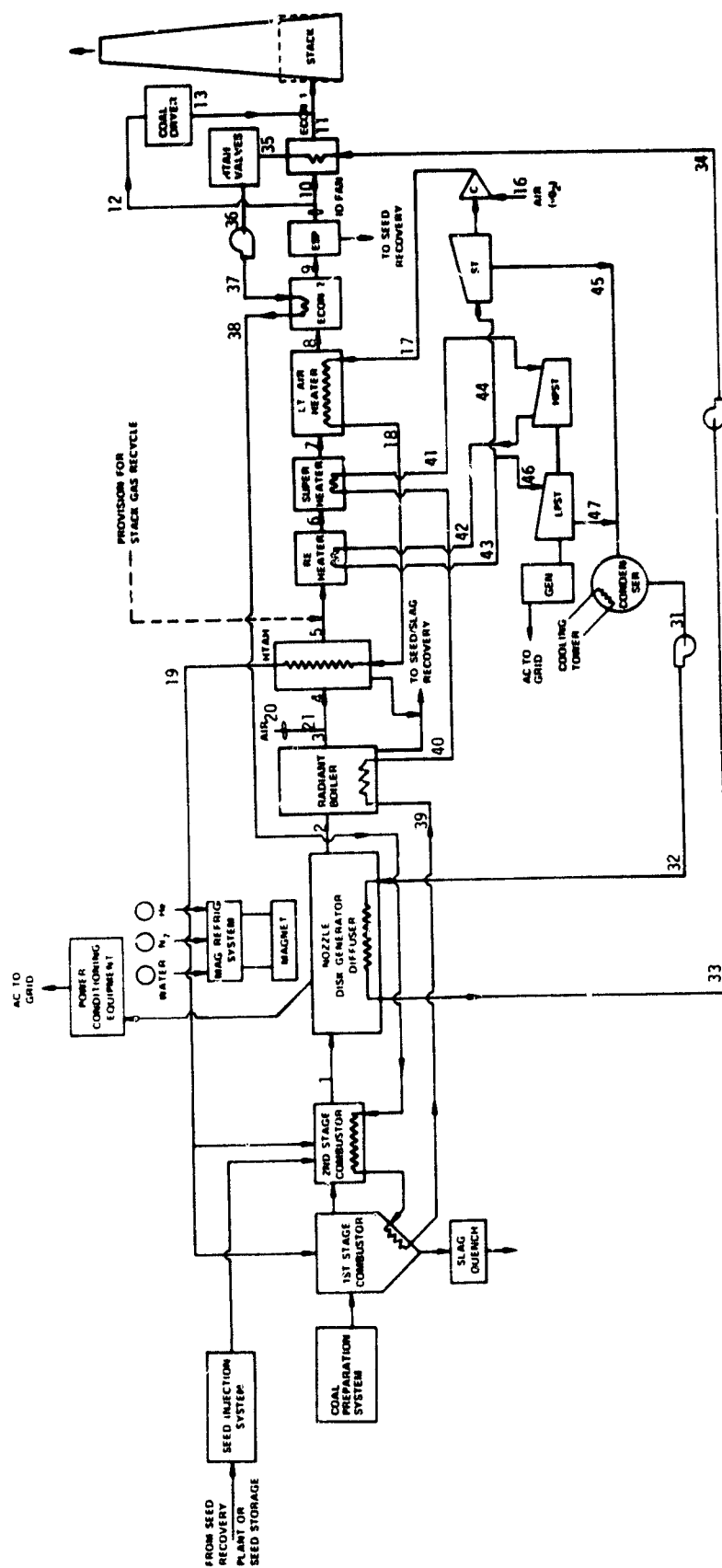


TABLE 5.4.8 GAS AND AIR SIDE STATEPOINTS

FOR 1920 K DIRECTLY FIRED OCD SYSTEM (CASE 1A)
(Station Numbers Correspond to Figure 5-4-4)

STATEPOINT STATION NUMBER	W MASS FLOW (kg/s)	P PRESSURE (100 kPa)	T TEMPERATURE (K)	h SPECIFIC ENTHALPY (MJ/kg)
1	735.98	6.152	2839	0.9616
2	735.98	1.083	2451	0.0787
3	735.98	1.051	2150	-0.6109
4	803.71	1.045	2107	-0.5671
5	803.71	1.003	1463	-1.5689
6	803.71	0.993	1235	-1.8715
7	803.71	0.974	1100	-2.0427
8	803.71	0.954	916	-2.3894
9	803.71	0.925	611	-2.6265
10	566.99	1.030	631	-2.6039
11	566.99	0.999	408	-2.8474
12	236.72	1.030	631	-2.6039
13	255.36	0.999	408	-3.1773
14				
15				
16	643.48	1.013	288	-0.0957
17	643.48	7.100	523	0.1443
18	643.48	6.893	922	0.5774
19	643.48	6.687	1920	1.7804
20	67.73	1.013	288	-0.0957
21	67.73	1.051	292	-0.0919



GT-1400-28

Figure 5-4-4. Directly Fired OCD MHD/Steam System - Statepoint Stations for Optimized Design Cases 1A and 1B

TABLE 5.4.9 GAS AND AIR SIDE STATEPOINTS FOR
1650 K DIRECTLY-FIRED OCD SYSTEM (CASE 1B)
(Station Numbers Correspond to Figure 5-4-4)

STATEPOINT STATION NUMBER	W MASS FLOW (kg/s)	P PRESSURE (100 kPa)	T TEMPERATURE (K)	h SPECIFIC ENTHALPY (Mj/kg)
1	809.58	4.973	2731	0.6649
2	809.58	1.083	2407	-0.0393
3	809.58	1.051	1834	-1.0911
4	884.08	1.036	1828	-1.0069
5	884.08	0.994	1345	-1.7287
6				
7	884.08	0.974	1100	-2.0427
8	884.08	0.955	794	-2.4159
9	884.08	0.926	611	-2.6266
10	623.49	1.030	631	-2.6041
11	623.49	0.999	408	-2.8474
12	260.59	1.030	631	-2.6041
13	260.59	0.999	408	-3.1773
14				
15				
16	707.82	1.013	491	0.1113
17	707.82	5.740	491	0.1113
18	707.82	5.573	922	0.5774
19	707.82	5.406	1650	1.4443
20	74.51	1.013	288	-0.0957
21	74.51	1.051	292	-0.0919



TABLE 5.4.10 GAS AND AIR SIDE STATEPOINTS FOR
1920 K SEPARATELY-FIRED OCD SYSTEM (CASE 2)
(Station Numbers Correspond to Figure 5-4-5)

STATEPOINT STATION NUMBER	W MASS FLOW (kg/s)	P PRESSURE (100 kPa)	T TEMPERATURE (K)	h SPECIFIC ENTHALPY (Mj/kg)
1	515.18	6.152	2839	0.9618
2	515.18	1.083	2450	0.0761
3	515.18	1.051	2150	-0.6109
4				
5	515.18	1.040	1796	-1.1434
6	562.60	1.036	1794	-1.0548
7	562.60	1.015	1100	-2.0427
8	562.60	0.995	816	-2.3894
9	562.60	0.965	611	-2.6266
10	789.77	1.030	620	-2.5555
11	789.77	0.999	408	-2.7871
12	174.43	1.030	620	-2.5555
13	187.47	0.999	408	-3.5127
14				
15				
16	450.43	1.013	288	-0.0957
17	450.43	7.100	523	0.1443
18	450.43	6.893	922	0.5774
19	450.43	6.687	1920	1.7804
20	47.41	1.013	288	-0.0957
21	47.41	1.051	292	-0.0919
61	401.61	6.606	2111	-0.5288
62	401.61	6.342	1072	-1.9321
63	401.61	6.215	895	-2.1489

TABLE 5.4.10 GAS AND AIR SIDE STATEPOINTS FOR
1920 K SEPARATELY-FIRED OCD SYSTEM (CASE 2) (CONT'D)
(Station Numbers Correspond to Figure 5-4-5)

STATEPOINT STATION NUMBER	W MASS FLOW (kg/s)	P PRESSURE (100 kPa)	T TEMPERATURE (K)	h SPECIFIC ENTHALPY (Mj/kg)
64	401.61	1.030	616	-2.4751
65	964.20	1.030	620	-2.5555
66	355.92	1.013	288	-0.0957
67	355.92	7.327	528	0.1494
68	152.53	7.327	528	0.1494
69	203.38	7.327	528	0.1494
70	203.38	7.181	922	0.5774

TABLE 5.4.11 GAS AND AIR SIDE STATEPOINTS FOR
OCD SYSTEM WITH OXYGEN AUGMENTATION (CASE 3)
(Station Numbers Correspond to Figure 5-4-6)

STATEPOINT STATION NUMBER	W MASS FLOW (kg/s)	P PRESSURE (100 kPa)	T TEMPERATURE (K)	h SPECIFIC ENTHALPY (Mj/kg)
1	542.80	8.128	2839	-0.4028
2	542.80	1.083	2447	-1.3377
3	542.80	1.051	2150	-2.0962
4				
5	542.80	1.040	1788	-2.6589
6	620.02	1.036	1791	-2.3392
7	620.02	1.015	1100	-3.3476
8	620.02	0.995	880	-3.6255
9	620.02	0.965	611	-3.9474
10	343.48	1.030	622	-3.9342
11	343.48	0.999	408	-4.1717
12	276.54	1.030	622	-3.9342
13	297.78	0.999	408	-4.8169
14				
15				
16	441.75	1.013	288	-0.0786
17	441.75	9.100	561	-0.1968
18	441.75	8.835	922	-0.5868
19				
20	77.22	1.013	288	-0.0957
21	77.22	1.051	292	-0.0919
22	349.31	1.013	288	-0.0957
23	92.44	1.013	288	-0.0093

TABLE 5.4.12 PERFORMANCE SUMMARY FOR OPTIMIZED OCD SYSTEMS

	DIRECTLY-FIRED 1920 K PREHEAT	DIRECTLY-FIRED 1650 K PREHEAT	SEPARATELY-FIRED 1920 K PREHEAT	O ₂ ENRICHED
Coal Input to Plant, MW _t				
MHD Combustor	2077.1	2284.8	1453.9	2367.8
Gasifier	-	-	1039.4	-
Seed Regeneration	41.5	45.7	29.1	47.4
Total	2118.6	2330.5	2522.4	2415.2
Gross Power Out, MW _e				
MHD (dc)	595.9	522.3	407.4	450.6
Steam	627.4	738.6	727.9	810.2
Gas Turbine	-	-	131.0	-
Total	1223.3	1260.9	1266.3	1260.8
Power Consumption, MW _e				
Cycle Air Compressor	154.4	146.5	108.1	124.1
Boiler Feed Pumps	21.6	25.1	24.8	27.7
Oxygen Plant	-	-	-	71.9
NO _x Scrubber	12.2	-	-	-
Other	72.1	77.3	149.6	59.1
Total	260.3	248.9	282.5	282.8
Generator Inlet Pressure - Atm.	6.15	4.97	6.15	8.13
Generator Mass Flow - kg/s	736.0	809.6	515.2	542.8
Generator Inlet Temperature - K	2839	2731	2829	2839
Disk Inlet Radius (m)	1.26	1.31	1.05	0.92
Disk Outlet Radius (m)	5.21	5.18	4.91	5.35
Radial E - field (kv/m)	12	12	12	12
Voltage (kV)	47.4	46.5	46.3	53.1
Total Enthalpy in (MW)	3102.5	3174.8	2171.8	2466.0
Enthalpy Extraction (%)	19.2	16.5	18.8	18.3
Generator Isentropic eff. (%)	69.9	66.9	68.3	62.5
Plant Net Power Out, MW _e	963.0	1012.0	983.8	978.0
Plant Efficiency, %	45.5	43.4	39.0	40.5

6.0 OPEN CYCLE DISK SYSTEMS - MAJOR COMPONENT AND SUBSYSTEM DESIGN

6.1 DISK GENERATOR, NOZZLE, AND DIFFUSER DESIGN

The general layout of the disk generator design which was developed for application to open cycle MHD systems is that of two monolithic pierced disks, which mate at their outer circumferences with structural members of the diffuser. A central hole is provided in one of the disks to permit combustion gas plasma entry; the plasma, after passing through the flow channel formed by the shaped upper and lower disk inner surfaces, then exhausts to a diffuser connected to the outer circumference of the disk structure. The supersonic nozzle is formed by a necking-down of the inner surfaces of each disk, just radially downstream of the central plasma inlet.

The diffuser itself is an annular structure surrounding the disk generator, and accepting its exhaust at its inner circumference. Deceleration of the supersonic disk exhaust plasma is accomplished by means of a sonic transition set up just at the exit of the disk (a normal shock is assumed for calculational purposes) followed by diffusion of the high-subsonic annular flow through a set of parallel equivalent straight-wall diffusers formed by the placement of a number of splitter vanes in the annulus. The diffuser exhausts at 1.068 atmospheres to the radiant furnace arrangement through a set of collection ducts arranged symmetrically about its outer periphery.

6.1.1 NOZZLE AND DISK GENERATOR DESIGN

The disk generator and diffuser structural concept is illustrated in Figure 6-1-1. This concept is by no means an optimized structural solution and many of the fabrication and assembly details have not been addressed; however, the concept has been developed to the degree necessary to permit the preparation of valid weight and cost estimates. Design parameters for the disk generators and nozzles of each of the 4 OCD system designs are provided in Tables 6.1.1A through 6.1.1D.

TABLE 6.1.1A
UCD POWER SYSTEM - CASE 1A
NOZZLE AND DISK GENERATOR
DESIGN DATA
(1920K DIRECTLY-FIRED DISK SYSTEM)

● TYPE	Radial Outflow Hall Generator with Swirl
● OPERATING MODE	Supersonic Near-Impulse Mode
● DIMENSIONAL DATA, PLASMA-WETTED SURFACES	
Disk Inlet Radius	1.256 m
Disk Inlet Height	0.419 m
Disk Outlet Radius	5.206 m
Disk Outlet Height	0.243 m
● PLASMA PROPERTIES	
Mass Flow	736 kg/s
Inlet Pressure	96 kPa
Inlet Temperature	2267 K
Inlet Swirl Ratio	0.5
● NOZZLE DATA	
Inlet Pressure	615 kPa
Inlet Temperature	2839 K
Nozzle Outlet Area	2.95 m ²
● COOLING SYSTEM DATA	
Type	Low Pressure Regenerative
Cooling Water Pressure	1013 kPa
Cooling Water Flow	179.2 kg/s
Cooling Water Inlet Temperature	312 K
● DISK ELECTRICAL DATA	
Design Hall Field (Constant)	-12 kV/m
Total Terminal Voltage Difference	47.4 kV
MHD dc Power	595.9 MW _e
● MISCELLANEOUS	
Total Weight (top & bottom sections)	136,000 kg
Cooling System Piping	2" Sch 40S Stainless Steel
Disk Structural Material	Fiberglass
Thickness	0.23 m
Inner Insulating Wall Operating Temperature	2000 K
Design Axial Magnetic Field	7 T

TABLE 6.1.1B
OCD POWER SYSTEM-CASE 1B
NOZZLE AND DISK GENERATOR
DESIGN DATA
(1650K DIRECTLY-FIRED DISK SYSTEM)

● TYPE	Radial Outflow Hall Generator with Swirl
● OPERATING MODE	Supersonic Near-Impulse Mode
● DIMENSIONAL DATA, PLASMA-WETTED SURFACES	
Disk Inlet Radius	1.309 m
Disk Inlet Height	0.436 m
Disk Outlet Radius	5.184 m
Disk Outlet Height	0.254 m
● PLASMA PROPERTIES	
Mass Flow	809.6 kg/s
Inlet Pressure	63 kPa
Inlet Temperature	2207 K
Inlet Swirl Ratio	0.5
● NOZZLE DATA	
Inlet Pressure	497 kPa
Inlet Temperature	2731 K
Nozzle Outlet Area	3.21 m ²
● COOLING SYSTEM DATA	
Type	Low Pressure Regenerative
Cooling Water Pressure	993 kPa
Cooling Water Flow	195.1 kg/s
Cooling Water Inlet Temperature	312 K
● DISK ELECTRICAL DATA	
Design Hall Field (Constant)	-12 kV/m
Total Terminal Voltage Difference	46.5 kV
MHD dc Power	522.3 MW _e
● MISCELLANEOUS	
Total Weight (top & bottom sections)	134,000 kg
Cooling System Piping	2" Sch 40S Stainless Steel
Disk Structural Material	Fiberglass
Thickness	0.23 m
Inner Insulating Wall Operating Temperature	2000 K
Design Axial Magnetic Field	7 T

Table 6.1.1C
OCD POWER SYSTEM-CASE 2
NOZZLE AND DISK GENERATOR
DESIGN DATA
(1920K INDIRECTLY-FIRED DISK SYSTEM)

● TYPE	Radial Outflow Hall Generator with Swirl
● OPERATING MODE	Supersonic Near-Impulse Mode
● DIMENSIONAL DATA, PLASMA-WETTED SURFACES	
Disk Inlet Radius	1.051 m
Disk Inlet Height	0.350 m
Disk Outlet Radius	4.909 m
Disk Outlet Height	0.180 m
● PLASMA PROPERTIES	
Mass Flow	515.2 kg/s
Inlet Pressure	96.1 kPa
Inlet Temperature	2267 K
Inlet Mach Number	1.90
Inlet Swirl Ratio	0.5
● NOZZLE DATA	
Inlet Pressure	615 kPa
Inlet Temperature	2839 K
Nozzle Outlet Area	2.07 m ²
● COOLING SYSTEM DATA	
Type	Low Pressure Regenerative
Cooling Water Pressure	1013 kPa
Cooling Water Flow	192.2 kg/s
Cooling Water Inlet Temperature	312 K
● DISK ELECTRICAL DATA	
Design Hall Field (Constant)	-12 kV/m
Total Terminal Voltage Difference	46.3
MHD dc Power	407.5 MW _e
● MISCELLANEOUS	
Total Weight (top & bottom sections)	123,000 kg
Cooling System Piping	2" Sch 40S Stainless Steel
Disk Structural Material	Fiberglass
Thickness	0.23 m
Inner Insulating Wall Operating Temperature	2000 K
Design Axial Magnetic Field	7 T

TABLE 6.1.1D
OCD POWER SYSTEM-CASE 3
NOZZLE AND DISK GENERATOR
DESIGN DATA
(OXYGEN-AUGMENTED DISK SYSTEM WITH
METALLIC AIR HEATER)

● TYPE	Radial Outflow Hall Generator with Swirl
● OPERATING MODE	Supersonic Near-Impulse Mode
● DIMENSIONAL DATA	
Disk Inlet Radius	0.922 m
Disk Inlet Height	0.308 m
Disk Outlet Radius	5.349 m
Disk Outlet Height	0.182 m
● PLASMA PROPERTIES	
Mass Flow	542.8 kg/s
Inlet Pressure	132 kPa
Inlet Temperature	2331 K
Inlet Mach Number	1.90
Inlet Swirl Ratio	0.5
● NOZZLE DATA	
Inlet Pressure	840 kPa
Inlet Temperature	2839 K
Nozzle Outlet Area	1.594 m ²
● COOLING SYSTEM DATA	
Type	Low Pressure Regenerative
Cooling Water Pressure	993 kPa
Cooling Water Flow	213.6 kg/s
Cooling Water Inlet Temperature	312 K
● DISK ELECTRICAL DATA	
Design Hall Field (Constant)	-12 kV/m
Total Terminal Voltage Difference	53 kV
MHD dc Power	450.6 MWe
● MISCELLANEOUS	
Total Weight (top & bottom sections)	143,100 kg
Cooling System Piping	2" Sch 40S Stainless Steel
Disk Structural Material	Fiberglass
Thickness	0.23 m
Inner Insulating Wall Operating Temperature	2000 K
Design Axial Magnetic Field	7 T

Disk Pressure Wall

The disk pressure walls are made of fiberglass to provide the required electrical insulation between the current collector electrode rings. Each fiberglass wall is fabricated in the form of a pierced monolithic flat disk, approximately 0.23 m (9 inches) in thickness. A central hole of approximately 2.5-3 m in diameter is provided in the lower disk for plasma entrance from the combustor, since all the open cycle generator systems selected for conceptual design will operate in the outflow mode.

The fiberglass structural wall is protected from the hot channel gases by a thickness of magnesia refractory which is supported by a series of water-cooled stainless steel tube rings. Welded studs are provided on the tube rings to promote the adhesion of the ceramic mass; the tube rings themselves are attached to the fiberglass by a bolted support. (Most fasteners and metallic members in this region should be fabricated of nonmagnetic materials since they operate in the central field of the magnet). The bulk of the magnesia refractory is installed as a rammed mass, shaped to provide the appropriate channel lofting. A finish coat of plasma jet-sprayed magnesia is applied to the rammed mass surfaces.

Disk Wall Refractory

Magnesia was selected as the reference refractory for the disk generator application due to its known capability to resist slag-and seed-laden plasma deterioration. The design wall operating temperature of 2000 K (3140°F) is only slightly higher than the currently-accepted upper limit of 3000°F for reliable operation of water-cooled magnesia walls. As demonstrated in the open-cycle parametric evaluations, the operating wall temperature of the disk does not appear to be a performance-critical parameter in the 1600 K - 2000 K range, and a tradeoff between slightly lower wall temperature (hence higher disk heat losses) and surface longevity could thus be made, if the higher wall temperature is determined to be detrimental to the integrity of the magnesia surfaces.

Disk Wall Cooling Water System

Disk wall cooling is provided by a series of circumferential cooling water tubes in the disk refractory wall. These headers are located on a fixed radial pitch (0.1 meter or 4" chosen for this study) and carry in parallel approximately one-half of the total steam plant condensate flow (at 312K inlet temperature) for regenerative cooling of the disk generator wall. The low pressure and temperature of the cooling water permits use of a relatively thin-wall stainless steel tubing (2" schedule 40S was selected for the reference design), allows operation of the entire disk fiberglass wall at a constant temperature to eliminate deflections caused by differential thermal stresses between inner and outer wall sections, and eases the difficulties of providing electrical isolation of the individual circumferential tubes from one another and from ground. Cooling water is supplied to each line from a combined supply header through a length of insulating hose and returns to another header through another equivalent hose length. Each circumferential tube run must be provided with a pair of connecting necks penetrating the fiberglass and ending in a coupling which connects to the insulating hoses from the condensate supply and return headers. The disk generator is designed to operate with a grounded exit, so that the cooling tubes will be at a higher potential the closer they are to the disk axis. The inner tube runs must thus be provided with the longest hoses to ensure electrical isolation.

Disk Generator Electrodes

The electrode system for a disk generator can in principle be made very much simpler than that for a typical linear generator of equivalent power output. At the design point, the disk generator can in theory achieve adequate performance while operating with only two sets of electrodes (the single-load Hall generator). As demonstrated in Section 5.3.4, however, the off-design characteristics of the disk generator mandate the inclusion of intermediate electrodes between anode and cathode to provide current control capability and stability under actual operating conditions. No more than four or five sets of such intermediate electrodes are thought to be required, thus maintaining a simple disk design when compared to linear generators.

The metallic cold-wall slagging electrode is proposed as the reference electrode design for this study. The relatively low temperature of the metallic surface will result in the buildup of a liquid layer of slag over the electrode, providing thermal insulation and protection from abrasion by the particulates and condensed vapors carried in the high-velocity combustion products. Because of the high current concentrations resulting from electrothermal instabilities at the slag/plasma and slag/electrode interface, the base material of the electrode must be selected to provide exceptional thermal diffusivity as well as adequate conductivity[1]. Copper is the material selected for the disk generator electrodes. Protective caps of oxidation-resistant materials must also be provided, especially on the anode, in order to limit electrode surface oxidation in the presence of high currents.

The average surface current density for linear MHD generator electrodes has been limited to 10 kA/m^2 . For the disk, with electrodes widely separated by insulating walls and with no sidewall effects to enhance current concentrations on electrode surfaces, a higher average loading may be possible, say $100\text{-}500 \text{ kA/m}^2$.

Electrodes for the disk generator are fabricated by bending rectangular-section extruded copper piping into continuous rings of the proper diameter for each electrode position. The design current loadings for any electrode in any of the four OCD design cases will be limited to a maximum of approximately 30 kA/m^2 with an exposed electrode surface of width 25.4 mm (1 inch) at any ring circumference equivalent to or greater than that for the disk inlet radius. At the segment short-circuit currents characteristic of the disk designs proposed, maximum current densities are on the order of 50 kA/m^2 (assuming both upper and lower electrodes of any pair are equally loaded). The plasma-and slag-contacting surfaces of the electrodes are capped with an oxidation-resistant material. Suitable choices would be noble metals such as platinum or palladium for the anode. Less costly materials, for example tungsten, could serve for the cathode and intermediate electrode cap material.

The retention of a slag coating on linear generator electrode surfaces is aided by the inclusion of an inset strip of refractory material. This may not be necessary for the disk electrodes, since they are well separated and surrounded by a refractory wall which could provide a slag adhesion surface. The high temperature of the insulation walls may not be amenable to liquid slag retention, however, since slag condensation temperature is on the order of 1900 K. This design factor must be investigated in greater detail if further work with cold-electrode disk generators is proposed.

In the future, the hot electrode concept will probably be more adaptable and acceptable for disk generators, although the protective slag layer does offer a greater electrode lifetime with the supersonic flows with which disk performance is optimized.

If the electrode positioning criteria indicated by the off-design calculations of Section 5.3.4 are applied to each of the four OCD system cases, potential electrode positions can be proposed and the specific performance parameters for each disk electrode system may be calculated. For a disk with four separate segments, designed with the constant Hall field constraint ($E_r = 12$ kV/m across the disk) the segmentation lengths should decrease from inner to outer radius. Taking a rough segmentation requirement of 2 m/1 m/0.5 m/0.5 m as the base design case, each of the four disk generators proposed for the OCD cases will have electrode system design parameters as noted in Table 6.1.2, with a reference electrode width (that is, outer surface radius minus inner surface radius) of 25.4 mm. The rectangular copper piping has exterior dimensions of 25.4 x 50.8 mm, with a wall thickness of approximately 6.3 mm (1/4 inch). The cap thickness is assumed to be 0.75 mm (30 mils). Heat losses to the electrode cooling system are estimated based upon a slag temperature of 1800 K and assuming that all heat transfer occurring in the generator is through convection. The total electrode system heat loss is less than 7 percent of the generator total (wall and electrode) heat loss in every case. Even with a significantly wider anode (say 125 mm) the total electrode system heat loss would be only 10 percent of the generator total heat loss.

TABLE 6.1.2 OPEN CYCLE DISK SYSTEM DATA

	CASE 1A	CASE 1B	CASE 2	CASE 3
Electrode Radius				
(m)				
Anode	1.26	1.31	1.05	0.92
Electrode 2	3.25	3.25	3.00	3.00
Electrode 3	4.23	4.23	3.95	4.05
Electrode 4	4.72	4.72	4.55	4.75
Cathode	5.21	5.18	4.91	5.35
Disk Load Current				
(A)				
(Constant E_r				
Constraint)	12578	11246	8804	8457
Total Electrode				
Surface Area				
(m ²)	5.96	5.97	5.57	5.57
Estimated Heat Loss				
to Electrode Cooling				
System MW_t				
(% of Disk Total Loss)	3.1 (6.6)	2.6 (6.8)	2.9 (6.8)	3.7 (6.3)
Electrode Loading				
at Design Point				
(kA/m ²)				
Anode	31	27	26	29
Cathode	8	7	6	5

For the percentage heat losses noted above, it becomes feasible to use a cooling system for the electrodes which is entirely independent of the bottoming plant. This is an important advantage of the disk generator over currently-proposed linear generators, since it eliminates the possibility of copper ions entering the feedwater stream. It has been demonstrated that copper or copper-bearing alloys, when used in the lower-temperature regions of a high pressure steam-raising system, will cause increased corrosion rates in high heat flux regions of the steam plant, particularly in regions where phase changes are occurring in the working fluid. The use of all stainless-steel piping in the regenerative cooling sections of the disk, diffuser, and combustor has been proposed in order to provide materials in these sections identical to that utilized in the radiant furnace waterwalls, thus eliminating all sources of copper from the system.

The copper electrode rings for the disk are supported by studs held in place in the fiberglass insulating walls of the disk. The design of the electrode support system must include provision for containing the reaction forces caused by the motion of the load current in a plane nominally perpendicular to that of the magnet axial field vector, as well as by the skew forces resulting from the increasing radial field near the outer periphery of the magnet. The details of the force containment structure for the electrode rings have not been determined, as they are beyond the scope of this study.

A schematic representation of the electrode integration with the disk wall, and the current extraction provisions for electrodes, are shown in Figure 6-1-1 Detail D. Cooling water can be introduced through a downcomer brazed to an opening in the outer wall of each circular electrode, entering through an insulating section of hose from the combined electrode/inverter cooling system. This system is independent of the bottoming plant systems, rejecting heat directly to the plant component cooling or service water system. Water treatment must be as comprehensive as that for the disk/diffuser/combustor cooling systems, in order to provide an extremely low conductivity fluid. Temperature can be kept in the 373-423 K range with relatively low fluid pressures. After cooling the electrode ring, the water is extracted at a

(point diametrically opposed to its injection point, again through an insulated connection which returns the heated fluid to the heat exchangers and demineralizers. The total heat load in a single ring electrode from ohmic heating at short circuit current is less than 100 kW. The system is thus effectively sized for removal of heat transferred from the disk plasma to the electrode walls.

No cooling is required for the pair of 25.4 x 76.2 mm insulated copper bus bars which extract the current at opposite sides of each ring electrode. Four bus bars are connected to form the combined current lead-in from one electrode pair to one terminal of the inverter bank servicing a single segment.

Disk Generator Supersonic Nozzle

The nozzle which achieves the final acceleration of the combustor swirling exit flow to the supersonic velocities needed for disk generator power extraction is formed by a continuous circular constriction in the flow passage between the upper and lower disk walls just downstream of the combustor exhaust outer radius. To minimize stagnation pressure losses it is necessary to turn the axial component of plasma flow leaving the combustor while it remains subsonic, and to achieve the bulk of the acceleration to supersonic velocity after the conversion of this axial flow component to either radial or tangential flow. The correct design of the supersonic nozzle requires a detailed effort for each individual disk generator application, which is well beyond the scope of this study.

Cooling of the nozzle walls is provided by the disk generator cooling system previously described. Since all portions of the disk generator structure inside the radius of the inner electrode will operate at a constant potential above ground, the design of the cooling system in the nozzle region can rely upon multiple headers and larger, more closely spaced cooling passages, if necessary, to protect the nozzle surfaces and those of the upper disk section directly opposed to the combustor exit. For this design concept, the disk cooling line separation of 0.1 m has been assumed to be maintained in the nozzle region to facilitate estimation of costs and weights.

6.1.2 ANNULAR DIFFUSER FOR DISK GENERATOR

Conceptually, the most efficient diffuser for a disk generator with radial outflow would be a radial (i.e., constant angular momentum) diffuser of the type utilized in turbomachinery. This would provide for relatively high pressure recovery with minimal heat loss. With the operating parameters and applications chosen for the open-cycle disk generators in this study, however, the use of a pure radial diffuser is complicated by the absence of any significant disk outlet swirl and by the necessity to couple the disk exhaust to a steam bottoming plant. The diffuser concept selected was thus that of an annular diffuser surrounding the disk generator, which couples the disk exhaust to a limited number of discrete radiant furnaces located about the diffuser periphery.

6.1.2.1 Diffuser Layout

The disk diffuser is composed in concept of a set of radially-disposed equivalent linear diffusers, whose walls are formed by splitter vanes running from the roof (upper horizontal surface) to the floor (lower horizontal surface) of the annular diffuser. The splitter vanes act as locating and supporting members for the diffuser structure and provide access between the upper and lower disk surfaces for service connections passing through their interior.

6.1.2.2 Diffuser Aerodynamic Design

The number of splitter vanes and their aerodynamic shapes are dictated by the precise application. The design must provide equivalent backpressure on the disk exhaust at any azimuthal location along the exit radius, while attaining maximum pressure recovery and turning the flow into a limited number of symmetrically-placed radiant furnace inlet ducts. At any radial position the rate of increase of the floor-to-roof and wall-to-wall dimensions between splitter pairs must be selected to prevent stall and to provide maximum pressure recovery in analogous fashion to that for a purely linear diffuser. For the open-cycle generator cases and parameters selected for the optimized system designs in this study, it was determined that a diffuser with a maximum outlet radius of about 10 meters and a splitter pattern of 24 separate vanes equally positioned in azimuth could be calculated to provide reasonable annular diffuser performance[2]. This diffuser design was then assumed fixed for all four of the open-cycle cases. (The inlet radius of the diffuser was taken to be equal to the outlet radius of the disk generator for each individual case.) Each flow path between splitter vanes is assumed to carry mass flow equal to the total disk generator flow divided by the number of equivalent flow paths in the diffuser.

Supersonic to Subsonic Transition

For the transition from supersonic to subsonic flow, the disk generator performance model assumes the existence of a normal shock at the disk generator exit. The inlet Mach number for the subsonic portion of the diffuser will depend upon the Mach number at which the sonic transition occurs. This is set

by the diffuser outlet condition, which specifies the disk exit radius. In practice, an oblique shock system will be set up at the disk exit radius; the system will undoubtedly move up and down the channel slightly, even given the provision of a very sophisticated combustor/inverter integrated control system. A limited distance, over which the sonic transition can occur through a series of oblique shocks is provided after the disk exit radius and prior to the leading edge of the splitters. Flow deceleration will occur without resort to a complicated wall separation design in this region, since the equivalent flow area for constant floor-roof separation increases linearly as the radius. Maintaining a constant channel height in this area may not promote maximum pressure recovery, however. Each application of the diffuser requires an extensive aerodynamic evaluation, not only for design point operation but for normal fluctuations about the design point, and for maneuvering. These detailed evaluations were not made as part of this study.

6.1.2.3 Diffuser Cooling

The diffuser roof and floor surfaces are cooled by circumferential cooling lines similar to those used in the disk wall cooling system. These lines carry cooling water which has previously been directed through the disk cooling system. The splitter vanes are cooled by high pressure boiler feedwater, which flows through the splitter vane cooling system from the combustor cooling system and thence to the radiant furnace waterwalls.

The roof, floor, and splitter vanes are protected from the seed-and slag-laden plasma by a surface layer of plasma-jet-sprayed magnesia, backed by a thickness of rammed magnesia supported by the studding on the internal cooling tubes. The studding also aids in heat transfer from the refractory to the cooling water system. The vanes and walls will operate at a surface temperature of 2000 K to prevent condensation and buildup of slag films within the diffuser. This relatively high wall temperature and the restricted dimensions of the diffuser flow sections between vanes will limit the amount of heat transfer to the walls from the plasma, particularly in the lower-velocity regions where convective heat transfer becomes small.

The exterior surfaces of the diffuser can be covered with a fiber blanket insulating layer to limit heat loss to ambient, since wall cooling is provided by the low temperature condensate system. The cooling tubes are bolted to the stainless steel wall plates; these walls will therefore operate at about maximum metal temperatures for the tube walls in the cooling system, with the exterior blanket installed.

6.1.2.4 Disk/Diffuser Structural Design

The structural designs of the disk and diffuser have been integrated to provide a reasonably strong and stiff structure with a minimum of structural members being required in the disk area; this reduces the amount of interference with the disk service connection layout requirements and with the magnet and combustor subsystem service connections. Lack of a heavy structural framework for the disk generator itself also permits the possibility of a more rapid changeout of the disk if necessary by rise of the overhead crane, thus enhancing availability and maintainability of the disk generator systems.

The 0.23 meter thickness of the disk fiberglass walls will limit the maximum bending deflection under operating pressure loadings typical of the supersonic open-cycle disk generators to approximately 4.3 mm (0.17 inch), assuming simply-supported conditions at the inner and outer diameters. This thickness was established primarily from deflection considerations. The assumption of simple support conditions requires that appropriate structural support be provided for the fiberglass disks from the diffuser at the outer disk diameter, and from the combustor (below) and a system of bracing (above) at the inner diameter.

The inner diameter of the lower fiberglass disk is supported from the extension of the combustor exhaust neck which penetrates the annular hole in the magnet. The combustor assembly itself is supported from a concrete foundation by means of a fiberglass and steel electrically-insulating structure.

The inner diameter of the upper fiberglass disk is supported against the high pressure gas forces in the nozzle inlet plenum region by means of a system of

bracing. The arrangement shown in Figure 6-1-1 employs a support cylinder and a web of spoke-like stainless steel rods which reinforce the upper disk wall and transfer loads due to the high pressure gas forces in the nozzle out to the diffuser structure. The resulting loads applied to the diffuser roof by the spokes are in the outward direction and tend to balance the inward acting gas forces, thus reducing the tendency of the diffuser roof to deflect inward.

The diffuser structure consists of upper and lower structural walls fabricated from stainless steel plate, and stiffened by wide flange stainless steel beams. The roof and floor are separated by 24 radial flow splitters which are utilized to maintain the relationship between the upper and lower walls in the diffuser subsonic portion, promote efficient diffusion in a short radial distance, turn the flow into the radiant furnace inlet ducts at the completion of the diffusion process, and provide access between upper and lower sections of the disk and diffuser.

In the arrangement illustrated in Figure 6-1, the fiberglass disks are bolted at their outer diameters to stainless steel ring members welded to 12.7 mm (0.5 inch) thick stainless steel plate walls and 8 x 8 WF beam radial stiffening members. These 8 x 8 WF beams provide the necessary strength and stiffness to transfer the channel disk support loads, and the diffuser gas loads, outward to the 12 x 12 WF beam ring members, which in turn transfer the loads to the splitters. The configuration of Figure 6-1-1 results in a deflection of approximately 8 mm or less at the channel support rings. To this value must be added the fiberglass disk deflection of 4.3 mm to arrive at a total wall deflection of approximately 13 mm (0.5 inch). This deflection will occur in both walls, and the maximum channel narrowing is approximately 25 mm (1 inch), being 11% of the minimum channel height for the illustrated disk. As previously noted, this deflection will be reduced by the effect of the upper wall stiffening system, which transfers an outward gas pressure force from the disk hub to the diffuser roof, thus tending to balance the inward gas pressure force. Tailoring of the unloaded channel gas surface profile can also be utilized to allow for the deflections under operating conditions.

The discussion above relates only to deflections due to gas pressure loads, and assumes that the channel lower wall is supported by the combustor at its inner diameter, and that the stiffening structure supports the upper channel wall. During the assembly of the upper channel wall onto its (outer) support ring, the fiberglass disk will sag approximately 30 mm (1.2 inches) at its inner diameter under its own weight and that added by the cooling tubes and ceramic. (This estimate assumes no structural contribution from the tubes.) Allowance for this initial deflection must be designed into the unstressed shape of the channel so that when loaded by its own weight the inner disk wall surfaces conform to the required channel profile. An additional allowance must also be made for the deflection of the upper wall which will occur as the stiffening structure spokes are installed. Nominal pretensioning may be required to minimize deflection under load.

As noted previously, the deflection of the fiberglass disks expected from the presence of a thermal gradient between their inner and outer surfaces can be eliminated by applying a layer of fiber wool thermal insulation on the exterior surface of the disks. The stress levels in the fiberglass disks are well below the limiting stresses for the resulting temperature of the material, due to the low operating temperature of the cooling water system.

When loaded by the high pressure gas forces in the central region of the upper disk half, the stiffening structure will deflect approximately 5 mm (0.2 inch), allowing a corresponding increase in channel height in this region. This component of deflection is particularly critical in that the nozzle throat area and therefore the flowrate under choked flow conditions is directly affected. Adjustment of the throat area is possible after assembly by adjusting the pretensioning of the stiffening structure spokes.

An alternative approach to stiffening the upper channel wall during operation is to use the gantry crane which will be provided as part of the facility. An insulated support cylinder could transfer the central gas pressure load to the traveller of the crane. The crane stiffness characteristics would have to be assessed and found suitable for such purpose. Since the load path obtained by

this approach is less direct than that of the spoked stiffening structure, it can be expected to involve much heavier structural members. This, however, may not be inconsistent with the gantry crane lifting capability necessary for handling the magnet components and the combustor.

The main support load paths from the diffuser structure to ground will be via the lower outer ring girder shown on Figure 6-1-1, and a ring of post members adjacent to the periphery of the magnet. No disk or diffuser support loads will need to be transferred through the magnet. For certain diffuser/radiant boiler arrangements (see Section 6.5 for further discussion), the outer ring girder could conceivably be utilized to transfer the deadweight loads of the inner walls of the radiant furnaces to ground. The diffuser splitters would require modification to permit the transfer of these loads.

6.1.3 ADDITIONAL DESIGN CONSIDERATIONS

Some other aspects of disk generator detail design which will require attention are the provisions for access to the space between the channel and magnet for securing cooling lines, electrical conduits, etc. The inner ring girder can be interrupted in the region of each splitter to provide access, given the design of a suitable structural transition from ring girder to splitter. Provision must also be made in the diffuser structure design to facilitate its disassembly and removal in the event that access to the magnet is required. The capability of disassembling portions of the diffuser upper surface to provide access to local areas of the interior for maintenance, refurbishment, etc. appears to be mandatory in view of the restricted access afforded by the narrow gas passage dimensions. The details of gas sealing between disk, combustor, diffuser, and radiant furnace have not been established.

6.1.4 ADVANCED DISK GENERATOR DESIGN CONCEPTS

The disk generator and diffuser design concepts presented in the preceding sections have been limited to straightforward approaches utilizing normal structural materials which appear to satisfy the design requirements and applicable design constraints. Advanced developments of disk generator designs to accommodate improved aero dynamics and structures can be envisioned.

As an example, the disk generator pressure wall to accommodate a flow normal to the magnetic vector could be prefabricated in the form of a set of dome-shaped fiberglass disks, rather than flat disks. The shape would provide additional stiffness to the pressure walls, thus permitting thinner sections and requiring less bracing against deadweight and gas pressure loads.

The ring and radial girder structure of the annular diffuser could be replaced by a lighter structure similar to the formers and stringers used in aircraft fuselages. Since the diffuser wall cooling is provided by a relatively low temperature cooling water system, the stainless steel plate and support members could be replaced by a strong and light non-magnetic material such as aluminum, without approaching limiting stresses at the operating temperature, even with external insulation applied to limit heat losses to ambient.

6.2 COAL COMBUSTOR

The combustor configuration selected for application to the four open cycle disk generator system design cases is a two-stage vertically-firing type, with high exit swirl. The larger first (gasifier) stage is situated directly beneath the second stage, which exhausts through an adapter section to the supersonic nozzle formed by the upper and lower disk generator sections just inside the inner radius of the power extraction region. The combustor is supported by a stainless steel and fiberglass insulating and support skirt, and in turn supports the lower disk generator at the inner circumference through the adapter section. The combustor is located in a pit sunk directly beneath the central axial hole in the disk magnet, and fires through this hole to the disk generator. Figure 6-2-1 indicates the general configuration of the disk generator/magnet/combustor geometry. All service and control connections to the combustor pass through tunnels in the magnet support pad. Access to the combustor is through personnel tunnels which also penetrate the support pad.

6.2.1 COMBUSTOR CONFIGURATION SELECTION

The selection of combustor type is intimately connected with the choice of disk flow direction, i.e. either radial inflow or radial outflow. The radial

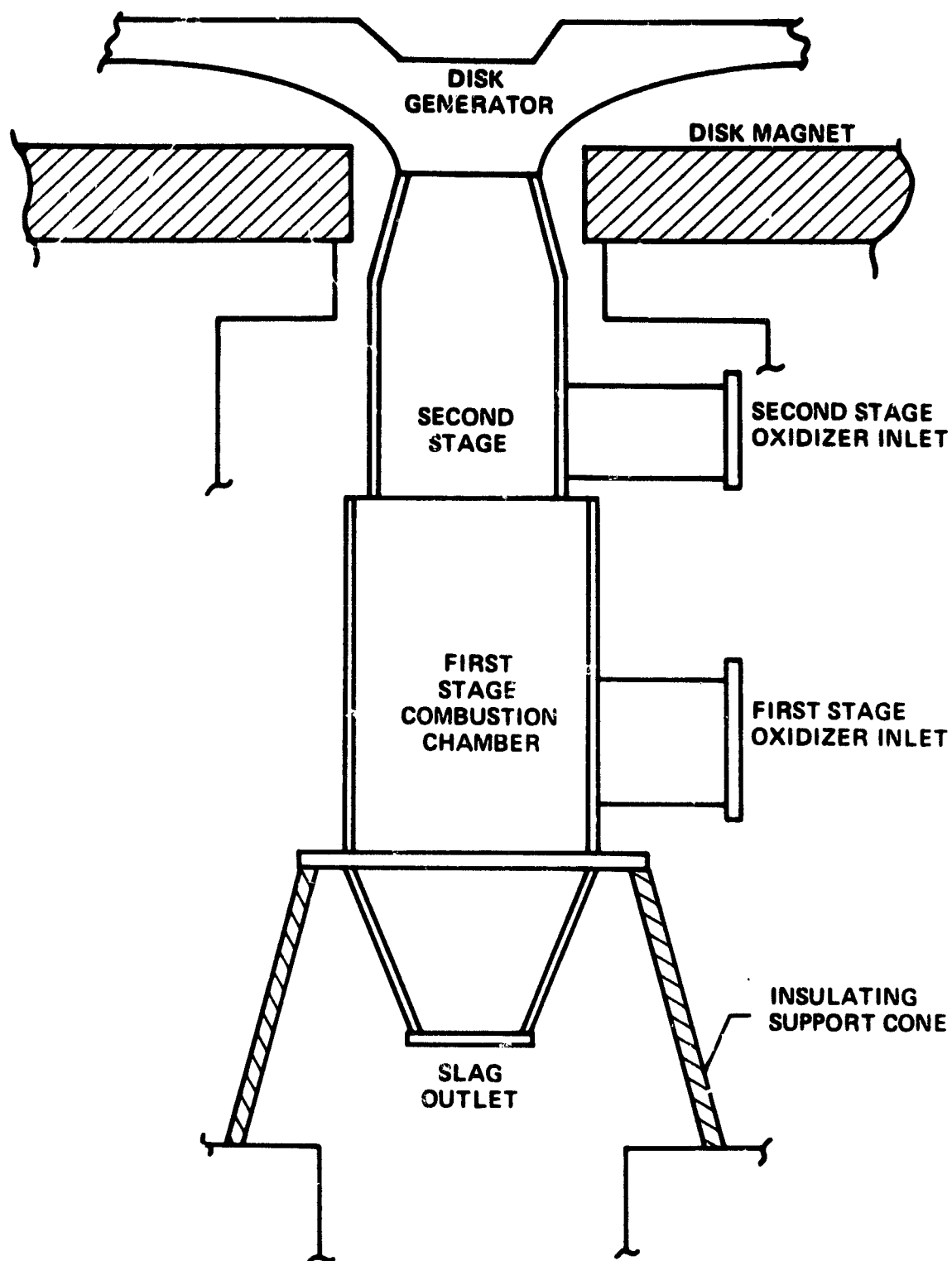


Figure 6-2-1. Disk Combustor Outline Drawing (Elevation)

inflow disk provides marginally better performance when compared to a radial outflow disk with the same disk inlet stagnation conditions and mass flow. This occurs because the inlet swirl ratio can be maintained in the radial inflow case by the conservation of angular momentum in the gas as it flows through the disk. However, with a fixed oxidant, fuel, and preheat condition it is not possible to obtain identical inlet stagnation conditions for the inflow and outflow disks, principally because of the implied requirement for a circumferential inlet plenum between the combustor and the disk power extraction region in the inflow case.

In the disk generator modeling section (Section 5.1), losses for both types of combustors were discussed, and the values assumed for the disk suboptimization studies were listed in Table 5.1.1. It was concluded during the early part of the disk generator suboptimization process that the radial inflow configuration offered no performance advantage over the radial outflow disk. The problems in power train layout and magnet design resulting from the use of the inflow configuration and its large central disk exhaust duct were also considered in making the decision to focus the study upon the outflow disk.

For the study, a rough comparison scheme for evaluation of combustor heat losses was developed. This comparison process is reviewed in Appendix A. For the specific combustor configurations evaluated in the Appendix (a single 2-stage axially-firing combustor and a series of tangentially-firing 2-stage combustors with the same mass flow as the single combustor) it was concluded that for all practical choices of combustor geometries, the heat loss of the combustor plus nozzle combination of an inflow disk will be several times greater than that for an equivalent outflow disk. As a limiting ratio, the heat loss ratio must always be at least 2.5 times greater in the inflow system than in the outflow system, given the same general combustor/nozzle configurations assumed for the analysis of Appendix A.

Estimated heat losses for the (radial outflow) two stage high-swirl combustors used in the optimized open cycle disk generator systems defined by this study range from 5 percent to 7 percent of the fuel higher heating value. Thus, the

equivalently sized radial inflow combustor/nozzle configuration can be expected to exhibit heat losses in the range 13 percent to 20 percent of HHV fuel. For the base 1920 K preheat condition, an increase of combustor heat loss of 10% (from 7% to 17%) results in an estimated decrease in combustor flame temperature of over 100 F, translating into a performance loss of 2-3 percentage points for directly-fired OCD systems designed by the methods developed in the study.

A comparison of the expected performance of an inflow disk when compared to an outflow disk with the same inlet operating conditions is made in a recent paper by Nakamura and Jenkins[1].

For the same inlet condition to the generator, with identical magnetic induction, disk wall temperature, inlet enthalpy flux, and diffuser conditions, a supersonic radial inflow disk operating in the impulse mode showed a slightly lower enthalpy extraction ratio than did a comparison radial outflow generator operating with supersonic flow in the impulse mode. The assumption of a radial inflow/outflow configuration for the disk resulted only in an increase of 1.5 percentage points in the generator enthalpy extraction ratio. When considered in light of the fact that a constant preheat temperature would provide significantly lower inlet stagnation temperature in a radial inflow disk system as compared to an analogous outflow disk system, it is apparent that the radial inflow configuration will not match the radial outflow performance for OCD operation with identical preheat levels, if the derived relationship for combustor heat losses, is correct.

It was therefore decided to focus the systems parametric analysis upon the radial outflow disk generator. This, in turn, set the basic configuration of the coal combustor for the OCD plants.

6.2.2 COMBUSTOR GENERAL DESIGN REQUIREMENTS

The general design requirements for a coal combustor to be used with an open cycle disk MHD generator are in no significant way different from those of any other MHD coal combustor. The normal requirements of coal volatilization,

carbon conversion, seed vaporization and ionization, stable operation, slag rejection, etc. must be provided for the disk as well as linear MHD generator application of the combustor. Certain design requirements must, however, receive more emphasis in the specification of combustor details for the disk generator application. These include:

- Minimization of combustor heat and pressure losses;
- Design for suitable lifetime at the extreme combustion temperatures required for the disk generator;
- Compatibility with the radial outflow configuration of the disk generator.

For the disk generator, the minimization of heat and pressure losses in the combustion gas is particularly important, since the requirement to accelerate the combustion gas to supersonic velocities causes a depression in channel inlet conductivity with respect to a subsonic linear generator, for the same combustor stagnation conditions. Therefore, the disk generator combustor design should reflect this through a minimization of combustion chamber wall area. For the radial outflow disk this requirement is best met by a 2-stage axially-firing combustor located coaxially with the disk generator, as shown in Figure 6-2-1. An additional consideration in this area is the necessity for providing a swirl velocity (tangential velocity component) at the disk generator inlet, to enhance its performance by compensating for the induced swirl component with opposite direction. A high exit swirl velocity implies the presence of guide vanes placed in the combustion gas flow, with attendant heat and pressure losses. Such guide vane losses can be reduced if the design of the combustor second stage permits the attainment of a reasonable swirl without the need for vanes.

The present study presumes that a swirl ratio of 0.5 can be obtained without resort to guide vanes in the combustor outlet flow. Section 5.1.2 describes the modeling for enthalpy and pressure losses arising from the introduction of

guide vanes. Parametric cases 1-10 (directly-fired, swirl = 1.0) and 2-8 (separately fired, swirl = 1.0) are the high-swirl cases in the parametric analyses. Neither case exhibits a performance improvement over the respective base case with the nominal swirl ratio of 0.5.

The modeling of swirl losses referred to above reflects the assumption that a vaneless combustor/nozzle combination can provide at least a swirl of 0.5. The validity of this assumption has not been proven. Given the lack of performance improvement with the higher-swirl cases over the 0.5 swirl cases, it was decided to specify for the optimized OCD systems vaneless combustors with design swirl at the disk inlet of 0.5. The vaneless disk inlet passage can be expected to result in a more reliable (i.e., longer MTBF) combustor design, thus contributing to plant availability.

6.2.3 COMBUSTOR DESIGN DETAILS

The design details of the combustor for each of the four OCD cases have been developed to the degree necessary to permit a reasonable cost estimate to be made for each unit. The specific design of combustor auxiliary systems such as seed and coal injection has not been addressed. These service systems, while important to the overall plant performance, are in no major aspect different from those required for a linear MHD plant combustor. Thus, the details of nozzle placement for coal injection and mixing, slag removal and/or electrical isolation, etc. are not considered in the following.

6.2.3.1 Combustion Conditions

The combustion volumes of the first stage and second stage were selected on the basis of the following criteria, recognizing that the residence-time and shape values chosen will very likely be modified in the light of the experimental data from the current DOE/MHD intensive MHD cool combustor R&D program. These data were not available for this study, so "best estimates" have been used to allow sizing and costing of components.

- The overall combustion stoichiometric ratio is $\phi = 0.95$ for all combustors.

- The first stage volume was chosen on the basis of providing a minimum gas residence time of 70 milliseconds. This residence time limit provides the minimum acceptable time to permit volatilization and maximize carbon utilization in the assumed fuel-rich mixture ($\phi \approx 0.40$).
- The second stage volume was chosen to provide a minimum gas residence time of 20 milliseconds. This permits complete vaporization and ionization of the potassium seed.

The use of extremely fuel-rich mixtures for final combustion conditions in the disk combustors to minimize NO_x formation (an especially critical area with the open cycle disk generator system with high preheat level and directly-fired preheaters) was not investigated for this study. Stoichiometric ratios $\phi \approx 0.85$ would be the minimum allowable due to the significantly decreased utilization efficiency of the combustor below this value. The stagnation temperature attainable with such rich mixtures would begin to decrease below the $\phi = 0.95$ temperature somewhere in the vicinity of $\phi \sim 0.90$, again a critical consideration for maximum disk generator performance potential. It is likely that a combustion stoichiometric ratio of $\phi \sim 0.92$ - 0.93 would optimize the combustion conditions with respect to NO_x formation and stagnation temperature. For this study only the value $\phi = 0.95$ was utilized in evaluating the performance of the "optimized" OCD systems.

6.2.3.2 Combustor Geometry

The combustion chamber shape was assumed to be a right circular cylinder for each stage, with a slightly restrictive nozzle (or "finder") between the first and second stages. The L/D of each stage was held at slightly more than 1.0 to minimize surface-to-volume ratio while providing suitable mixing within the gas in each stage. The outside diameter of the second stage in each combustor design was constrained to be less than 3 meters, to permit the coupling of each combustor by a conical adapter with the disk generator inlet neck through the warm bore of the disk magnet.

The axially-firing linear combustor was selected not only for its minimum heat and pressure loss potential, but also because it provides for ease of slag removal system design. The slag is removed from the combustion mixture principally by the centrifugal forces generated in the swirling mixtures, and gravitational forces cause it to flow downwards in the combustion chamber towards the slag outlet neck. The diameter of the neck was taken to be approximately 0.25 times the diameter of the first stage combustion chamber, to limit the potential for complete blockage of the outlet by slag buildup during long-term high power level operation while minimizing the available area for radiation losses through the slag system. The heat losses attributable to slag removal from the combustor have been estimated and are considered in the final systems performance analysis for each case.

6.2.3.3 Combustor Electrical Isolation

The disk generator design anticipates the operation of the system with the downstream radius (i.e. diffuser and beyond) grounded. Thus, the combustor must operate at the full Hall potential developed across the disk generator, which for the four OCD cases evaluated will be approximately 50 kV. The combustor support and all service/control lines must therefore permit full isolation from ground. For the cooling water, air, seed, and electrical connections various methods have been proposed for previous linear generator designs, and these are no different in principle or in detail from those required by the disk generator combustors. These isolation provisions are therefore not considered in the conceptual design for these combustors. For the isolation of the combustor structure from ground, a fiberglass/stainless steel combination support and insulating ring is proposed. Shaped as a truncated circular cone, this ring supports the deadweight loads of the combustor and lower disk half inner section, and isolates the Hall potential from ground. The structure has been sized on support and isolation considerations only, in order to permit a rough major materials plus fabrication cost evaluation. Details of interface with the combustor first stage and concrete support have not been developed, nor has the requisite information concerning detection of impending loss of isolation.

6.2.3.4 Combustor Cooling System

Combustor cooling is provided by a series of circumferential cooling lines located in the wall of the first and second stage and the slag outlet neck. These lines are provided with supercritical bottoming plant working fluid from the high pressure boiler feedwater pump through a 10 inch Schedule 160 stainless steel header that runs vertically up the side of the combustor from top to bottom. Following the passage of the fluid through the high pressure high temperature electrical isolation section from the main feedwater header, it enters the individual cooling coils through welded couplings at the various stations along the header, flows circumferentially around the walls of the combustor, and leaves to mix with the bulk of the heated fluid in a return header parallel to and identical with the inlet header. Both headers are fully insulated to reduce heat losses from the cooling system.

The combined flow from the individual cooling coils is routed through an electrical isolation section, through the diffuser splitter vane cooling lines, to the radiant furnace inlet duct cooling lines and hence to the radiant furnace. Thus, the bulk of the heat lost in the combustor is recovered for steam generation in the bottoming plant.

Since the steam plant working fluid is routed through both the disk and combustor cooling systems, which operate at the full Hall potential, it is necessary to provide the utmost purity and thus minimize conductivity in this fluid by the use of a full-flow demineralization unit in the cooler condensate portion of the system. This requirement is shared with the disk generator system by any linear MHD system which has direct coupling between the MHD component cooling system and the bottoming plant working fluid.

The cooling coils within the walls of the combustor are fabricated from 2 inch Schedule 160 full-studded piping. These coils are welded to the 10 inch Schedule 160 supply and return headers. The inlet and outlet headers themselves are part of the combustor structure. The total pressure loss in the combustor cooling system, from inlet to outlet flanges at the electrical isolation sections is estimated to be approximately 50 to 100 kPa at full flow full-power conditions.

6.2.3.5 Combustor Wall and Structural Design

The wall design selected for the OCD coal combustors is depicted in Figure 6-2-2. The pressure envelope is formed from 13 mm (0.5") thick stainless steel. Since the combustor operates directly in the field of the disk magnet, all metallic components will of necessity be fabricated from non-magnetic materials. The use of stainless steel is indicated because of its high strength at the high temperatures at which the wall and piping must operate. Since at their outer circumference the circumferential cooling coils will be supported by the combustor wall, the wall will operate at the maximum metal temperature of the cooling system (with thermal insulation applied to limit wall heat losses to ambient). The vertical pitch of the 2-inch cooling lines was chosen to be 100 mm (4 inches) in the first stage, and 75 mm (3 inches) in the second stage.

The combustor wall is set with rammed magnesia refractory to protect the steel cooling coils and outer steel pressure jacket. Each stage is finished with a plasma-jet-sprayed coating of refractory, magnesia for the first stage and yttria-stabilized zirconia for the second. Magnesia exhibits good resistance to slag at temperatures up to 2000 K but it is necessary to use the stabilized (cubic) form of zirconia as a final wall coating in the second stage of the combustor due to the extreme gas temperatures. In the presence of a reducing environment, and seed materials, the stabilized form of zirconia will revert to the anisotropic structure after some time, thus resulting in the potential for spalling and cracking of the applied surface layer. This is judged to be a serious problem for the combustor design, at least for the 1920 K preheat case. For lower preheat temperatures, the presence of an insulating slag layer (in the first stage at least) may obviate the necessity for a significant refractory lining in the combustor. Such a problem is not uniquely disk generator-related, but due to the necessity to operate the disk with the highest available stagnation conditions to maximize plasma conductivity after acceleration to supersonic flow, it poses a severe handicap to achieving equivalent performance to that of a subsonic linear generator, with high availability. Thus the national MHD coal combustor R&D program should be addressed to attaining these plasma parameter requirements also.

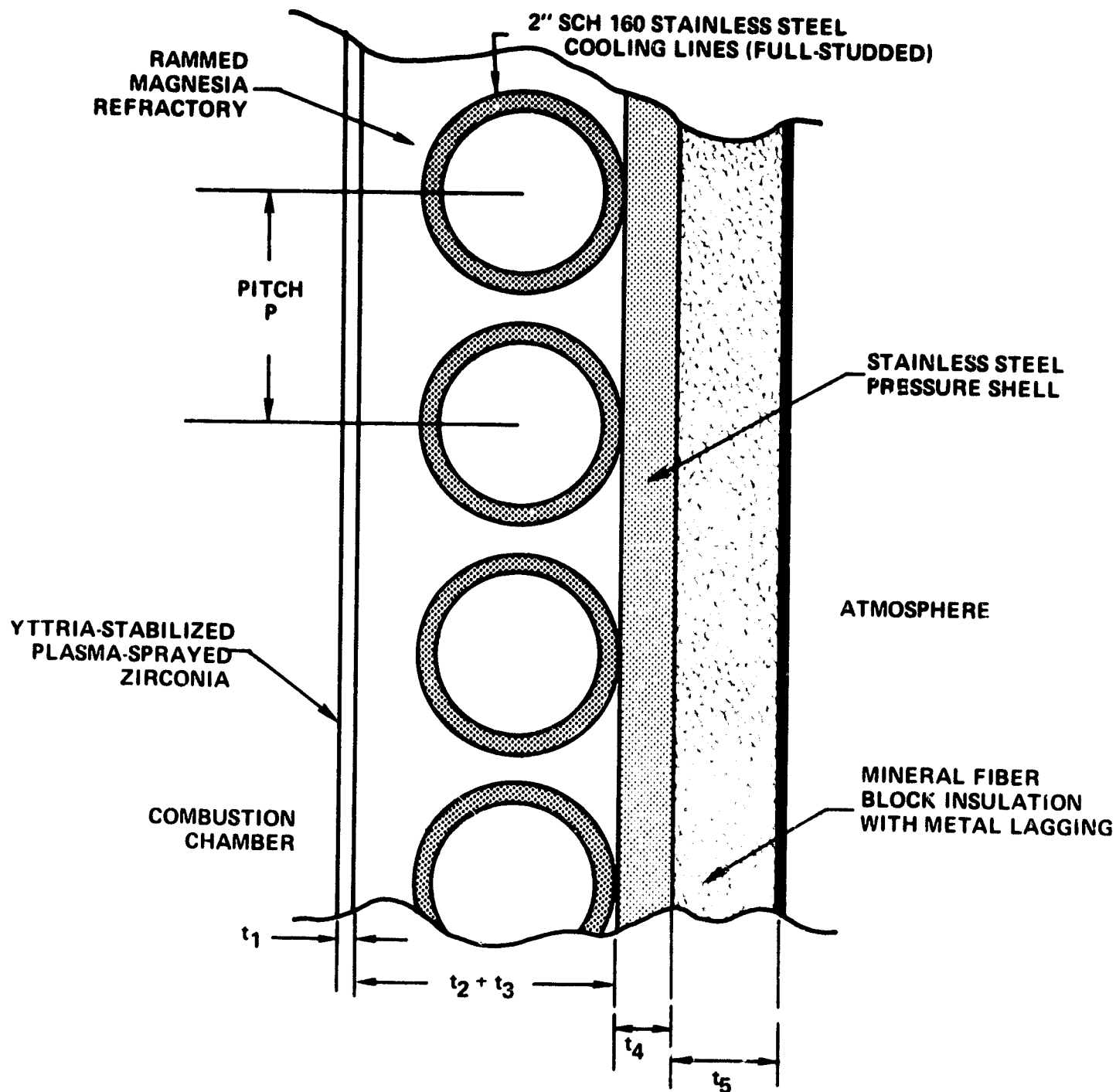


Figure 6-2-2. Disk Combustor Wall Design Concept

The combustor wall is covered by an external blanket of mineral wool insulation, to limit heat loss to ambient. The blanket itself is covered with a thin layer of stainless steel lagging material to provide support.

The entire combustor can be shop-fabricated and shipped as a unit to the plant site. The combustor can be installed in its pit prior to the installation of the magnet. For removal of the combustor after plant construction is complete, the overhead crane can lift the combustor free of its support skirt following disk generator removal; the combustor can be tilted to the horizontal and removed via a specially-sized access tunnel under the magnet.

6.2.3.6 Final Case Design Parameters

The design parameters for the coal combustors of each OCD case are given in Tables 6.2.1A through 6.2.1D. The dimensional data for each combustor design is contained in Table 6.2.2.

TABLE 6.2.1A
MHD COAL COMBUSTOR DESIGN DATA
FOR
OPEN CYCLE DISK GENERATOR SYSTEM
WITH DIRECTLY-FIRED AIR PREHEATERS
1920 K PREHEAT

● General Data	
Combustor Type:	2-Stage Cyclone
Fuel:	Pulverized Coal
Fuel Type:	Montana Rosebud, 5% Moisture
Fuel Carrier Gas:	Flue Gas
Oxidant:	Air
Seed	Mixed K_2CO_3 and K_2SO_4
Seed Carrier Gas:	Air
● Combustion Data	
Fuel Conditions: Mass Flow	81.36 kg/s
Coal Thermal Input	2077.1 MW _t
Carrier Gas Flow	8.14 kg/s
Carrier Gas Temp.	408 K
Oxidant Conditions:	
Mass Flow	643.48 kg/s
Temperature	1920 K
Pressure	669 kPa
Combustion Gas Conditions, First Stage:	
Plasma Stagnation Temp.	2143 K
Residence Time	70 ms
Overall Combustion Stoichiometry:	0.95
Combustion Gas Exit Conditions: Mass Flow	735.98 kg/s
Temperature	2839 K
Pressure	615 kPa
● Seed Feeding System Data	
Seed injection Rates:	K_2CO_3 - 2.02 kg/s K_2SO_4 - 8.80 kg/s
Seed Injection Temperature:	350 K
Plasma Exit Conductivity:	11.24 mho/m

TABLE 6.2.1A
MHD COAL COMBUSTOR DESIGN DATA
FOR
OPEN CYCLE DISK GENERATOR SYSTEM
WITH DIRECTLY-FIRED AIR PREHEATERS
1920 K PREHEAT

● Combustor Cooling System Data	
Design Heat Duty:	145.4 MW _t
Cooling System Type:	High Pressure Regenerative
Cooling Water Conditions:	
Mass Flow	385.16 kg/s
Pressure	26.3 MPa
Inlet Temperature	555 K
Outlet Temperature	622 K
● Slag Separation Data	
Slag Rejection Coefficient:	0.90
Slag Flow to Quench System:	7.83 kg/s
Ash/Slag Carryover to Channel:	0.87 kg/s
Slag Rejection Heat Loss	11.2 MW _t
● Miscellaneous Data	
Combustor Shell Material	18-8 Stainless Steel
Combustor Cooling Line Material	2" Sch. 160 Stainless Steel
	Full Studded
Shell and Cooling System Maximum Operating Temperature:	727 K
Insulating Jacket Design Outer Temperature	339 K
Combustor Structural Floating Potential	48 kV
Combustor Weight	40,468 kg
1st Stage Air Inlet Header Diameter	2.00 m
2nd Stage Air Inlet Header Diameter	1.65 m
Slag Neck Diameter	0.73 m

TABLE 6.2.1B
MHD COAL COMBUSTOR DESIGN DATA
FOR
OPEN CYCLE DISK GENERATOR SYSTEM
WITH DIRECTLY-FIRED AIR PREHEATERS
1650 K PREHEAT

- General Data

Combustor Type:	2-Stage Cyclone
Fuel:	Pulverized Coal
Fuel Type:	Montana Rosebud, 5% Moisture
Fuel Carrier Gas:	Flue Gas
Oxidant:	Air
Seed:	Mixed K_2CO_3 and K_2SO_4
Seed Carrier Gas:	Air
- Combustion Data

Fuel Conditions: Mass Flow	39.51 kg/s
Coal Thermal Input	2284 MW _t
Carrier Gas Flow	8.95 kg/s
Carrier Gas Temperature	408 K
Oxidant Conditions:	
Mass Flow	707.82 kg/s
Temperature	1650 K
Pressure	541 kPa
Combustion Gas Conditions, First Stage:	
Plasma Stagnation Temp.	
Residence Time	70 ms
Combustion Gas Conditions, Second Stage:	
Plasma Stagnation Temp.	2750 K
Residence Time	20 ms
Overall Combustion Stoichiometry:	0.95
Combustion Gas Exit Conditions: Mass Flow	
Temperature	2731 K
Pressure	497 kPa
- Seed Feeding System Data

Seed Injection Rates:	K_2CO_3 - 2.22 kg/s
	K_2SO_4 - 9.68 kg/s
Seed Injection Temperature:	350 K
Plasma Exit Conductivity:	8.34 mho/m

C - 3

TABLE 6.2.1B
MHD COAL COMBUSTOR DESIGN DATA
FOR
OPEN CYCLE DISK GENERATOR SYSTEM
WITH DIRECTLY-FIRED AIR PREHEATERS
1650 K PREHEAT

● Combustor Cooling System Data	
Design Heat Duty:	159.9 MW _t
Cooling System Type:	High Pressure Regenerative
Cooling Water Conditions:	
Mass Flow	453.56 kg/s
Pressure	26.3 MPa
Inlet Temperature	521 K
Outlet Temperature	592 K
● Slag Separation Data	
Slag Rejection Coefficient:	0.90
Slag Flow to Quench System:	8.64 kg/s
Ash/Slag Carryover to Channel:	0.96 kg/s
Slag Rejection Heat Loss	12.3 MW _t
● Miscellaneous Data	
Combustor Shell Material	18-8 Stainless Steel
Combustor Cooling Line Material	2" Sch. 160 Stainless Steel
	Full Studded
Shell and Cooling System Maximum Operating Temperature:	700 K
Insulating Jacket Design Outer Temperature	339 K
Combustor Structural Floating Potential	46.5 kV
Combustor Weight	38,290 kg
1st Stage Air Inlet Header Diameter	2.20 m
2nd Stage Air Inlet Header Diameter	1.80 m
Slag Neck Diameter	0.68 m

TABLE 6.2.1C
MHD COAL COMBUSTOR DESIGN DATA
FOR
OPEN CYCLE DISK GENERATOR SYSTEM
WITH SEPARATELY-FIRED AIR PREHEATERS

● General Data	
Combustor Type:	2-Stage Cyclone
Fuel:	Pulverized Coal
Fuel Type:	Montana Rosebud, 5% Moisture
Fuel Carrier Gas:	Flue Gas
Oxidant:	Air
Seed:	Mixed K_2CO_3 and K_2SO_4
Seed Carrier Gas:	Air
● Combustion Data	
Fuel Conditions: Mass Flow	56.96 kg/s
Coal Thermal Input	1453.9 MW _t
Carrier Gas Flow	5.70 kg/s
Carrier Gas Temp.	408 K
Oxidant Conditions: Mass Flow	450.43 kg/s
Temperature	1920 K
Pressure	669 kPa
Combustion Gas Conditions, First Stage:	
Plasma Stagnation Temp.	2138 K
Residence Time	70 ms
Combustion Gas Conditions, Second Stage:	
Plasma Stagnation Temp.	2861 K
Residence Time	20 ms
Overall Combustion Stoichiometry:	0.95
Combustion Gas Exit Conditions:	
Mass Flow	515.18 kg/s
Temperature	2839 K
Pressure	615 kPa
● Seed Feeding System Data	
Seed Injection Rates:	K_2CO_3 - 1.42 kg/s K_2SO_4 - 6.16 kg/s
Seed Injection Temperature:	350 K
Plasma Exit Conductivity	11.24 mho/m
● Combustor Cooling System Data	
Design Heat Duty:	102.8 MW _t
Cooling System Type:	High Pressure Regenerative
Cooling Water Conditions:	
Mass Flow	447 kg/s
Pressure	26.3 MPa
Inlet Temperature	514 K

TABLE 6.2.1C
MHD COAL COMBUSTOR DESIGN DATA
FOR
OPEN CYCLE DISK GENERATOR SYSTEM
WITH SEPARATELY-FIRED AIR PREHEATERS (CONT'D)

● Slag Separation Data	
Slag Rejection Coefficient:	0.90
Slag Flow to Quench System:	5.48 kg/s
Ash/Slag Carryover to Channel:	0.61 kg/s
Slag Rejection Heat Loss:	7.8 MW _t
● Miscellaenous Data	
Combustor Shell Material:	18-8 Stainless Steel
Combustor Cooling Line Material:	2" Sch. 160 Stainless Steel (Full Studded)
Shell and Cooling System Maximum Operating Temperature:	723 K
Insulating Jacket Design Outer Temperature	339 K
Combustor Structure Floating Potential	47 kV
Combustor Weight	35,039 kg
1st Stage Air Inlet Header Diameter	1.70 m
2nd Stage Air Inlet Header Diameter	1.40 m
Slag Neck Diameter	0.64 m

TABLE 6.2.1D
MHD COAL COMBUSTOR DESIGN DATA
FOR
OPEN CYCLE DISK GENERATOR SYSTEM
WITH OXYGEN AUGMENTATION

● General Data	
Combustor Type:	2-Stage Cyclone
Fuel:	Pulverized Coal
Fuel Type:	Montana Rosebud, 5% Moisture
Fuel Carrier Gas:	Flue Gas
Oxidant:	Oxygen Enriched Air $O_2=1.07$
Seed :	Mixed K_2CO_3 and K_2SO_4
Seed Carrier Gas:	Air
● Combustion Data	
Fuel Conditions:	
Mass Flow	92.76 kg/s
Coal Thermal Input	2367.8 MW _t
Carrier Gas Flow	9.28 kg/s
Carrier Gas Temp.	408 K
Oxidant Conditions:	
Mass Flow	441.75 kg/s
Temperature	922 K
Pressure	913 kPa
Combustion Gas	
Conditions, First Stage:	
Residence Time	70 ms
Combustion Gas	
Conditions, Second	
Stage:	
Residence Time	20 ms
Overall Combustion	
Stoichiometry:	0.95
Combustion Gas Exit	
Conditions: Mass Flow	
Temperature	542.80 kg/s
Pressure	2839 K
	840 kPa
● Seed Feeding System Data	
Seed Injection Rates:	
	K_2CO_3 - 1.48 kg/s
	K_2SO_4 - 6.45 kg/s
Seed Injection	
Temperature:	350 K
Plasma Exit	
Conductivity:	6.45 mho/m

TABLE 6.2.1D
MHD COAL COMBUSTOR DESIGN DATA
FOR
OPEN CYCLE DISK GENERATOR SYSTEM
WITH OXYGEN AUGMENTATION (CONT'D)

● Combustor Cooling System Data	
Design Heat Duty:	165.8 MW _t
Cooling System Type:	High Pressure Regenerative
Cooling Water Conditions:	
Mass Flow	496.8 kg/s
Pressure	26.3 MPa
Inlet Temperature	483 K
Outlet Temperature	555 K
● Slag Separation Data	
Slag Rejection Coefficient:	0.90
Slag Flow to Quench System:	8.91 kg/s
Ash/Slag Carryover to Channel:	0.99 kg/s
Slag Rejection Heat Loss	12.7 MW _t
● Miscellaneous Data	
Combustor Shell Material	18-8 Stainless Steel
Combustor Cooling Line Material	2" Sch 160 Stainless Steel (Full-Studded)
Shell and Cooling System Maximum Operating Temperature:	650 K
Insulating Jacket Design Outer Temperature	339 K
Combustor Structural Floating Potential	53 kV
Combustor Weight	28,380 kg
1st Stage Air Inlet Header Diameter	1.00 m
2nd Stage Air Inlet Header Diameter	0.80 m
Slag Neck Diameter	0.53 m

TABLE 6.2.2
OPEN CYCLE DISK GENERATOR SYSTEM COAL
COMBUSTOR DIMENSIONAL DATA

	DIRECTLY(1) FIRED	DIRECTLY(2) FIRED	SEPARATELY FIRED	WITH O ₂ AND NO HTAH
<u>FIRST STAGE</u>				
Inside Diameter (D ₁), m	2.90	2.70	2.56	2.10
Length (L ₁ + L _s), m	4.50	4.30	4.05	3.50
Pressure Vessel Wall Thickness (t ₄), m	1.27 x 10 ⁻²	1.27 x 10 ⁻²	1.27 x 10 ⁻²	1.27 x 10 ⁻²
Magnesia Refractory Thickness (t ₂ + t ₃), m	7.98 x 10 ⁻²	7.98 x 10 ⁻²	7.98 x 10 ⁻²	7.98 x 10 ⁻²
Plasma-Sprayed Zirconia Thickness (t ₁), m	3.81 x 10 ⁻⁴	3.81 x 10 ⁻⁴	3.81 x 10 ⁻⁴	3.81 x 10 ⁻⁴
Cooling System Tube Pitch (P), m	1.02 x 10 ⁻¹	1.02 x 10 ⁻¹	1.02 x 10 ⁻¹	1.02 x 10 ⁻¹
Outer Insulating Jacket Thickness (t ₅), m	2.62 x 10 ⁻²	2.62 x 10 ⁻²	2.62 x 10 ⁻²	2.62 x 10 ⁻²
Outside Diameter (D ₃), m	3.14	2.94	2.80	2.34
Slag Neck Diameter (D _s), m	0.79	0.68	0.64	0.53
<u>SECOND STAGE</u>				
Inside Diameter (D ₂), m	2.60	2.40	2.40	2.00
Length (L ₂), m	2.90	2.70	2.60	2.15
Pressure Vessel Wall Thickness (t ₄), m	1.27 x 10 ⁻²	1.27 x 10 ⁻²	1.27 x 10 ⁻²	1.27 x 10 ⁻²
Magnesia Refractory Thickness (T ₂ + T ₃), m	6.59 x 10 ⁻²	6.59 x 10 ⁻²	6.59 x 10 ⁻²	6.59 x 10 ⁻²
Plasma-Sprayed Zirconia Thickness (t ₁), m	4.45 x 10 ⁻⁴	4.45 x 10 ⁻⁴	4.45 x 10 ⁻⁴	4.45 x 10 ⁻⁴
Cooling System Tube Pitch (P), m	7.62 x 10 ⁻²	7.62 x 10 ⁻²	7.62 x 10 ⁻²	7.62 x 10 ⁻²
Outer Insulating Jacket Thickness (t ₅), m	2.62 x 10 ⁻²	2.62 x 10 ⁻²	2.62 x 10 ⁻²	2.62 x 10 ⁻²
Outside Diameter (D ₄), m	2.81	2.61	2.51	2.21

(1) 1920 K Preheat
(2) 1650 K Preheat

6.3 MAGNET SUBSYSTEM

The superconducting magnet system for the disk MHD generator consists of the magnet, the cryogenic support equipment, and the power supply and protection systems. While a linear MHD channel requires a complicated magnet coil and structural arrangement that completely surrounds it, thus posing service connection and line routing problems, and making channel inspection and repair/replacement difficult, the working volume of a disk generator channel can be effectively magnetized by a single solenoid magnet system. Such a single solenoid magnet can provide maximum accessibility and places virtually no limitations on plasma flow paths to and from the disk generator itself.

Previous disk MHD channels have been magnetized by a "split pair" coil (i.e. Helmholtz pair) formed by two solenoid coils with a common axis, having the disk located between and coaxial with the coils. This type of magnet requires a massive support structure to hold the coils apart against their mutual magnetic attraction; such a force containment structure requires posts which must operate at cryogenic temperatures to pass through the disk and diffuser of an outflow disk generator. Although such a magnet type can be utilized by passing the supports through the interior of the splitter vanes in the annular diffuser, it was decided that the single coil magnet was more acceptable from the standpoints of design simplicity and ease of access to the power train components.

6.3.1 DISK GENERATOR MAGNET DESIGN CRITERIA

The basic design criteria developed for the disk generator magnets to be used in the open cycle disk systems were as follows:

- The magnet should be simple to design and construct, to maintain and extend the conceptual simplicity of the disk generator power train, and to minimize costs;
- The layout should minimize interference with the choice of plasma flow paths for the disk generator;
- The configuration chosen should permit access to the disk generator and diffuser, and minimize obstructions and design constraints for their service connections;

- The size of the effectively magnetized volume should provide margins such that close tolerancing is not required for locating the disk generator with respect to the magnet.

These design criteria could apply to a magnet for virtually any disk generator configuration; following the choice of the radial-outflow configuration for the OCD system disk generators, it was possible to define design requirements which fixed the general magnet configuration.

6.3.2 DISK GENERATOR MAGNET CONFIGURATION SELECTION LOGIC

For the four open-cycle disk generator systems being considered, the diameter of the disk generators was on the order of 10 m, thus indicating that a magnet of substantial size was required. After a review of possible magnet configurations for the disk generator systems, it was decided to configure the disk magnet as a solenoidal magnet, in the form of a flattened right circular cylinder. The cylinder would have a central axial hole provided, through which the coal combustor second stage could exhaust to the disk generator supersonic nozzle. Such a magnet could be supported with its cylindrical axis disposed either vertically or horizontally. The single coil design also was capable of providing a relatively large volume of magnetization at minimum cost, thus permitting the placement of the disk generator at an altitude above its face sufficient to permit the interposition of cooling, electrical, and instrument lines, and structural support members between the disk and the magnet dewar outer surface. The complexity of the force containment structure for such a design is minimal in comparison to virtually any other magnet design.

The large diameter of the disk generator and the necessity of coupling its exhaust to a set of radiant furnaces of substantial size, with minimum turning losses and simple diffuser designs, finally restricted the selection of magnets to those with vertical axes of symmetry. To permit maximum access to the disk generator and diffuser, these are located on the upper horizontal face of the disk magnet, with the magnet supporting itself from the floor. The central axial hole in the magnet is penetrated by the combustor exhaust duct. The combustor is located below the magnet in a pit, with access permitted by tunnels under the magnet support floor for service lines and for maintenance or

repair. The disk design selected requires no support from the magnet, thus eliminating a possible high heat load situation which would require a substantially enlarged cryogenic system capacity. Specific magnet parameters and important dimensions which were defined as a result of the open-cycle disk generator parametric studies are as follows:

- The axial component of the magnetic induction throughout the volume of interaction in each disk generator design is specified as 7 T. This value is to be attained at any point in the disk working volume with an allowable variation of ± 1 T.
- To provide sufficient clearance between disk under surface and magnet upper surface, the working volume of each disk (in which the 7 ± 1 T requirement given above is to be met) is to be located in a vertical region beginning at 0.60 m and ending at 1.02 m above the upper magnet dewar surface.
- The minimum free radius of the central hole in the magnet coils should be 1.5 m. This will provide clearance to pass the exhaust duct of the combustor second stage through the magnet to the disk generator nozzle, while simultaneously allowing flow velocities sufficiently low to minimize pressure losses for the mass-flow rates being considered.

With the magnet configuration and layout chosen, the cryogenic systems and power supply and protection systems for the superconducting magnet can be located an adequate distance from the magnet to avoid significant magnetic interactions.

6.3.3 DISK GENERATOR MAGNET DESIGN DETAILS

6.3.3.1 Magnet Subsystem

The magnet subsystem for each of the open cycle disk generators treated in this study consists of an outer ring of conductors gap-filled by epoxy to form a monolith, and an inner stack of flat plates supporting conductors. These are depicted in Figures 6-3-1 and 6-3-2 as Regions A and B, respectively. The outer monolithic structure is required to accommodate the higher current densities present in that region. Internally-cooled, cabled superconductors are shown in the Figures, the properties of which are described below.

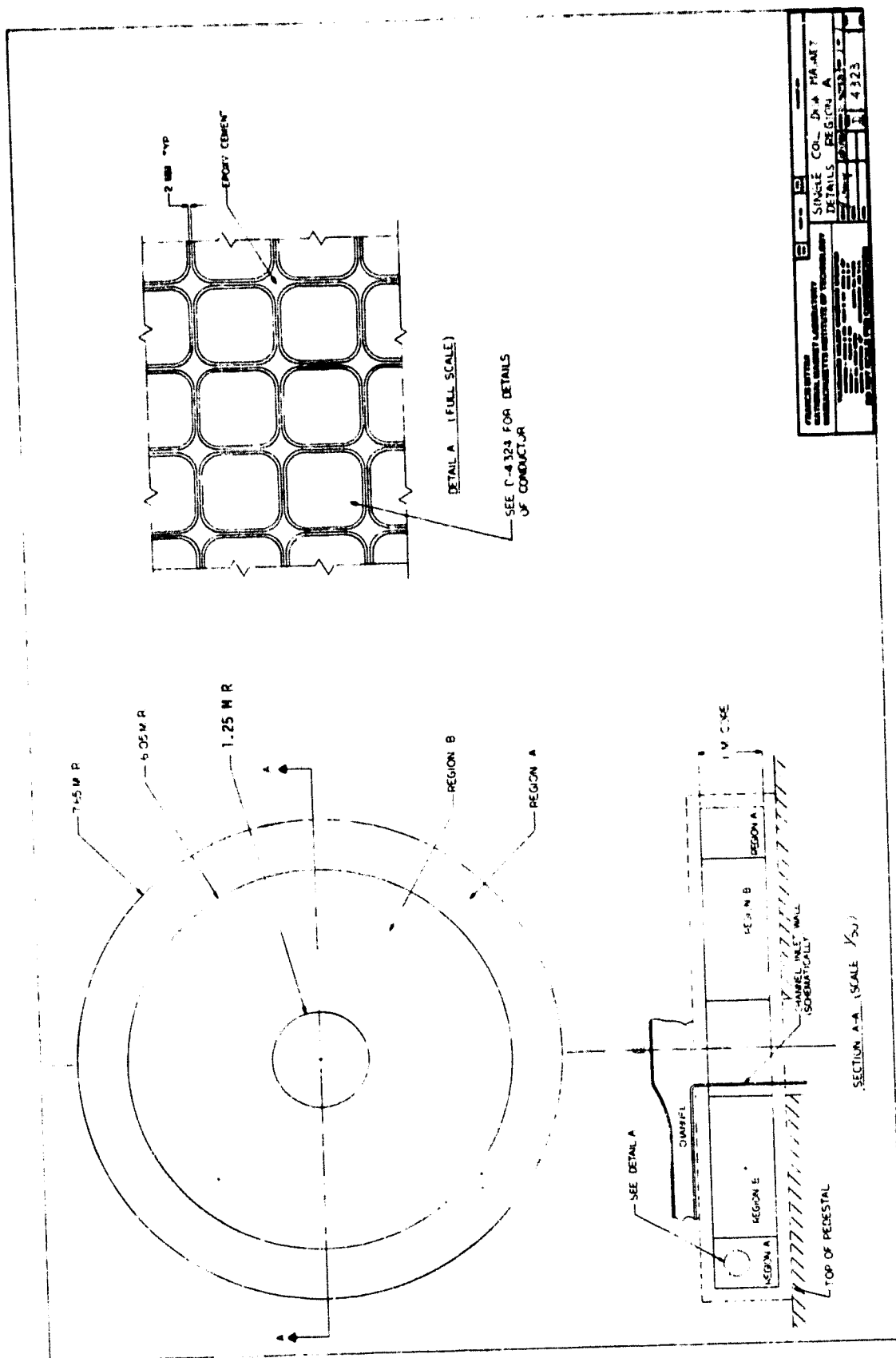


Figure 6-3-1. Single Coil Disk Magnet General Configuration and Structural Details (Coil Region A)

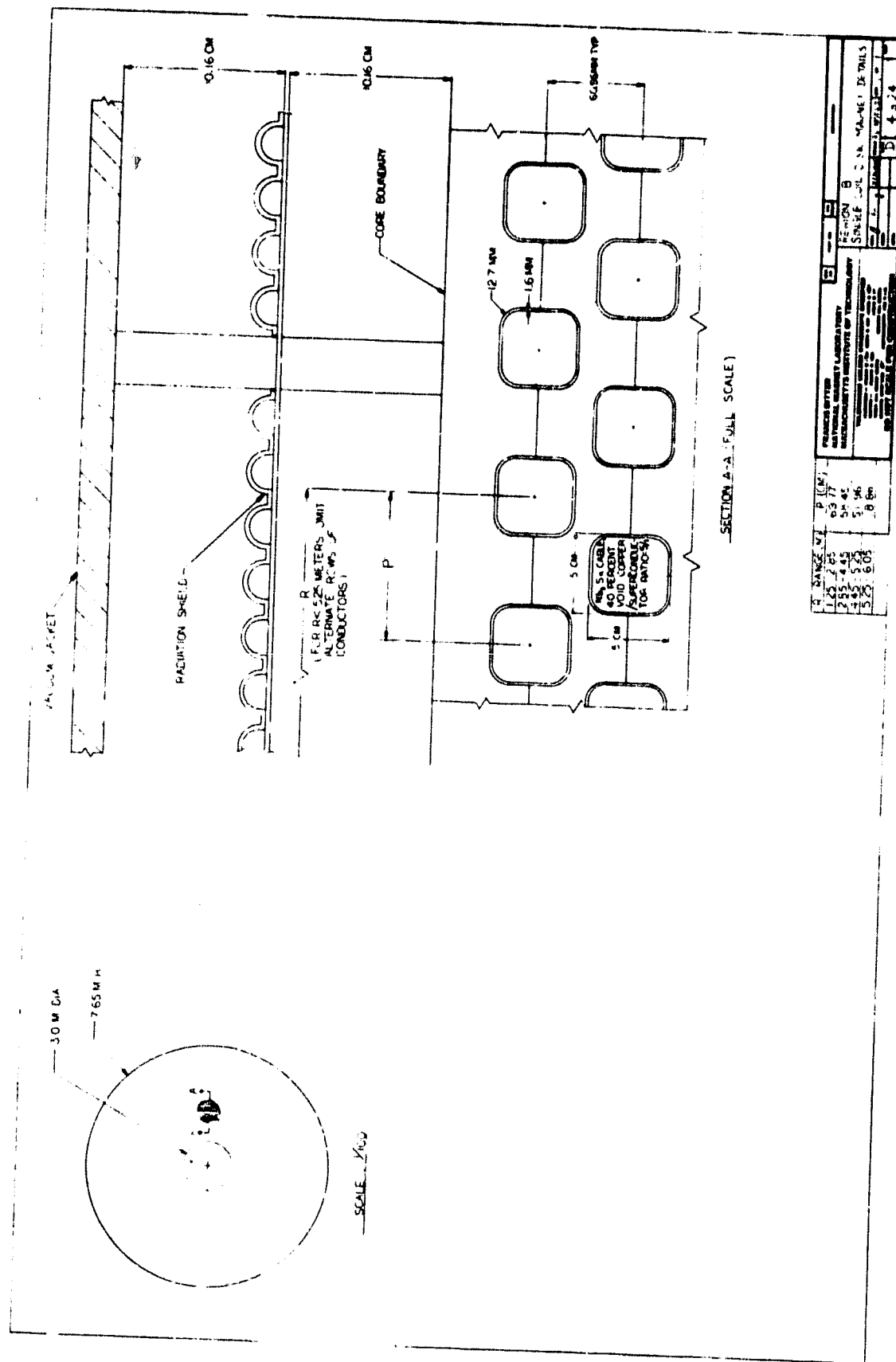


Figure G-3-2. Single Coil Disk Magnet Structural Details of Dewar and Coil Region B

The magnet coil subsystem is thermally insulated by a radiation shield and vacuum jacket held in place by standoffs, as shown in Figure 6-3-2. The standoffs are concentric G-10 fiberglass cylinders designed to permit relative radial thermal expansion.

The dimensions of each magnet and the extent of Regions A and B vary with the application to each of the four OCD systems, as described in the following text. The fundamental design and general layout of the interior components of the magnet subsystem do not, however. The description of design details, dimensions, operating parameters, etc. in the following sections are specific to a 7.65 m coil radius superconducting magnet suitable for use in the OCD system using 1920 K oxidant preheat and incorporating a 5.21 m (outer radius) disk generator (Case 1A). A subsequent section on magnet scaling details the parameters and scaling laws appropriate to the single disk solenoidal magnet design, which permits a single evaluation of costs, weights, and sizing for other disk generator radii based on the 7.65 m magnet design. Table 6.3.1 contains major design parameters for the disk magnets for each of the four OCD system cases.

Conductors

The internally-cooled cabled superconductors (ICCS) have a cross section approximating a 50 mm (2-inch) square with rounded corners. They are capable of carrying 50 kA current at 4.5 K to 5 K with a copper/superconductor ratio of 5:1, using Nb_3Sn superconductor. The 40 percent void in this case results in an average current density of 25 MA/m^2 . This is consistent with 6 GJ of stored-energy in the field and a discharge voltage of 750 V, with a temperature rise to 200 K.

Other Materials

The conductor case and support plates for the inner region of conductors are fabricated of 304L stainless steel with 0.14 percent nitrogen addition. The radiation shield and vacuum vessel are also 304 stainless steel. This

TABLE 6.3.1
OCD SYSTEMS - MAJOR MAGNET DESIGN PARAMETERS

	CASE 1A	CASE 1B	CASE 2	CASE 3
● MAGNET DIMENSIONS (m)				
- Coil Outside Diameter	15.30	15.55	14.75	16.05
- Coil Thickness	1.00	1.00	1.00	1.00
- Total Diameter	15.80	16.05	15.25	16.55
- Total Thickness	1.50	1.50	1.50	1.50
- Central Clear Bore	2.90	2.90	2.90	2.90
● MAGNET AND DEWAR				
WEIGHT (tonnes)	1352	1395	1255	1490
● MAGNET DESIGN AXIAL				
FIELD (T)	7	7	7	7
● MAGNET CONDUCTOR				
Type	Stabilized Nb ₃ Sn (5:1 Cu/SC*)	Same	Same	Same
Operating Temperature	5 K	5 K	5 K	5 K
Average Current Density	25 MA/m ²	25 Ma/m ²	25 MA/m ²	25 MA/m ²

material and others of comparable strength are under evaluation for application to superconducting magnet designs of this nature, in testing programs being carried out at room temperature as well as at cryogenic temperature.

The G-10 fiberglass standoffs are an E-glass cloth in an epoxy matrix.

Fields and Forces

The magnet currents necessary to provide the near-constant 7 T magnetic induction throughout the region of interaction of the OCD disk generator also induce a substantial radial field, as shown in Figure 6-3-3. The axial field passes through zero midway through the outer potted conductor ring, and becomes negative at 5 T at the outer periphery of the coil. This results in the balancing of radial loads in the outer ring since the (positive) inner 5 T field generates an outward loading from the 7.65 m point. Radial loads thus do not begin to accumulate until within the 6.05 m radius. The peak value of 165 MPa (24,000 psi) occurs at the 1.25 m inner radius. It should be noted that while the magnet diagram of Figure 6-3-1 depicts a coil with a 1.15 m inner radius, it is possible with very little difficulty to provide a slightly larger radius by a removal of conductor in the central region, without any significant effect on the performance of the magnet in the region of interaction within the disk generator. Thus, after final design details of the combustor exhaust neck area have been defined, it is possible to arrive at the required base size without significant impact on the previous magnet design efforts.

Figures 6-3-1 and 6-3-2 shows that the superconductor density in the coils is graded as a function of radius. Such a design approach provides several positive effects. It permits the maintenance of a relatively constant 7 T axial field within the working volume of the disk generator. It allows the use of more structural material near the hole in the magnet to minimize the circumferential stresses. Finally, it permits optimization of the structural efficiency near the 5.25 m radius where the overall required current density is high enough to necessitate use of a large portion of the magnet cross section for conductor.

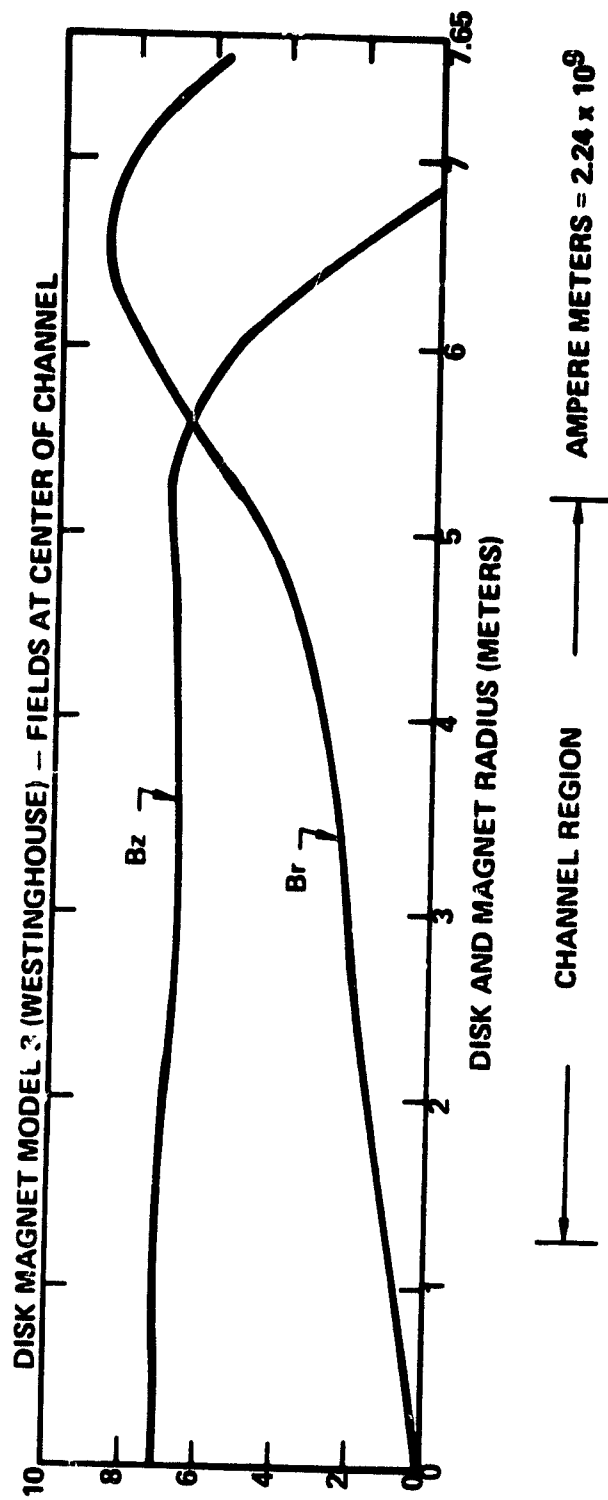


Figure 6-3-3. Data for Direct Fired MHD Disk Generator Magnet

Stresses

The stresses in the principal structural components of the disk generator magnet appear in Table 6.3.2, together with the factors of safety based on typical material property data taken from the published literature. The allowable stress is $1/3$ of the static ultimate tensile strength or $2/3$ of the yield strength, whichever is lower.

The vacuum jacket is designed at the minimum size required for fabrication and handling, which accounts for the low applied stress.

6.3.3.2 Cryogenic Subsystem

The cryogenic subsystem is designed to cool the magnet coil and structure to the operating temperature of 4.5 K and to maintain them at that temperature continuously while the MHD generator is in service. A mechanical refrigerator/liquefier is used to supply primary refrigeration for coil and power lead cooling. A separate closed-loop system, cooled by the primary refrigeration equipment, is provided within the magnet enclosure itself to circulate supercritical helium through the magnet coils. A bulk liquid nitrogen system provides refrigeration for initial cooldown of the magnet system, for intermediate shield cooling, and for helium refrigerator pre-cooling. The complete cryogenic subsystem consists of helium refrigerator and compressor equipment, a helium purifier, gas and liquid storage containers, a helium circulating pump, heat exchangers for the closed-loop circulating system associated with the internally-cooled conductor, initial cooldown and warmup piping, instrumentation, safety devices, and controls including provisions for automatically maintaining required temperatures and liquid levels in the system. A simplified block diagram of the cryogenic system is shown in Figure 6-3-4.

Heat Loads

The estimated steady state heat loads which the cryogenic system must handle are summarized in Table 6.3.3.

Refrigerator and Compressor Equipment

The refrigerator and compressor equipment will be designed to have a margin in rated capacity of at least 25% above the estimated maximum heat loads of the

TABLE 6.3.2: EVALUATION OF SAFETY FACTORS FOR MAJOR STRUCTURAL COMPONENTS OF DISK MAGNET

STRUCTURAL COMPONENT	MATERIAL	OPERATING TEMPERATURE K	σ_{app} APPLIED STRESS MPa (ksi)	σ_{app} ALLOWABLE STRESS MPa (ksi)	SAFETY FACTOR $\sigma_{all}/\sigma_{app}$
Disk Plate	304L Stainless Steel +0.14N	4	424 (61.5)	460 (66.7)	1.08
Vacuum Jacket	304 Stainless Steel	Room Temperature	24.8 (3.6)	184 (26.7)	7.4
Standoff	G10 Fiberglass	4 to Room Temperature	138 (20)	172 (25)	1.25

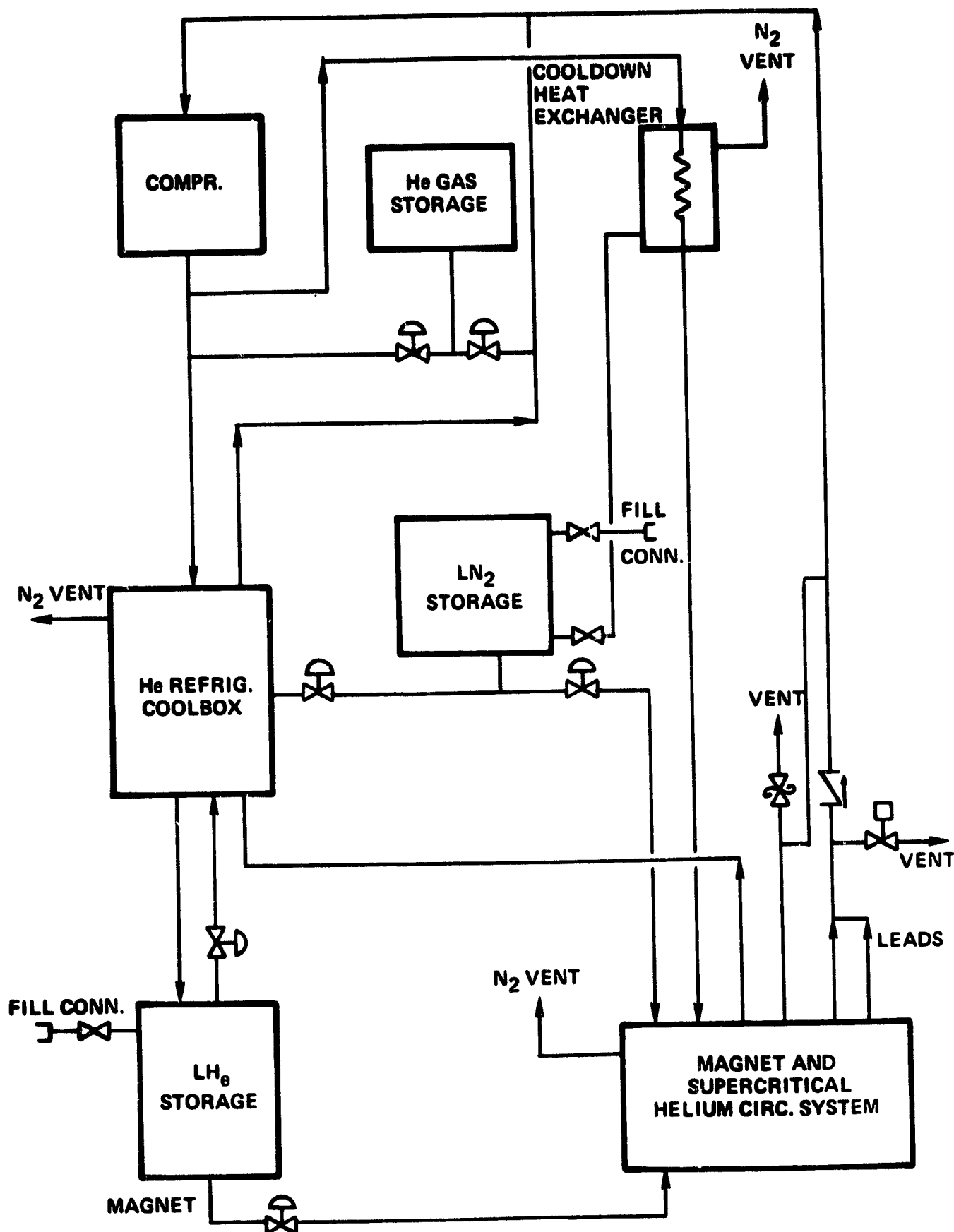


Figure 6-3-4. Block Diagram for MHD Magnet Cryogenic System

leads and 4.5 K region given in Table 6.3.3. The magnet system can be maintained at operating temperature using liquid helium from the storage container during repair and/or maintenance of refrigerator and compressor equipment.

The cryogenic system includes high-pressure gaseous helium storage capacity sufficient for the complete system charge of helium. Emergency atmospheric pressure helium recovery containers are not included, and in the event of magnet quench, a portion of the helium charge may be released into the atmosphere through the vent stack.

Closed-Loop Coil Cooling System

A closed-loop system with heat exchangers, pump, and manifolds will circulate supercritical helium at about 4 atm pressure and slightly above 4.5 K through the internally cooled conductor of the magnet coil. Heat absorbed by the supercritical helium in the coil passages will be removed by heat exchange with 4.5 K helium of the primary refrigeration system.

Magnet Cooldown and Warmup

Cooldown of the magnet from room temperature will be accomplished by forced circulation of cold helium gas through the magnet coils. The refrigerator compressor will be utilized to force the gas through the system while the cooldown heat exchanger, supplied with liquid nitrogen from bulk storage, will primarily cool the helium gas to approximately liquid nitrogen temperature.

Warmup of the magnet will also be accomplished by means of forced circulation of helium gas using the refrigerator compressor. Gas at room temperature will be delivered to the shield and coil cooling system. Return gas which has been cooled by heat exchange with the magnet coils and structure will be warmed back to room temperature in warming coils provided in the return line to the compressor suction.

**TABLE 6.3.3: DISK GENERATOR MAGNET
SUMMARY OF ESTIMATED HEAT LOADS FOR CRYOGENIC SUBSYSTEM**

REMOVAL OF HEAT ENTERING 4.5 K REGION OF MAGNET

Radiation from intermediate shield	30 W
Conduction through supports	25 W
Conduction through stack	5 W
Pump and circulating system losses	2 kW (Note 1)
Resistive heating in conductor splices (100)	<u>100 W</u>
Total refrigeration at 4.5 K	2.16 kW
Refrigerant flow required to remove 2.16 kW	
LHe in at 4.5 K; gas out at 4.7 K	0.104 kg/s (3,000 l/hr)

REFRIGERATION FOR CURRENT LEADS

(50 kA pair)

Two-stage leads (Note 2)

● 1st Stage	1.8×10^{-3} kg/s
LHe in at 4.5 K; gas out at 80 K	(52 l/hr)
● 2nd Stage	5.3×10^{-3} kg/s
He gas in at 80 K; gas out at 300 K	

REMOVAL OF HEAT FROM 80K REGION

(Intermediate shield and heat stations)

Radiation from vacuum jacket walls	430 W
Conduction through supports	118 W
Conduction through stack	<u>25 W</u>
Total refrigeration at 80 K	573 W
Refrigerant flow, (LN ₂) required to remove 573 W:	13 l/hr

NOTE 1: Required only during energizing. Pumping losses during steady state operation are negligible. Estimate is based on continuous rating and is therefore conservative.

NOTE 2: The two-stage leads are more efficient in use of refrigerant than conventional single-stage leads. The use of two-stage leads is preferred for relatively high design currents because lead refrigeration is a significant portion of total refrigeration required during steady state operation.

6.3.3.3 Magnet Power Supply and Discharge Subsystem

The power supply and discharge subsystem is designed to charge the magnet, to maintain automatically the desired steady state magnetic field, and to discharge the magnet under both routine and emergency conditions. The subsystem will consist of a solid state rectifier unit designed for 60 Hz input from the powerplant bus, current and voltage controls, an emergency dump resistor, a circuit breaker to activate the emergency resistor, and the control equipment necessary to actuate the emergency dump system automatically in response to a signal from the coil quench monitoring system. A simplified diagram of the power supply and discharge system is shown in Figure 6-3-5. Design characteristics of the subsystem are given in Table 6.3.4.

Rectifier Power Supply Unit

The power supply unit will provide direct current to the magnet for charging and will maintain the desired (constant) current in the magnet coils during MHD generator service use. The unit will be so designed that the voltage can be reversed to provide for controlled discharge of the magnet with stored energy returned to the power plant bus. Controls will permit operation at currents from 0 to 50 kA with voltage 0 to ± 18 V. Automatic control of current at any desired setting is possible with the power supply control systems.

Emergency Circuit Breaker

The circuit breaker is capable of breaking up to 50 kA direct current under emergency conditions. The opening of the circuit breaker interrupts the current in the low impedance power-supply magnet loop, causing the full magnet current to pass through the dump resistor.

Emergency Dump Resistor

The resistor is designed as a water-cooled unit which is capable of absorbing all of the stored energy in the fully-charged magnet. Under normal steady-state operating conditions the resistor will remain as a shunt across the coil terminals and will carry only a small current as determined by the voltage drop across the power leads.

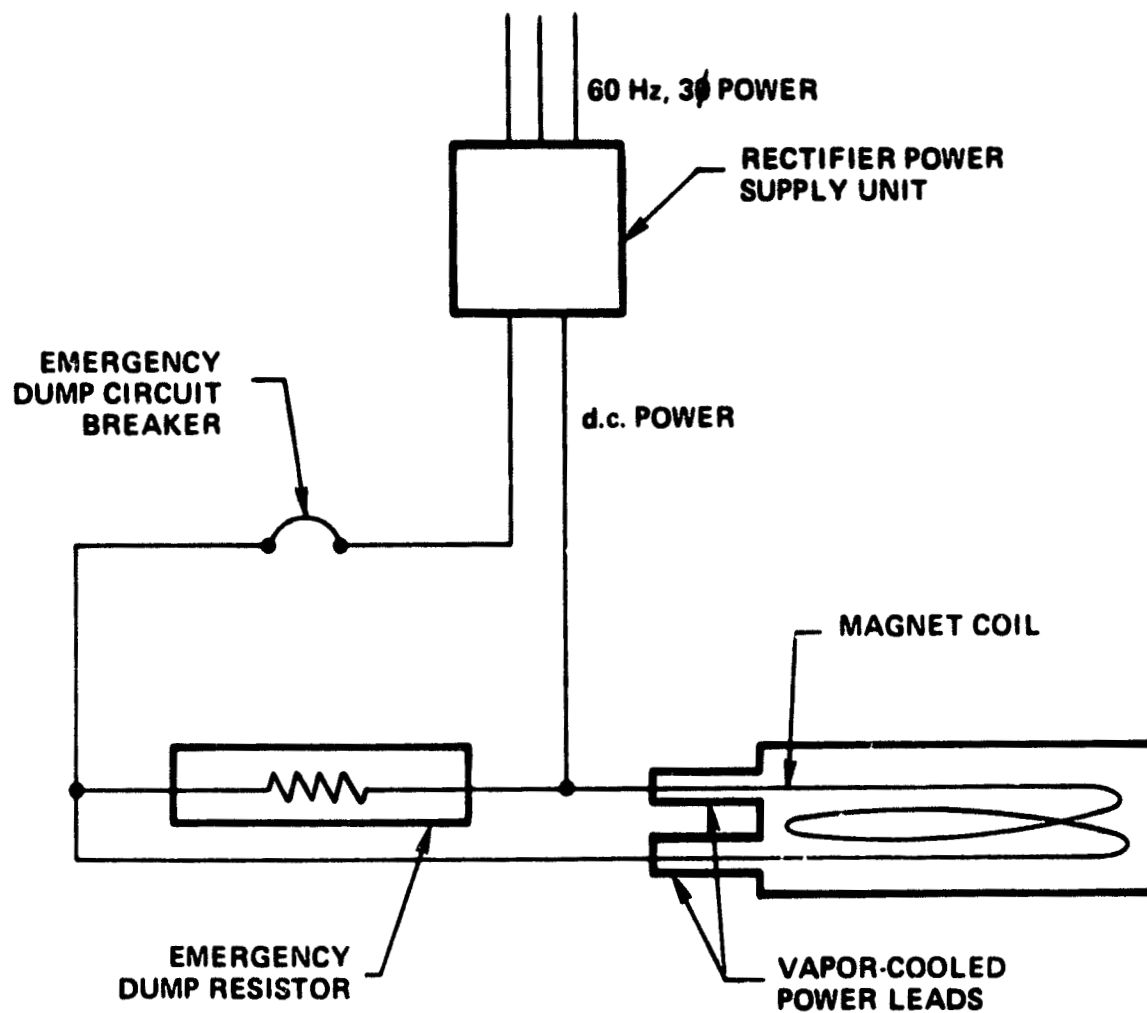


Figure 6-3-5. Power Supply and Discharge Subsystem for MHD Magnet

TABLE 6.3.4: DESIGN DATA FOR SUPERCONDUCTING MAGNET POWER SUPPLY SUBSYSTEM

Power Supply Unit

Maximum charge/discharge rating:

Current, maximum	50 kA
Voltage, maximum	± 18 V
Charge time, minimum	4 hr
Discharge time, minimum	4 hr

Normal Rating (steady state)

Current	50 kA
Voltage	<1 V

Emergency Circuit Breaker

Current, maximum	50 kA
Voltage, maximum	1 kV

Emergency Dump Resistor

Resistance	0.2 ohm
------------	---------

6.3.4 DISK MAGNET SCALING LAWS

The design information provided in the previous subsections is specific to the 7.65-m solenoidal magnet which is appropriate for the 1920 K preheat open-cycle disk generator having an outer radius of 5.2 m. In order to provide a means of evaluating the size, cost, and performance of magnets of the same basic design for the disks of various sizes specified for the remaining three OCD systems, magnet scaling laws were derived. These scaling laws are believed to hold over the range of disk sizes proposed for the OCD generator systems treated herein, subject to the appropriate constraints discussed in each subsection below. The magnet scaling laws provided are also adaptable to magnets for disk generators other than those described in this report.

6.3.4.1 Disk Magnet Parameters

The principal parameters of a solenoidal disk magnet are as follows:

- R - outer radius of winding, m
- t - thickness of winding, m
- B - field strength, T
- $j\lambda$ - overall current density, A/m²
- N - coil parameter directly relatable to cost, A-m
- C - cost, dollars

Each disk magnet must be designed to generate the field intensity and geometry required in the channel region, to function satisfactorily for the required magnet life, and to be available at the lowest possible cost. This involves a choice of the proper conductor for the fields within the magnet and selection of appropriate materials for conductor structural support, insulation, and cooling.

6.3.4.2 Channel Size Scaling

The disk magnets that have been examined in this study have been limited to those which are capable of providing a 7 T axial field in the channel region. The maximum current densities are in all regions less than 3×10^7 A/m², which is an upper bound chosen to minimize magnet size while remaining

consistent with reliable performance. This limiting current density led to a winding thickness of 1 m, which provided a reasonable magnet outer radius for the radial extent of the axial field required. Study of a few cases revealed that the magnet outer radius could set at 1.5 times the channel outer radius for the channel size range of interest, and with the 1 m coil thickness taken as a fixed dimension.

In basic design, the disk magnet is a large flat solenoid composed of a main winding with several smaller trim coils to flatten the axial field within the channel volume.

The axial field for various magnet designs was determined at several positions in the channel region for several ratios of outer radius to inner radius of the coil system. Little variation in field level is expected in the region between 0.6 m and 1.1 m from the centerplane which would encompass channels with volumes of 20 to 40 m³.

These preliminary investigations led to the realization that approximate scaling for the disk magnets involves selecting the magnet thickness to be constant at 1 m and the outer radius to be 1.5 times the channel outer radius, R_C . As a result magnet volume (V) for any disk magnet considered would be proportional to R_C^2 .

These results apply to a magnet with constant 7 T axial field. If the field level were required to change, the thickness would then necessarily change in the same proportion. Then V would be proportional to $R_C^2 B_z$.

6.3.4.3 Stress Scaling

The electromagnetic loading per unit conductor length q , on the magnet coil is equal to $I \times B$ at any location. If the channel radius were to be changed then for a given field strength at the magnet axis, it has been assumed, conservatively, that I would vary with R . As a result, q would vary with R . In a circular flat plate, the stress would be $\sigma = 2q/t$ and the stress still would be proportional to R but at twice the unpunctured value.

6.3.4.4 Disk Power Level Scaling

If the channel power level, P , is increased by expanding both the entrance height and radius proportional to $(P)^{1/2}$, then it can be shown that the channel outer radius should increase by $(P)^{1/4}$ in order to make the magnetized volume proportional to P . The disk magnet volume, V , is proportional to R^2 and, consequently, to $(P)^{1/2}$.

If both sides of the disk magnet were to be used then the available power would double with no change in the magnet. Ensuing power-related magnet variations would follow the above relations.

6.3.4.5 Cost Scaling

A synthesis of production costs of linear magnets was conducted by Hatch [1]. He plotted cost (C) logarithmically as a function of VB^2 , which reflects energy in the magnet warm bore. The data display considerable scatter. However, the mainstream of the information appears to lie along a band with slope 0.6 in the large magnet range so that C is proportional to $V^{0.6} B^{1.2}$.

Detailed cost studies were conducted for a 6 m disk magnet as well as the 7.65 m disk magnet with 7 T nominal fields. The costs of the two magnets were found to be approximately 35.6 million dollars and 47.2 million dollars, respectively (mid 1978 basis). Using the same cost scaling factors as were found appropriate for the linear magnet, the costs should be proportional to $(6.0/7.65)^{1.2} = 0.75$ since the nominal magnetic induction is the same for each magnet design. The ratio of costs determined by the detailed estimating procedures (results for the 7.65 m magnet are given in Section 7.0 of this report) is $35.6/47.2 = 0.75$, which is in good agreement with the scaling factor result.

For the development of costs for the three remaining solenoidal magnet designs proposed for application to the OCD systems, the scaling factor $C_1/C_2 = (R_1/R_2)^{1.2}$ was utilized, with the 7.65 m magnet as the reference design.

6.3.5 OTHER MAGNET DESIGNS FOR DISK GENERATORS

6.3.5.1 Split Pair Magnets

In order to evaluate the suitability of a split pair magnet design for large-scale disk MHD power generation systems, a detailed design effort extending beyond the scope of the present Disk MHD Generator Study would be required, since the structural and cryogenic system design complexities for the split pair magnet far exceed those for the solenoidal single-coil magnet described previously.

One significant advantage of such a magnet design would be the elimination or reduction of the radial field set up by a flat disk magnet design component at the outer radii of the disk generator, thus configuring the field to provide only an axial component throughout the region of interaction. This field geometry matches that assumed in the current disk generator performance evaluation and design codes, thus increasing the probability that the calculated performance of the disk generator would be more closely matched by the actual equipment in service than in the case where a high radial field component were present.

Additionally, the design of a split-pair magnet to provide equivalent axial magnetic induction intensity for a similar disk channel requires the use of less superconductor than in the flat plate disk magnet design. As noted previously, the force containment structure of the split-pair magnet design would necessarily penetrate the plasma-carrying regions of the disk generator and diffuser; it is estimated that for the size of disk generator being considered and the required magnetic induction of 7 T, approximately half the channel circumference would be blocked by magnet structural members at the disk outer radius.

The inner coil region of the split-pair magnet would encroach upon the cylindrical space within which the channel lies, thereby diminishing accessibility for channel maintenance, repair, or replacement. The structural design of the magnet, channel, and diffuser would necessarily be more closely integrated than in the case of the single-coil disk magnet.

Summary cost evaluations for the split-pair magnet design indicate that the costs are roughly similar to those of the single coil disk magnet for the same size OCD system. The effect of the cost reduction due to removal of superconductor is clearly lost by the necessity for a more complicated magnet structure.

6.3.5.2 Advanced Single Coil Disk Magnet

The choice of a single-coil solenoidal magnet as the reference magnet design for the open cycle disk generator systems studies was based primarily upon its relatively low cost, simple structural design, and minimum interference for access to the hot-gas-carrying components of the MHD system. The price paid for these positive features is the appearance of a relatively high radial field component at the larger disk radii. The presence of such a radial field component results in a deviation of the actual physical situation from the ideal quasi-one-dimensional geometry assumed for the MHD interaction in a disk generator of the planar flow type used in the open-cycle power systems described herein.

At the expense of a slightly more complicated conductor design and structural design, it is possible to utilize a magnet of the basic single coil solenoidal design and configure the disk generator flow geometry to take advantage of the radial field component. This would provide a more compact overall design, since the plasma path is longer than a radial line.

As described previously in Section 6.1.4, the disk generator can be formed from shaped rather than from flat-plate fiberglass sections, thus providing increased stiffness to the structure while decreasing external support requirements for compensation of gas forces and deadweight loads at the inner and outer radii of the disk. The figure selected for the disk generator can be chosen simultaneously with the design of the magnet itself. By a combination of conductor thickness and density differences between the main coils and trim coils, and by requiring that the magnet field be configured so that the plasma flow surface at channel center be normal to the resultant field ($B_{r,r} + B_{z,z}$) rather than constraining the magnet design to provide a

constant axial field component (B_z) across the disk, it appears possible to provide an advanced disk generator/magnet integrated design which retains the advantages of the single coil (flat) magnet while also decreasing component size and improving generator performance.

Thus, the potential advantages of such a domed shaped disk design are:

The possibility of reducing the amount of conductor required. The resultant field will be constrained to a nominal value of 7 T; as shown in Figure 6-3-6, the resultant field of a single coil flat plate disk magnet attains values higher than the 7 T nominal value at radii near the disk generator edge, when measured along the path at which plasma flow would be normal to the resultant magnetic induction vector. The reduction of the resultant field at the larger radii can be accomplished by reducing the thickness of the outer coils and/or the conductor density in these coils.

The plasma flow path traveled in a domed disk generator is longer for the same outer radius when compared to a flat plate disk. This implies that the advanced (integrated disk/magnet) system will be smaller for the same MHD enthalpy extraction, given similar interaction conditions.

Some obvious disadvantages also accrue when utilizing the curved flow path flow the plasma.

Pressure losses in the disk generator are increased due to the turning losses in the supersonic flow;

Coupling of the disk generator exhaust to the diffuser is more complicated and may result in a degradation of overall system performance due to a decrease in diffuser pressure recovery capability.

Additional effort to define the possible advantages and disadvantages of such an integrated disk/magnet design was not within the scope of the study. This type of disk generator and magnet design appears to offer promise of increased performance, and should be investigated further.

6.4 DISK GENERATOR POWER MANAGEMENT SYSTEM

The Hall-connected disk MHD generator can be expected to show a definite advantage in the power management system design over comparably-sized linear MHD generators. For the disk it is possible to conceive of such a system,

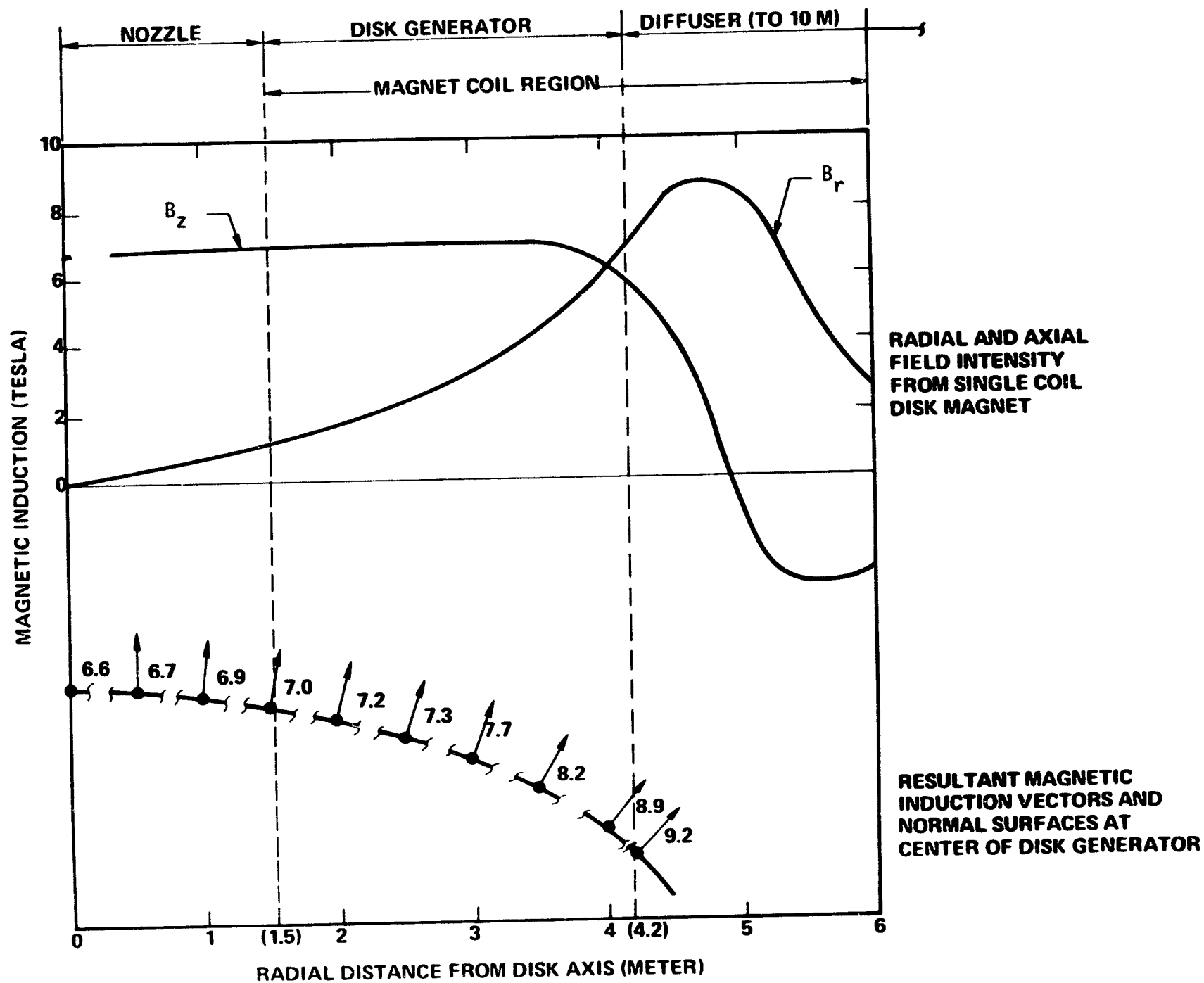


Figure 6-3-6. Effect of Radial Field Component in Solenoidal Single Coil Magnet

designed around a two-terminal machine, with no consolidation circuitry. However, the evaluation of off-design performance for the supersonic OCD generator (Section 5.3.4) revealed that several intermediate electrodes between anode and cathode would be required to realize linear electrical characteristics in the disk. A multiple-electrode disk generator still permits the use of a power management system with no current consolidation equipment, thus promising superior reliability and electrical efficiency when compared to any Faraday or diagonal MHD generator. The cost of such a power management system can also be anticipated to be much less than that of a system with similar power handling capability for the linear generator.

For this study, the design for a nominal 500 MW disk generator power management system was prepared, using as a basis the reference disk generator design described in Section 5.3.4. The results of the design effort were utilized with appropriate scaling laws to estimate the cost of such a system for each of the four OCD generator systems described in Section 5.4. From the design data, it was also possible to estimate costs for OCD generator system power management equipment.

6.4.1 GENERAL SYSTEM DESCRIPTION

The specific disk generator conditions for which the reference disk power management system was designed is described in Table 6.4.1. (This is the reference generator of Section 5.3.4, as noted previously). At the generator design point, with the constant radial Hall field design constraint, all segment currents are equal. As a result, no current is extracted from the disk generator through the three intermediate electrodes in this condition.

Minimum allowable segment currents (i.e., maximum allowable segment voltages) have not been determined. These are set both by the wall breakdown voltage and the channel gas dynamic response under load. A greater understanding of the characteristics of multiple-load supersonic disk generators operating under off-design conditions must be achieved in order to facilitate the delineation of the definitive disk power conversion system design. The design details for both the reference disk generator and power management equipment have been

TABLE 6.4.1
Reference Open Cycle Disk MHD Generator Design Point
Electrical Data for MHD Power Management System

- Generator Type: Hall connected, supersonic near-impulse mode
- Generator Inlet Radius: 1.226 m
- Generator Outlet Radius: 4.106 m
- Design Total Power: 527.3 MW (dc)
- Design Voltage Difference: 34.56 kV (-12 kV/m radial Hall field constraint)

Segment	Electrode Upstream	Radius, m Downstream	Segment Voltage, V	Segment Current, A	Segment Impedance, Ohms	Segment Short Circuit Current, A
1	1.226 (Anode)	2.216	11,880	15,258	9.7 ± 0.1	16,500
2	2.216	3.116	10,800	15,258	14.0 ± 0.3	16,210
3	3.116	3.626	6,120	15,258	5.3 ± 0.6	16,480
4	3.626	4.106	5,760	15,258	7.5 ± 2.5	16,050

sufficiently developed in this study for cost evaluations and comparisons with linear MHD generator power management equipment.

Figures 6-4-1 and 6-4-2 are elemental dc and ac side schematics of the reference disk power management system, respectively. The converter component list is given in Table 6.4.2. Each of the four separate dc voltage levels which result from the annular segmentation of the disk generator is served by eight parallel-connected 6-pulse bridge current-sourced line-connected thyristor converters. The converters are operated in pairs feeding delta-wye connected transformers so that a 12-pulse system is synthesized both at the ac side and in the combined dc ripple.

DC disconnects (S1) are furnished to permit isolation for maintenance of individual bridges. The dc input capacitors (C1) serve two purposes. One of their functions is to reduce converter ripple injection to the generator to less than 3 percent (peak). This is a most important feature, as the off-design performance investigation of the supersonic OCD generator has displayed. Imposition of even very slight current variations about the design point current results in significant effects on channel pressure drop. It is likely that even greater suppression of ripple injection will be required in order to permit disk generator operation with the effective impedances for each annular segment as seen in the reference generator. In the event of a catastrophic single bridge open circuit failure, the dc input capacitors also serve to limit the transient voltage increase to approximately 110 percent of initial voltage.

The current sourcing reactors (L1) for the converters provide a proper dc interface, allowing 20 percent peak ripple current and limiting peak transient fault currents.

The freewheel diodes (Q1) prevent the reversal of input capacitance and generator voltages when the bypass or fault switches are closed. The bypass switches (Q2) provide a means for clearing converter commutation faults. The fault switches (S2) will close to maintain an indefinite generator short circuit if a converter fault fails to clear and the ac system must be disconnected.

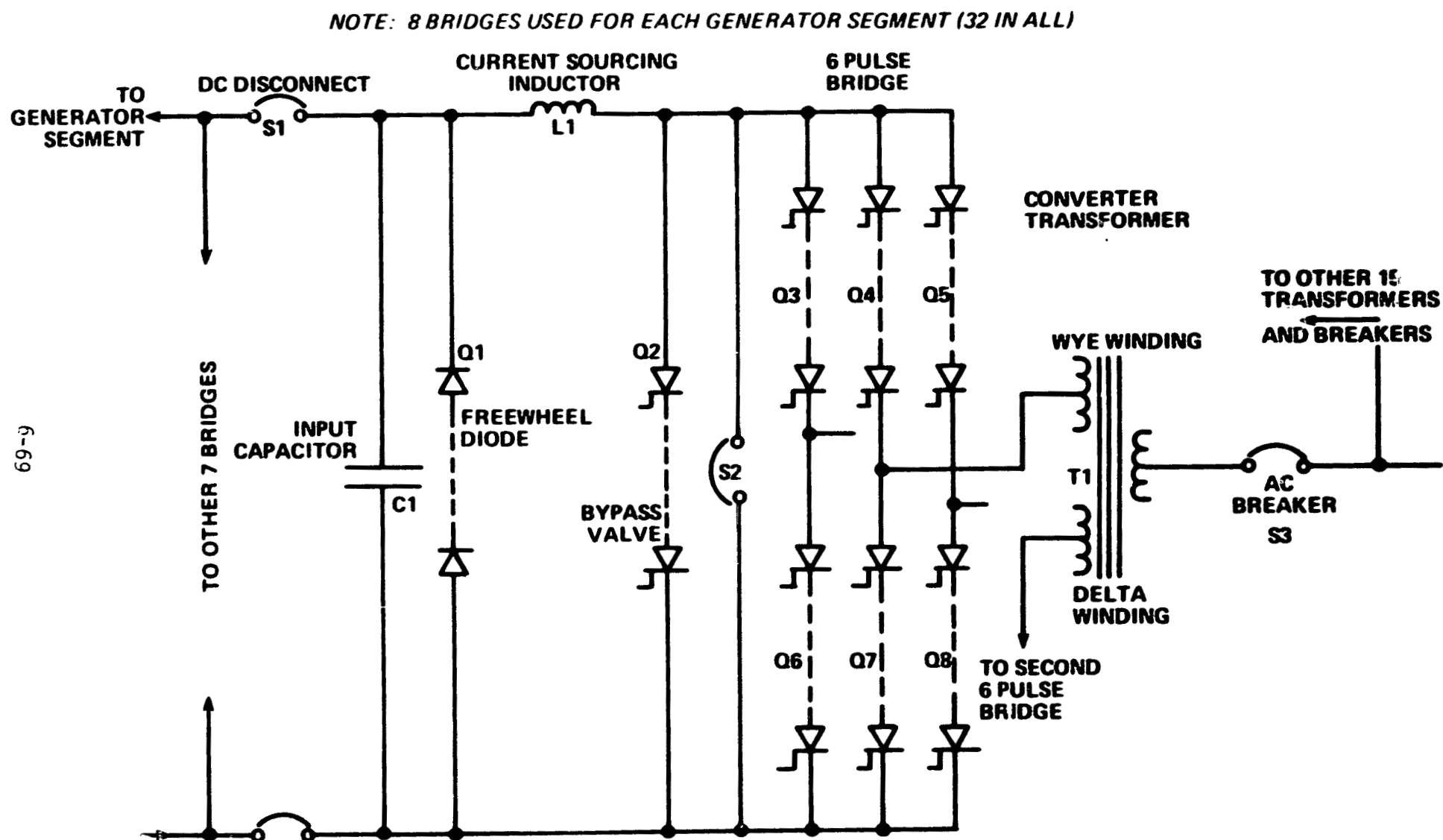


Figure 6-4-1. 500 MW Disk Power System Elemental Converter Conditioning Schematic

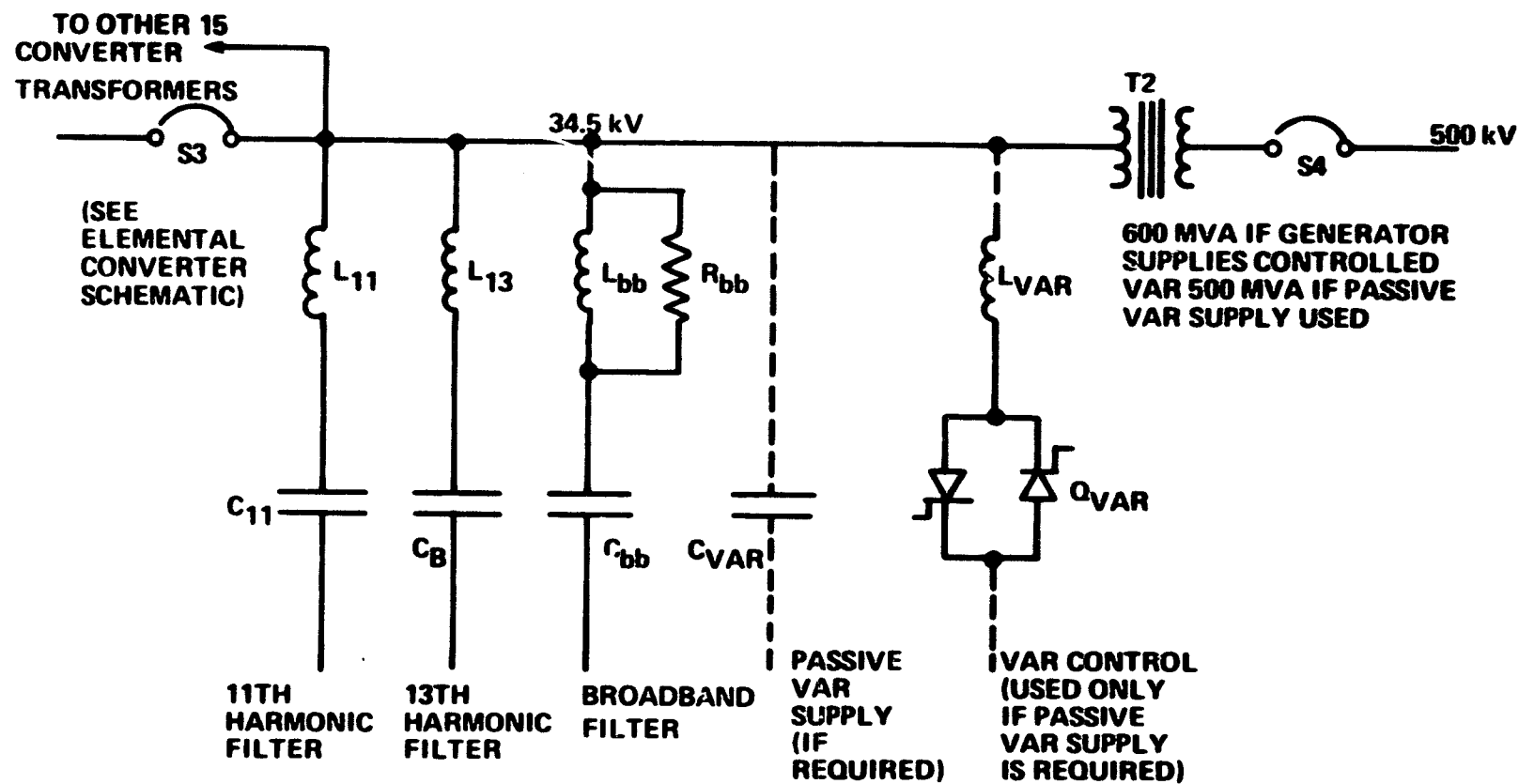


Figure 6-4-2. Single Line Diagram for AC Interface of 500 MW Disk Power System

TABLE 6.4.2
COMPONENT LIST FOR 500 MW DISK CONVERTER

- S1: Two-pole 15 kV/2000 A load break switch, motor-operated
- C1: 375 μ F 15 kV dc for 11880 V and 10800 V segments
750 μ F 7.5 kV dc for 6120 V and 5760 V segments
- L1: 8.25 mH for 11880 V segment
7.5 mH for 10800 V segment
4.25 mH for 6120 V segment
4.0 mH for 5760 V segment
- Q1: 16 x 3 kV/2000 A devices for 11880 V and 10800 V segments
8 x 3 kV/2000 A devices for 6120 V and 5760 V segments
- Q2: 24 x 2200 V/2000 A thyristors for 11880 V and 10800 V segments
12 x 2200 V/2000 A thyristors for 6120 V and 5760 V segments
- Q3-Q8: 16 x 3600 V/1500 A devices for 11880 V and 10800 V segments
8 x 3600 V/1500 A devices for 6120 V and 5760 V segments
- S2: Single pole 15 kV/2000 A load break switch, motor-operated
- T1: Primary 34.5 kV, wye
Secondaries:
11880 V segment: 12500 V rms wye and delta
10800 V segment: 11400 V rms wye and delta
6120 V segment: 6450 V rms wye and delta
5760 V segment: 6070 V rms wye and delta
Ratings: 70 MVA for 11880 V and 10800 V segments
40 MVA for 6120 V and 5760 V segments
- S3: Outdoor oil breaker 34.5 kV/1200 A/40 kA fault

The converter transformers (T1) operate to an intermediate ac voltage level of 34.5 kV at which level filtering (and passive VAR correction if required) is applied. Individual ac breakers (S3) are provided for each converter transformer, serving both to protect the transformer in the event of sustained system faults, and to isolate pairs of converter bridges and the transformer for maintenance.

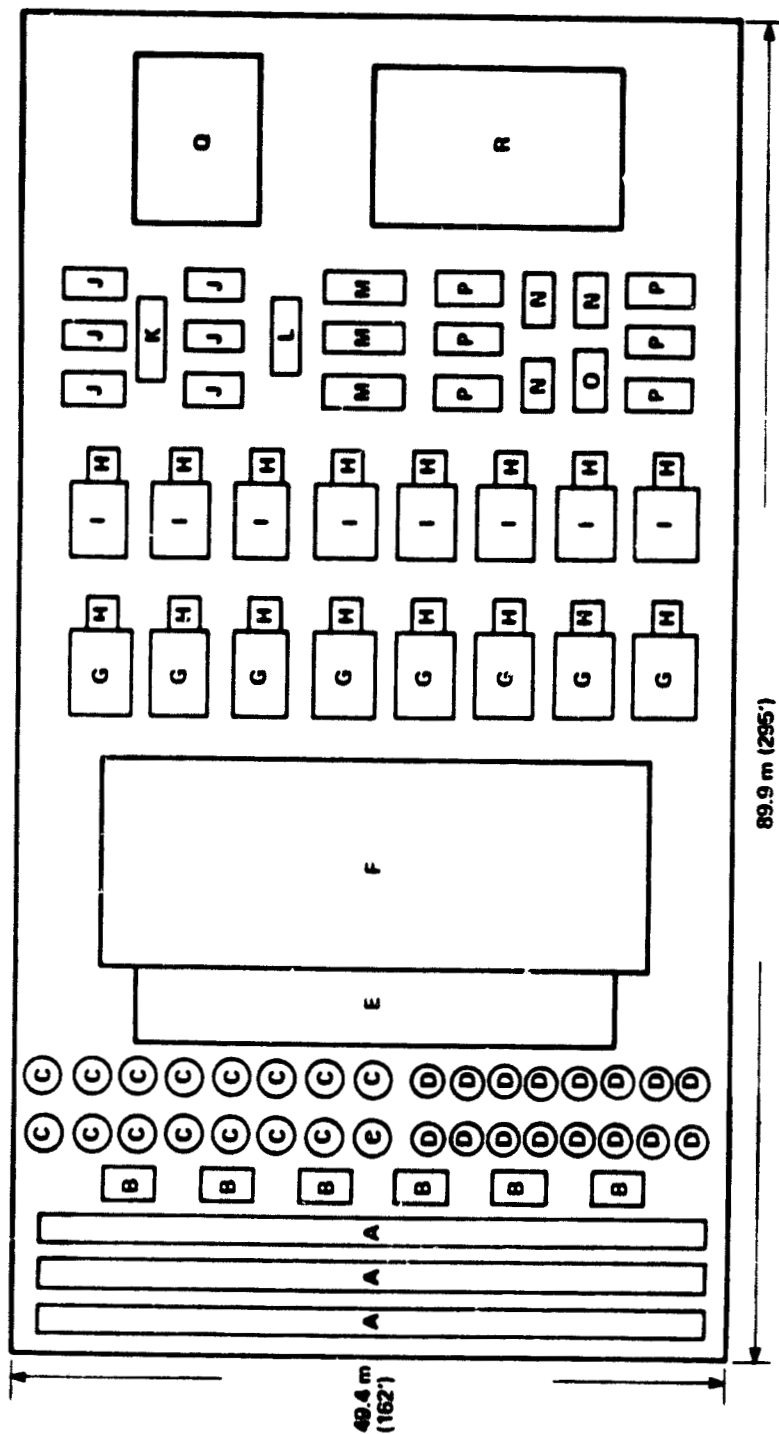
High-Q tuned traps are used to filter the 11th and 13th harmonics to less than one percent voltage at the 34.5 kV bus; a damped broadband branch is provided to filter the 23rd and higher order harmonics to the same degree. The leading VAR supply of these filters is approximately 210 MVA.

For the remaining VAR correction, it is expected that it will be supplied by the on-site ac generator; the ac machine rating can be increased from roughly 500 MW to 600 MW (MVA) to supply the difference. If the ac generator supplies the (controllable) VAR correction, the main transformer (T2) between the MHD generator 34.5 kV bus and the 500 kV grid bus will be a 600 MVA unit, with a 500 kV SF₆ breaker (S4) furnishing protection and isolation.

Passive VAR Compensation

If the VAR correction is not ac generator-supplied, an additional 290 MVA of capacitive VAR together with 500 MVA of thyristor-controlled reactors is needed. The passive correction components would consist of 18 reactors (LVAR), each 27.8 MVA, arranged in three 3-phase groups, two in each phase being controlled by thyristor switches (QVAR) comprised of 96 thyristors (3600V, 1100A) in each phase of each group; 48 in each direction of the inverse parallel connected strings being provided.

The layout of all system components is illustrated in Figures 6-4-3 (overall yard layout) and 6-4-4 (valve hall and control building layout), with component dimensions chosen for the specific design case treated (527 MW dc reference generator).



LEGEND:

- A - DC SWITCHGEAR
- B - DC CAPACITOR BANKS
- C - DC INDUCTORS, 11880V/10800V CONVERTERS
- D - DC INDUCTORS, 6120V/5760V CONVERTERS
- E - CONTROLS BUILDING (108' x 18' x 10' H)
- F - VALVE HALL (124' x 48' x 32' H)
- G - CONVERTER TRANSFORMERS FOR 11880V/10800V CONVERTERS
- H - 34.5 kV THROAT-MOUNTED BREAKERS
- I - CONVERTER TRANSFORMERS FOR 6120V/5760V CONVERTERS

- J - 11TH HARMONIC FILTER CAPACITOR BANKS
- K - 11TH HARMONIC FILTER INDUCTORS, RACK MOUNTED
- L - 13TH HARMONIC FILTER INDUCTORS, RACK MOUNTED
- M - 13TH HARMONIC FILTER CAPACITOR BANKS
- N - BROADBAND FILTER DAMPING RESISTORS
- O - BROADBAND FILTER INDUCTORS
- P - BROADBAND FILTER CAPACITOR BANKS
- Q - MAIN TRANSFORMER
- R - 500 kV SF₆ BREAKER

NOTE: VAR COMPENSATING PASSIVE COMPONENTS NOT SHOWN. IF PASSIVE COMPENSATION IS REQUIRED, ADDITIONAL COMPONENTS WOULD BE 18 CAPACITOR BANKS, 18 REACTORS INTERPOSED BETWEEN THE FILTERS AND THE MAIN TRANSFORMER AND BREAKER. THIS WOULD ADD 20 METERS TO SITE LENGTH. VAR CONTROL VALVES WOULD BE LOCATED IN THE VALVE HALL.

Figure 6-4-3. Open Cycle Disk Generator MHD/Steam Power Plant 500 MW Power Conditioning System Overall Yard Layout

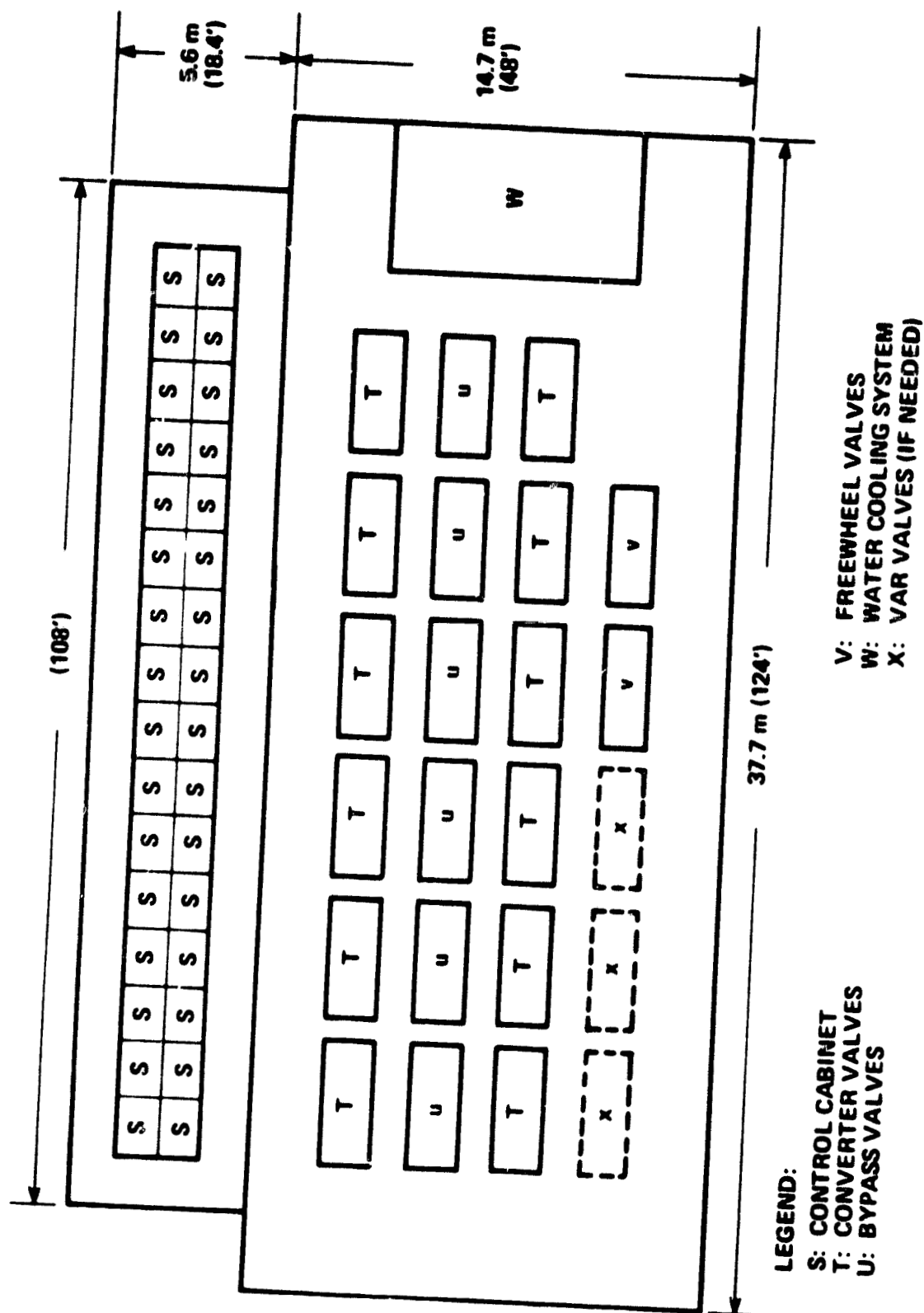


Figure 6-4-4. Open Cycle Disk Generator MHD/Stream Power Plant 500 MW Power Conditioning System Valve Hall and Control Building Layout

Appendix E contains estimated dimensions and weights of the reference power conditioning system equipment.

6.4.2 SYSTEM OPERATION

Normal operation of the system is straightforward. The converters are run at approximately 0.7 power factor, requiring all the correction supplied by the filter circuits and the generator (or passive VAR). The major transients of startup, shutdown, and fault protection are discussed briefly below.

System Startup

The converters are ac energized prior to MHD generator startup. They are then run up from inversion end stop to slightly less than 90 degree delay (just into the rectification quadrant) to circulate 200 - 300 A dc via the freewheel diodes at essentially zero applied voltage difference. The dc disconnects are then closed and the MHD generator can be started. As soon as the generator short circuit capability exceeds the established freewheel current level, it will overhaul the diodes and begin to raise the input capacitor voltage at a rate not exceeding 5.5 v/us. The inverters then move into the inversion region, picking up generator power as it becomes available. The idling (freewheel) mode can be sustained indefinitely if needed.

System Shutdown

It is assumed that system shutdown will be initiated by a shutdown of the MHD generator itself. As the generator segment V and I collapse, the inverters will follow and finally reassume the freewheel mode. The converter system may then be shutdown manually or automatically by running the converters back into the inversion condition, thus quenching the freewheel current, and then opening in sequence the ac breakers and the dc disconnects.

System Fault Clearing

An inverter commutation fault, from any cause, will be sensed by observing inverter ripple current slope and commutator overlap time. Upon sensing a fault, the protection system will trigger all the faulted converter's group bypass valves to short circuit the affected generator electrical segment and clear the converter current.

If the converter current does clear, as it will if the fault is not catastrophic, then the converters are transiently advanced into the rectification region to extinguish the bypass valves and thus resume inversion for the affected generator segment.

Should the converter current not clear following bypass valve triggering, a catastrophic fault has occurred. The fault switches are then closed to maintain short circuit on the MHD generator segment and the ac breaker of the affected converter is opened. The generator must then be shut down before the fault switches can be reopened and service restored, following repair.

The response of the supersonic OCD generator to fault clearing actions of this nature must be investigated further. The generator operates close to the short circuit condition on each segment at the design point. It is likely that a coordinated combustor runback must be provided as an adjunct action to each protective action, in order to prevent choking of the flow within the channel. The operation of the channel under transonic conditions may also be permissible for short times and this would perhaps obviate the necessity for a parallel combustor runback on a commutation fault which can be cleared immediately.

6.4.3 ADDITIONAL SYSTEM DESIGN CONSIDERATIONS

With the power management equipment design detailed above, it is necessary to provide a cooling system using high-purity water to remove heat generated in the conversion bridges. For bridge currents limited to 2000 A, no chilling of the cooling water is necessary, and the reference power conversion system design assumes that the use of 313 K (105°F) water is sufficient. The cooling water flow required at this temperature is approximately 160 kg/s, for a total heat load of 4 MW_t. Since the cooling water conditions selected for the power management system are also appropriate for the cooling of the disk electrodes, it is possible to envision some cost savings and increased efficiency to be derived from using a single system for both services. Neither system will recover heat for use in the steam bottoming plant.

System Efficiency

For the OCD parametric analyses and for the final performance evaluations, a dc to grid efficiency of 97.5 percent was assumed for the MHD power management system. The reference system design described in this section has been evaluated with regard to expected performance, both for the case of generator-supplied VAR compensation and for the passive VAR compensation case. The results of loss calculations for both cases are given in Table 6.4.3. The component losses, given in kW at full rated load, result in calculated efficiencies in the 97.1 - 97.2 percent range. This is in good agreement with the assumed value of 97.5 percent.

A Faraday linear channel of approximately the same dc power output, with 1000 electrode pairs, requires the inclusion of consolidation circuitry; this circuitry is estimated to result in an additional 1/2 percentage point loss in conversion system efficiency.

6.4.4 SYSTEM COST

For the reference 527.3 MW generator power management system, the estimated materials and fabrication costs are given in Table 6.4.4. Again, these are provided for both the generator VAR compensation and the passive VAR compensation cases. The specific costs (\$ per kW) are not fixed values over any dc power range, but depend upon the details of generation scaling such as voltage and current relationships, number of annular segments, etc. The passive VAR compensation costs can be used to estimate the cost of CCD power management systems constrained to operate at the match point, as were the CCD systems investigated in this study and described in Section 8.0.

For the 1000 electrode pair Faraday linear channel of 500 MW dc output, the necessary equipment is estimated to cost approximately the same as that for the disk generator. However, the consolidation circuitry for such a generator can be expected to add an additional \$30 million to the quoted costs for the disk power management equipment.

TABLE 6.4.3
OCD MHD GENERATOR SYSTEM
LOSSES FOR 527.3 MW POWER MANAGEMENT EQUIPMENT

INPUT DC POWER: 527,416.5 kW

<u>COMPONENT</u>	<u>LOSSES kW AT FULL LOAD</u>	
	GENERATOR VAR	PASSIVE VAR
Main Transformer	2596.8 (600 MVA)	2201.4 (500 MVA)
VAR Capacitors	0.0	582.0
Harmonic Filter Capacitors	420.7	420.7
Harmonic Filter Inductors	56.6	56.6
Broadband Filter Resistors	2616.1	2616.1
Converter Transformers	3771.7	3771.7
Converter Bridges	3686.4	3686.4
DC Sourcing Inductors	1595.6	1595.6
Cooling Water Pumps	<u>184.3</u>	<u>184.3</u>
Totals	14928.2*	15114.8
Output Power, kW	512388.3	512201.7
Efficiency	97.17%	97.13%

* Does not include increased generator loss due to uprating for VAR correction.

TABLE 6.4.4
COST ESTIMATES FOR 527.3 MW DISK MHD
GENERATOR POWER MANAGEMENT EQUIPMENT

All Costs are FOB for Site Delivery, Mid-1980 Dollars

	With Generator VAR Compensation	With Passive VAR Compensation
Main Breaker	554,210	554,210
Main Transformer	2,075,980	1,868,970
Generator Δ VAR	1,255,000	
VAR Capacitors		1,338,600
VAR Reactors		921,590
VAR Control		1,333,990
Filter Capacitors	967,690	967,690
Filter Inductors	82,750	82,750
Filter Damping Resistors	<u>237,460</u>	<u>237,460</u>
Sub-total for dc Interface	5,173,040	7,305,260
34.5 kV Breakers	365,300	365,300
Converter Transformers	6,555,880	\$ 6,555,880
Converters and Bypass Values	3,983,230	3,983,230
Cooling System	1,448,000	1,448,000
DC Reactors	1,014,310	1,014,310
DC Capacitors	579,600	579,600
DC Switchgear	660,920	660,920
Freewheel diodes	256,260	256,260
Controls	<u>1,760,000</u>	<u>1,760,000</u>
Total Cost	\$21,796,540	\$23,928,760
527.3 MW/Base	\$41.34/kW	\$45.38/kW
Delivered Power Base (see efficiency)	\$42.54/kW	\$46.72/kW

The four OCD "optimized" generators described in Section 5.4 have segmentation similar, but not identical, to the reference disk generator segmentation. The major difference is found in the segment voltage for the first (entrance) segment; this is approximately twice the voltage for the reference disk first segment. The total voltage for each disk is approximately 50 kV, rather than the 35 kV of the reference disk. Table 6.4.5 contains the relevant system interface information for each of the OCD cases representing "optimized" disk power systems. As noted in the discussion of electrode system design (Section 6.1), the choice of segmentation radii is somewhat arbitrary; it does reflect the results of the off-design joint disk performance review contained in Section 5.3.4, which indicated that a monotonically decreasing segmentation distance would provide reasonably equivalent segment impedances throughout the generator.

The costs of the power management systems for the four OCD cases described in Table 5-4-12 can be calculated from the cost breakdown of Table 6.4.4. The scaling for various contributions to the total cost is assumed to be as follows:

- Converters: scale linearly with specific cost values of Table 6.4.4.
- Switchgear: scale linearly with specific cost values of Table 6.4.4.
- Magnetics (filters, transformers, inductors, generator MVA): scale as $(VI)^{0.87}$, with reference values being the specific costs in Table 6.4.4.
- Other: scale linearly with specific cost derived from Table 6.4.4.

The number of bridges for each segment in each of the four OCD cases was set by the 2000 A per bridge limit previously discussed. It is apparent that for a real disk system design, the segmentation selected will most probably not be identical to the segmentation selected here; the tradeoff between disk gas dynamic performance characteristics and electrical system design must be investigated in much greater detail than has been done for this study. For

TABLE 6.4.5
DISK POWER MANAGEMENT SYSTEM DESIGN DATA
DISK/CONVERTER INTERFACE

Case 1A	Voltage, V	Current, A	Number of Converters	Bridge Power
Segment 1	23878	12577.5	8	37.5 MW
Segment 2	11750	12577.5	8	18.5 MW
Segment 3	5875	12577.5	8	9.2 MW
Segment 4	5875	12577.5	8	9.2 MW
$V = 47378 \quad I_L = 12577.5$			Total Power = 595.9 MW	
Case 1B	Voltage, V	Current, A	Number of Converters	Bridge Power
Segment 1	24070	11245.5	6	45.1 MW
Segment 2	11800	11245.5	6	22.1 MW
Segment 3	5875	11245.5	6	11.0 MW
Segment 4	4700	11245.5	6	8.8 MW
$V = 46445 \quad I_L = 11245.5$			Total Power = 522.3 MW	
Case 2	Voltage, V	Current, A	Number of Converters	Bridge Power
Segment 1	23284	8804.3	6	34.2 MW
Segment 2	11400	8804.3	6	16.7 MW
Segment 3	7250	8804.3	6	10.6 MW
Segment 4	4350	8804.3	6	6.4 MW
$V = 46284 \quad I_L = 8804.3$			Total Power = 407.5 MW	
Case 3	Voltage, V	Current, A	Number of Converters	Bridge Power
Segment 1	26279	8457.4	6	37.0 MW
Segment 2	12600	8457.4	6	17.8 MW
Segment 3	8400	8457.4	6	11.8 MW
Segment 4	6000	8457.4	6	8.5 MW
$V = 53279 \quad I_L = 8457.4$			Total Power = 450.6 MW	

example, the additional savings inherent in selecting segmentation such that a large number of identical converter bridges could be used (VI's about the same for two or more segments) would be traded off against the performance improvements possible by having non-identical segment lengths.

6.5 RADIANT FURNACE DESIGN

The slag furnace (radiant furnace) design for the OCD generator is a critical transitional element in converting the essentially radial and planar combustion gas flow from the diffuser exit into a compact linear flow suitable for introduction into HTAH hot gas supply headers or to the seed recovery furnace. The selection of an optimum configuration must be based on evaluation of multiple effects such as plant interferences, minimum diffuser exit perturbations, heat loss potential, layout considerations, and NO_x reduction potential. These items must be combined into a design which also permits the recovery of combustion gas heat at the rates required by the plant performance design calculations while providing a removal point for the majority of the slag carried over from the combustor.

6.5.1 TOP-LEVEL DESIGN REQUIREMENTS

The salient top-level design requirements for the OCD radiant slag furnace can be summarized as follows:

- The furnace must provide for the requisite heat recovery from the combustion gas in the bottoming plant working fluid
- The furnace must permit removal of a major fraction of the slag carried over from the combustor by condensing and collecting it during the first phase of gas cooling after the MHD power extraction
- The furnace must permit near-complete separation of seed and slag by operating under conditions which result in slag condensation but no significant seed condensation
- The furnace must accept the axisymmetric radial flow from the OCD annular diffuser, and convert it to an essentially linear flow stream of compact proportions suitable for introduction into more conventionally-designed downstream equipment such as seed recovery furnaces or HTAH gas inlet ducts.

The design requirements for the radiant slag furnace of an OCD MHD/steam power plant thus differ from those of the slag furnace for any other open cycle MHD plant only in the addition of the final item listed above. As previously noted, emphasis in the present OCD systems conceptual design was placed upon the maximum utilization of conventional equipment for the bulk of the power system. Thus, the seed recovery furnace and downstream equipment normally associated with the slag furnace and closely integrated with it (at least in separately-fired open cycle MHD/steam systems, and those with only metallic preheaters) have been considered to be of typical design, accepting a compact linear flow of combustion gas. It would likely be possible to provide an integrated slag/seed radiant furnace and convective section design for an OCD separately fired system; however, for the purposes of a "first-cut" conceptual power system design, it is assumed that the radiant furnace for all the OCD systems is the slag furnace only. This maintains a consistent basis from which to compare the various OCD systems reported upon herein.

NO_x CONTROL CONSIDERATIONS

In addition to the explicit functions described previously, the slag furnace of most open cycle MHD/steam power plants is also assigned the subsidiary mission of effecting NO_x reduction in the combustion gas by providing cooling rates and residence times compatible with the kinetics of NO_x removal reactions in the 2200 K to 1800 K temperature range. Following the NO_x decomposition in the radiant furnace, secondary combustion is required to burn the MHD exhaust gases to an oxidant-rich combustion product. This oxidant-rich product is then suitable for use in the reheating of HTAH matrices or in downstream bottoming plant heat recovery equipment.

Acceptable performance from a supersonic open cycle disk generator with swirl can only be obtained with a relatively high oxidant preheat temperature, using air alone as the oxidant. The increased heat losses in the swirl-type combustor and the subsequent requirement to accelerate the plasma from combustor stagnation conditions to supersonic velocity both contribute to a depression of inlet plasma conductivity for the disk generator, in comparison to subsonic

linear generators with equivalent combustor stagnation conditions and seed fractions. The upper limit on combustor stagnation temperature is set by a combination of combustor design features, oxidant, and oxidant preheat level. 1920 K has been selected as the maximum supportable oxidant preheat temperature resulting from the use of regenerative ceramic matrix heat exchangers reheated with coal or coal-derived fuels burned in air. This temperature limit applies both in the directly-fired and in the separately-fired air preheater cases.

In the case of the directly-fired disk generator system, the upper approach temperature difference necessary to assure a reliable air preheat temperature of 1920 K requires that the radiant furnace outlet gas temperature be in the range 2100 K - 2150 K. Use of the radiant (slag) furnace to eliminate the bulk of the NO_x formed in the combustor is thus not possible in this case, since the secondary combustion process must be accomplished prior to the introduction of radiant furnace exhaust gasses into the HTAH reheat system. Use of a lower preheat temperature (say 1650 K) permits the utilization of the slag furnace for NO_x removal, but at the expense of reduced topping cycle performance. Both types of systems, i.e., high (1920 K) preheat and lower (1650 K) preheat with direct firing of HTAH by the radiant (slag) furnace exhaust gases are considered in this study.

For the separately-fired disk system, and for the oxygen-enriched system without HTAH, NO_x control can presumably be accomplished by use of the combined effects of the cooling and residence time in the slag furnace, and/or in the separate seed furnace and downstream convective equipment. Since the system conceptual design task did not encompass a delineation of the seed furnace and bottoming plant convective equipment detail design parameters, nor the metallic air heater parameters, it is not possible to delineate the expected NO_x performances for these cases. The radiant (slag) furnace was therefore sized only on the basis of heat duty and layout considerations for the 1920 K preheat level directly-fired case, the separately-fired, and oxygen-augmented cases. For the 1920 K preheat level directly-fired disk

generator system, an NH_3 scrubber (similar to the Exxon DeNO_x process) will be required; the 1650 K slag furnace can be sized to permit its use as the primary NO_x removal point in the combustion gas train.

6.5.2 PRELIMINARY FURNACE CONFIGURATION SELECTION

Various configurations for the OCD radiant furnace design were considered. These included configurations with the disk generator arranged so that its axis of symmetry was both vertical and horizontal. The more promising of the two arrangements was considered to be that with a vertical axis of symmetry since this type of arrangement permitted simple magnet support and the use of a vertically-firing coal combustor without the necessity for an outlet adapter to turn the flow.

For the radial outflow disk configuration, the use of an annular diffuser surrounding the disk is required. To couple such a diffuser to a single radiant furnace, several layout options were considered. These included:

- Disk generator diffuser, magnet, and combustor located directly beneath and coaxially with a single cylindrical radiant furnace;
- Disk generator and diffuser exhausting into a large scroll collector which was ducted directly to a single radiant furnace;
- Disk generator and diffuser exhausting into an annular radiant furnace surrounding the diffuser, with tapered dimensions to permit access and equipment changeout with minimum lift requirements for the plant crane.

Two of these proposed layouts are shown in Figures 6-5-1 and 6-5-2. Following consideration of their merits, none of the three options mentioned above was chosen as the baseline layout. For the first-mentioned, access to the power train components would be strictly limited, requiring a near teardown of the radiant furnace for magnet, disk, or diffuser maintenance or replacement. Routing of service connections, instrument lines, etc., to the power train components would be difficult. The available flow area in the diffuser is reduced considerably by the requirement for passing all such service lines through the diffuser, as well as major support members for the furnace itself.

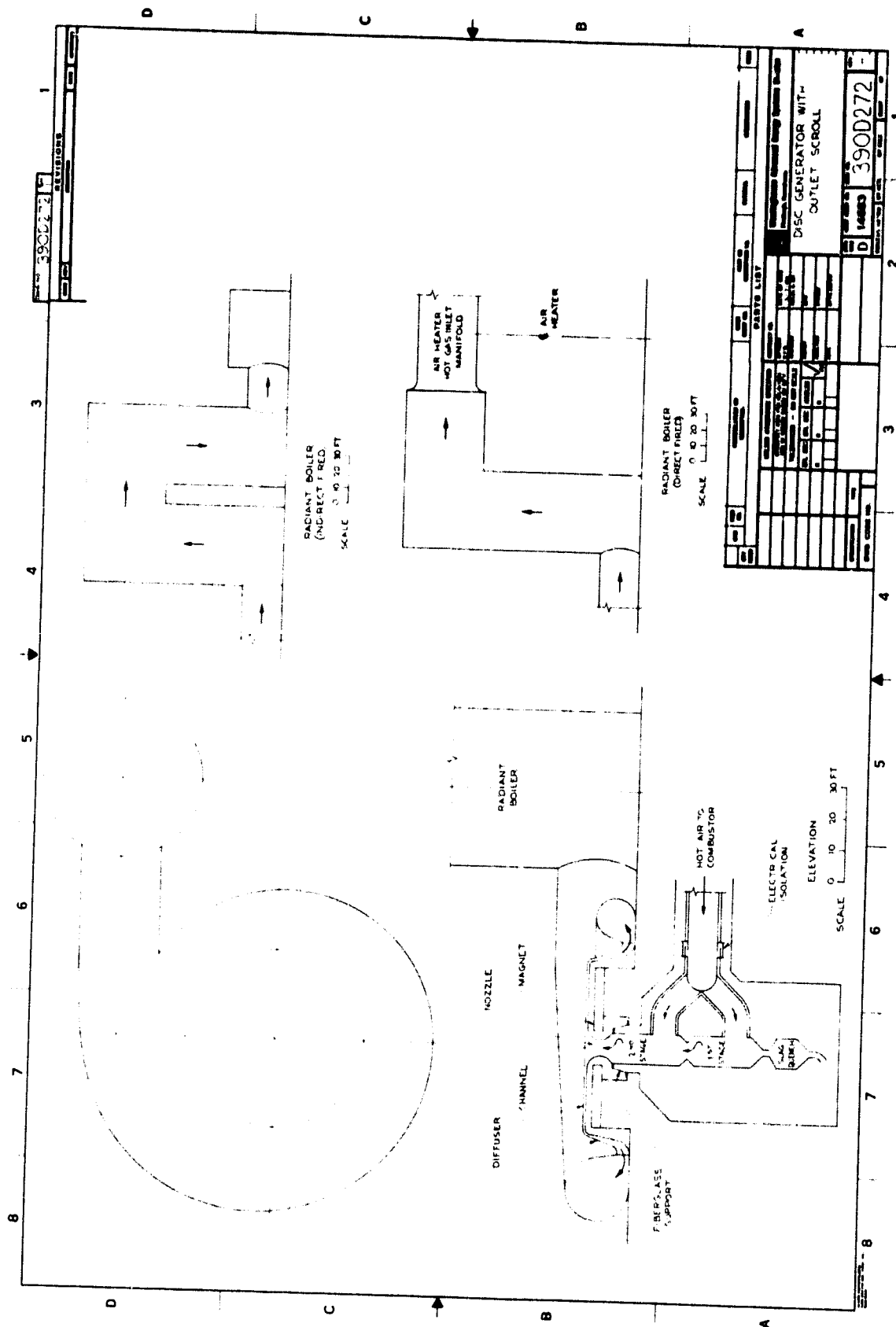


Figure 6-5-1. Disk Generator Diffuser and Radiant Furnace Interface with Outlet Scroll Collector

The large single radiant furnace supplied by a scroll collector on the diffuser outlet is probably the most immediately obvious arrangement for coupling a radial outflow disk to standard bottoming plant components. However, such a scheme entails the addition of extensive surface area to the combustion gas system and thus exacerbates the problem of heat loss to ambient. With the scroll designed to form part of the radiant furnace heat exchange system, such an increased surface area could possibly be acceptable, but the varying flow lengths inherent in this geometry may impose unacceptable variations in cooling rates, residence times, and diffuser exhaust back-pressure for the various streamlines. An additional complication would be found in the design of the slag collection and handling system for such a boiler arrangement. The design of the supercritical fluid piping systems would also be more difficult with such an arrangement. Accessibility of the power train components is relatively good in this configuration.

The closely integrated disk generator/radiant furnace arrangement of Figure 6-5-2 was developed in an attempt to minimize heat losses while still providing a single radiant furnace structure and reasonable access to power train components. Careful engineering of the furnace/diffuser interfaces will be required to accommodate the sealing requirements and thermal expansion motions, while providing support for the boiler deadweight loads. The outer ring girder of the lower diffuser structure would be utilized in such an arrangement to transfer the deadweight loads from the inner furnace wall to ground. The splitters in the diffuser would require suitable reinforcement or must otherwise be modified to permit the transfer of these loads across the combustion gas stream. The radiant furnace inner and outer walls would consist of water walls supported in pendular fashion from a cool external steel structure. Analyses of flow and temperature patterns within such an annular furnace structure revealed the possibility of large variations in pressure and heat transfer rates for various flowpaths within the furnace. While it seems possible to envision the development of a design such as this which could provide equivalent cooling rates and constant backpressure on the diffuser for flow at any circumferential location in the diffuser exhaust, the designs studied were not considered to be acceptable and were therefore discarded as a basis for the OCD conceptual layout.

The final power train arrangement to be considered was that shown in Figure 6-5-3, having multiple cylindrical radiant furnaces arrayed symmetrically about the periphery of the annular diffuser. Each furnace is free-standing without a requirement for passing any of its deadweight load through the diffuser to ground. Each furnace is coupled to the diffuser exhaust by means of a relatively compact transition duct, thus producing more uniform diffuser backpressure and gas residence time for the split flow streams from the diffuser. The design does, however, complicate to some extent the exhaust trunk arrangement from the furnaces to the high temperature air heaters or the seed recovery furnace/convective equipment downstream. This type of arrangement is analogous to the typical layout of the major steam-raising equipment for a large central station pressurized water reactor plant, which is arranged about the centrally located reactor heat source. This final arrangement, which holds promise of providing reasonable accessibility to the power train components while minimizing design complications, was selected as the basis for the conceptual design of the OCD radiant furnace.

6.5.3 DESIGN BASIS FOR OCD CYLINDRICAL RADIANT FURNACES

Following the selection of the multiple cylindrical radiant furnace configuration as the most appropriate for the OCD generator systems, it was possible to further refine the layout and proceed with the conceptual design of the furnaces.

6.5.3.1 Number of Furnaces

The basic selection criteria leading to the choice of an appropriate number of cylindrical radiant furnaces were:

- Relative ambient heat loss potential;
- Coupling losses between annular diffuser and furnaces;
- Accessibility of disk, diffuser, and magnet;
- Coupling losses for furnace exhaust to downstream components;
- Steam/feedwater piping integration.

(For purposes of selection, the accessibility of components interior to the ring of radiant furnaces surrounding the disk generator was considered as the primary requirement. This provides a plant design which permits full utilization of the simplicity of design of the disk generator with respect to ease of access and repair, with concomitant positive effect upon plant availability. Limited access would be provided by arrangements having virtually any number of furnaces. However, it was considered important to maintain the capability for a removal of each disk generator section (upper and lower), without the necessity for making an excessive lift over the top of the radiant furnaces. Thus, the configuration selected must provide sufficient clearance between the outer walls of adjacent furnaces to pass a component with a maximum diameter equivalent to that of the disk generator upper and lower sections. This clearance can be provided even for a relatively large number of furnaces, if these were positioned at a significant radial distance from the disk axis. However, the choice of about a 10 m maximum radius for the annular diffuser exit (based upon aerodynamic considerations) and the approximate 5 m radius of the disks being considered, limited the selection to arrangements with 5 or less identical symmetrically-disposed furnaces.

The major consideration pointing to the selection of a larger rather than smaller number of furnaces was the expected minimum effect upon diffuser exhaust gas flow symmetry, with more furnaces, thus providing increased potential for pressure recovery. However, a larger number of furnaces also implies greater ambient heat losses and draft losses. Combining the exhaust gas flow from as many as five separate furnaces also poses a distinct problem, requiring a ring header with increasing diameter if it is required that no gas ducts pass over the disk/diffuser region and thereby limit access to the interior of the radiant furnace array.

A similar argument regarding the combination of furnace exhaust flows also applies to the 4-furnace array, although it provides increased clearance for component removal and limits ambient heat losses and draft losses even further below those of the 5-furnace array. The diffuser-to-furnace flow coupling is

expected to be relatively easy to accomplish in the case of 4 furnaces, as no significant turning of the horizontal flow patterns is required.

For the 3-furnace array, it is possible to extract the furnace exhaust gases from each furnace singly by use of nearly straight ductwork running to a large header which combines all flow for use in the downstream oxidant preheating or steam raising equipment. This simplicity of layout is enhanced by the fact that three furnaces can be located relatively close to the diffuser exit while still permitting sufficient clearance for removal of disk generator half sections. Draft losses and heat losses to ambient are also expected to decrease with the smaller number of furnaces. The furnace exhaust ducting can be positioned so that it is extracted from the power train area in a direction opposite to that in which the gantry rails leave the same area. The HTAH or convective heat exchange equipment for the bottoming plant is thus located together, away from the required disk laydown, installation, or repair area to which the gantry crane runs. The 3-furnace array was selected as the reference radiant furnace concept for OCD system design and layout.

For a 3-furnace array, the flow patterns from the annular diffuser to the furnaces are not as simple as those for a larger number of furnaces, and the flow must be directed by means of shaped splitter vanes and turning walls in the furnace-to-diffuser transition ducts. The potential for reduced diffuser efficiency is increased with a decreased numbers of furnaces, because of these more complicated flow patterns. It is expected that reasonable diffuser efficiencies can be provided for with an integrated diffuser/furnace inlet duct design, for arrays with a minimum of three or more identical radiant furnaces. The detailed design of these integrated diffusers/inlet ducts will be a critical part of the OCD systems design effort for plants using the separate cylindrical furnace configuration.

6.5.3.2 Slag Furnace Heat Transfer Model

The heat transfer model used to estimate the size of the radiant furnaces for each of the four OCD system cases was similar to that described in a recent Argonne National Laboratory report [1]. Uniform vertical combustion gas flow

was assumed within the cylindrical section of the furnace. Only convective and radiant heat transfer terms were considered. Gas/particle emissivities and absorptivities were estimated for 10 percent slag carryover and a mean radiating length of $2/3 D$ from Figures 2 and 3 of the referenced Argonne report. The furnace inside surfaces were assumed to be covered by a uniform, thin layer of liquid slag with an emissivity of 0.9 at its mean temperature of 1600 K. The furnace walls and floor were assumed to be of the waterwall type, with supercritical bottoming plant working fluid contained within tubes forming the waterwall. The radiant furnace inlet ducts were considered to be part of the total heat transfer unit associated with the radiant furnaces, as were the diffuser splitter vanes. Both of these latter surfaces were taken to operate at 2000 K wall temperature, in a non-slagging mode.

The heat transfer requirements for the radiant furnace system in each case were determined from the final optimized system performance calculations, using the Westinghouse SPA code. These heat transfer requirements and the estimated contributions of each of the three heat transfer elements comprising the overall radiant furnace system are given in Table 6.5.1. In Case 1B, the required 1850 K furnace outlet temperature was achieved by absorbing the heat transfer requirement of the "superheater" (as determined by the SPA code) into the radiant furnace heat transfer section. Normally, the "superheater" section is assumed to be a partly or fully convective heat transfer section following the seed furnace in the gas flow path. (The quotation marks are used to emphasize the fact that the term "superheater" refers to an active transfer section for gas to bottoming plant heat transfer, but which for the supercritical steam plant assumed provides no actual superheat function. Since there is no distinct phase differentiation in a supercritical fluid, there is no superheating in the precise sense of the word. The "superheater" nomenclature is retained only for ease of reference to the results of the SPA code which identifies a discrete heat transfer unit by this name.)

TABLE 6.5.1
OPEN CYCLE DISK GENERATOR SYSTEMS
RADIANT FURNACE SUBSYSTEM HEAT TRANSFER DATA

	OCD DF		OCD SF	OCD + O ₂
	1920 K	1650 K		
	CASE 1A	CASE 1B	CASE 2	CASE 3
Total Heat Transfer Required, (MW _t)	508	851 ¹	354	402
Heat Transfer in Radiant Furnace Proper (MW _t)	448	816	300	355
Heat Transfer in Furnace Inlet Duct (MW _t)	40	21	38	37
Heat Transfer in Diffuser Splitters (MW _t)	20	14	16	10
Design Heat Transfer per Cylindrical Furnace, (MW _t) (3 Furnaces)	150	272	100	118

(1) "Superheater" heat transfer requirement absorbed into slag furnace to permit gas temperature reduction to 1850 K at outlet.

6.5.3.3 Sizing of Radiant Furnaces

Furnace sizing was accomplished by assuming a furnace diameter compatible with the OCD systems design basis and known constraints, and calculating the height required to provide the stated heat transfer at design conditions.

For an MHD/steam plant, the furnace diameter is chosen normally to permit adequate residence time for the gas in the NO_x -removal-critical temperature range of 2200 K - 1850 K, while the gas is yet in a fuel-rich condition. As described before, this constraint cannot be met in the 1920 K preheat directly-fired disk generator system. Thus, the furnace diameter for Case 1A was specified only upon layout and heat transfer considerations, to provide a compact set of three slag furnaces which offered reasonable access to the disk/diffuser area for repair, maintenance, or replacement purposes. 10 meters was chosen as a base diameter for the slag furnaces in this case.

In order to compare the relative cost and estimated performance of a disk generator system which was capable of providing NO_x removal by means of controlled radiant slag furnace residence time alone to the 1920 K preheat case, a lower preheat temperature case with direct firing of high temperature air heaters was investigated. This case assumed 1650 K air preheat temperature, which permitted the utilization of combustion gas cooling within the three radiant furnaces as the principal NO_x removal mechanism. The furnace diameter was selected using a correlation given in a recent technical paper⁽²⁾ as shown below:

$$\ln C_e^* = 11.7 \phi - 0.669 \ln D_1 + 0.0148 B - 3.17$$

with D_1 in meters;

C_e^* "frozen" NO_x concentration in ppm;

ϕ combustion stoichiometry;

B slag carryover in percent.

On applying this relation for a stoichiometry of 0.95, to obtain a required NO_x level of 350 ppms, the required radiant boilers geometry was found to be unacceptable.

Therefore, for the purposes of designing the radiant boiler, the stoichiometry was assumed to be 0.92. The resulting diameter for the boilers is 16.5 m. The effect of this change in stoichiometry on the remainder of the system is felt to be minimal. It should be noted that the required diameter computed from the above equation is independent of flow rate and thus the number of furnaces.

Using this diameter, the furnace length was computed using the same heat transfer model used in Reference (2) and found to be 11 meters.

With the diameter of 16.5 meters selected for the slag furnace in Case 1B, the relative cost of the radiant furnace assembly was expected to be greater for the lower preheat case; this is in addition to the decreased performance expected as a result of lowering the preheat temperature from 1920 K to 1650 K, and the more restricted layout of the power train components. The required outlet temperature of ~1850 K results in the requirement that the total heat transfer duty for the slag furnaces of Case 1B be significantly greater than for Case 1A, as indicated in Table 6.5.1.

For Cases 2 and 3, it is possible to size the slag furnace to provide NO_x reduction to below the required concentrations. However, it is conceptually just as feasible to provide such reduction in the seed recovery furnace downstream of the combined slag furnace outlet ducts (since no high temperature air heaters are interposed between these furnaces). For this study, the use of the seed furnace for NO_x control was assumed; the diameter of the 3 slag furnaces for each case was thus taken to be 10 meters, identical to the Case 1A diameter. One advantage of limiting the gas temperature decrease in the slag furnace is the potential for a better partition of seed and slag between the furnaces; since the bulk of the seed does not begin to condense from the gas until the average temperature drops below about 2000 K, while a large fraction of the slag can be removed from the gas at the walls of the slag furnace.

6.5.4 RADIANT FURNACE DESIGN DETAILS

6.5.4.1 Cylindrical Section

The radiant furnace design selected for the OCD cases was a typical modern slag-tap type with a full-stud tube wall and inner casing. Waterwalls are formed from vertical runs of stainless steel piping set in rammed magnesia refractory walls. The piping is studded to promote the presence of an insulating slag layer on all interior surfaces of the furnace. 2-inch Schedule 160 piping set on a 0.75 m (3 inch) circumferential pitch was chosen in order to limit the stresses to valves below the limiting stress for this material at the design conditions of the supercritical system. The tube walls are welded to circumferential support plates fastened to the inner casing of carbon steel. This inner casing provides the gas pressure boundary for the furnace. It can be fabricated from carbon steel since the remanent field of the disk magnet is very small at the radius of the inner wall of the furnace nearest the power train axis. The shell is approximately 3 mm (1/8") thick, and is supported with the waterwalls in pendant fashion from carbon steel structural members. A 0.1 meter thickness of medium temperature insulating block separates the pressure casing (which operates at maximum cooling water temperature) from the exterior casing of 1.5 mm thick carbon steel lagging.

6.5.4.2 Furnace Inlet Ducts

The furnace inlet duct pressure walls are formed from carbon steel plate 13 mm (1/2") thick. These walls are supported by external beams similar to those used in the diffuser structure. Waterwalls of 2-inch Schedule 160 studded stainless steel piping set in a refractory layer of MgO surround the gas duct from the diffuser exit to the cylindrical furnace inlet. Water from the combustor cooling system passes through the diffuser splitter vanes and the inlet duct cooling lines on its way to the lower ring header for the radiant furnace proper. The average MgO thickness for the inlet duct is approximately 60 mm. A 50 mm layer of mineral wool insulation is applied to all air surfaces of the inlet duct casing and structure to limit heat losses to ambient. The inner walls of the duct are designed to operate at 2000 K to prevent a liquid slag buildup within the duct.

The maximum entrance velocity of the combustion gas into the cylindrical furnace section is less than 80 m/s, set by the height of the duct at the furnace wall. Gas flows vertically upward through the cylindrical furnace at about 12 m/s (Cases 1A, 2 and 3) or less than 8 m/s (Case 1B) to the centrally-located exhaust opening in the furnace roof. The cooled combustion gas is collected and directed through individual exhaust ducts to the combined exhaust gas header. Flow velocities are limited to about 65 m/s in this section of the combustion gas system.

6.5.4.3 Slag Collection and Handling

Liquid slag collects on the cooled walls of the cylindrical radiant furnaces and flows down these walls to the floor of each furnace, where it is removed through a central opening in the water-cooled floor of the furnace. Since the slag collection and handling system for this type of furnace is no different from the furnace for a linear MHD plant, no details of this system were developed as part of the study. It is expected that the necessity of providing 3 slag collection points for the disk instead of a single point as for the linear radiant furnace will increase the cost of such a system for the OCD power plants, even though the capacities of the distributed and single systems are identical. Figure 6-5-4 illustrates the general layout of a single cylindrical section and inlet duct. The details of the gas sealing between the diffuser and inlet duct have not been defined in this study. These most probably will present a difficult problem, since the diffuser and inlet duct designs must provide some accessibility for inspection and repair of the refractory surfaces at intervals over the design life of the plant. In Table 6.5.2 the outside dimensions and estimated weights for the radiant furnace of each OCD Case considered are provided.

6.5.5 ADDITIONAL COMMENTS

For the furnace configuration discussed herein, the inlet duct is an integral part of the diffuser for the disk generator. The duct must therefore be designed to provide the maximum aerodynamic performance when coupled with the annular diffuser and the cylindrical radiant furnace. A more detailed evaluation of the multiple-furnace array surrounding the radial outflow

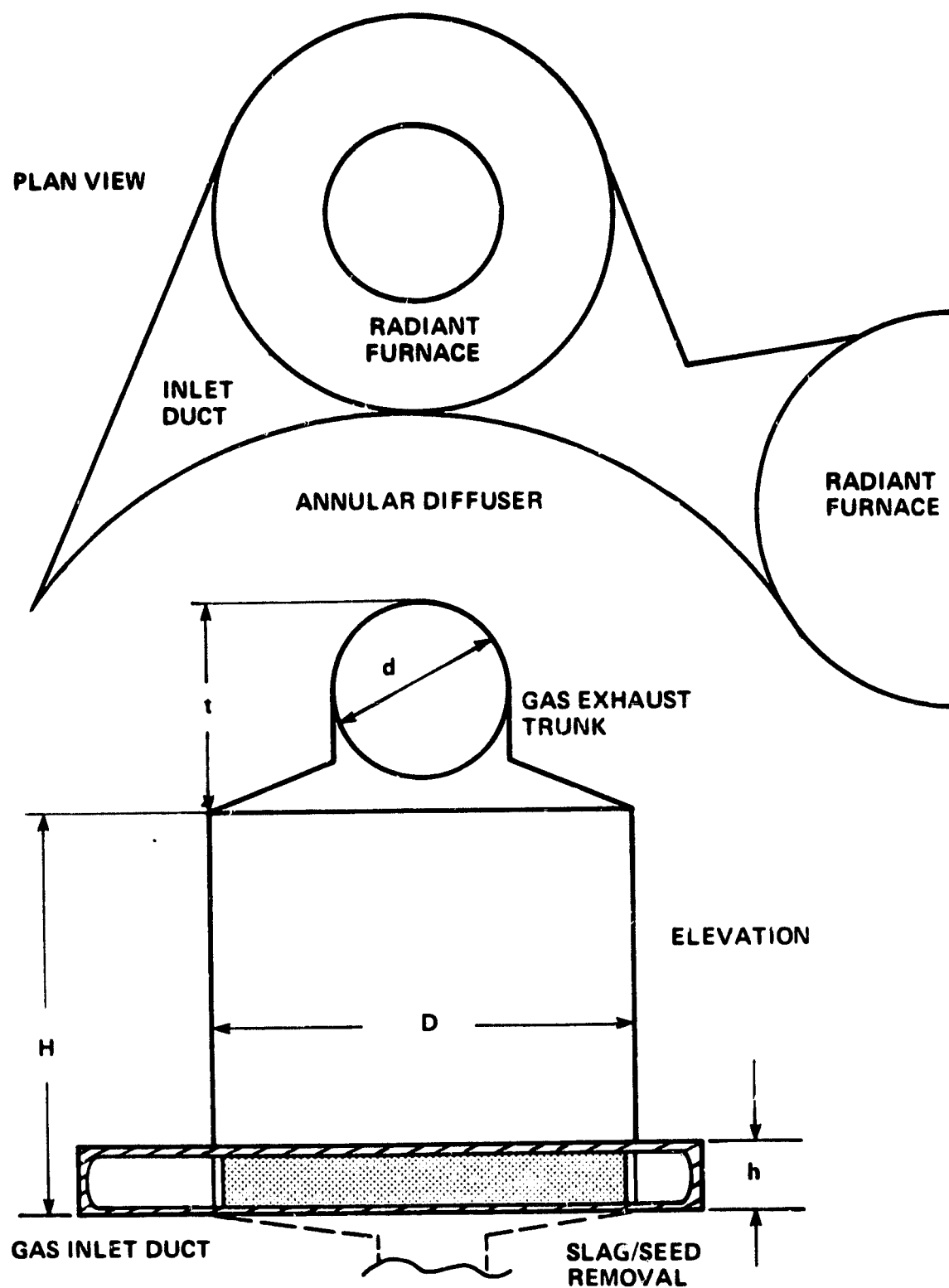


Figure 6-5-4. Open Cycle Disk Generator System Radiant Furnace Arrangement

combustion gas disk generator must be carried out in order to precisely characterize the performance potential of the OCD systems utilizing this configuration. The overall pressure recovery coefficient of 0.6 assumed for this study is probably very near the theoretically attainable upper limit for the selected design.

TABLE 6.5.2
OCD RADIANT FURNACE DIMENSIONS
AND WEIGHTS

	OCD DF		OCD SF	OCD + O ₂
	1920 K	1650 K		
	CASE 1A	CASE 1B	CASE 2	CASE 3
Number of Furnaces	3	3	3	3
Furnace Outside Diameter, Meters	10.6	16.7	10.6	10.6
Cylindrical Casing Height, Meters	16.5	11.0	10.0	14.0
Exhaust Trunk Height, Meters	6.5	6.5	5.3	5.5
Inlet Duct Height, Meters	1.15	1.15	1.05	1.00
Estimated Combined Weight of Furnace and Inlet Duct (one set) (includes structural steel framework)	592,000 kg	719,000 kg	385,000 kg	492,000 kg

6.6 AIR HEATER SYSTEMS

The design of oxidant preheater systems for OCD MHD power plants is no different in principle from the design of preheaters for linear MHD power plants. However, the necessity for supersonic operation of the disk generator in order to achieve acceptable performance levels implies that the OCD systems must be designed for the highest possible combustor stagnation temperature. For air-blown coal combustors, this naturally requires the use of maximum obtainable preheat levels. As part of the disk generator study, therefore, one subtask was assigned which led to a review and specification of likely design features and performance parameters for air preheaters suitable for use at the maximum credible temperature levels. This task encompassed a delineation of features for both a directly-fired preheater system (representing the expected mature development of air heater technology for MHD applications) and an indirectly fired system (for intermediate disk MHD systems).

6.6.1 SELECTION OF MAXIMUM PREHEAT TEMPERATURE

The maximum supportable preheat temperature was taken to be 1920 K (2996°F) in the case of directly-fired and indirectly-fired air preheaters. The logic behind this selection is discussed in the following paragraphs.

Current air heater technology (based on the design of blast furnace stoves) requires clean fuel and can provide air preheat levels on the order of 1800 K. Some experience with advanced clean-fuel-fired air preheaters in the USSR has been obtained at preheat levels up to 2270 K, and at 2000 K for reasonable periods of operation. For the disk generator systems study, the clean fuel for indirectly-fired preheaters is assumed to be provided by an advanced pressurized gasifier supplying the HTAH reheat burners with a low BTU fuel gas. Initially, it was thought that with such a system the attainment of preheat levels up to 2270 K was possible; however, for the specific constraints and fuel/oxidant type considered, it was determined that such preheat levels could not be reached. Therefore, the upper limit for clean-fuel-burning preheaters was set at 1920 K, since this level gave promise of the possibility of designing air heater matrices with Al_2O_3 materials

instead of requiring the use of the much more costly zirconia in the hotter regions of the bed. This value of 1920 K was chosen as the base case preheat level for the indirectly-fired OCD parametric study.

Clearly, the basis for use of the 1920 K preheat level in OCD indirectly-fired units does not carry over into the selection of an identical preheat level for the OCD directly-fired system. The presence of relatively large amounts of slag and seed in the reheat gas complicates the design of such a preheater system. However, given the correctness of the assumption that the directly-fired disk systems would only be the result of a matured MHD development program, it seemed reasonable to assume that the 1920 K preheat level could be obtained, albeit with a higher risk. The 1920 K preheat was therefore chosen as the base preheat level for the OCD directly-fired disk systems as well. This selection also permits a more reasonable comparison to be drawn between the final "optimized" system performances of the OCD directly-fired and indirectly-fired cases.

6.6.2 AIR PREHEATER SYSTEM CHARACTERISTICS

The characteristics of air preheater systems designed for maximum preheat are considered in the following subsections. Two reference cases were analyzed in detail, one each for a 1000 MW_e (nominal) directly-fired unit and for a 1000 MW_e (nominal) indirectly-fired unit.

In each case, the delivered air temperature is 1920 K (2996°F). This temperature level and the directly-fired conditions require an extension of the state-of-the-art as compared with present commercial practice as described above. A conservative approach was therefore taken in sizing the heaters, valves, and ducting. Cost estimates were made for each of the systems considered; the cost estimate will tend to represent early rather than mature technology since it is based upon limited knowledge of development requirements to obtain such preheater performance.

The effect of the conservative approach is most significant in the directly-fired case. In this case, one of the major remaining development

needs is the method of supporting the heater beds. A high temperature support is needed to allow drainage of the seed and slag (the temperature must reach about 1366 K on each operating cycle). It was decided to use small bed diameters, consistent with present commercial practice for comparable high temperature supports (e.g., as in secondary ammonia reformers). This limited the bed diameter to about 4.3 m (14 feet), and to accommodate the flow for a 1000 MW_e OCD system required a total of 28 heaters. Further developments in support technologies could be expected to reduce this number.

6.2.2.1 Directly-Fired Air Heaters for Open Cycle MHD Systems

General Considerations

The design of the directly-fired HTAH is dominated by the presence of seed and slag in the reheat gases. The presence of seed and slag presents two problems. First, they are corrosive to many refractory materials. Second, they pass through the heater system (heater beds, valves, ducts) in a temperature range where they condense and solidify. The latter introduces the possibility of fouling of the heater beds and valves.

Development in these areas is being supported by DOE and carried out as part of the DOE MHD program. Considerable progress has been made and the current status is described below. The results of this work has been applied to the design described here.

Description of Heater System

A conceptual layout of a typical heater system was initially prepared without reference to any particular plant arrangement. Its sole purpose was to provide a basis for the cost estimate and to give an indication of overall size. No study of preferred arrangements or more compact arrangements were made. The final layout of the air heater system for the OCD directly-fired system (Case 1A) in Section 6.7 was chosen with regard to all system constraints.

Details of the system are presented in Table 6.6.1. The number of heaters (28) resulted from the decision to use a relatively small bed diameter, as discussed

TABLE 6.6.1
SIZE AND OPERATING CONDITIONS
FOR 1000 MW_e OPEN CYCLE DIRECTLY-FIRED CASE

Gas and Air Conditions

Gas Inlet Temperature, K (F)	2080 (3286)
Gas Outlet Temperature, K (F)	1261 (1811)
Air Inlet Temperature, K (F)	920 (1191)
Air Outlet Temperature, K (F)	1922 (3000)
Gas Inlet Pressure, kPa (psi)	120 (17.4)
Air Inlet Pressure, kPa (psi)	600 (87)
Gas Flow Rate, kg/sec, (lbm/sec)	849 (1865)
Air Flow Rate, kg/sec, (lbm/sec)	766 (1690)
Gas Pressure Drop, kPa, (psi)	5.2 (0.75)
Air Pressure Drop, kPa, (psi)	14.5 (2.1)

Number of Heaters

On Air	7
On Gas	19
Press./Depress.	2
Total	28

Cycle Times

Air, sec	664
Gas, sec	1800
Press./Depress., sec	191
Full, sec	2655

Dimensions

Cored Brick Hole Diameter, mm (in)	19 (0.75)
Cored Brick Web Thickness, mm (in)	9.5 (0.375)
Bed Height, m (ft)	7.0 (23)
Bed Diameter, m (ft)	4.3 (14)

Valve Flow Diameter

Gas Inlet, m (ft)	2.1 (7.0)
Gas Outlet, m (ft)	1.7 (5.5)
Air Inlet, m (ft)	1.0 (3.3)
Air Outlet, m (ft)	1.5 (4.8)

Ripple in Delivered Air Temperature, K (F) + 36 (64)

Total Heat Loss, MW (Btu/hr) 35 (120 x 10⁶)

Air Loss from Valve Leakage and
Press./Depress., kg/sec (lb/sec) 7.9 (17.5)

previously. As noted there, the diameter of 4.3 m is based upon present commercial practice with high temperature bed supports. The complications of cycling temperature and the need to accommodate seed and slag removal both represent extensions of the state-of-the-art and therefore, it was decided not to add the further extension of an increase in diameter. The study did not include examination of HTAH costs with various numbers of heaters, but it is very likely that a smaller number would have a lower cost.

The ducts and manifolds were sized to give a gas/air velocity of 200 ft/s, based on estimated erosion and pressure drop limitations.

Another factor in the selection of relatively small beds is that the corresponding valve sizes are also reduced. The valve sizes and temperature levels are within current blast furnace stove practice. The small size should improve individual valve reliability, a factor that needs to be examined relative to the number of valves. The major difference between the HTAH valve requirement and current practice is the presence of seed and slag.

Refractory materials for various parts of the system are identified in Table 6.6.2. The major limitation in these selections is that the high temperature level is above that for which suitable materials have been found and tested as part of the DOE MHD program. Further discussion of this factor is given below.

An estimate of component weights and costs is given in Table 6.6.3. It should be noted that this estimate cannot be compared directly with that for the indirectly-fired heater; while the directly fired heater is a complete component, the indirectly-fired heater requires an extensive set of ancillary equipment whose costs have not been estimated as part of this study.

Development Status of Directly-Fired Air Heaters

The major development requirements involve high temperature materials resistant to seed and slag and having satisfactory life and cost: heater operating conditions that will prevent fouling of the flow passages with seed and slag, a

TABLE 6.6.2
REFRACTORY MATERIALS
FOR 1000 MWe OPEN CYCLE DIRECTLY-FIRED CASE

Heater Beds:	Fused Cast Magnesia/Alumina Spinel		
Heater Bed Liner:	Fused Grain Spinel Bricks		
Insulation:	<u>Hot Liner</u>	<u>Mid Layer</u>	<u>Outer Layer</u>
Hot Gas Inlet	Cast Spinel	3300 F Castable	2800 F Castable
Hot Gas Outlet	Cast Spinel	2000 F Castable	2000 F Castable
Air Inlet	Heavy Castable	2000 F Castable	2000 F Castable
Air Outlet	Cast Spinel	3300 F Castable	2800 F Castable

TABLE 6.6.3
ESTIMATED HEATER SYSTEM COST*
OPEN CYCLE DIRECTLY-FIRED CASE

		<u>Cost, 10⁶\$</u>	
	<u>Weight, m. tons</u>	<u>Materials</u>	<u>Labor</u>
<u>Heaters</u>			
Bed	5290	17.5	3.2
Insulation	4940	11.1	4.0
Vessel	850	0.6	2.0
<u>Ducts and Manifolds</u>			
Insulation	40	12.7	3.0
Steel	830	0.6	1.9
Flanges	1640	3.60	
Expansion Joints		1.2	
<u>Valves</u>	840	19.7	
<u>Bed Support</u>	890	3.4	0.4
<u>Structural Steel</u>	3600	2.8	7.5
<u>Instrumentation/Controls</u>		1.2	
SUBTOTALS	27600	74.4	22.0
TOTAL SYSTEM COST, 10 ⁶ \$			96.4

*Direct costs are shown, i.e. contractors overhead and profit are not included. Installation is included in labor component. All costs are in mid-1979 dollars.

bed support that meets the requirements of the heater operating conditions, and valves with satisfactory reliability and cost. Development in each area is proceeding at Fluidyne Engineering Corporation under contract with DOE. The current status is described in the following.

Materials

Heater bed, hot gas inlet duct and upper dome lining, and heater bed lining must be constructed of seed/slag resistant material. The present development program has concentrated on evaluation of commercial materials which could be produced in large quantities. Testing of over one hundred materials has shown that magnesia alumina spinel and some chromia-containing materials have good corrosion resistance. One material in particular has performed well, a fusion-cast substance composed of magnesia grains embedded in a spinel matrix.

Current estimates are that these materials will have satisfactory life and cost for delivered air temperatures to 1520 K (2700°F). A temperature of 1920 K (2996°F) will require search for materials that are not now in commercial production.

Operability

Seed/slag present in the reheat gas must not accumulate in the air heaters or their associated inlet and outlet ducts. Tests with a cumulative duration of 1100 hours have been completed with a 5.2 m (17 ft) high bed under simulated directly fired operation with seed and slag. These results have been encouraging and indicate that the seed and slag does not accumulate if the bottom of the bed is heated above the seed freezing point (about 1350 K) during each operating cycle. These tests were made with an oxidizing reheat gas and with Montana Rosebud ash. A single test of long duration is needed to confirm these results and tests under other operating conditions are also needed.

The inlet air temperature to the heater was 922 K for these tests. This represents a reasonable maximum level for the outlet temperature of metallic HTAH's which are part of the overall MHD systems design. Additional tests could determine if a lower inlet air temperature can be accommodated.

Bed Support

The foregoing discussion points up the need for a bed support which will endure temperatures at least as high as 1370 K (2000°F). Fluidyne has studied possible methods and has identified a ceramic dome structure as a promising approach. Part of the basis for this choice is experience with secondary NH_3 reformers where a perforated ceramic dome is used as a catalyst bed support. Reformers operate at bottom-of-the-bed temperatures of 1280 K (1850°F) to 1310 K (1900°F) and combined static and dynamic load of 200 kPa (30 psi), conditions which compare favorably with those which would obtain in MHD HTAH service. However, regenerative heaters cycle in temperature while NH_3 reformers operate at steady conditions. Testing of a full-scale or near full-scale dome is needed to verify satisfactory operation in response to thermal cycles.

Valves

Six valves are required for operation of each heater in the HTAH system; these are: gas inlet and outlet, air inlet and outlet, pressurization, and depressurization. With the exception of air inlet and pressurization valves, the others require some development or at least verification testing.

The gas inlet valve will be exposed to the most severe conditions. A test of a small prototype valve has been run with encouraging results. This test valve is a gate valve in which the gate and a follower ring form an integral structure which slides back and forth in the body of the valve. The follower ring protects the body seat from fouling by seed/slag in the hot gas. Both the gate/follower ring and the valve body are water-cooled and protected with a refractory lining.

Each of the aforementioned issues is being addressed in the MHD heater development program and in none of these areas is there evidence of a barrier to development for air temperature levels to 1760 K (2700°F). However, more work is needed in order to demonstrate feasibility and provide the data needed to support design. The availability of materials for the higher preheat temperatures is uncertain.

6.6.2.2 Indirectly-Fired Air Heaters for Open Cycle MHD Plants

General Considerations

The primary feature of this design case is the use of pressurized combustion gases for reheat of the air heaters. Fuel is furnished by a coal gasifier. The gas is cleaned of particulates and condensibles and supplied to the burners which operate at 1720 kPa (250 psi) in the design discussed here. For the OGD parametric analyses, a matched air/gas pressure was assumed.

The use of a clean reheat gas brings the air heater requirements close to the state-of-the-art than for the directly-fired case. However, there still are significant differences from the most advanced blast furnace stove practice. These are delivered air temperature, 1920 K versus about 1650 K; air flow rate, 575 kg/sec versus about 185 kg/sec; pressure level, 1670 kPa versus about 670 kPa, and pressurized versus atmospheric combustion.

The complete air heater system would consist of the air heaters, pressurized combustors, coal storage and handling equipment, and power recovery expanders. The cost estimate covers only the air heaters and therefore cannot be compared with the directly-fired case.

Power recovery expanders in use in petroleum refineries could be used for recovering energy from the reheat gas leaving the HTAH. These devices are used on the vent from catalytic cracker regenerators in which catalyst is regenerated by burning off carbon. The vent stream must be cleaned of particulates and high efficiency cyclones have been developed by the Shell Oil Company for cleaning these streams. When these cyclones are used with power recovery expanders manufactured by either Elliott Company or Ingersoll-Rand Company, performance guaranties are provided. Whether enough dust would be carried out of the HTAH with the reheat gas to require use of the high-efficiency cyclones is not known. Some dusting will occur but it may not be enough to require use of these separators.

Description of Heater System

The use of reheat gases that are at higher pressure than the air is the reverse of the situation for the directly-fired case. Because of pressure drop limitations, the gas at the lowest pressure requires a larger number of heaters (at any given time) and consequently a shorter cycle time. In the present case, therefore, the number of heaters on gas is less than the number on air.

Details of the operating conditions and component sizes are given in Table 6.6.4. The cored brick hole size was made only 13 mm (1/2 in) because the clean gases eliminate problems of fouling. The system consists of ten heaters, each having a bed of 4.88 m (16 ft) diameter and 10.36 m (34 ft) height.

The refractory materials chosen are listed in Table 6.6.5. A high density-high purity alumina is specified for the highest temperature regions. The most critical design limitation will be creep at the high temperature. The specified temperature of 1920 K is technically feasible but very difficult in a large system.

An estimate of component weights and costs is given in Table 6.6.6. As described earlier, this estimate does not include the ancillary equipment and therefore, cannot be compared with the estimated cost of the directly-fired heater.

Development Status of Indirectly-Fired Air Heaters

The greatest uncertainty in the design is caused by the high temperature levels: gas inlet at 2075 K (3275°F) and air outlet at 1920 K (2996°F). Maximum refractory temperatures will approach 2033 K (3200°F). This temperature level requires the selection of high purity alumina for those regions. However, the potential for creep exists. Data at these high temperatures is not available and extrapolation from lower temperature data is fraught with risk. High temperature creep data is needed for these materials, and, perhaps, a test of at least a portion of a heater structure to assure that creep would not cause serious problems.

TABLE 6.6.4
SIZE AND OPERATING CONDITIONS
FOR 1000 MW_e OPEN CYCLE INDIRECTLY-FIRED CASE

Gas and Air Conditions

Gas Inlet Temperature, K (F)	2075	(3275)
Gas Outlet Temperature, K (F)	786	(955)
Air Inlet Temperature, K (F)	533	(500)
Air Outlet Temperature, K (F)	1931	(3017)
Gas Inlet Pressure, kPa (psi)	1720	(250)
Air Inlet Pressure, kPa (psi)	600	(87)
Gas Flow Rate, kg/sec, (lbm/sec)	567	(1250)
Air Flow Rate, kg/sec, (lbm/sec)	576	(1270)
Gas Pressure Drop, kPa (psi)	32	(4.6)
Air Pressure Drop, kPa (psi)	14	(2.1)

Number of Heaters

On Air	6
On Gas	3
Press./Depress.	1
TOTAL	10

Cycle Times

Air, sec.	996
Gas, sec.	498
Press./Depress., sec.	166
Full, sec.	1660

Dimensions

Cored Brick Hole Diameter, mm (in)	12.7	(0.5)
Cored Brick Web Thickness, mm (in)	9.5	(0.375)
bed Height, m (ft)	10.4	(34)
Bed Diameter, m (ft)	4.9	(16)

Valve Flow Diameter

Gas Inlet, m (ft)	1.2	(3.8)
Gas Outlet, m (ft)	0.7	(2.3)
Air Inlet, m (ft)	0.7	(2.4)
Air Outlet, m (ft)	1.4	(4.5)

Ripple in Delivered
Air Temperatures, K (F)

80 (145)

Total Heat Loss, MW (Btu/nr)

9.1 (31 x 10⁶)

Air Loss from Valve Leakage
and Press./Depress. kg/sec (lb/sec)

8 (18)

TABLE 6.6.5
REFRACTORY MATERIALS FOR 1000 MW_e
OPEN CYCLE INDIRECTLY-FIRED CASE

Heater Beads:	Upper 40Δ	High density alumina
	Mid 25Δ	Vega
	Lower 35Δ	Bison

Heater Bed Liner:	Castable
-------------------	----------

Insulation:	<u>Heat Liner</u>	<u>Mid Layer</u>	<u>Outer Layer</u>
Gas Inlet	3300F castable	2800F castable	2600F castable Gas
Outlet		All 2000F castable	
Air Inlet		All 2000F castable	
Air Outlet	3300F castable	2800F castable	2600F castable

TABLE 6.6.6
ESTIMATED HEATER COST WITHOUT ANCILLIARIES*
OPEN CYCLE INDIRECTLY-FIRED CASE

<u>Heaters</u>	<u>Weight, m. tons</u>	<u>Cost of Mat. 10⁶\$</u>	<u>Labor Cost 10⁶\$</u>
Bed	3250	4.1	1.9
Insulation	400	0.3	0.4
Vessel	1300	0.9	3.1
<u>Ducts and Manifolds</u>			
Insulation	720	0.7	0.4
Steel	520	0.3	1.2
Flanges	280	0.6	
Expansion Joints		0.3	
<u>Valves</u>	210	5.1	
<u>Structural Steel</u>	1010	0.8	2.1
<u>Bed Support</u>	70	0.3	
<u>Instrumentation/Controls</u>		0.4	
SUBTOTALS	7760	13.8	9.1
TOTAL SYSTEM COST 10 ⁶ \$			22.9

*Does not include cost of coal handling and gasification, hot gas cleanup, pressurized combustor and pressure energy recovery equipment.

Direct costs are shown, i.e. contractors overhead and profit are not included. Installation is included in the labor component. All costs in mid 1979 dollars.

There are three additional areas when the design requires an extension of the state-of-the-art with blast furnace stoves.

- The temperature of the gas leaving the bottom of the bed is nearly 1033 K (1400°F), which will require a bed support structure of higher temperature capability than those for blast furnace stoves (about 811 K).
- The maximum pressure level is 1670 kPa (250 psi) versus about 670 kPa (100 psi) as noted previously. The principal effort of this difference would be a change in the valve construction.
- Pressurized combustors have not been used with blast furnace stoves.

Each of these three items represent extensions of the technology but they can all be accommodated with careful design and some development and verification testing.

6.7 OCD SYSTEMS POWER TRAIN LAYOUT REPRESENTATIONS AND FURNACE DUCT DESIGN

The OCD system designer must have in mind a general configuration for the disk power train layout prior to beginning the conceptual design phase for the major components of the disk generator power train. In this sense, the integration of these components into a workable power train is a less demanding task than for a linear MHD system. However, the non conventional flow patterns necessary with the gas-carrying components of the disk power train also challenge the system and component designers by requiring a much higher level of interdependence and matching of components to synthesize a workable system. The central problem in the OCD power system layout is the disk power train layout itself, that is, the layout of combustor, nozzle, disk, diffuser, and radiant furnace. Since the magnet is a vital component of any MHD system, and impacts the design of features relating to channel servicing, it must also be considered to be a vital element in the disk power train layout.

For the present study, it has been assumed that all components of the OCD power systems downstream of the radiant furnace(slag furnace), where the planar flow pattern of the outflow disk exhaust is reconfigured into the more conventional compact linear flow stream, are of typical design. Emphasis in the layout of the OCD power train has therefore been placed on the major disk-related components, as defined by NASA. The general layout of the overall OCD plant was not attempted, since the sizing of components downstream of the radiant furnace was not undertaken. From the study of high temperature air heater systems for disk generator systems, made as part of the overall disk evaluation effort, typical designs for HTAH systems were taken, although these are in general not "disk-specific" but apply to any MHD plant with high preheat levels. The coupling of the HTAH with the disk power train has been shown in the layouts which follow.

6.7.1 SCOPE OF LAYOUT REPRESENTATIONS

Three drawings were prepared which represent possible arrangements of the equipment which is unique to a disk MHD power plant. As noted previously, this equipment includes the combustor, nozzle, disk generator, annular diffuser, radiant furnace, and furnace transition ducting to the HTAH (for directly-fired plants) or downstream heat recovery equipment (for separately-fired or oxygen-augmented OCD plants). The drawings were based upon the optimized design Case 1A, in order to illustrate the integration of the 1920 K HTAH with the disk power train. The MHD power conditioning system is not a critical element with respect to disk power train layout, although its design is clearly affected by the disk versus linear generator choice. The layout of a typical power conditioning system of an OCD plant is shown in Figures 6-4-3 and 6-4-4 of this report.

Figure 6-7-1 (Burns and Roe Drawing SM0050) is a general arrangement drawing for Case 1A showing an overall plan view and elevation with sectional views of the combustor pit beneath the disk magnet, and typical HTAH vessels and ducting. A partial plan view of the combustor and high temperature air ducting to the combustor is also shown. Figure 6-7-2 (Burns and Roe Drawing SM0051) is an isometric drawing of the Case 1A combustor, disk

generator, diffuser, radiant furnace, furnace exhaust ducting, and HTAH system hot gas main and hot air ducting. The equipment arrangement is identical to that shown in Figure 6-7-1.

Figure 6-7-3 (Burns and Roe Drawing SM0052) is similar in content to Figure 6-7-1, but shows an alternate arrangement of the equipment.

6.7.2 DISCUSSION OF LAYOUT CONCEPT/DRAWINGS SM0050 AND SM0051

One of the primary objectives of preparing layout drawings is to permit the identification of component interfacing problems, and access problems, and to identify possible means for solution of such problems. With respect to the present study, problems highlighted by the preparation of layout drawings for the OCD power train are:

- Interconnection difficulties for hot gas flow between the radiant furnaces and the HTAH array;
- Interconnection difficulties for hot air flow between the HTAH and the combustor;
- Access to disk generator for maintenance and for removal/replacement;
- Access to combustor for maintenance and for removal/replacement.

As illustrated on Figures 6-7-1 and 6-7-2, the radiant furnace array has been arranged so that one of the three exhaust ducts is routed directly over the vertical extension of the disk power train axis of symmetry (generator axis). This particular arrangement can be expected to restrict potential methods for disk generator removal. One method which has been proposed is the use of an overhead travelling crane which can lift the upper and lower sections of the generator (one lift for each monolithic section) and transfer each to a location beneath the HTAH hot gas main, where they may be placed on a vehicle for transport to a remote location (storage/laydown area or on-site refurbishment shop). The vertical beams of the crane rail support structure must clear the radiant furnace inlet ducts and diffuser outer periphery. The furnace exhaust ducts and the HTAH hot gas mains are at a sufficient elevation

to provide room for movement of the generator sections beneath them. There is also sufficient width between adjacent hot gas main structural supports for access by vehicle to effect lateral transfer of the individual disk halves.

Combustor access is achieved by means of tunnels connecting to the combustor pit beneath the magnet and disk generator. The combustor can be removed with the magnet in place by lifting the combustor with the overhead crane to permit removal of the support cone; the combustor may be tilted with its axis placed horizontally on a flatbed vehicle on which it can be moved through the access tunnel (rails not shown) to an open area beneath the HTAH hot gas main. The combustor can then be lifted from the pit in this area if it is lifted still in the horizontal position.

Preheated combustion air is injected tangentially into the combustor through the first and second stage air inlet ducts. Two separate hot air lines are taken from the HTAH hot air main and can be run to the combustor through the common access pit. A single large hot air duct could also be provided which would split in the vicinity of the combustor for injection to the first and second stages.

6.7.3 ALTERNATE ARRANGEMENT (DRAWING SMO052)

In the arrangement shown in Figure 6-7-3, the radiant furnace orientation has been selected to eliminate the necessity for routing a furnace exhaust duct over the axis of the power train. This arrangement is preferred, as noted previously in Section 6.5.

This increases the number of available options by which the disk generator can be removed and replaced. Access to diffuser sections for removal/replacement is also enhanced. The alternate arrangement illustrates the same type of overhead crane as in the first-mentioned arrangement. However, the radiant furnace rearrangement permits the transference of the disk sections by crane to a laydown area directly away from the HTAH array, rather than towards the array. The access pit for combustor servicing is also located on the side of the generator away from the HTAH array. The hot air supply ducts running to

the combustor require individual tunnels which are widely separated in order to avoid fouling the slag removal equipment and foundations of the interposed radiant furnace vessel.

6.7.4 RADIANT FURNACE EXHAUST DUCTING

The radiant furnace exhaust ducting which carries the hot combustion gases away from the individual furnaces can be considered to be a disk-related component, since the disk generator configuration requires the provision of multiple furnaces rather than a single furnace at the diffuser outlet. For this reason, it is appropriate to add the costs of this ducting into the basis for the overall disk power train costing. The specific arrangement of the ducting cannot be selected until the general layout of the power train has been defined.

For OCD Cases 1A and 1B, (direct fired) the ducts carry radiant furnace exhaust gas to the high temperature air heater system. For OCD Cases 2 and 3, (separately-fired and O_2) the ducts carry gas to the heat recovery-seed recovery (HRSR) components downstream of the furnaces. For costing purposes, the conceptual design for the ducting associated with OCD Case 1A (keyed to Figures 6-7-1, 6-7-2, and 6-7-3) was used.

For the initial Case 1A layout (Figures 6-7-1 and 6-7-2) there are 2 ducts approximately 12 m in length, and one duct of 37 m length. The alternate arrangement shown in Figure 6-7-3 requires two 37 m ducts and a single 12 m duct. The total ducting length required is either 61 m or 86 m, depending upon the case chosen. Since the plant arrangements have not been defined in all Cases, the costs will be estimated on the basis of 75 m (250 feet) of ducting for the basic case. Adjustments in cost estimates for specific layouts can be applied if required, following detailed layout definition for each Case.

6.7.4.1 Duct Design Conditions

The internal diameters of the three radiant furnace exhaust ducts are determined on the basis of limiting average flow velocity to approximately 60 m/sec (200 ft/sec). The flowrate, pressure, and gas temperature for each OCD design case, and the selected duct internal diameter, are given in Table 6.7.1.

TABLE 6.7.1

RADIANT FURNACE EXHAUST DUCT DESIGN CONDITIONS

<u>CASE</u>	<u>GAS FLOW *</u> <u>RATE, kg/s</u>	<u>GAS</u> <u>TEMPERATURE, K</u>	<u>DUCT INTERNAL</u> <u>DIAMETER, METERS</u>
1A (Direct Fired, 1920 K)	736	2150	5.15
1B (Direct Fired, 1650 K)	810	1850	4.96
2 (Indirect Fired)	447	2150	4.01
3 (+O ₂)	543	2150	4.43

* Total gas flow at 1 atmosphere pressure, Molecular Weight = 30.

6.7.4.2 Ducting Mechanical and Thermal Design

The ducting is assumed to be fabricated of carbon steel with internal refractory insulation. The insulation reduces heat losses to ambient and protects the inner steel surface from the corrosive high-temperature gas. The insulation is applied as three separate layers of refractory brick, with the addition of a final plasma-jet-sprayed coating of magnesium oxide to enhance its resistance to the highly reducing seed-laden gas. Refractory materials selected for the three brick layers were extra-high alumina brick for the innermost layer, and 2 separate grades of insulating firebrick for the intermediate and outermost layers. Table 6.7.2 gives the refractory materials data for the design and cost evaluations.

The thicknesses of individual brick layers for each of the two temperature levels (2150 K for Cases 1A, 2, and 3; 1850K for Case 1B) are detailed in Table 6.7.3. The thicknesses are based upon ducting designs for previous open-cycle MHD plant studies. Selection of intermediate thicknesses of brick to "fine-tune" the design is impractical, as bricks having the standard dimensions are available at substantial savings over specially-made brick.

The carbon steel ductwork must be designed to withstand any pressure differentials existing across its boundary; the deadweight loads imposed by the brickwork and itself across the span between the furnace outlet and the downstream hot gas main may be supported either by the ductwork itself or by additional structural steel. If the steel thickness is sufficiently great, and/or if stiffening members are provided on the ducting, no structural steel will be required. For this study, the thickness of steel required has been determined on the basis of conservative estimates of stresses generated internally, and it has been assumed that the resulting thickness is sufficient to provide adequate stiffness for structural support. Table 6.7.4 lists the parameters upon which determination of steel thickness is based. The largest component of internal stress is that due to thermal expansion of the refractory lining. The required thickness, estimated on the basis of a common outside diameter is approximately 3.8×10^{-2} m (1.5 inches). This thickness is assumed common to all four Cases.

TABLE 6.7.2

REFRACTORY MATERIALS DATA FOR OCD RADIANT FURNACE
EXHAUST DUCT INSULATION

<u>Material</u>	<u>Density (lbm/ft³)</u>	<u>Cost (\$/lbm)</u>
Extra-High Alumina Brick (99AD)	190.5	0.70
Insulating Firebrick (A. P. Green G-33)	80.5	0.76
Insulating Firebrick (A. P. Green G-26)	50.5	0.30
MgO Spray Coating	175.0	(85 ft ² a' lied)*

* Includes all indirect charges

TABLE 6.7.3

THICKNESSES OF INSULATION LAYERS FOR
OCD RADIANT FURNACE EXHAUST DUCTS

	<u>CASES 1A, 2, 3</u>	<u>CASE 1B</u>
Design Gas Temperature, K	2150	1850
Layer 1 (99 AD)		
Thickness, m	3.4×10^{-1}	2.3×10^{-1}
Layer 2 (G-33)		
Thickness, m	7.62×10^{-2}	1.1×10^{-1}
Layer 3 (G-26)		
Thickness, m	7.62×10^{-2}	7.62×10^{-2}
Weighted Average Density (lbm/ft ³)	152	135
Weighted Average Unit Cost (\$/lbm)	\$104.06	\$92.18

TABLE 6.7.4

PARAMETERS FOR DETERMINING OCD
FURNACE DUCT STEEL WALL THICKNESS

Design Gas Pressure	200 kPa	(15 psig)
Design Refractory Expansion Pressure	1.22 MPa	(175 psi)
Pipe Outside Diameter	5.79 m	(19 feet)
Design Temperature	533 K	(500 F)
Maximum Allowable Stress	122 MPa	(17,500 psi)
Corrosion Allowance	3.175 mm	(0.125 inches)

7.0 COSTING OF MAJOR OPEN CYCLE COMPONENTS

One of the principal objectives of the present study was the estimation of costs for the disk-related components of open/cycle disk MHD/Steam Systems. The conceptual designs prepared for the major components of the four optimized OCD systems described in Section 6.0 of this report were utilized as the basis for the required cost estimates.

7.1 COST BASIS

7.1.1 COSTING GROUND RULES

The cost estimate format, guidelines and modified FPC Code of Accounts which were used previously in the MHD Engineering Test Facility (MHD-ETF) conceptual design studies have been applied to the costing efforts in the present study, as required by NASA in the original contract documents. The final costs for the major components are reported in Mid-1978 dollars. All costs for the disk components quoted in this section of the report were initially calculated in terms of Mid-1980 dollars, and de-escalated to Mid-1978 dollars by assuming a fixed cost increase rate of 10 percent per year, resulting in a de-escalation multiplier of 0.83 for the 2-year period of difference.

7.1.2 ELEMENTS OF COMPONENT COSTS

The elements of component costs used in reporting the final overall cost of each major component included:

- Materials and Fabrication Costs
- Transportation Costs
- Installation Costs (Direct Labor)
- Indirect Costs

The cost breakdown for the following components was made in terms of these elements: disk generator, diffuser, combustor, radiant furnace. For the disk magnet, the costs of design, engineering, fabrication, transportation, installation, and checkout for a reference magnet design were provided by the Francis Bitter National Magnet Laboratory. Together with the applicable scaling relationships found in Section 6.3, this reference cost was used to determine the equivalent total cost for each of the other OCD design cases.

Section 6.4 contains the cost breakdown for the reference disk power management system. Installed costs were estimated to be 125 percent of major materials and fabrication costs. The costs for individual cases were determined by use of these reference costs and the scaling factors given in Section 6.4.4 of this report. For the remainder of the components, the following reviews the key assumptions used in arriving at the individual cost element values.

Materials and Fabrication Costs

In this category costs were calculated from materials and operations lists prepared for each major component during the component conceptual design phase. Where costs were not individually calculated for each case, scaling relationships were derived for estimating costs and these are given under the appropriate component heading in Section 7.2.

Transportation Costs

Transportation cost estimates were prepared for each component based upon the weight of the component determined during the conceptual design phase. Each component has been assumed to have been transported over a distance of 1000 miles, at a cost of 100 dollars per ton (Mid-1980 valuation).

Direct Labor Cost Estimates

The direct labor cost for installation of each component is based upon component weight. 60 man-hours of labor is assumed to be required for each ton of equipment. A weighted average labor rate of \$15.65 per manhour is derived from the following data based upon current labor rates in St. Louis, Missouri:

Foreman	(15%) at \$18.38 per hour
Pipe Fitter	(40%) at \$16.71 per hour
Millwright	(35%) at \$13.68 per hour
Operating Engineer	(10%) at \$14.45 per hour

Indirect Cost Estimates

Estimated indirect costs are based upon the direct labor costs. The ratio of indirect costs to direct labor costs is taken to be 1.2764 to 1 on the basis of the following breakdown:

A. Direct Labor Cost	
B. Craft Support Labor	= 0.2 (A)
C. Insurance on Labor	= 0.18 (A + B)
D. Non Craft Support Labor	= 0.17 (A)
E. Small Tools and Consumables	= 0.075 (A + D)
F. Equipment Rentals	= 0.1 (A + D + E)
G. Overhead and Profit	= 0.15 (A + B + C + D + E + F)
H. Contingency	= 0.1 (A + B + C + D + E + F + G)
I. Total Indirect Cost	= B + C + D + E + F + G + H

7.1.3 COMPONENTS TO BE COSTED

The components to be costed for the study, given in order of their appearance in the Modified FPC Code of Accounts breakdown for MHD plants, are as follows:

<u>Account Number</u>	<u>Component</u>
312.3	Radiant Furnace
317.1	Coal Combustor
317.2	MHD Generator Subsystem
317.3	Magnet Subsystem
317.4	Inverters (Power Management System)

The cost reporting is done in terms of the four design cases (1A, 1B, 2, 3) defined for optimized designs of open cycle MHD/Steam systems, as described in Section 5.4. An example cost estimate form for a single case is shown in Figure 7-1-1.

<u>ACCOUNT</u> <u>NUMBER</u>	<u>ACCOUNT</u> <u>DESCRIPTION</u>	<u>UNIT</u>	<u>QUANTITY</u>	<u>MATERIAL COST*</u>	<u>INST.</u> <u>COST</u>	<u>INDIRECT</u> <u>COST</u>	<u>TOTAL</u> <u>COST</u>
312.3	<u>Radiant Section</u>						
312.3.1	Slag Furnace and Ducts	Each	3				
317.1	<u>Combustion Equipment</u>						
317.1.1	Coal Combustion	Each	1				
317.2	<u>MHD Generator Subsystem</u>						
317.2.1	Disk Generator and Nozzle	Each	1				
317.2.2	Diffuser	Each	1				
317.3	<u>Magnet Subsystem</u>	Each	1				
317.4	<u>Power Management Subsystem</u>	Each	1				

* Includes Transportation and Fabrication

Figure 7-1-1 Sample Disk Generator Study Cost Estimate

7.2 MAJOR COMPONENT COSTS

Major component costs reported in this section are given in terms of Mid-1978 dollars. The basis and scaling factors for each component are treated in the individual component subsections.

7.2.1 DISK GENERATOR AND NOZZLE

Materials and fabrication costs and weights were calculated separately for the disk generators of Cases 1A and 2 (1920 K preheat directly-fired disk, and 1920 K preheat separately-fired disk). The costs for Cases 1B and 3 (1650 K preheat directly-fired disk, and oxygen-augmented disk) were estimated from the following derived scaling relationships:

- (1) Weight of disk assembly $\approx 5000 R_0^2$ (kg) where
 R_0 = disk outer radius, meters
- (2) Materials and fabrications costs = \$11.90/kg.

The disk generator halves may be completely shop-fabricated, with final mating and alignment carried out at the plant site. All transportation, installation, and indirect costs were calculated from the individual weights of each disk generator assembly, using the methods given in Section 7.1.2.

7.2.2 COAL COMBUSTOR

Materials and fabrication costs and weights for each coal combustor were separately calculated. The combustor can be completely shop-assembled, with only mating to service lines and the disk generator inlet required upon installation. Costs of seed and coal feeding equipment are not included in the overall combustor costs, nor were the costs for the slag handling equipment.

Transportation costs, installation costs, and indirect costs were calculated from the component weights.

7.2.3 ANNULAR DIFFUSER

Certain annular diffuser subassemblies (such as the splitter vane cooling, systems and internal framework) may be shop fabricated. The bulk of the diffuser assembly must be carried out upon installation into the power train. Materials and fabrication costs include the basic fabrication necessary to complete the diffuser assembly, such as cooling header bending and welding, wall sector welding, and I-beam welding. The installation costs reflect charges for rigging, handling, final hookup, etc., as for all other major components. Again, transportation, installation, and indirect costs are based upon the individual assembly weights, which were separately calculated for each case, along with the materials and fabrication costs.

7.2.4 RADIANT FURNACES AND INLET/EXHAUST DUCTS

All major fabrication operations for the radiant furnaces and their inlet and exhaust ducts must be carried out on-site. The quoted materials and fabrication costs include the basic fabrication steps such as pressure wall welding, tube/header welding, insulating block and refractory installation, and installation of lagging. The installation (direct labor charge) covers the rigging, handling, etc. accompanying the erection of the furnaces and their inlet and exhaust ducts. The slag collection system for each furnace has not been costed.

Transportation, labor, and indirect charges are based on the individually-calculated weights of each set of furnaces and ducts.

7.2.5 DISK MAGNET

The total installed costs for the disk magnet of OCD Case 1A (the 7.65 meter magnet) are given in Table 7.2.1. These costs were prepared by the National Magnet Laboratory. Since each magnet for the remaining OCD design cases has a 7 T design magnetic induction, and a 1-meter thickness, the cost scaling factor

$$\frac{C_1}{C_2} = \left(\frac{R_1}{R_2} \right)^{1.2}$$

TABLE 7.2.1. COST ESTIMATE - DISK MAGNET CASE 1A
(FID-1980 BASIS)

<u>ITEM</u>	<u>WEIGHT</u> (10 ³ kg)	<u>UNIT COST</u>	<u>TOTAL</u> <u>COST</u> (\$1000's)
Nb ₃ Sn-Cu Conductor Wire (2.24 X 10 ⁹ Am)	455	\$64/kg	29,120
Conductor Sheath	95	\$10/kg (includes installation)	950
Insulation	5	\$20/kg	100
Structure (Stainless Steel)	640	\$18/kg	11,520
Radiation Shield	25	\$14/kg	350
Vacuum Jacket	130	\$14/kg	1,820
Cold Mass Support	2	\$25/kg	50
Subtotal	<u>1,352</u>		<u>43,910</u>
Packing and Shipping for 1352 X 10 ³ kg		\$1.7/kg	2,300
On-Site Assembly		\$2.0/kg	2,700
Cryogenic Subsystem (Installed)			2,500
Power Supply/Dump (Installed)			400
Instrumentation (Installed)			250
Checkout and Testing			500
Project Management			2,800
Analysis and Design			<u>4,000</u>
TOTAL COST			59,360

given in Section 6.3.4.5 can be used to determine their installed costs from the cost quoted for the 7.65 meter magnet. No cost breakdown is given in the final summaries for the disk magnets of Cases 1B, 2, or 3.

7.2.6 DISK POWER MANAGEMENT SYSTEM

The materials and fabrication costs for two types of power management equipment for the reference disk of Section 6.4 are given in Table 6.4.3. Using these and the scaling factors for the major items of the power management system given in Section 6.4.4, it was possible to estimate costs (F.O.B. for site delivery) for each of the four OCD design cases treated herein. The system specific costs (\$/kW) can be expected to change with the gross power and the number of inverters required for each disk segment. The reference system and Case 1A system have 8 inverters per segment, 32 in all, while the remaining OCD Cases have fewer inverters required (24 total per system for Cases 1B, 2, and 3).

The installed costs for the power management system, as previously noted, are based on a cost increase of 25% over F.O.B. costs for each system. The specific costs calculated for each case are as follows (Mid-1980 basis, F.O.B.):

- Reference Case: \$41.34/kW (gross MHD power)
- Case 1A: \$40.49/kW
- Case 1B: \$40.29/kW
- Case 2: \$41.16/kW
- Case 3: \$41.17/kW

7.2.7 DISK COMPONENT COST SUMMARIES

Table 7.2.2 through 7.2.5 contain cost summaries for the major equipment of the four nominal 1000 MWe open cycle disk MHD Systems. The costs are quoted in Mid-1978 values. The "Major Component Costs" column includes materials, fabrication, and transportation costs. No BOP were calculated for these components.

7.3 COMPARISON OF DISK AND LINEAR MHD COMPONENT COSTS

For the specific components costed in Section 7.2, a comparison was made with equivalent linear MHD components in order to determine the relationships between costs. The cost results obtained in the latest linear MHD systems studies (the AVCO and General Electric PSPEC studies) were selected as the reference linear values. The costs for components in both studies were also given in Mid-1978 dollars, thus facilitating the comparison process.

To provide a reasonably accurate comparison, it is required that the disk system characteristics and critical design parameters for the disk major components be similar to those for the comparison plants and components. Since the PSPEC studies focussed upon MHD/steam plants with early commercialization potential, they were based upon separately-fired MHD units and those with no HTAH systems but with oxygen augmentation of the combustor oxidant; the equivalent comparison cases among those investigated as part of this study are OCD Cases 2 and 3, respectively. Cases 1A and 1B provide information on more advanced disk MHD systems, but there are no analogous parameteric cases in the PSPEC studies with which to compare these directly-fired systems.

7.3.1 EXPECTED RELATIONSHIPS

One reason for pursuing a systems study for disk MHD/steam power systems is the expected capital cost advantage to be gained by using the disk design. It was anticipated early in the development of the disk generator that simple configurations for the generator power conditioning equipment and the magnet could be used, thus tending to minimize the costs associated with these components. Since the magnet and conversion/consolidation costs are

TABLE 7.2.2 DISK GENERATOR STUDY COST ESTIMATE
CASE 1A - 1920K PREHEAT DIRECTLY-FIRED SYSTEM
NET ELECTRICAL POWER OUTPUT: 963 MWe
COST IN \$1000's, MID-1978 BASIS

<u>ACCOUNT NUMBER</u>	<u>ACCOUNT DESCRIPTION</u>	<u>UNIT</u>	<u>QUANTITY</u>	<u>MATERIAL COST</u>	<u>INST. COST</u>	<u>INDIRECT COST</u>	<u>TOTAL COST</u>
312.3	<u>Radiant Section</u>						
312.3.1	Slag Furnace and Ducts	Each	3	18,958	2,693	3,438	25,089
317.1	<u>Combustion Equipment</u>						
317.1.1	Coal Combustor	Each	1	838	35	44	917
317.2	<u>MHD Generator Subsystem</u>						
317.2.1	Disk Generator and Nozzle	Each	1	1,626	117	149	1,892
317.2.2	Diffuser	Each	1	2,402	227	290	2,919
317.3	<u>Magnet Subsystem</u>	Each	1	-	-	-	49,302
317.4	<u>Power Management Subsystem</u>	Each	1	20,036	-	-	25,045

TABLE 7.2.3 DISK GENERATOR STUDY COST ESTIMATE
CASE 1B - 1650K PREHEAT DIRECTLY-FIRED SYSTEM
NET ELECTRICAL POWER OUTPUT: 1012 MWe
COST IN \$1000's, MID-1978 BASIS

<u>ACCOUNT NUMBER</u>	<u>ACCOUNT DESCRIPTION</u>	<u>UNIT</u>	<u>QUANTITY</u>	<u>MATERIAL COST</u>	<u>INST. COST</u>	<u>INDIRECT COST</u>	<u>TOTAL COST</u>
312.3	<u>Radiant Section</u>						
312.3.1	Slag Furnace and Ducts	Each	3	24,355	2,848	3,634	30,837
317.1	<u>Combustion Equipment</u>						
317.1.1	Coal Combustor	Each	1	808	33	42	883
317.2	<u>MHD Generator Subsystem</u>						
317.2.1	Disk Generator and Nozzle	Each	1	1,606	115	147	1,869
317.2.2	Diffuser	Each	1	2,271	217	277	2,765
317.3	<u>Magnet Subsystem</u>	Each	1	-	-	-	50,198
317.4	<u>Power Management Subsystem</u>	Each	1	17,466	-	-	21,833

TABLE 7.2.4 DISK GENERATOR STUDY COST ESTIMATE
CASE 2 - 1920K PREHEAT SEPARATELY-FIRED SYSTEM
NET ELECTRICAL POWER OUTPUT: 984 MWe
COST IN \$1000's, MID-1978 BASIS

<u>ACCOUNT NUMBER</u>	<u>ACCOUNT DESCRIPTION</u>	<u>UNIT</u>	<u>QUANTITY</u>	<u>MATERIAL COST</u>	<u>INST. COST</u>	<u>INDIRECT COST</u>	<u>TOTAL COST</u>
312.3	<u>Radiant Section</u>						
312.3.1	Slag Furnace and Ducts	Each	3	15,852	1,931	2,465	20,248
317.1	<u>Combustion Equipment</u>						
317.1.1	Coal Combustor	Each	1	738	30	38	806
317.2	<u>MHD Generator Subsystem</u>						
317.2.1	Disk Generator and Nozzle	Each	1	1,479	106	135	1,720
317.2.2	Diffuser	Each	1	2,366	226	289	2,881
317.3	<u>Magnet Subsystem</u>	Each	1	-	-	-	47,112
317.4	<u>Power Management Subsystem</u>	Each	1	13,931	-	-	17,414

TABLE 7.2.5 DISK GENERATOR STUDY COST ESTIMATE
CASE 3 - OXYGEN AUGMENTED DISK SYSTEM
NET ELECTRICAL POWER OUTPUT: 978 MWe
COST IN \$1000's, MID-1978 BASIS

<u>ACCOUNT NUMBER</u>	<u>ACCOUNT DESCRIPTION</u>	<u>UNIT</u>	<u>QUANTITY</u>	<u>MATERIAL COST</u>	<u>INST. COST</u>	<u>INDIRECT COST</u>	<u>TOTAL COST</u>
312.3	<u>Radiant Section</u>						
312.3.1	Slag Furnace and Ducts	Each	3	17,241	2,292	2,927	22,460
317.1	<u>Combustion Equipment</u>						
317.1.1	Cost Combustor	Each	1	546	24	31	601
317.2	<u>MHD Generator Subsystem</u>						
317.2.1	Disk Generator and Nozzle	Each	1	1,716	123	157	1,996
317.2.2	Diffuser	Each	1	2,080	198	251	2,529
317.3	<u>Magnet Subsystem</u>	Each	1	-	-	-	52,219
317.4	<u>Power Management Subsystem</u>	Each	1	15,399	-	-	19,299

very large portions of the total power train costs, the overall system cost could be expected to be favorably affected by adoption of the disk generator geometry. The Hall connected electrical system of the disk was expected to provide benefits in the costs, resulting from a total voiding of the requirement for consolidation circuitry if a 2-terminal generator were to be realized.

The costs of combustors for disk systems would be expected to be not significantly different from those for linear systems with similar combustion conditions, power, and preheat levels.

For the generator itself, the high costs of fabrication for the nominal linear MHD channel are related to its design features, but savings in costs could be foreseen with a disk if a significant number of electrodes were not required.

Previous evaluations of the disk configuration had not specifically addressed the design of the diffuser nor of the radiant furnace. It was realized that these components would be very much different from their linear counterparts if a radial outflow-type disk were utilized. These difference tended to imply larger costs for disk system diffusers and radiant furnaces when compared to linear system components, because of the unusual flowpaths required for combustion gases.

As previously stated, the conceptual designs for all the aforementioned major components of disk generator systems were selected with the intent of extending the conceptual simplicity of the disk MHD generator configuration into the component design and power train integration areas. As such, the costs for these items are likely to reflect this intent in that they represent a lower level in the range of costs expected for such components. They are therefore indicative of the potential costs of fully-developed disk system components.

7.3.2 COMPARISON CASES

The AVCO and General Electric PSPEC cases used as comparison points for disk generator system major component costs were selected on the basis of the

following considerations:

- general systems similarity;
- similar thermal and net electrical power levels;
- similar oxidant enrichment and oxidant preheat levels;
- identical fuel type;
- similar combustor operating parameters;
- similar magnet system parameters.

The cases selected are described, in terms of salient design characteristics, in Tables 7.3.1 and 7.3.2. The detailed features of the component designs have not been compared; however, the benefits of delving into such detail comparisons are judged not significant with respect to the quality of the overall conclusion on relative costs for these conceptual system designs.

7.3.3 COMPARATIVE COMPONENT CASE

The elements of the three costing studies (GE and AVCO PSPEC and this study) which provide the best comparison basis are the Materials Costs (including BOP and transportation costs). These are the values utilized in the comparison chart, Table 7.3.3.

The material costs for the GE PSPEC cases (2.11 and 3.2) were taken from Tables 4.2-2 and 4.2-3 of Reference [1] respectively. These values are reported in Mid-1978 dollars. For the AVCO PSPEC cases (Case II, Parametric Point 1 and Case III, Parametric Point 1) Tables 5-2 and 5-3 of Reference [2] were used for Materials Costs. The disk Case 2 and 3 values are taken from the Materials Costs columns of Tables 7.2.4 and 7.2.5, respectively.

Some of the subaccounts for the disk and the linear (PSPEC) components could not be compared directly. For the case of the GE PSPEC Combustor Costs, the values reported in Tables 4.2-2 and 4.2-3 of Reference [1] were corrected to exclude the costs of coal drying, coal rejection, and slag collection equipment by multiplying the table values by a factor of 0.145. This is the approximate relationship shown for the combustor costs per se in the AVCO PSPEC report to the costs for the entire MHD Combustion Equipment category

TABLE 7.3.1. AVCO PSPEC COMPARISON CASES FOR
DISK/LINEAR COMPONENT COSTS

FOR DISK CASE 2: AVCO CASE II, PARAMETRIC POINT 1

Nominal Net Power:	900MWe
Fuel:	Montana Rosebud, 5% Moisture
MHD Combustor:	Single-Stage, 80% Slag Rejection
Oxidizer:	Air, 3000 F Preheat in Separate Gasifier-Fired Regenerative HTAH
MHD Generator:	Diagonal, Subsonic, Diffuser CPR = 0.6. Channel Length: 18.9 m
Magnet:	Graded Field, 6-5 T
MHD Component Cooling:	By Condensate and Feedwater

FOR DISK CASE 3: AVCO CASE III, PARAMETERIC POINT 1

Nominal Net Power:	900 MWe
Fuel:	Montana Rosebud, 5%
Moisture MHD Combustor:	Single-Stage, 80% Slag Rejection
Oxidizer:	Air with 34% O ₂ by Volume, 1100°F Preheat ² in Metallic Heater
MHD Generator:	Diagonal, Subsonic, Diffuser CPR = 0.5. Channel Length: 19.7 m
Magnet:	Graded Field, 6-5 T
MHD Component Cooling:	By Condensate and Feedwater

TABLE 7.3.2. GE PSPEC COMPARISON FOR
DISK/LINEAR COMPONENT COSTS

FOR DISK CASE 2: GE CASE 2.11

Nominal Power:	900 MWe
Fuel:	Montana Rosebud
MHD Combustor:	Single-Stage, 80% Slag Rejection
Oxidizer:	Air, 3000°F Preheat in Separate Pressurized Cyclone Combustor- Fired Regenerative HTAH
MHD Generator:	Faraday, Subsonic, Diffuser CPR = 0.6. Channel Length: 20 m
Magnet:	Graded Field, 6-5 T
MHD Component Cooling:	By Condensate and Feedwater

FOR DISK CASE 3: GE CASE 3.2

Nominal Power:	
Fuel:	Montana Rosebud
MHD Combustor:	Two-Stage Cyclone, 85% Slag Rejection
Oxidizer:	Air + 40% Oxygen, 1300°F Preheat in Metallic Heater
MHD Generator:	Faraday, Subsonic, Diffuser = CPR 0.6 Channel Length = 25 m
Magnet:	Graded Field 6-5 T
MHD Component Cooling:	By Condensate and Feedwater

TABLE 7.3.3. COMPARISON OF COSTS FOR MAJOR COMPONENTS OF
OPEN CYCLE DISK AND LINEAR MHD/STEAM POWER SYSTEMS
(BASIS: MAJOR EQUIPMENT MATERIAL COSTS IN \$1000's, MID-1978)

ITEM	SEPARATELY-FIRED SYSTEMS			OXYGEN-AUGMENTED SYSTEMS		
	OCD CASE 2	AVCO PSPEC CASE III PP-1	GE PSPEC CASE 2.11	OCD CASE 3	AVCO PSPEC CASE III PP-1	GE PSPEC CASE 3.2
COMBUSTOR	738	832		546	832	
MHD GENERATOR	3,845	5,280	18,000	3,796	5,300	23,000
Channel & Nozzle	1,479	4,306	13,300	1,716	4,347	17,300
Diffuser	2,366	974	4,700	2,080	953	5,700
MAGNET SYSTEM	39,175	44,480	91,500	43,422	44,030	107,000
POWER MANAGEMENT SYSTEM	13,931	35,000	31,700	15,399	33,700	38,600
RADIANT FURNACE	15,852	-	11,300	17,241	-	14,500

reported under account number 317.1. The disk generator combustor costing excluded all costs except those for the combustor itself.

For consistency in comparison of radiant furnace costs, only the GE PSPEC results could be used, since these represent the costs of the part of the HRSR systems analogous to the disk radiant slag furnaces reported upon and costed herein. The AVCO radiant furnace costs could not be extracted from the cost values reported for subaccount 312.4 (Steam Generator) in Reference [2], Tables 5-2 and 5-3.

All other accounts could be directly compared on a Materials Cost basis, with the addition of a transportation cost adder to the Disk Power Management Subsystem Materials subaccount. This cost adder was calculated on the basis of equipment weights for the reference 527.3 MW power management system design described in Section 6.4, using the transportation cost estimating procedures in Section 7.1.2. The total weight of all equipment is 2500 tons; the resultant transportation costs are estimated at \$250,000 (Mid-1980 basis) or \$207,500 de-escalated to Mid-1978.

Comparison of the materials costs (i.e. materials plus fabrication plus BOP equipment, including transportation to the site) for each component are given in the following.

MHD Generator

This category includes the nozzle, duct, and diffuser. The overall cost of the disk generator in both cases is less than that quoted for either PSPEC linear system, as shown in Table 7.3.3. The simple design of the disk is evident when its costs are compared with those for the AVCO diagonal channels, or for the more complicated Faraday channel used for the GE PSPEC study. The large difference in cost between the GE and AVCO linear channels is not explainable; however, it is considered likely that the cost for a "representative" linear generator will fall somewhere within the range between these two values, thus giving the disk generator an overall cost advantage with respect to equivalent linear generators.

Coal Combustor

There is no significant difference in costs for combustors of either linear system, or the disk system, in the separately-fired cases. For the oxygen-augmented cases, the disk generator combustor is operated at a stagnation pressure of (9.3 atm), while the AVCO single-stage combustor is operated at a lower pressure (8.3 atm). The decrease in cost of the disk generator combustor with respect to the AVCO combustor is understandable in this case. The breakdown of costs on the combustor in the GE PSPEC was not sufficient to allow comparison.

Magnet

The linear magnet costs presented for both AVCO and GE cases are based upon the AVCO ETF circular saddle coil magnet design concept. The difference in costing for magnets of the same field, design, and almost identical length and warm bore diameter is interesting. The National Magnet Laboratory, which prepared the disk generator magnet design and cost summary (see Sections 6.3 and 7.2), has estimated the cost of a linear MHD generator magnet for a 1000 MWe nominal MHD/steam plant to be approximately \$150 millions, installed, on a Mid-1980 basis. Correcting to a materials plus transportation basis and de-escalating to Mid-1978 dollars, the resultant cost would be approximately \$103.5 millions, in good agreement with the GE magnet cost estimates. Overall, the disk magnet designs proposed in this study show a cost advantage over the magnets for linear MHD generators of equivalent power.

Power Management Subsystem

Compared to the estimated costs of both the AVCO and GE power management equipment, the costs for the disk generator power management equipment are less than half those for the linear MHD/steam systems of the same configuration and nominal power level.

Radiant Furnace

The cost comparison between the GE linear systems radiant furnace materials costs, and materials costs for the comparison disk systems, show a definite advantage for the linear generator systems. It is anticipated that this

difference would be more exaggerated had the detailed design of the gas sealing and expansion joints between diffuser and radiant furnace been included in the disk furnace costs.

7.3.4 SUMMARY

The cost comparisons made in the preceding subsection tend to validate the expected cost differences between linear and MHD major components. The significant areas of difference, in favor of the disk, were the generator itself ($1/3$ the cost of an equivalent linear machine); the magnet (approximately $1/2$ the cost for a linear magnet of representative design); and the power management system (again approximately $1/2$ the cost for the Faraday or diagonal-connected linear generator power management equipment). The linear system shows an advantage in the radiant furnace costs, due to the more compact arrangement of the HRSR system which is possible. There is no significant difference in combustor costs, at least for the radial outflow disk configuration which can utilize a combustor which has design features closely approximating those for a linear generator system combustor.

8.0 CLOSED CYCLE DISK SYSTEMS STUDIES

This section of the report summarizes the results of the CCD systems studies carried out during the Disk MHD Generator Study. The CCD study was not as extensive as that for the OCD systems. Inherent difficulties in determining an acceptable design procedure and in the integration of disk and systems models limited the scope to the direct-fired case. Performance evaluations for base load CCD systems were carried out. The design implications of off-design-point performance were not investigated for the CCD generator as was done for the OCD generator. The systems model used in the CCD performance evaluation was less sophisticated than that used for the OCD systems evaluation in that steam extraction for feedwater heating was not included and a fired arrangement of system components was assumed. The overall systems performance calculations covered a range of power levels, and assessed the sensitivity of the CCD system to critical parameter variations.

8.1 CLOSED CYCLE DISK GENERATOR MODELING

Performance optimization in the closed cycle nonequilibrium disk generator is a more complex process than for open cycle disk generators because of the additional factors which control the interaction, and because of the imposed systems constraint (i.e. match point operation), which requires an integrated disk/systems code. In the OCD, for a given magnetic field density, seed fraction, and fixed generator inlet stagnation conditions the effective electrical properties σ_e and β_e are uniquely determined by the choice of inlet Mach number and swirl. The electrical loading is determined by the additional specification of a design constraint, which sets the current. In the CCD case, the electron population is not in thermal equilibrium with the surrounding gas, and electron temperature becomes an additional variable. Two additional parameters are also introduced in the CCD case; these are plasma turbulence level and impurity level in the disk working fluid. The effective electrical properties σ_e and β_e depend strongly upon the electron temperature and electron density for the characteristically high level of interaction. Electron mobility is, in most cases, dominated by coulombic collisions. The determination of channel lofting is extremely sensitive to

changes in the electron density, and seed fraction becomes an important parameter since it can therefore be used to control the level of interaction. For a given Mach number and swirl the short circuit current density is not constant in the CCD, and depends upon the electron density and the electron temperature. Therefore, the loading is not linearly proportional to the radial current density as is the case in OCD (c.f. discussion -Appendix B).

8.1.1 LOCAL PERFORMANCE CHARACTERISTICS

Local performance characteristics for a typical CCD generator are illustrated in Figures 8-1-1 through 8-1-3 for the specific conditions

$$T_c = 1920 \text{ K}$$

$$P_o = 913 \text{ kPa (9 atmospheres)}$$

$$B = 4.5 \text{ T (axial field only)}$$

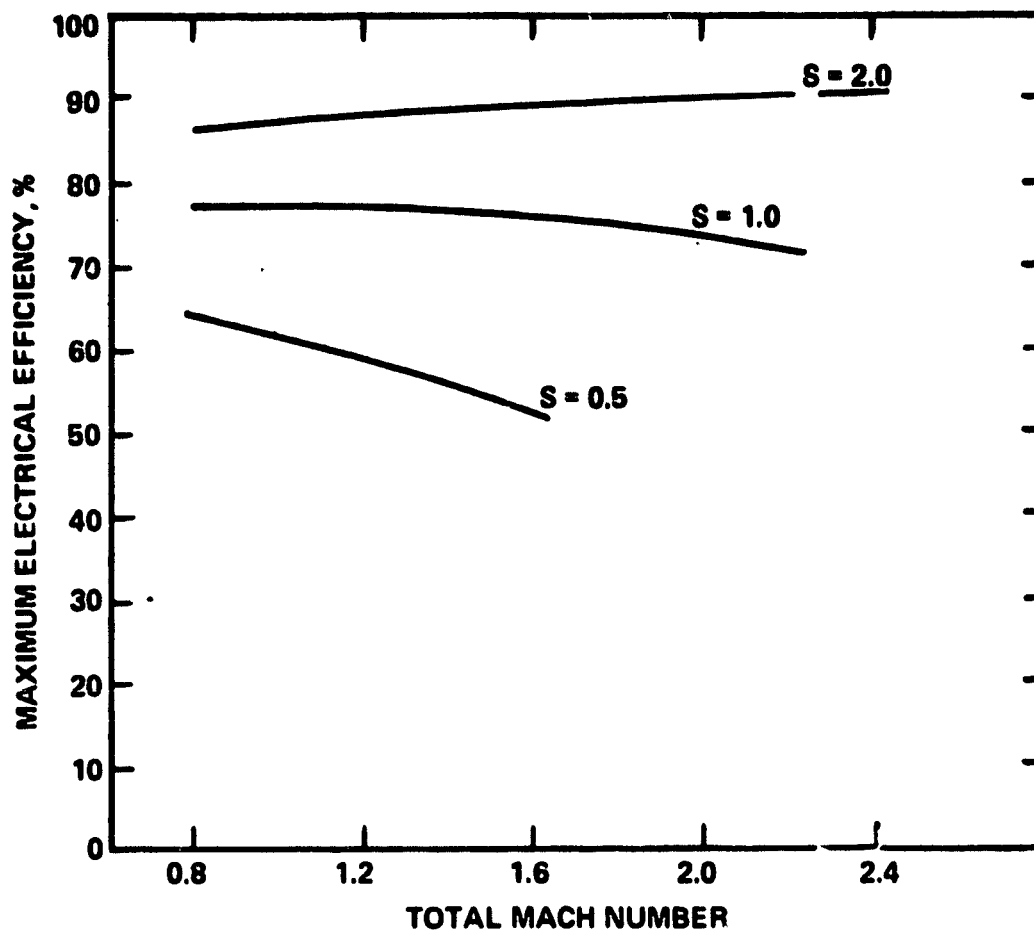
$$x = 0.3 \text{ percent}$$

$$\hat{S} = 0.2$$

(\hat{S} = turbulence level parameter).

Figure 8-1-1 depicts the relationship of the maximum electrical efficiency to the parameters, Mach number and inlet swirl. In general, it is seen that the efficiency of the CCD increases with an increase in swirl. For moderate swirl values, as exemplified by the $S = 0.5$ curve, the efficiency is seen to fall rapidly with increasing Mach number. These results are a consequence of the relatively high level of interaction attained in the CCD. As the inlet Mach number increases for a given swirl, the electron density (and therefore the interaction) increases, as shown in Figure 8-1-2. With high interaction (again for the $S = 0.5$ case) the Hall parameter is coulomb dominated and decreases as M and Ne increase (see Figure 8-1-3). For a lower interaction level (the $S = 2.0$ case) the Hall parameter is partially controlled by the electron density and partially by the pressure; each effect tends to offset the other as pressure falls and Mach number increases.

The enthalpy extraction length (Le) is a measure of the generator size required at the local operating condition for a given extraction ($\Delta h_o/h_o$).



705352-4A

INLET STAGNATION CONDITIONS: 1920K, 9 ATM
SEED FRACTION: 0.3% CESIUM IN ARGON
TURBULENCE LEVEL: 0.2
MAGNETIC INDUCTION: 4.5T
 $K = K_{OPT}$

Figure 8-1-1. Maximum Electrical Efficiency Versus Mach Number for CCD Generator

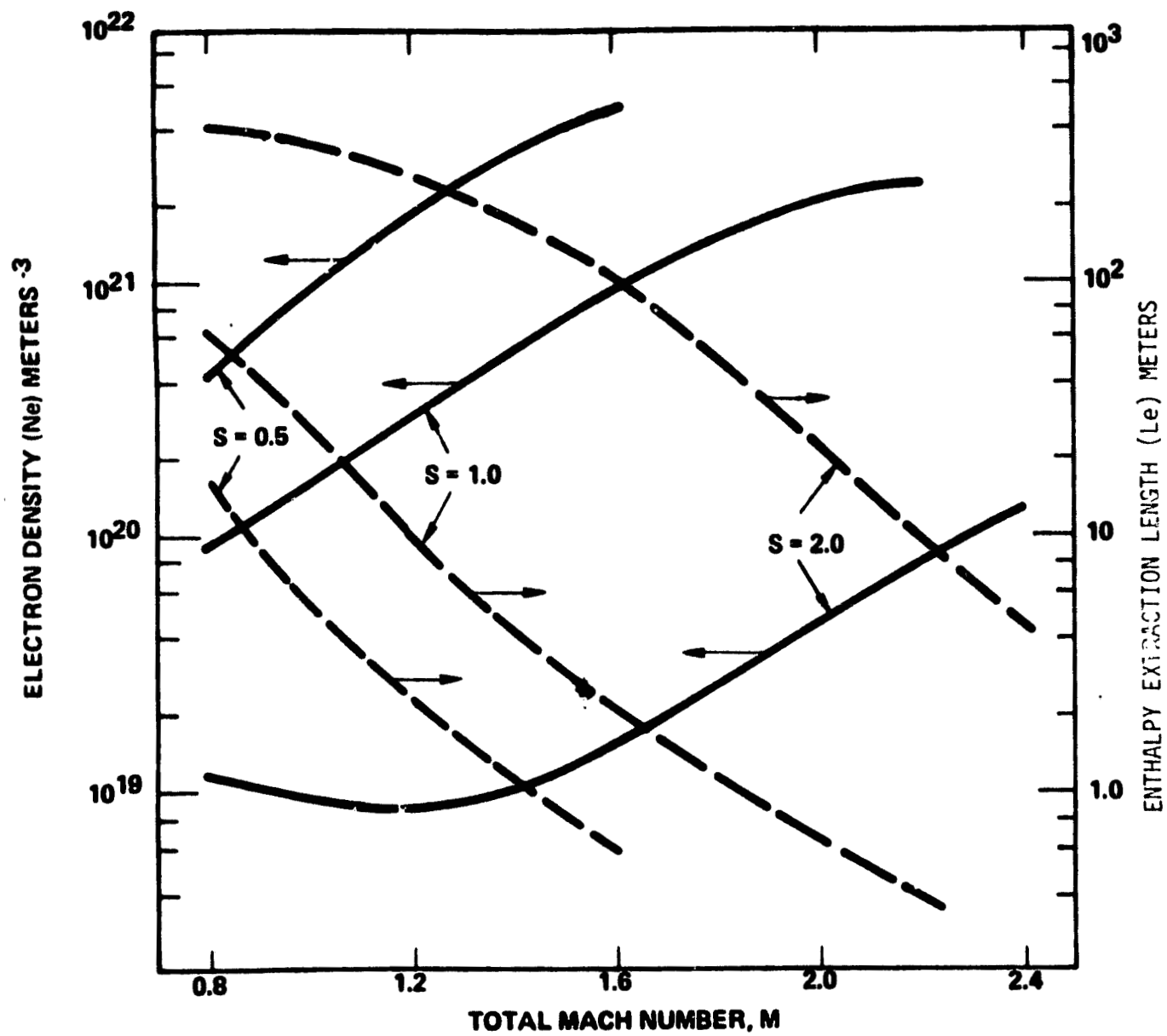


Figure 8-1-2. Electron Density and Enthalpy Extraction Length Versus Mach Number for Conditions of Figure 8-1-1

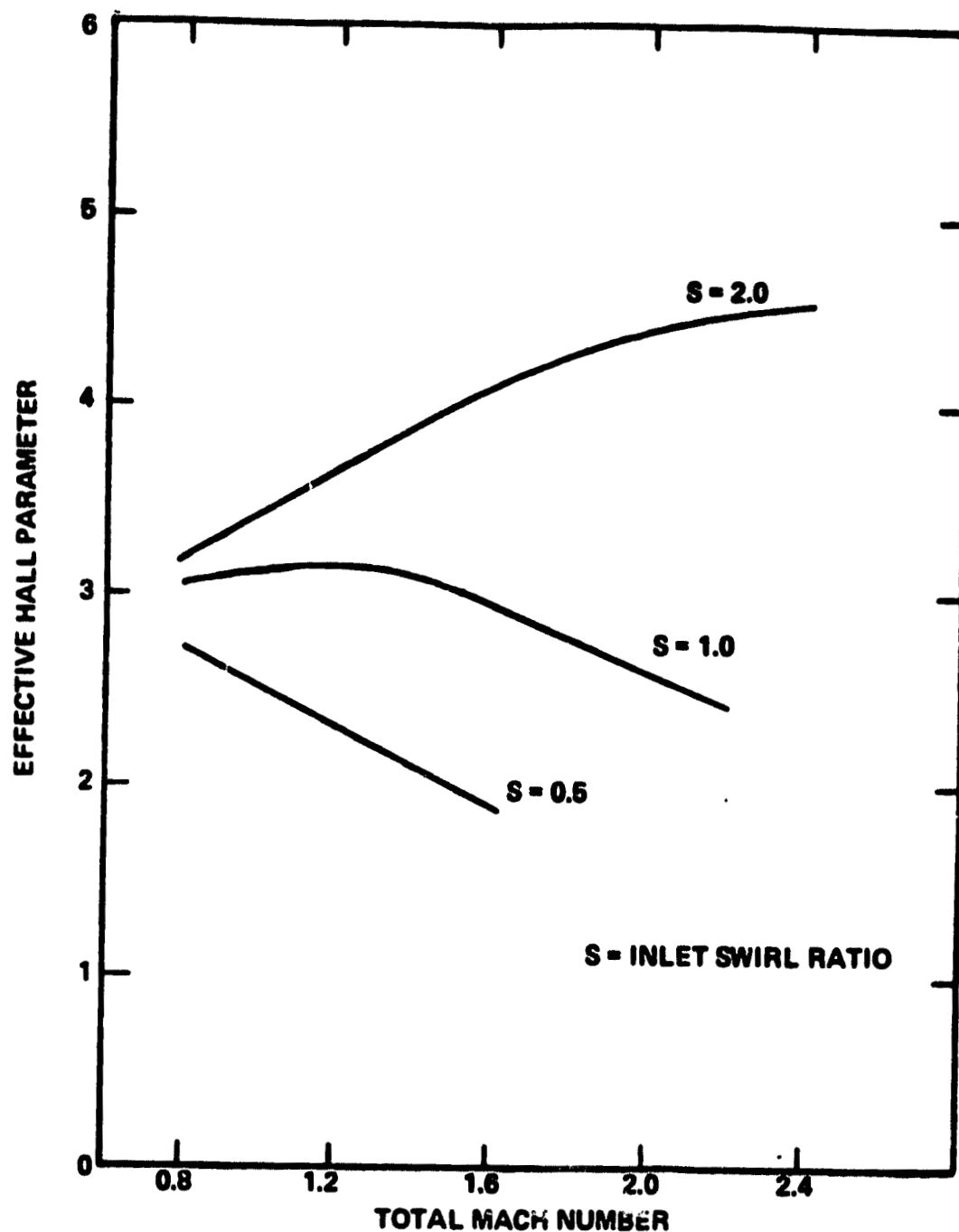


Figure 8-1-3. Effective Hall Parameter Versus Mach Number for CCD Generator of Figure 8-1-1

The enthalpy extraction length characteristics of the CCD are also shown in Figure 8-1-2. Two aspects of the information presented thereon are noteworthy. Firstly, there exists no minimum value of Le (or put another way, optimum Mach number) as is the case for the OCD generators, where conductivity decreases directly with decreasing temperature. Secondly, Le increases rapidly as the swirl increases at a constant Mach number, since electron density decreases with swirl increasing. The opposite type of behavior is characteristic of the OCD, where Le decreases slightly with increasing swirl for operation at the maximum local electrical efficiency.

These observations suggest that the advantages of high swirl will be offset to some degree in the CCD by the increase in extraction length unless the inlet Mach number is kept relatively high (above about 2.0). For this example the maximum Hall field developed was less than 5 kV/m.

8.1.2 CCD GENERATOR MODEL FORMULATION

The "two-temperature" generator model for the closed cycle disk which was utilized in this study is described in this subsection and in Appendix B.

As described previously in Section 4.1, the CCD working fluid assumed was cesium-seeded argon. Channel flow is quasi-one-dimensional and friction losses are accounted for in a manner similar to that used in the OCD generator model. Finite-rate electron kinetics and energetics have been incorporated for analysis of the ionization relaxation processes which occur at the generator inlet, and for cases where the seed becomes fully ionized[1]. The effective conductivity and Hall parameter are determined from reduction formulae developed by Louis[2]. These formulae are applicable for near-isotropic turbulence and express the effective properties in terms of their ideal values and a plasma turbulence parameter. The effects of molecular impurities or other contaminants in the channel working fluid are modeled by the inclusion of separate collisional loss factors for each species of interest. Incorporation of these factors permits a more accurate evaluation of the recombination rate constants and the energy averaged collision frequency. Cross-section data given by Spencer and Phelps are used [3].

The generalized model formulation consists of six conservation equations (four for heavy gas particles, and two for the electrons). In addition, a design constraint equation, the equation of state, and Ohm's Law are required to solve for the nine dependent variables which characterize the design. These variables are as follows:

- n - neutral gas number density
- N_e - electron number density
- u_r - radial gas velocity component
- u - total gas velocity
- E_r - radial electric field (Hall field)
- T_{gas} - gas temperature
- T_e - electron temperature
- P - gas pressure
- z - channel height.

For the majority of cases examined in this study the relaxation length was determined to be negligibly small relative to the generator interaction length. Consequently, the kinetics were suppressed and the electron density was calculated from the Saha equation.

The system of equations and method of solution is outlined in Appendix B.

For the CCD cases investigated in this study, it was assumed that effective Hall parameters would be restricted to values less than 5. Shock tunnel experiments with small-scale disk devices have yielded somewhat lower limiting values[4]; for conditions with moderate degrees of ionization but the relationships governing scaling of these results to the larger CCD generators considered herein are not known. For cases where the seed is near full ionization effective Hall coefficients as high as 8 were measured at the Tokyo Institute of Technology[5]. For the generator itself, an adiabatic wall has been assumed. This assumption parallels that used in a previous GE study[6] and can be realistically proposed for closed cycle MHD devices since the recovery temperatures are less than 2000 K, which is within the realm of

current state-of-the art for wall materials technology. The pressure loss for the diffuser is calculated using a pressure recovery coefficient $C_p = 0.8$. Since in the CCD the interaction length is relatively short, the boundary layer will be thin with respect to both the core flow and the thicknesses expected in the longer linear CC generators. It is therefore assumed that such high performance diffusers are possible in the CCD cases, guide vanes with internal cooling would be required to insure that the boundary layer remains attached.

One further assumption concerns the neglect of electrode voltage drop. For the CCD, the anode and cathode are most likely required to be located outside the region of interaction. The cathode may need to be distributed in the core flow near the channel exit radius, while the anode can be located upstream of the nozzle in the vicinity of the stagnation region. Such electrode geometry has been used in small-scale shock tube-driven disk generator experiments at MIT and elsewhere. With this type of electrode system design, electrode voltage drops can be minimized. Of key importance is the fact that the Faraday current in a disk is electrode-free, i.e; the current loop is closed in the gas.

8.1.3 GENERATOR DESIGN CONSTRAINT

Selection of an appropriate generator design constraint was shown to be critical to the final performance characteristics and design details of the OCD generator in Section 5.3. In the closed cycle case, the constant radial Hall field constraint used for the OCD is not appropriate, since the performance of the CCD will be limited by the effective Hall parameter rather than the Hall field. Ionization instabilities which lead to plasma turbulence are minimal in the OCD case, but these must be catered for in the design of the CCD.

It was apparent that acceptable CCD designs (i.e., compact disks with relatively high power output) could be achieved through imposition of a design constraint which requires the generator to operate at the local maximum electrical efficiency at each radial position within the region of

interaction. This overcomes to some degree the performance limitations imposed by the low effective Hall parameters achievable in the nonequilibrium case. When this maximum efficiency constraints is coupled with the overall system constraint (see below), an indirect maximization of enthalpy extraction is also achieved.

8.1.4 OVERALL SYSTEM CONSTRAINT

Section 4.1 has defined the operating mode selected for the CCD systems: "match point" operation. The designs of the system and the generator become interdependent with this type of operation specified, and the generator design code must be integrated with a systems model in order to determine the generator cutoff point. At each radial station in the CCD generator calculation, the design process assesses the balance between the required shaft work and the steam plant power. When these are equivalent, the "match point" has been reached and the generator is terminated (i.e., the size of the generator has been determined). A detailed description for the model used to impose this systems constraint is given in the following section.

The selection of match point operation as the nominal operating mode for the CCD MHD/steam system was predicated upon the need to achieve a high availability with the power system in a commercial application. At present, the use of mixed steam turbine and electric motor drives for a single MHD cycle compressor is not feasible, at least for the compressor size required in a 1000 MWe plant. An arrangement having parallel steam-turbine-driven and motor-driven compressors is conceivable, but the difficulties inherent in parallel operation of such high capacity, high discharge pressure machines are significant. The use of a single large steam turbine driven compressor, fully utilizing the available steam power (after feed pump turbine and air compressor turbine work has been provided) has therefore been chosen as the basis for this study.

8.2 CLOSED CYCLE DISK MHD SYSTEMS MODELING

The overall efficiency of a closed cycle MHD/steam power plant is dependent upon a large number of factors, each of which must be carefully assessed with

respect to the attainment of a configuration capable of providing optimum or near optimum system performance. The proper design of the system requires that the fullest use must be made of all energy delivered to the MHD working fluid. Large amounts of energy remaining in the MHD working fluid at the generator outlet must be extracted down to temperatures which approach those of the plant's ultimate heat sink.

A low compressor inlet temperature permits the attainment of the required pressure increase without the consumption of excessive amounts of power. As noted in the previous section, the selection of parameters and operating modes for the overall system will have a direct impact upon the design of the CCD generator itself, through imposition of the "match point" constraint. The delineation of the optimum CCD MHD/steam system configuration and parameters requires the use of a highly sophisticated system code.

The systems model used in the present study is simplified in order to permit the evaluation of a large number of CCD cases; it is, however, capable of providing sufficient information to determine the optimum operating range for CCD systems within the context of a fixed arrangement for the system components and without steam extraction for feedwater heating. The system was designed for a 1000 MWe plant and applied to other power levels by scaling the combustion gas flow rate to the argon flow rate. A more refined systems code is needed in order to achieve a fully optimized result (i.e. global optimization) for CCD system performance.

8.2.1 SYSTEM MODEL CONFIGURATION

The configuration used in the CCD systems model is shown in Figure 8-2-1 and consists of twenty units. The flowstreams for air, water, coal, combustion gas, and argon are depicted in the Figure. The model features were specific for the coal-combustor-fired regenerator system, which has been described in some detail in Section 4.1.2. All model parameters used in the CCD systems analyses were selected to be characteristic of this type of system.

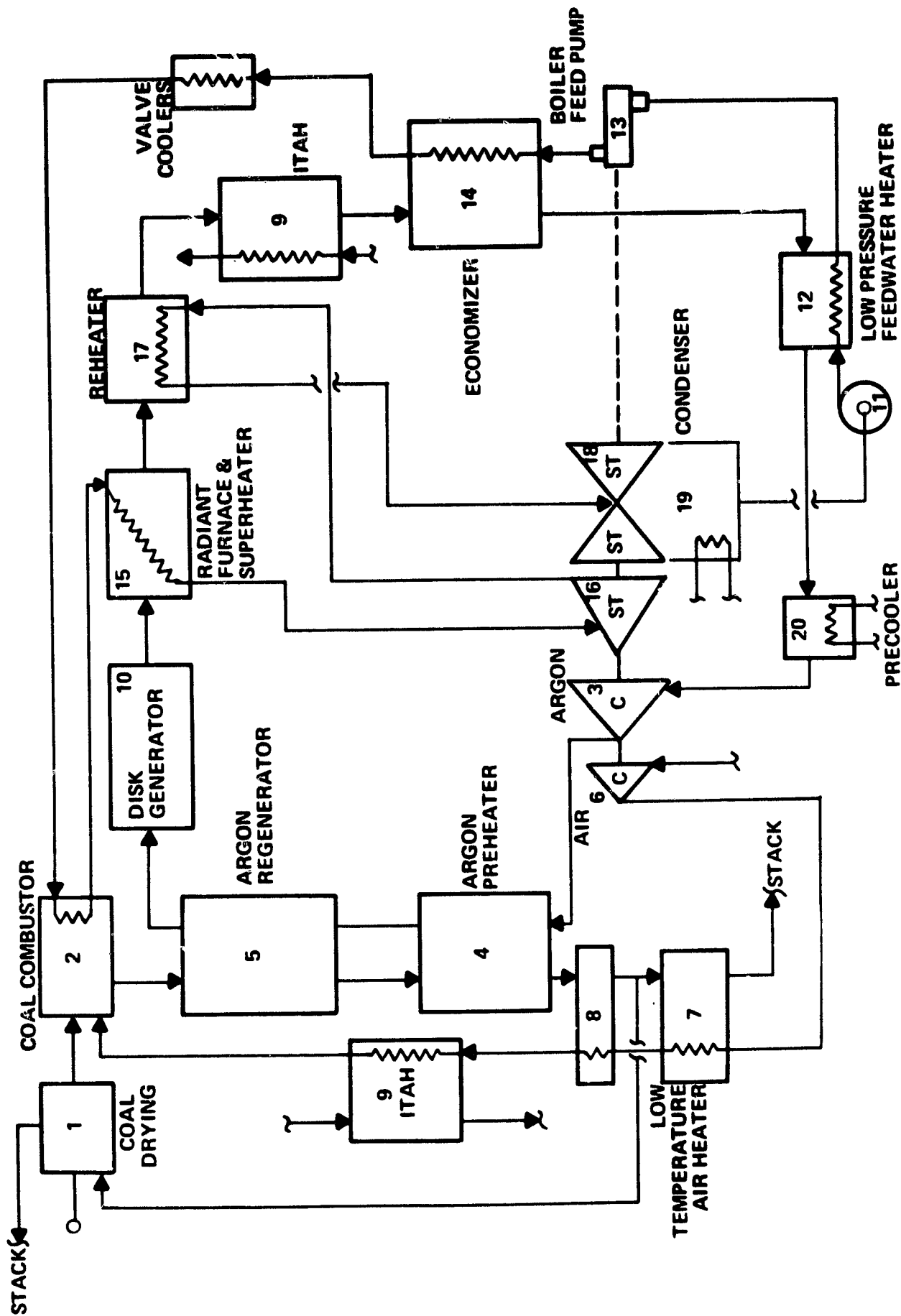


Figure 8-2-1. Closed Cycle Disk Generator System Model for Performance Studies

Combustion must be carried out to an oxygen-rich final condition in this type of system, in order to prevent the rapid destruction of the regenerator matrix material in a reducing environment. The combustor operates with only a slight overpressure with respect to atmosphere, in order to drive the combustion gases through the heater system, recuperators, and other downstream equipment. Since the combustion gases are not mixed with a seeding material that can scavenge SO_2 , as in the OCD cases, removal of this contaminant must be carried out by use of a separate scrubbing system in the gas exhaust train, before the plant stack.

The combustion gases will also contain a relatively high concentration of NO_x , since the combustion process is carried out in an oxygen-rich state. For $\phi = 1.05$, the NO_x levels at the combustor outlet can exceed 5000 ppm. The combustion gases are rapidly cooled upon passage through the regenerators, thus effectively freezing in the high concentrations typical of the combustion condition. In the CCD combustion gas system, there is no available component analogous to the OCD radiant furnace in which NO_x decomposition can take place in the critical 2200 K - 1800 K range. Therefore, some other means of removing NO_x from the gases prior to their release must be provided.

For the CCD systems considered herein, it was therefore assumed that NO_x removal would be accomplished by use of an ammonia injection system similar to that described in Appendix D for the OCD directly-fired case with high preheat level. The energy requirements associated with the inclusion of the separate emission control systems for NO_x and SO_2 in the CCD system design have been accounted for in the plant parasitic loads, which are considered in the final CCD system efficiency calculations.

The flame temperature in the combustor was estimated to be 2415 K with atmospheric combustion of Montana Rosebud coal dried to a 5% moisture level. A combustor heat loss of 7% of the fuel HHV is assumed. This energy is assumed recovered for reuse in the steam bottoming plant.

The maximum temperature of argon entering the disk generator is fixed at 1920 K and the regenerator inlet temperature for argon is fixed at 922 K. The temperature of the combustion gas at the outlet of the regenerator is fixed at 1090 K, which is used in this CCD systems model to scale the flow rate of combustion gas and coal in the system. The efficiency of the regenerator is assumed to be 0.95. 40% of the heat lost from the combustion gas in the regenerators is made available to the water stream (of the steam plant) through the regenerator valve coolers. A metallic recuperative preheater is used to heat the argon from the compressor outlet temperature to 922 K. The argon compressor is driven by steam, with its isentropic efficiency assumed fixed at 0.9. The enthalpy needed for argon preheating determines the outlet temperature of the combustion gas from the preheater, which like the rest of the heat exchangers in the system is assumed to operate at an efficiency of 99.5%. A minimum temperature approach of 8 K is permitted at the low temperature terminal of the argon preheater.

The combustion gas from the argon preheater is utilized in heating the air in two stages and for drying the coal before being discharged through emissions control equipment to the stack. The minimum temperature for coal drying is fixed at 611 K and a stream of combustion gas is branched off to the coal dryer to dry the coal to the specified conditions of the combustor. The air drawn at 288 K from the atmosphere is compressed and enters the first low temperature air heater at approximately 305 K where it is heated. A minimum temperature approach criterion of 20 K is set for any two streams exchanging heat throughout the system (with the single exception of the argon preheater). The final stack temperature of the combustion gas for both streams is fixed at 408 K, set by acid dew point considerations.

The final preheating of air is accomplished in an intermediate temperature air heater (ITAH) by energy taken from the argon stream exiting from the reheater of the steam plant. In this CCD model, the exit temperature of argon from the reheater is fixed at 1000 K and the temperatures of air across the air heater being known, the argon temperature at the outlet is determined by the

efficiency of the ITAH. This outlet temperature of argon constrains the heating of water in the economizer, as is discussed below.

The steam cycle that is assumed for the present plant configuration is a supercritical plant with a single reheat step operating with a high turbine pressure of 24.2 MPa (3500 psi) and a temperature of 811 K (1000°F), and with a condenser pressure of 6.8 kPa (2" HgA) and temperature of 312 K (102°F). The water from the condenser is pumped to about 1.0 MPa by the motor-driven condensate pump and then enters a low temperature feed water heater, where the water is heated by recovering energy from the argon stream and allowed to approach saturation conditions. Since the saturation temperature of water at the LPFH outlet is 451 K, and the argon temperature at the inlet of the low temperature feed water heater is fixed (20 K higher) at 471 K. The present CCD code has not been corrected to handle the steam feedheating in a deaerating feed tank, nor in extraction type feed heaters; hence the calculated efficiency of the steam cycle used in the modeling is slightly lower than optimum.

The water from the feed water heater at 451 K is pumped to high pressure by the main feed pump and is then heated in the economizer; the inlet temperature of argon to the economizer is determined by the ITAH air preheat requirement. The pressure of the bottoming plant working fluid at the outlet of the economizer is fixed at 26.6 MPa. The fluid then flows through the valve coolers, where it receives the recoverable heat from the regenerator, and through the combustor cooling system where it picks up heat from the walls. The efficiency of heat exchange to water at all points in the system is fixed at 99.5%.

Fluid with a pressure of 25 MPa is fed into the radiant furnace section, where it is heated to 811 K. The working fluid is then led into the high pressure steam turbine, where it expands to exhaust conditions of 564 K and 4.5 MPa. The low pressure steam is then reheated to 811 K and enters the low pressure steam turbine at a pressure of 4 MPa. The low pressure steam turbine finally expands steam to the specified condenser pressure. An isentropic efficiency of 90% is assumed for both the high and low pressure steam turbines. The

steam turbines are utilized solely to drive the air and argon compressors (and the boiler feed pumps) and do not generate electric power additional to that delivered by the MHD generator.

The heat required by water in the radiant furnace and the reheater is determined and the required enthalpy is assumed to be provided from the high temperature argon at an efficiency of 99.5%; the assumed argon pressure losses throughout the system are given in Table 8.2.1. The procedure enables one to calculate the temperature of the argon stream at the outlet of the reheater and this temperature is compared with 1000 K, which was fixed from the considerations of the intermediate temperature air heater approach requirement. The flow rate of water is then modified through the steam cycle such that a convergence of 1 K is established for the temperature of argon at the outlet of the reheater. Once the flow rate of water is determined, the final inlet temperature of argon at the precooler is computed from the heat balance across the low pressure feed water heater, and the heat budget and the plant efficiency are calculated. The argon compressor inlet temperature (and therefore the duty cycle of the precooler) varies in the range 311 K to 330 K depending upon the convergence of the cycle analysis for each particular set of generator operating conditions. All heat rejected in the precooler is lost to the ultimate heat sink. The use of a precooler is intended to minimize the required argon compressor power, and to permit operation of the compressor at discharge temperatures of less than 700 K, in recognition of materials limits for such a high-capacity, high pressure ratio machine.

TABLE 8.2.1: SUMMARY OF SYSTEM PARAMETERS
FOR CLOSED CYCLE DISK SYSTEM MODEL

Argon Stream

Pressure Losses:

Diffuser Pressure Ratio	.897	(Cp = .8)
(subsonic after inlet shock loss)		
Loss between diffuser and compressor	3.0% of total pressure	
Loss between compressor and nozzle	3.0% of total pressure	

Efficiencies:

Adiabatic Nozzle	.99
Compressors	.90
Heat Exchangers (except regenerator)	.995
Argon Regenerator	.95
Feed Pumps	.70

Statepoint Temperatures (K):

[Argon Loop]

Compressor Inlet	311 - 325
Compressor Outlet	Variable
Preheater Outlet	922
Regenerator Outlet	1920
Disk Generator Outlet	Variable
Radiant Furnace Outlet	Variable
Reheater Outlet	1000
ITAH Outlet	Variable
Economizer Outlet	472
LPFH Outlet	Variable
Precooler Outlet	311 - 330

TABLE 8.2.1 - Continued

[Steam Loop]

Hotwell	312
Condensate Pump Discharge	312.6
Low Pressure Feed Heater	451
Main Feed Pump Discharge	457.4
Economizer Out	Variable
Valve Cooler Out	Variable
Combustor Cooling Out	Variable
Radiant Furnace Out	811
HP Turbine Out	564
Reheater Out	811
LP Turbine Out	--
Condenser Out	312

[Air System]

Compressor Inlet	288
Compressor Outlet	305
LTAH 2 Outlet	Variable
LTAH 1 Outlet	Variable
ITAH Outlet	922

[Combustion Gas System]

Combustor	2415
Regenerator Out	1090
Argon Preheater Out	Variable
LTAH 1 Out	611
LTAH 2 Out	408
Coal Dryer Out	408

8.3 CLOSED CYCLE DISK SYSTEMS PERFORMANCE

Several hundred CCD system performance cases were investigated for the study, yielding twenty-seven final disk and system cases which provided near-optimum performance at the match point, over a wide range of net power outputs. These twenty-seven cases were characteristic of CCD system performance with low impurity levels and with moderate turbulence. An additional five cases were selected to delineate performance characteristics for CCD systems with higher turbulence levels. A single case was also developed to permit the evaluation of the effects of higher impurity levels in the MHD working fluid.

8.3.1 SYSTEM PERFORMANCE OPTIMIZATION

For all CCD cases investigated, the magnetic induction was held fixed at 6 T, and the inlet stagnation temperature was 1920 K. Two different plasma turbulence levels ($\hat{S} = 0.2$, $\hat{S} = 0.5$) were also considered. The turbulence parameter (\hat{S}) is defined as the mean square deviation of the fluctuations in electron density. An impurity level of 18 ppm CO_2 and 82 ppm of $\text{CO} + \text{N}_2$ was used except for one case where a 200 ppm impurity level was investigated. The effective Hall coefficient (β_e) is limited to values less than 5, as previously discussed. This is consistent with the assumptions made for the low-turbulence level linear closed cycle cases investigated in the GE study [x].

The stagnation pressure and inlet swirl were varied stepwise over the range 0.4 to 1.22 MPa (P_0) and 1.0 to 4.0 (S). For each distinct combination of P_0 and S the inlet Mach number and seed fraction are selected to yield an exit Mach number in the 1.0 to 1.1 range, and a generator pressure ratio which is compatible with system operation at the match point. The calculated system efficiency is not necessarily the maximum obtainable efficiency for the quoted generator parameters, since enthalpy extraction and generator isentropic efficiency can both increase with increasing generator size (radius) beyond this point. Operation beyond the match point introduces cycle complexities, as previously described, which are judged unsuitable for a reliable commercial power generating system. Higher performance may also be obtained in certain cases by designing the generator with a slightly higher exit Mach number.

For all these calculations, the channel inlet height was fixed at 0.5 meters. The OCD criterion (inlet height set to approximately 1/3 inlet radius) was not used in the CCD case, since the interaction lengths are relatively short. The inlet radius was selected on the basis of mass flow and density considerations, with the minimum allowable radius being set at 1.5 meters.

Table 8.3.1 summarizes the computer calculated performance of the thirty-three distinct CCD system cases which have had their performances optimized with respect to the stated conditions and imposed constraints. In each case the following variables and parameters which characterize each CCD system are tabulated:

- S, inlet swirl
- P_o , inlet stagnation pressure
- M, inlet Mach number
- X, seed fraction
- β_e , effective Hall parameter (at midchannel)
- E.E., enthalpy extraction
- η_G , generator isentropic efficiency
- η_G & η_D , generator and diffuser isentropic efficiency
- L, interaction length
- P_G^r , generator pressure ratio
- P_{comp}^r , compressor pressure ratio
- R_o , generator inlet radius
- P, gross MHD power (VI)
- η_s , System Efficiency

The overall system efficiency η_s has been calculated by using the expression:

$$\eta_s = \frac{0.985 P}{HCOAL} - \text{Parasitic Load Decrement}$$

HCOAL is the assumed coal firing rate for the system and 0.985 is the converter efficiency. Transformer losses and plant parasitic loads were not included in the calculated plant efficiencies given in Appendix B. Table 8.3.2 was prepared estimating these losses and loads to be equivalent to 1.8

TABLE 8.3.1 CLOSED CYCLE DISK GENERATOR SYSTEM PERFORMANCE SURVEY
(INLET CHANNEL HEIGHT = 0.5 METER)

100 ppm Impurities; Turbulence Level 0.2														
Case No.	S	Atm P _o	M	% X	β_e	% E.E.	% η_G	% $\eta_{G\&D}$	% η_S	m L	P _G ^r	P _{COMP} ^r	m R _o	MW _e _P
1	2.0	4	2.02	.135	4.8	43.2	84.1	80.8	46.2	.29	4.01	4.93	2.5	376
2	2.0	4	2.00	.405	4.5	43.7	83.5	80.4	46.0	.28	4.14	5.08	3.0	459
3	2.0	6	2.22	.135	4.7	43.0	82.5	79.4	45.7	.15	4.17	5.17	2.1	416
4	2.0	8	2.25	.405	4.3	42.5	80.5	77.5	45.1	.86	4.10	5.07	3.0	763
5	2.0	10	2.50	.100	4.7	42.5	79.9	77.0	44.9	.92	4.34	5.44	2.5	674
6	1.5	6	2.00	.035	4.6	42.4	79.8	76.9	45.1	.36	4.32	5.30	1.5	420
7	1.5	6	2.08	.015	4.8	42.1	79.8	77.0	45.0	.43	4.27	5.26	1.5	396
8	1.5	6	1.95	.045	4.6	41.9	80.3	77.3	45.2	.36	4.15	5.08	2.5	712
9	1.5	6	2.01	.015	4.9	42.9	80.7	77.8	45.4	.51	4.32	5.30	2.5	703
10	1.5	8	2.26	.007	4.9	42.0	77.9	75.1	44.5	.80	4.44	5.50	1.5	467
11	1.5	8	2.05	.035	4.7	42.4	79.9	77.0	45.1	.61	4.32	5.31	3.0	1085
12	1.5	8	2.10	.015	4.9	42.7	79.9	77.0	45.1	.77	4.38	5.39	3.0	1057
13	1.5	10	2.20	.045	4.5	42.8	77.4	74.7	44.4	.67	4.51	5.58	1.5	608
14	1.5	10	2.13	.045	4.6	42.3	78.6	75.8	44.7	.82	4.44	5.47	2.5	1069
15	1.5	12	2.30	.045	4.4	41.5	76.3	73.6	44.0	.84	4.59	5.69	1.5	677
16	1.5	12	2.25	.045	4.5	41.5	77.2	74.4	44.3	.96	4.48	5.54	2.2	1027
17	1.5	12	2.21	.045	4.6	41.9	77.5	74.7	44.4	1.11	4.50	5.56	2.5	1206
18	1.0	8	1.95	.005	4.8	40.9	74.0	71.5	43.5	.84	4.76	5.83	1.5	715
19	1.0	8	1.93	.005	4.8	41.2	74.5	72.0	43.7	.86	4.75	5.81	1.8	875
20	1.0	8	1.91	.005	4.8	41.3	75.0	72.4	43.8	.88	4.70	5.75	2.2	1085
21	1.0	10	2.05	.005	4.7	40.6	73.0	70.6	43.2	.90	4.82	5.92	1.5	833
22	1.0	10	2.00	.005	4.6	40.9	73.5	71.1	43.4	.98	4.81	5.90	1.8	1039
23	1.0	10	2.00	.005	4.7	40.6	73.7	71.2	43.4	.96	4.70	5.77	2.0	1146
24	1.0	10	1.98	.005	4.7	40.8	74.0	71.5	43.5	1.00	4.73	5.80	2.2	1284
25	1.0	10	2.00	.005	4.7	41.0	74.2	71.7	43.6	.96	4.76	5.83	2.5	1449
26	1.0	12	2.10	.005	4.6	40.6	72.0	69.7	42.8	1.06	4.90	6.04	1.5	962
27	1.0	12	2.02	.005	4.6	40.4	73.4	70.9	43.3	1.24	4.79	5.88	2.5	1703
100 ppm Impurities; Turbulence Level 0.5														
28	4.0	4	2.35	.300	2.4	42.6	80.8	77.9	45.2	.42	4.26	5.30	2.5	162
29	4.0	4	2.35	.300	2.4	43.1	81.1	78.2	45.3	.42	4.34	5.40	3.0	197
30	4.0	6	2.75	.300	2.3	39.8	76.8	73.9	43.7	.43	4.43	5.22	1.5	104
31	4.0	8	2.95	.100	2.3	40.7	74.7	72.2	43.2	.61	4.61	5.89	1.5	125
32	4.0	10	3.02	.100	2.3	40.3	73.3	70.8	42.8	.95	4.73	6.06	2.5	246
200 ppm Impurities; Turbulence Level 0.2														
33	2.0	8	2.50	.405	4.4	42.0	78.6	75.8	44.5	1.13	4.38	5.48	2.5	531

TABLE 8.3.2
1000 MW_e Closed Cycle Disk Generator System
ESTIMATED PLANT PARASITIC LOADS FOR SYSTEM
WITH REGENERATORS FIRED BY COAL COMBUSTOR

- Electrical Losses during MHD Power Conversion

Inverter Efficiency: 0.985

Transformer Efficiency: 0.99

- Electrical Loads

Cesium Purification and Reclamation	1.0 MW
Argon Purge of Regenerator	2.0 MW
Combustion Gas Purge of Regenerator	1.5 MW
Argon Purification	1.0 MW
Cooling Towers	5.6 MW
Condensate Pump	0.6 MW
Magnet Systems	0.2 MW
Coal Handling and Processing	12.0 MW
Coal Transport Gas Compressor	0.5 MW
Electrostatic Precipitator	0.4 MW
Stack Gas Scrubbers	10.0 MW
(Includes ID Fan Power)	
Miscellaneous	<u>5.0 MW</u>
Total Parasitic Load	39.8 MW _e

- Efficiency Decrement for 2222 MW_t

(45% nominal efficiency): 1.8%

percentage points of plant efficiency for a 1000 MWe plant. The actual percentage value of parasitic loads will vary with plant size, but it is assumed that the variance is not substantial over the range of CCD system powers given in Table 8.3.1.

The actual statepoints for all generator cases described in Table 8.3.1 can be found in Appendix B to this report.

General observations regarding the results of the CCD system performance analyses may be made, as follows.

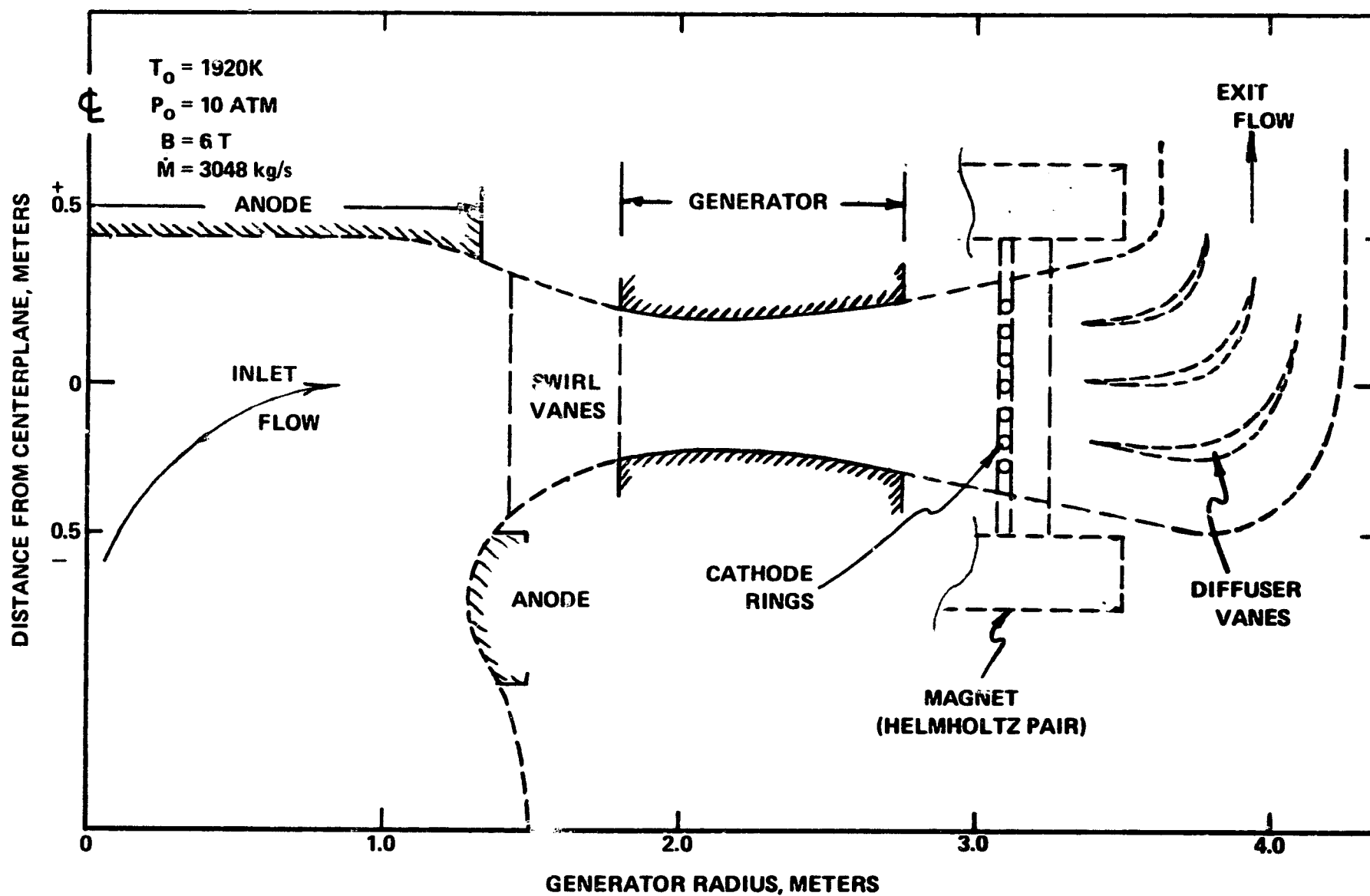
- (1) Levels of optimum system efficiency are comparable to those predicted for OCD generators in this report, and for those calculated for linear closed cycle channels which may require an interaction length of 10 meters or more. The relatively short interaction lengths attainable with the disk generator configuration operating in the supersonic regime result in less friction effects and permit more efficient diffusers to be used.
- (2) Excellent performance can be obtained from the CCD at relatively low power levels. The advantage of scale is relatively small for CCD systems.
- (3) The required inlet Mach number for "optimum" performance is high, consistent with the local performance characteristics discussed in Section 8.1. The Mach number increases as turbulence and impurity levels are increased.
- (4) To constrain the effective Hall parameter to values less than 5, the seed fraction was increased with swirl ratio. For inlet swirl ratios greater than 2 with low turbulence, more than a 1% seed fraction will be required. For the low swirl cases (1.0 and below) with low turbulence, the seed fraction is very low and is approaching a range within which adequate controllability of this parameter may be difficult for large-scale CCD plants. For high degrees of ionization ($S = 1.0$ results) lower turbulence levels (i.e. \bar{S} less than 0.2) should be more realistic if the ionization instability is the sole source of the turbulence. These lower turbulence levels will result in improved generator performance and better control of the generator loading (particularly when full ionization of the seed is reached).

- (5) For the higher turbulence level cases, where the effective Hall parameter is now restricted to $\beta_e \leq 2.3$, higher values of swirl and inlet Mach number must be used to obtain efficiencies comparable to those of the low turbulence systems.
- (6) The actual equilibrium values of impurity level in the MHD working fluid attainable in practice are not known. However, the effect of increasing impurity level from 100 to 200 ppm for this study is to reduce the maximum obtainable power at the match point. The efficiencies obtainable remain comparable to those of the low impurity level cases.
- (7) For the optimized cases presented, the interaction length increases and the efficiency decreases with increasing stagnation pressure.

8.3.2 EXAMPLE CCD GENERATOR DESIGNS

Two examples of the channel design and property profiles are given in Figures 8-3-1 through 8-3-6. In Figures 8-3-1 through 8-3-3, case # 22 from Table 8.3.1 ($\hat{S} = 0.2$) is shown. The operating conditions and resulting channel geometry are given in Figure 8-3-1. The generator is drawn to scale; other components (dashed lines) are shown schematically. As a result of the high interaction, the generator is relatively short ($L/D \leq 2.0$); two-dimensional electrical effects are important and would most likely require a cathode (e.g., tungsten rods) distributed across the exit plane of the channel. To insure a more uniform magnetic field, the split-pair (Helmholtz pair) magnet configuration would be preferred, with the cathode located in the vicinity of zero field. This magnet would be much more compact than an equivalent design for a 1000 MWe OCD, however. The anode can also be divided, as indicated in the figure, or the option of a central rod could be used. The latter affords the possibility of rotation or axial feeding for arc control and/or replenishment of consumable material. The electrical and transport properties for this channel are shown in Figure 8-3-2. Near the end of the generator the seed is over 80% ionized. The local power density is denoted as P_D in the figure. The gas properties for this case are given in Figure 8-3-3.

Generator designs for the high turbulence assumption are shown in Figures 8-3-4 through 8-3-6. The channels are strongly convergent relative to the $\hat{S} = 0.2$ cases as a result of the high swirl and lower interaction (compare Ne profiles). The current load factor $K = K_{opt}$ is reduced, and the generators



705352-5A

Figure 8-3-1. Example Closed Cycle Disk Generator Design (Case # 22)

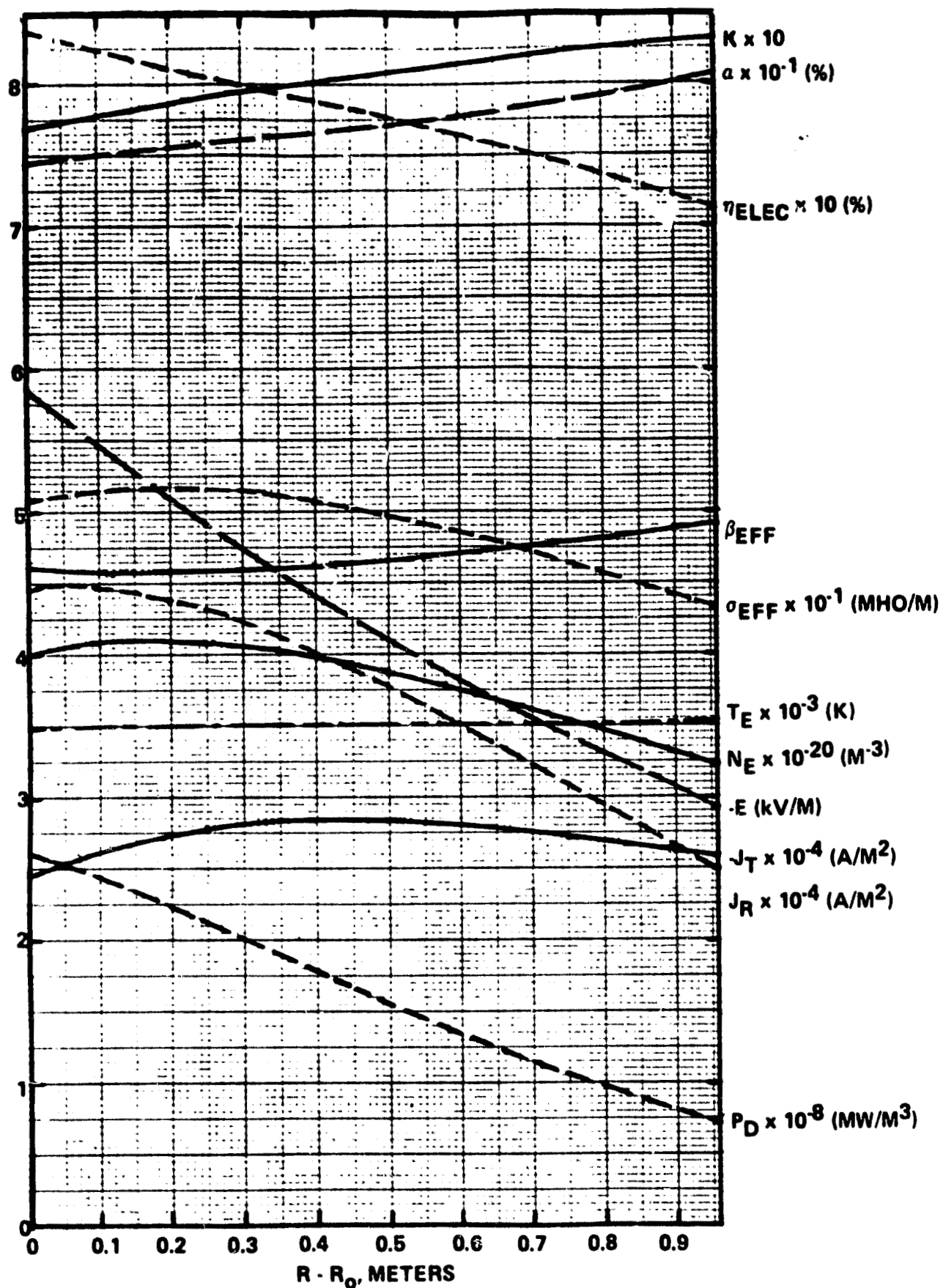


Figure 8-3-2. Electrical and Effective Transport Properties for the Generator
(Case # 22, $I_L = 251$ kA)

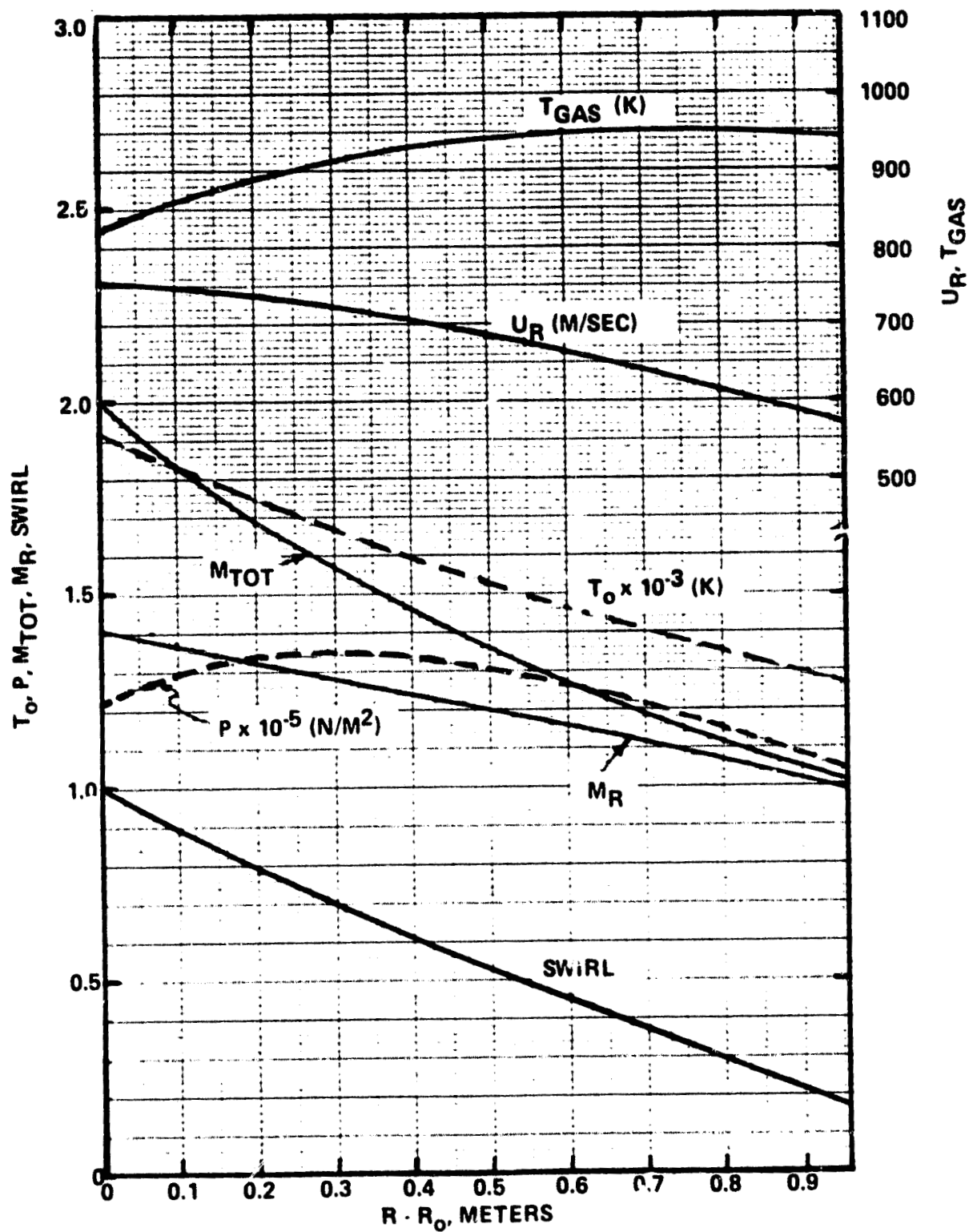


Figure 8-3-3. Profiles of the Fluid Properties for Case # 22 Disk Generator

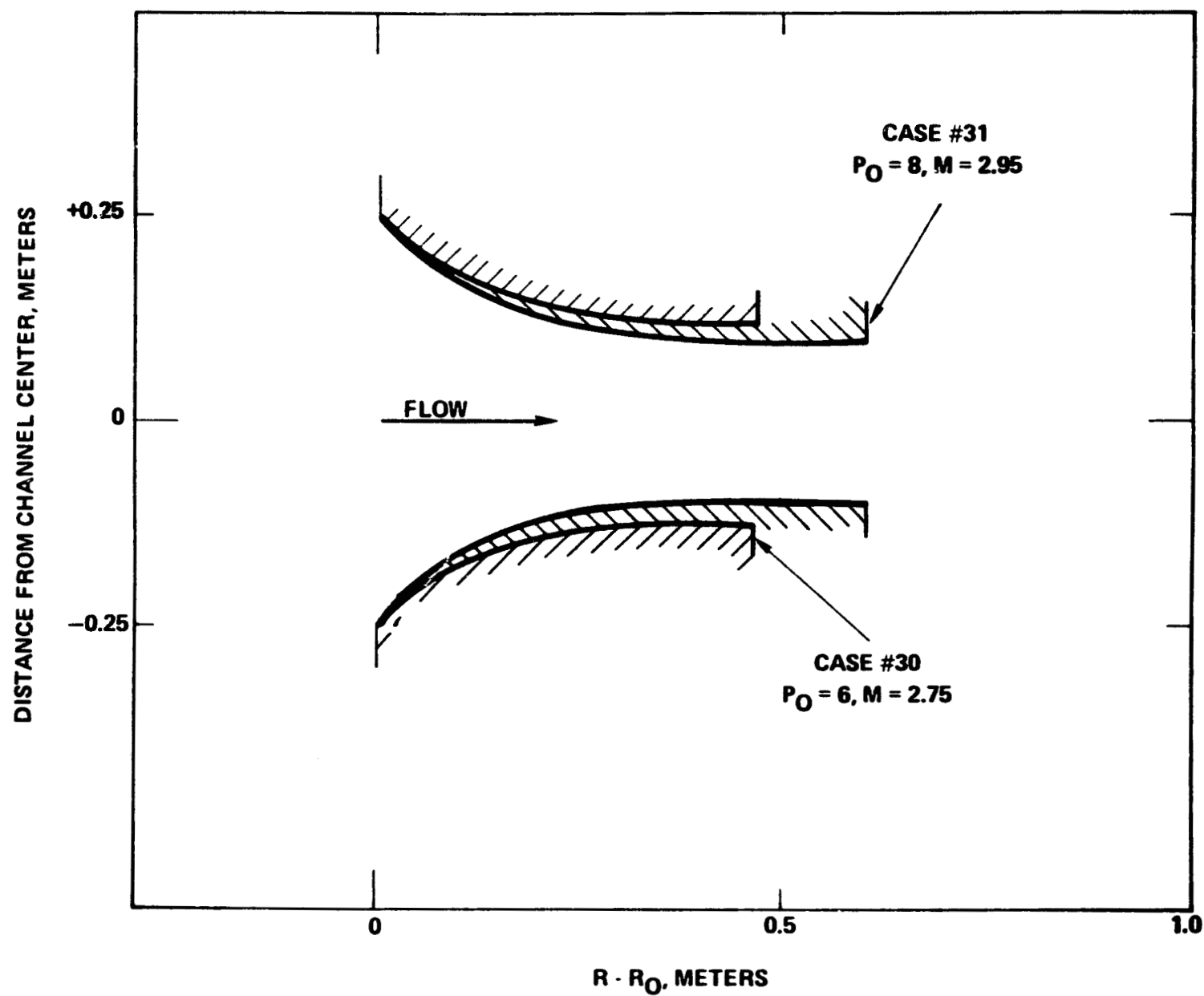


Figure 8-3-4. Example CCD Generator Designs for High Plasma Turbulence ($S = 0.5$)

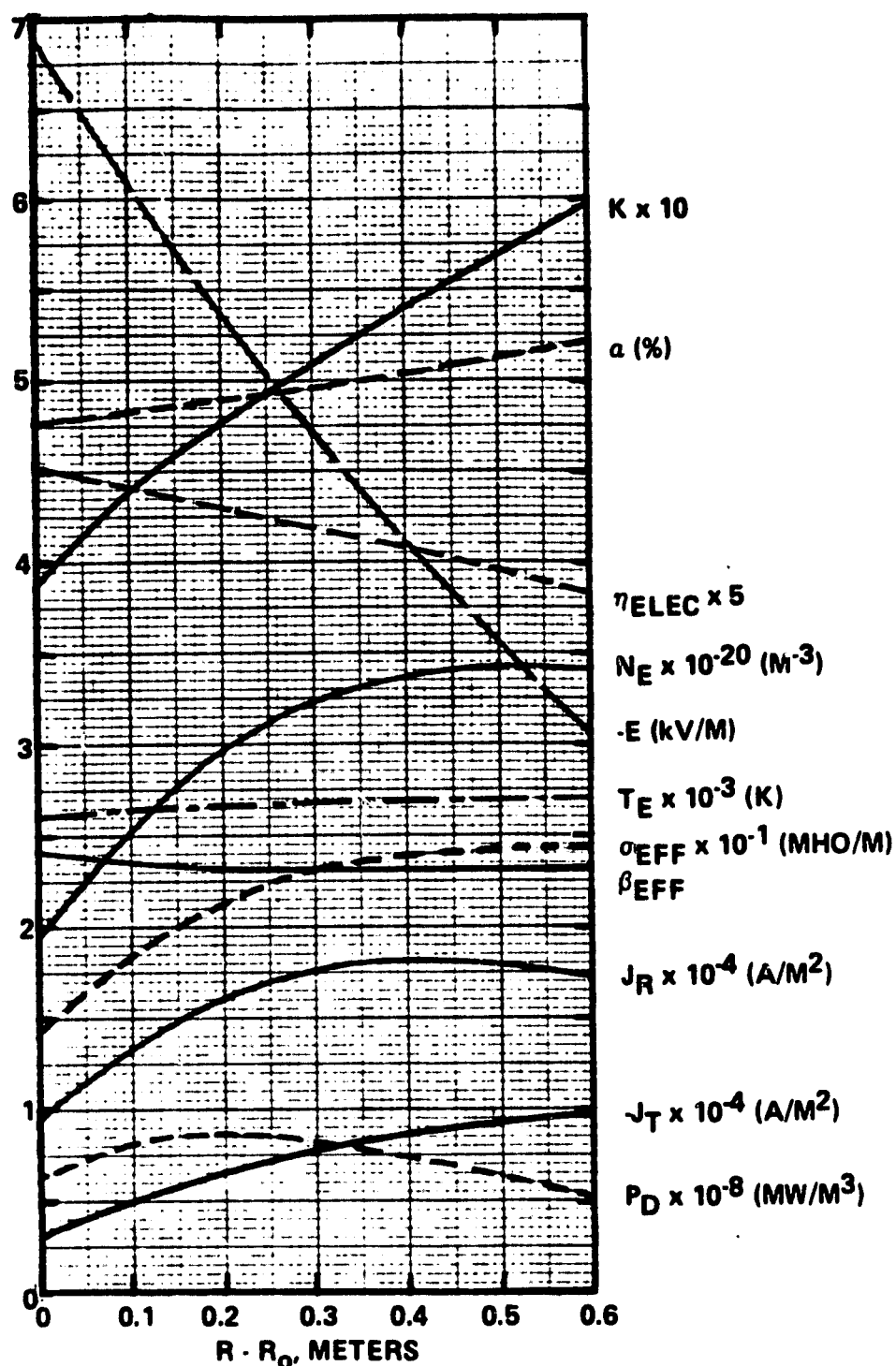


Figure 8-3-5. Electrical and Effective Transport Properties for the High Turbulence Disk Generator (Case # 31, $I_L = 41.7$ kA)

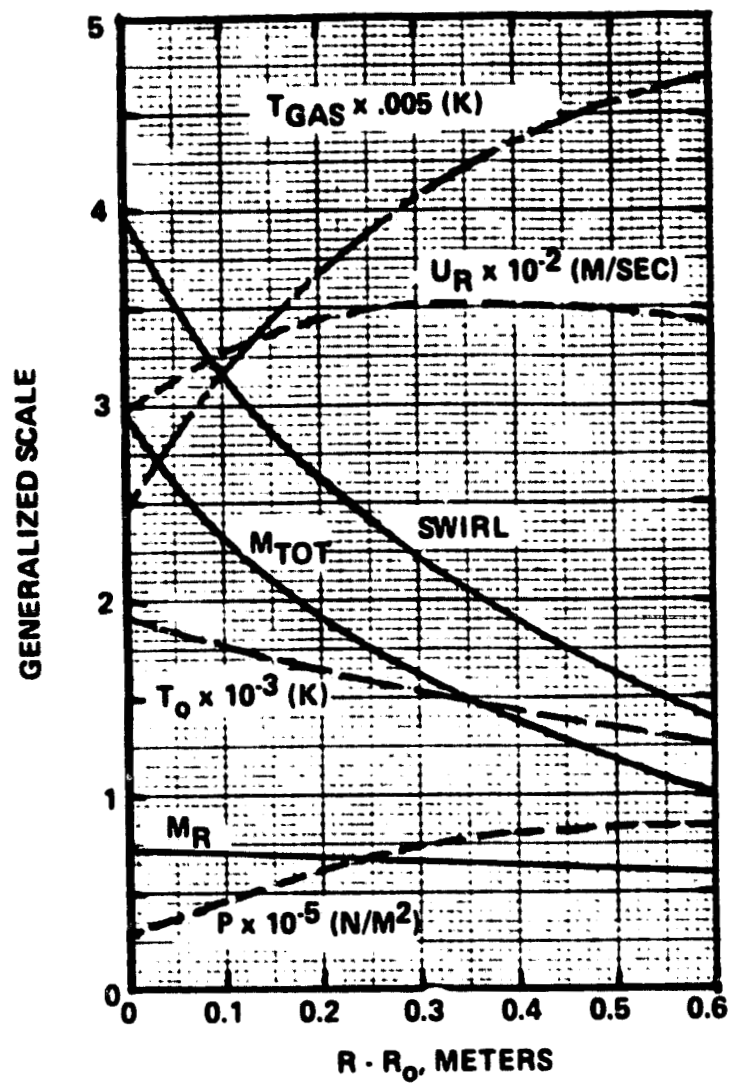


Figure 8-3-6. Profiles of the Fluid Properties for the High Turbulence Disk Generator (Case # 31)

operate near maximum power ($K = 0.5$) as well as maximum efficiency. In addition to generating high inlet swirl, some deswirling is required at the channel exit (see Figure 8-3-6). The operation more closely resembles the reaction mode; the radial Mach number is nearly constant and subsonic. However, the adverse pressure gradient for this case may be sufficient to cause boundary layer separation; this problem must be assessed in greater detail.

Figure 8-3-7 shows the gross enthalpy extraction versus the turbine efficiency of the combined generator plus diffuser for the cases given in Table 8.3.1. The data for G.E. ECAS 102/102A cases have been taken from Reference[6]; the extraction was calculated using the definition based on the temperatures given in the paper. The comparison shows that the disk achieves about a four point gain in turbine efficiency for the same enthalpy extraction. This suggests that the CCD can exhibit higher cycle efficiencies than the linear Faraday generator when similar system assumptions are used. This is to be expected since the disk is a more compact unit, having less friction effects because of the short L/D ratio, and can be provided with a more efficient diffuser. The diffuser recovery is primarily subsonic with a stagnation pressure ratio of 0.897 (for an assumed $C_p = 0.8$). The inlet shock is weak since the entrance Mach number is only slightly greater than unity. In addition, the assumption made here of an adiabatic diffuser for the CCD is more realistic than for the linear channel where diffuser lengths are of the order of tens of meters and $T_0 = 1200$ K. The combined generator diffuser pressure ratio is shown in Figure 8-3-8. Lower ratios (and hence less compressor work) are found for the disk, consistent with the higher isentropic efficiencies (for the same enthalpy extraction).

Figure 8-3-9 shows the overall system efficiency versus turbine efficiency for the disk data of Table 8.3.1. Curves are plotted for the $\hat{S} = 0.2$ and $\hat{S} = 0.5$ cases.

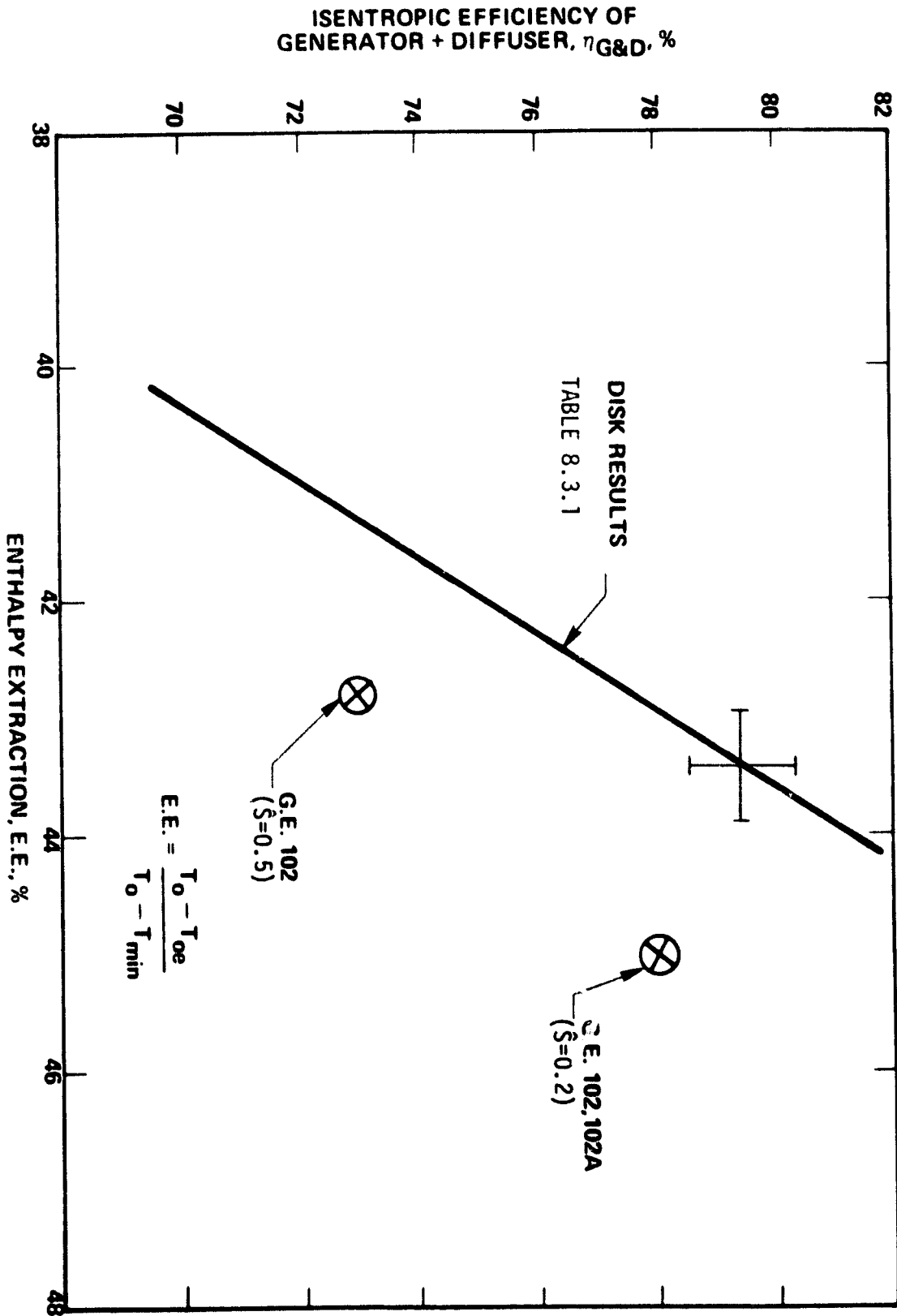


Figure 8-3-7. Comparison of Enthalpy Extraction Versus Turbine Efficiency of Generator Plus Diffuser for Disk and Linear Closed Cycle Systems

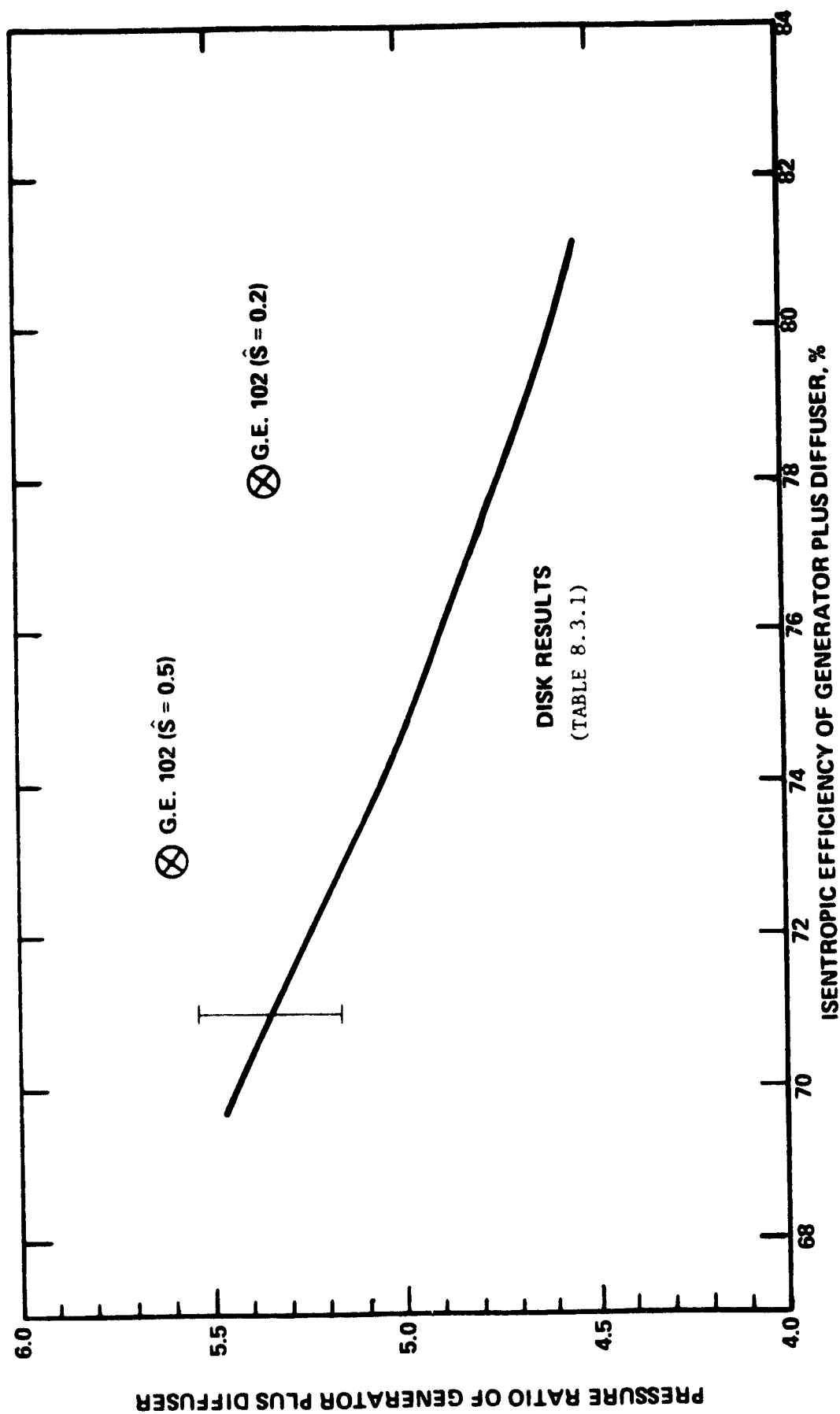


Figure 8-3-8. Pressure Ratio Versus Isentropic Efficiency Comparison of Disk and Linear Generators

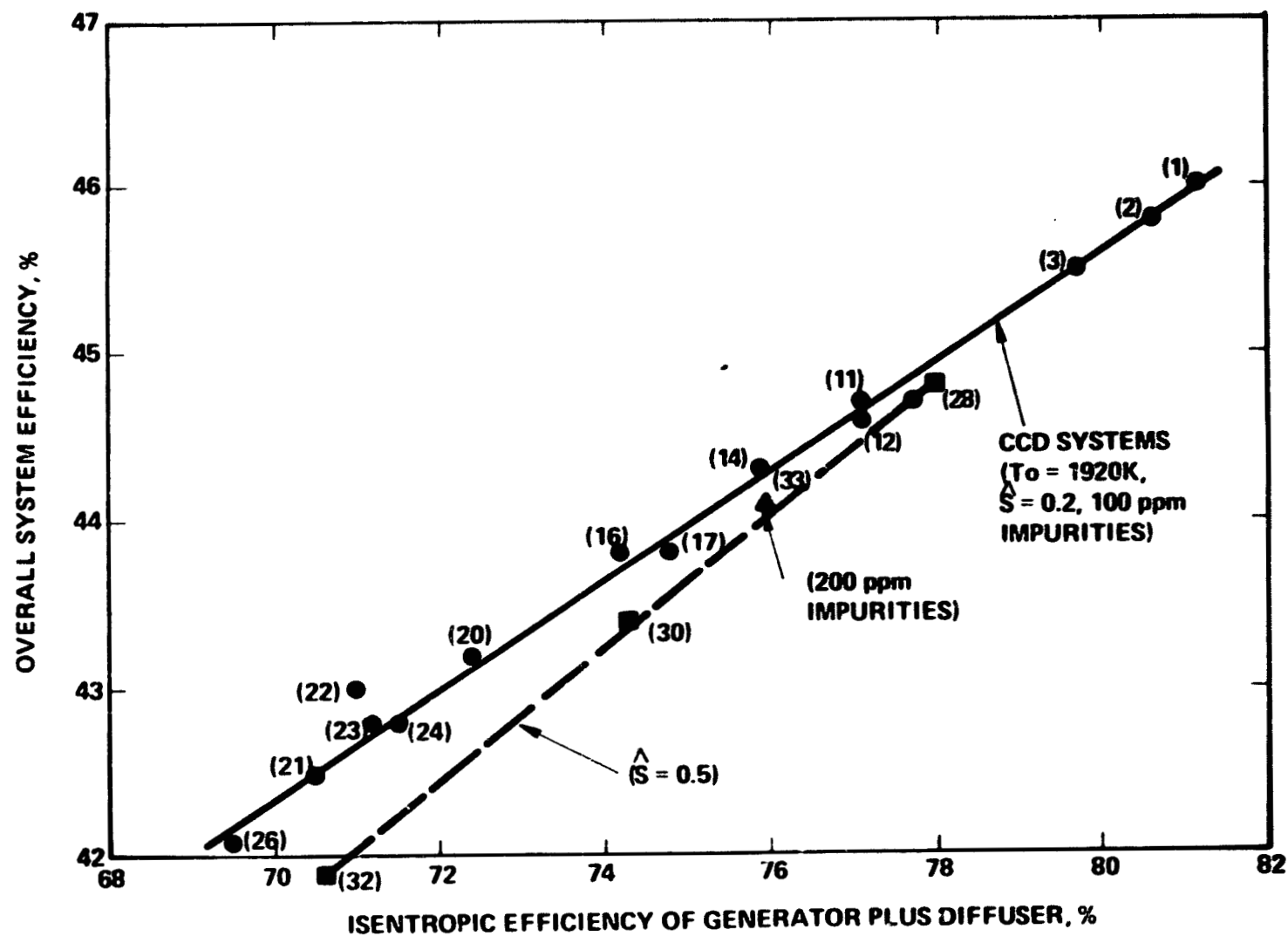


Figure 8-3-9. Estimated CCD System Performance With Match Point Operation and Atmospheric Combustion (Calculational Case Numbers Given in Parentheses)

8.4 HEATERS FOR CLOSED CYCLE MHD

8.4.1 GENERAL CONSIDERATIONS

The closed cycle MHD plant arrangement has two significant differences from the open cycle MHD plant that affect the heater design. First, seed is introduced downstream of the heater and, therefore, the seed will not pass through the heater. Second, contamination of the noble gas by residual products of combustion in the heater must be held to very low levels. This will be accomplished by evacuating or purging the heaters to remove the residual gas (primarily nitrogen, water vapor, and carbon dioxide).

Contamination measurements have been made by General Electric Company on a small heater (0.3 m diameter and 3 m high bed). This heater, because of its small size, had a much greater proportion of insulation materials relative to bed materials than would a full-scale heater. Hence, the results should be conservative. The measurements indicated levels below those which would cause significant deterioration of channel performance.

8.4.2 REHEAT WITH DIRECT COAL FIRING

In the direct coal firing arrangement the combustor is fired with coal and the products of combustion pass through the heaters. The combustor design will determine the amount of slag rejection, i.e., the amount of slag that enters the heaters. The major development requirement is to devise means of preventing heater fouling with slag and therefore, a high level of slag rejection is desirable.

Alternative approaches to the combustor design are the use of individual burners for each heater rather than a single large burner, and atmospheric pressure versus pressurized combustion. The choice will have a major effect on the high temperature valve requirements for the system. The use of individual pressurized burners eliminates the hot gas inlet valves, which are the valves that are exposed to the most severe service. Elimination of these valves is a substantial advantage and therefore, the use of individual pressurized burners is the preferred arrangement. Development of such a burner is being pursued by

General Electric Company. Another advantage of pressurized combustion is that heaters are smaller and therefore the system cost is reduced and the purge requirements are reduced.

The air heater system will look similar to that for the directly-fired heaters described in Section 6.5. The holes in the cored brick will need to be larger (relative to clean gas firing) to accommodate some slag accumulation without plugging.

Materials will need to be resistant to slag. This is a less demanding requirement than resistance to both seed and slag. However, the high temperature level will require development of data on the long duration effect of erosion and corrosion. Tests of materials under simulated conditions with atmospheric pressure reheat are being carried out at Montana State University.

One method of preventing plugging of the bed with slag has been examined at present. It is proposed to allow slag to accumulate until the pressure drop exceeds a predetermined limit, then take the heater off line for cleaning. Cleaning would be done by heating the entire bed to about 1650 K. Preliminary tests indicate this may be a feasible approach.

The ability to heat the entire bed to a temperature as high as 1650 K requires development of a suitable bed support. The dome support concept under development by FluidDyne for the open cycle directly-fired heater has been applied to the General Electric heater mentioned in Section 8.4.1. This heater will be operated with its pressurized burner and high temperature bed support during the year 1980. Further development of the bed support will require tests at larger scale. This work will be applicable to direct-firing of both open cycle and closed cycle MHD.

The valve development needs are related to the choice of combustor (individual or one large combustor and pressurized or not). The most demanding valve need is eliminated with the individual pressurized combustor approach. Redesign to accommodate high pressure and verification tests would be needed for the remaining valves.

The question of nitrogen oxide emission is similar to that for the open cycle indirectly-fired case. However, the presence of slag in the heater beds will diminish the probability that alumina materials will retain their catalytic properties, and therefore cause some reduction in the NO_x levels.

8.4.3 REHEAT WITH CLEAN COAL GAS

The requirements for this system are very similar to those for the open cycle case discussion in Section 6.5. The major difference is the additional need to evacuate or purge heaters to avoid contamination of noble gas. Therefore, the discussion presented in Section 6.5 applies to this case.

9.0 SUMMARY OF CCD MAJOR COMPONENT COSTS AND COMPARISON TO OCD COMPONENT COSTS

This section provides a summary comparison of the costs of major components for closed cycle disk and open cycle disk MHD/steam power systems of the same nominal electric power output. Conceptual designs for 1000 MWe OCD MHD/steam system major components were prepared and described in Section 6.0, and costed earlier in this Section of the report. It was therefore decided to select one of the nominal 1000 MWe CCD cases investigated and reported upon in the CCD Systems Analysis section to serve as the basis for development of rough CCD component costs. Case 22, with 1039 MWe gross MHD power output, and estimated net output of 968 MWe to the grid, was chosen to be the reference CCD case.

9.1 DISCUSSION OF REFERENCE CASE CCD SYSTEM

Case 22 of Table 8.3.2 is a typical example of the performance of a large CCD MHD/steam electrical generating system. All steam power generated in the bottoming plant is utilized to drive the main feed pump and MHD cycle compressor turbines; the calculated deviation from the match point is only + 0.23 MW as noted in the Case 22 data sheet of Appendix B. The MHD generator will be assumed to be operable as a single-load device, although it is likely that further investigation of off-design-point performance of such generators must be undertaken before the acceptability of such a design is proven.

The CCD generator is a low-voltage, high current device; dc power is delivered to the load at 251 kA through 4139 V. The low terminal voltage is close to the minimum allowable value for converter bridges of the type utilized in the recent converter system designs; the scaling relationships given in Section 6.4 will not hold if the disk is not taken to be a single load device in this CCD case, to maintain the minimum bridge voltage above this limiting level.

The Case 22 generator representation of Figure 8-3-1 depicts a Helmholtz pair magnet, but there appears to be no first-principle reason why the less complex single solenoidal coil magnet used for the OCD conceptual designs could not be

designed appropriately for CCD applications. The magnet warm bore required is equivalent to the size of the hole permissible in the inner coil structure of such magnets which can be provided without affecting field quality in the interaction region.

For the generator itself, the very high current implies an unusual electrode system of significant surface area with respect to the plasma-wetted surface area of the disk. The mechanical design of the disk for Case 22 should be reasonably consistent with those for the OCD described in Section 6.1. The nozzle or another structure must provide the required swirl at the generator inlet, and the diffuser can be envisioned as similar to the OCD design since the residual swirl at the generator exit is approximately the same for both designs.

The coal combustor design for the CCD case can be very similar to those developed for the OCD cases, since the slag rejection performance must be equal to or better than that provided by the designs of Section 6.2.

The conceptual design of a full heat recovery system for the OCD cases evaluated in this report was not carried out. The CCD heat recovery system may be of substantially different design than that for an OCD system. Further delineation of features for both types of disk heat recovery systems is required before a reasonable cost comparison basis is established.

9.2 RELATIVE COST ASSESSMENTS

9.2.1 DISK GENERATORS

The operating pressure, temperatures, swirl, and Mach number for the OCD and CCD disks (at least with respect to the comparison CCD Case) are approximately the same. Therefore, the structural design of the OCD can be presumed to be appropriate for the Case 22 CCD, and the scaling factors for disk cost described in Section 7.1 apply to the OCD/CCD comparison as well-- with the exception that the costs of the larger electrode system will need to be added on to the scaled disk costs in the CCD case.

The estimated cost relationship for the disk structures is

$$\frac{C_{OCD}}{C_{CCD}} \approx \frac{R_{OCD}^2}{R_{CCD}^2}, \text{ giving}$$

for the comparison between the OCD Case 1A disk and CCD Case 22 disk the cost relationship is $C_{CCD} = 0.3 C_{OCD}$. The largest disk size found in the Table 8.3.1 CCD cases with 1000 MWe output is for Case 12 with $R_0 = 3.77$ m, and the relationship gives a relative cost of $C_{CCD} \approx 0.52 C_{OCD}$ with the 5.21 m radius OCD Case 1A generator as reference. Hence, the structure costs for a CCD are likely to be approximately half those for an OCD in a similar output MHD/steam power system.

The electrode system costs are expected to be significant; in fact, the area required to limit current loading to the same range as for the OCD cases (i.e. 30-50 kA/m²) is about 17 m² for the Case 22 load current. Using an approach similar to that taken for the OCD generators, almost the entire plasma-wetted surface of the Case 22 generator interaction region would have to be electrode surface. The quasi-one-dimensional model used in defining CCD parameters in this report would therefore not be adequate to predict CCD performance with the resulting current; in order to achieve a reasonable operating configuration, the electrodes must be distributed over vertical surfaces (such as those associated with swirl vanes and diffuser splitters) placed directly in the generator flow stream. The cost of the generator must then increase substantially. To a first level of approximation, the CCD generator for an MHD/steam system appears to show little or no cost advantage over the OCD generator for a plant with similar electrical power output.

9.2.2 POWER MANAGEMENT SYSTEM

The information developed for the reference OCD generator power management system provides sufficient information to permit an assessment of the specific cost (\$/kWe) for the Case 22 CCD power conditioning system. Since no co-sited ac generating capability is available in the CCD MHD/steam power system, the

VAR compensation must be provided by passive components. Table 9.2.1 contains cost information for the CCD Case 22 power management system under the assumption that the CCD generator can be operated as a two-terminal device. All converters are of identical design and power rating, and are paralleled across the generator. 126 converters are necessary if the 2000 A per bridge constraint is honored. The bridge power, 8.25 MWe, is low in comparison to the typical bridge power for the OCD design cases. The \$48.52/kWe (gross MHD output basis) compares with the \$45.38/kWe for a passively-compensated OCD system of 500 MWe. The much larger number of converter bridges and the relatively low bridge power result in the inflation of specific cost for the CCD Case.

9.2.3 COAL COMBUSTOR

Assuming that the design of CCD and OCD combustors are essentially the same, the comparative costs will be set by the thermal power level and combustion conditions. For a rough comparison of costs, the relation for combustors of equivalent power level and $L/D \approx 1$ is approximately.

$$\frac{C_{OCD}}{C_{CCD}} = \left(\frac{T_{OCD} P_{CCD}}{T_{CCD} P_{OCD}} \right)^{2/3}$$

The Case 22 CCD coal combustor operates at 2415 K and approximately 1.2, while OCD combustor conditions are 2835 K and 700kPa. For these values, the size of the CCD coal combustor will require that

$$C_{CCD} \approx 3 C_{OCD}.$$

Since combustor thermal rating is the same in each case, the specific costs are in the same relationship.

9.2.4 MAGNET

The single coil magnet design for the OCD generator system is directly applicable to providing the field for the CCD generator. Section 6.3.4.5 described a study of magnet costs which resulted in a cost scaling relationship

$$C \propto V^{0.6} B^{1.2}$$

TABLE 9.2.1. COST ESTIMATE FOR CASE 22 CCD
MHD POWER MANAGEMENT EQUIPMENT

Design Data: Total Power: 1039 MWe (gross MHD output)
 Number of Bridges: 126
 Bridge Current: 1992 A at 4139 V
 Bridge Power: 8.25 MWe
 Passive VAR Compensation Provided

<u>ITEM</u>	<u>ESTIMATED COST, F.O.B., MID-1980 DOLLARS</u>
Main Breaker (500 kV)	\$ 1,092,000
Main Transformer (34.5/500 kV)	3,371,800
VAR Capacitors	2,415,000
VAR Reactors	1,662,600
VAR Control	2,628,500
Damping Resistors	467,890
Filter Capacitors and Inductors	1,895,900
Cooling System	2,853,200
Converters and Valves	7,842,000
Converter Transformers	14,773,000
dc Reactors and Capacitors	3,412,500
dc Switchgear	1,278,600
Freewheel Diodes	496,880
34.5 kV Breakers	751,910
Inverter Controls	5,545,200
TOTAL	\$50,487,000
Specific Cost	\$48.52/kWe

For the OCD magnets, all of a design with similar thickness and magnetic induction, this reduced to

$$\frac{C_1}{C_2} = \left(\frac{R_1}{R_2} \right)^{1.2}$$

With the lower 6 Tesla magnetic induction proposed for the Case 22 CCD magnet, the expected cost relationship will be

$$\frac{C_{\text{CCD}}}{C_{\text{OCD}}} = \left(\frac{B_{\text{CCD}} R_{\text{CCD}}}{B_{\text{OCD}} R_{\text{OCD}}} \right)^{1.2}$$

Comparing the 7.65 meter magnet of OCD Case 1A with the 4.21 meter magnet required for CCD Case 22, if the magnet thickness is held constant

$$C_{\text{CCD}} = 0.4 C_{\text{OCD}}$$

Thus, magnet costs for the CCD generator will be significantly less than for the OCD generator. Since the costs of a Helmholtz pair have been estimated by NML to be roughly equivalent to those of a single coil design, the possible reversion to the Helmholtz pair for the CCD because of the larger depth of the interaction region required would not affect this conclusion.

10.0 REFERENCES

Section 2.1

- [1] Hals, F., "Parametric Study of Potential Early Commercial MHD Power Plants" NASA CR-159633, December 1979 (AVCO PSPEC).
- [2] Marston, C. H., et al, "Parametric Study of Potential Early Commercial MHD Power Plants" NASA CR-159634, February 1980 (GE PSPEC).

Section 3.1

- [1] Klepeis, J., and Rosa, R. J., "Experimental Studies of Strong Hall Effects and $V \times B$ Induced Ionization," 5th Symposium on Engineering Aspects of Magnetohydrodynamics, MIT, April 1964, "Experimental Studies of Strong Hall Effects and $U \times B$ Ionization - II," 6th Symposium on Engineering Aspects of Magnetohydrodynamics, Pittsburgh, April 1965, pp. 26-30.
- [2] Vithshas, A. F., Golubev, V. S. and Malikov, M. M., "Investigation of an Electrical Discharge in a Magnetic Field in the Presence of a Gas Flow," Proceedings of the Third International Conference on Magnetohydrodynamic Electric Power Generation, Salzburg, 1966, pp. 591-609, "Investigation of Ionization Instability in a Disk-shaped Hall Channel," Proceedings of the Fourth International Conference on Magnetohydrodynamic Electrical Power Generation, Warsaw, 1968, Vol. 1, pp. 529-545.
- [3] Louis, J. F., "Studies on an Inert Gas Disk Hall Generator Driven in a Shock Tunnel," 8th Symposium on Engineering Aspects of Magnetohydrodynamics, Stanford, March 1967, pp. 75-88.
- [4] Klepeis, J. E. and Louis, J. F., "High Hall Coefficient Studies in a Disk Generator Driven by Molecular Gases," 10th Symposium on Engineering Aspects of Magnetohydrodynamics, MIT, March, 1968, pp. 202-204; and "Studies with a Disk Generator Driven by Molecular Gases," 11th Symposium on Engineering Aspects of MHD, Pasadena, March 1970, pp. 62-63.
- [5] Shioda, S. and Yamasaki, H., "Generation Experiments with a Disk MHD Generator Under the Conditions of Fully Ionized Seed," 6th International Conference on Magnetohydrodynamic Electrical Power Generation, Washington, D.C., June 1975, Vol. III, pp. 105-114.
- [6] Loubsky, W. J., Hruby, V. J., and Louis, J. F., "Detailed Studies in a Disk Generator with Inlet Swirl Driven by Argon," 15th Symposium on Engineering Aspects of Magnetohydrodynamics, Philadelphia, May 1976, pp. VI.4.1-VI.4.5.
- [7] Klepeis, J. and V. Hruby, "MHD Power Generation Experiments with a Large Disk Channel: Verification of Disk Scaling Laws," 15th Symposium on Engineering Aspects of Magnetohydrodynamics, Philadelphia, May 1976, pp. VI.3.1-VI.3.6.

- [8] Klepeis, J. and Hruby, V., "The Disk Geometry Applied to Open Cycle MHD Power Generation: Experiment and Theoretical Considerations," 16th Symposium on Engineering Aspects of Magnetohydrodynamics, Pittsburgh, 1977, pp. I.5.31-I.5.37 and addendum.
- [9] Nakamura, T. and Jenkins, M. K., "Performance of Disk Generators for Open-Cycle MHD Power Generation", 18th Symposium on Engineering Aspects of Magnetohydrodynamics, Butte, June 1979, pp.B.3.1-B.3.11.
- [10] Louis, J. F., "Disk Generator", AIAA Journal, Vol. 6, No. 9, September 1968, pp. 1674-1678.
- [11] Klepeis, J. E., Cole, J., Hruby, V. J. and Louis, J. F., "The Disk Generator Applied to Open Cycle MHD Power Generation," 6th International Conference on Magnetohydrodynamic Electrical Power Generation, Washington, D.C., June 1975, Vol. I, pp. 251-266.
- [12] Klepeis, J. E., "Open Cycle Disk Generator Studies", 4th US/USSR Colloq. on MHD Electrical Power Generation, Washington, D.C., October 1978, pp. 411-414.
- [13] Dvore, D. S., Martinez-Sanchez, M. and Shamma, S. E., "Two Dimensional Effects in Disk Generators", 17th Symposium on Engineering Aspects of MHD, Stanford, March 1978, pp. B.2.1-B.2.7.
- [14] Lytle, J. K., Loubsky, W. J., Rosenbaum, M., and Louis, J. F., "Nonequilibrium Disk Generator Studies", 18th Symposium on Engineering Aspects of MHD, Butte, June 1979, pp. D-2.5.1-D-2.5.7.
- [15] Rosenbaum, M., Shamma, S. and Louis, J. F., "Experimental and Theoretical Studies of the Effects of Nonequilibrium in Equilibrium MHD Generators", 7th International Conference on MHD Electrical Power Generation, MIT, June 1980, pp. 486-494.
- [16] McCune, J. E. and Donaldson, Colman, duP., "On the Magnetohydrodynamics of Compressible Vortices", presented at ARS Semi-Annual Meeting, Los Angeles, May 1960. Printed in, Energy Conversion for Space Power, edited by Snyder, N.W., Academic Press, 1961, pp. 715-741.
- [17] Donaldson, Coleman duP., "The Magnetohydrodynamic Vortex Power Generator: Basic Principles and Practical Problems", presented at the Second Symposium on the Engineering Aspects of Magnetohydrodynamics, Philadelphia, March 1961. Printed in Engineering Aspects of Magnetohydrodynamics, edited by Mannual and Mather, Columbia University Press, 1962, pp. 228-254.
- [18] Jenkins, M. K., Nakamura, T., Vilas, T. R. and Eustis, R. H. "Experimental Results of a High Magnetic Field Combustion Disk Generator", 7th International Conference on MHD Electrical Power Generation, MIT, June 1980, pp. 495-502.

Section 5.1

- [1] Omori, S., et al, "High Slag Rejection, High Carbon Conversion Rate, Air Cooled Cyclone Coal Combustor" 18th Symposium on Engineering Aspects of Magnetohydrodynamics, Butte, June 1979.
- [2] Rosenbaum, M., et al, "Experimental and Theoretical Studies of the Effects of Nonuniformities in Equilibrium MHD Generators" 7th International Conference on Magnetohydrodynamics, Cambridge, MA, June 1980.
- [3] Jenkins, M. K., et al, "Experimental Results of a High Magnetic Field Combustion Disk Generator" 7th International Conference on Magnetohydrodynamics, Cambridge, MA, June 1980.

Section 5.2

- [1] Svehla, R. A. and McBride, B. J., "FORTRAN IV Computer Program Calculation of Thermodynamic and Transport Properties of Complex Chemical Systems" NASA TN D-7056, 1973.
- [2] DOE Workshop on Chemical Equilibrium and Transport Properties, Germantown, MD, September 13-14, 1979.
- [3] Letter, D. L. Chubb (NASA-Lewis) to D. L. Black (Westinghouse AESD), dated October 3, 1979.
- [4] Lippert, T. E. and Weeks, K. D., "Open Cycle MHD Systems Analysis", Westinghouse R&D Center Report 79-5E61-SYMHD-R2.

Section 6.1

- [1] Demirjian, A., et al, "Electrode Development for Coal-Fired MHD Generators", 17th Symposium on Engineering Aspects of Magnetohydrodynamics, Stanford, March 1978.
- [2] Kline, S. J., et al, "Optimum Design of Straight-walled Diffusers" J. Basic Engrg Series D, No. 3, September 1959 p. 195.

Section 6.2

- [1] Nakamura, T. and Jenkins, M. K., "Performance of Disk Generators for Open Cycle MHD Power Generation" 18th Symposium on Engineering Aspects of Magnetohydrodynamics, Butte, June 1979.

Section 6.3

- [1] Hatch, A.M. "Cost Estimates and Cost Analysis Techniques for Superconducting MHD Magnets" NML Quarterly Report.

Section 6.5

- [1] Sistino, A. J., "Analytical Studies of NO_x Decomposition in the Radiant Boiler of an Open-Cycle MHD Power Plant" ANL/MHD-79/7, April 1979.
- [2] Hopenfeld, J., "Simplified Correlations for Prediction of NO_x Emissions from MHD Power Plants" J. Energy, V. 3, No. 6 p. 335.

Section 7.3

- [1] Marston, C. H., et al, "Parametric Study of Potential Early Commercial MHD Power Plants" NASA CR-159634, February 1980.
- [2] Hals, F., "Parametric Study of Potential Early Commercial MHD Power Plants" NASA CR-159633, December 1979.

Section 8.1

- [1] Lytle, J. K., et al, "Nonequilibrium Disk Generator Studies", 18th Symposium on Engineering Aspects of MHD, Butte, June 1979.
- [2] Louis, J. F., "Studies on an Inert Gas Disk Hall Generator Driven in a Shock Tunnel", 8th Symposium on Engineering Aspects of Magnetohydrodynamics, Stanford, March 1967.
- [3] Spencer, F.E., and Phelps, A. V., "Momentum Transfer Cross-Sections and Conductivity Integrals for Gases of MHD Interest" 15th Symposium on Engineering Aspects of Magnetohydrodynamics, Philadelphia, May 1976.
- [4] Loubsky, W. J., et al, Proceedings of 3rd US/USSR Colloquium on MHD Electric Power Generation, Moscow, 1976.
- [5] Shioda, S., et al, "Power Generation Experiments and Prospects of Closed-Cycle MHD with Fully Ionized Seed" 7th International Conference on MHD, MIT, June 1980.
- [6] General Electric Phase I Final Report: Energy Conversion Alternatives Study (ECAS), NASA CR-134948, February 1976.

Section 8.3

- [1] General Electric Phase I Final Report: Energy Conversion Alternatives Study (ECAS), NASA CR-134948, February 1976.
- [2] Zauderer, B. "Systems Studies of Coal Fired Closed Cycle MHD for Central Station Power", 15th Symposium on Engineering Aspects of Magnetohydrodynamics, Philadelphia, May 1976.

APPENDIX A

APPENDIX A

ESTIMATION OF RELATIVE HEAT LOSSES FOR COMBUSTOR/NOZZLE OF OUTFLOW AND INFLOW DISK GENERATORS.

Introduction

Although the absolute values of heat loss will vary greatly with the details of the combustor design, it is nevertheless possible to estimate, within reasonable error bounds, the relative heat losses for an outflow configuration having two combustion stages, and an inflow configuration having n two-stage combustors and a toroidal plenum to distribute their output around the periphery of the generator. The insulation/cooling technology for all the hot walls is assumed to be the same for each case. Figures A1-1 and A1-2 define the geometries assumed for this analysis.

If ρ_1 and ρ_2 are the first and second stage mean gas densities, respectively, then to a good approximation, we obtain the following expressions for the gas residence times and component wall areas:

$$\tau_1 = \frac{\pi \rho_1 \theta_1 d_1^3}{4m}$$

$$\tau_2 = \frac{\pi \rho_2 \theta_2 d_2^3}{4m}$$

$$a_1 = \pi d_1^2 (\theta_1 + \frac{1}{2})$$

$$a_2 = \pi d_2^2 (\theta_2 + \frac{1}{4})$$

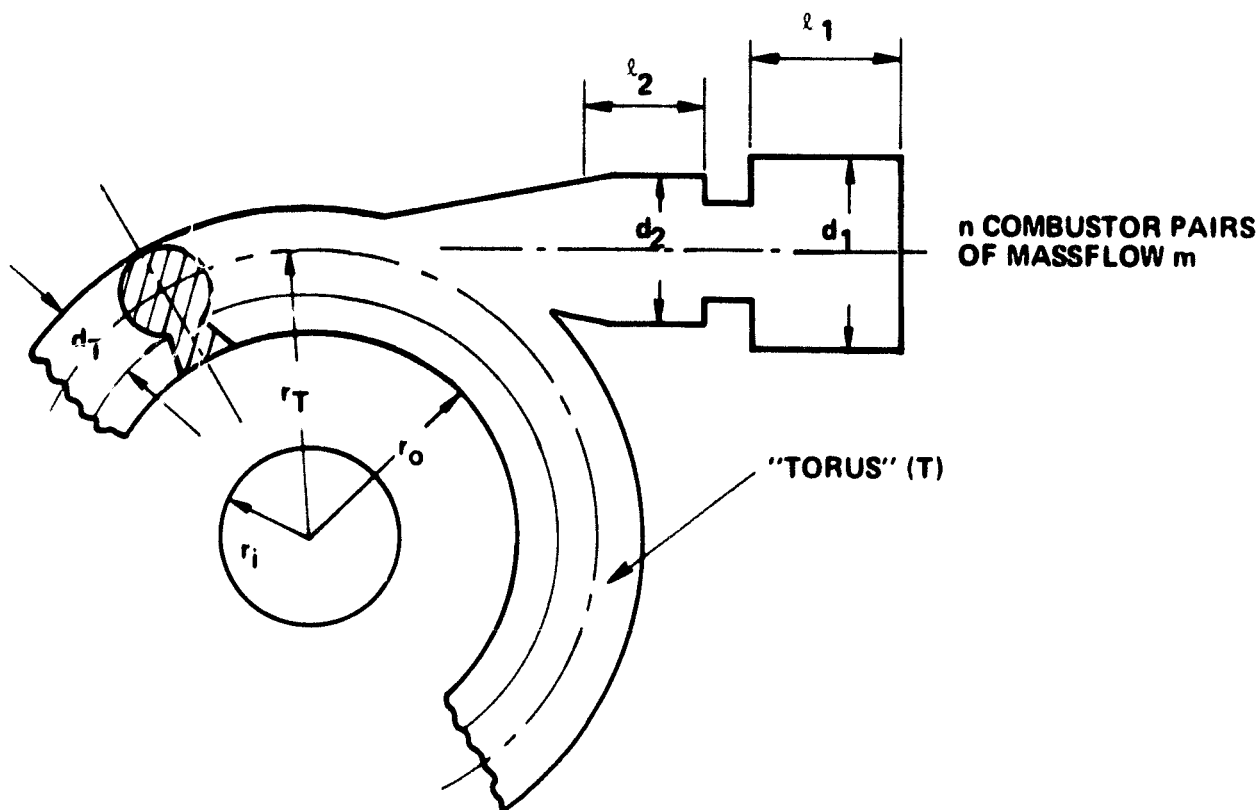
$$a_T = 2 \pi^2 \phi d_2 r_T$$

$$A_N = \pi [\sqrt{2}/4 D_2^2 + r_i (1 + \sqrt{2})]$$

$$t_1 = \frac{\pi \rho_1 \phi_1 D_1^3}{4M}$$

$$t_2 = \frac{\pi \rho_2 \phi_2 D_2^3}{4M}$$

We can now look at the component heat loss ratios in terms of various heat-transfer and scaling law models. For the first (gasifier) stage, use is made of a scaling proposed by Wright⁽¹⁾.



r_i = GENERATOR INNER RADIUS
 r_o = GENERATOR OUTER RADIUS
 r_T = TORUS/PLENUM MEAN RADIUS
 WALL AREAS $a_i, i = 1, 2, T$
 GAS RESIDENCE TIMES $\tau_i, i = 1, 2$

$$(l/d)_i \equiv \theta_i, i = 1, 2$$

$$r_o/r_i \equiv a$$

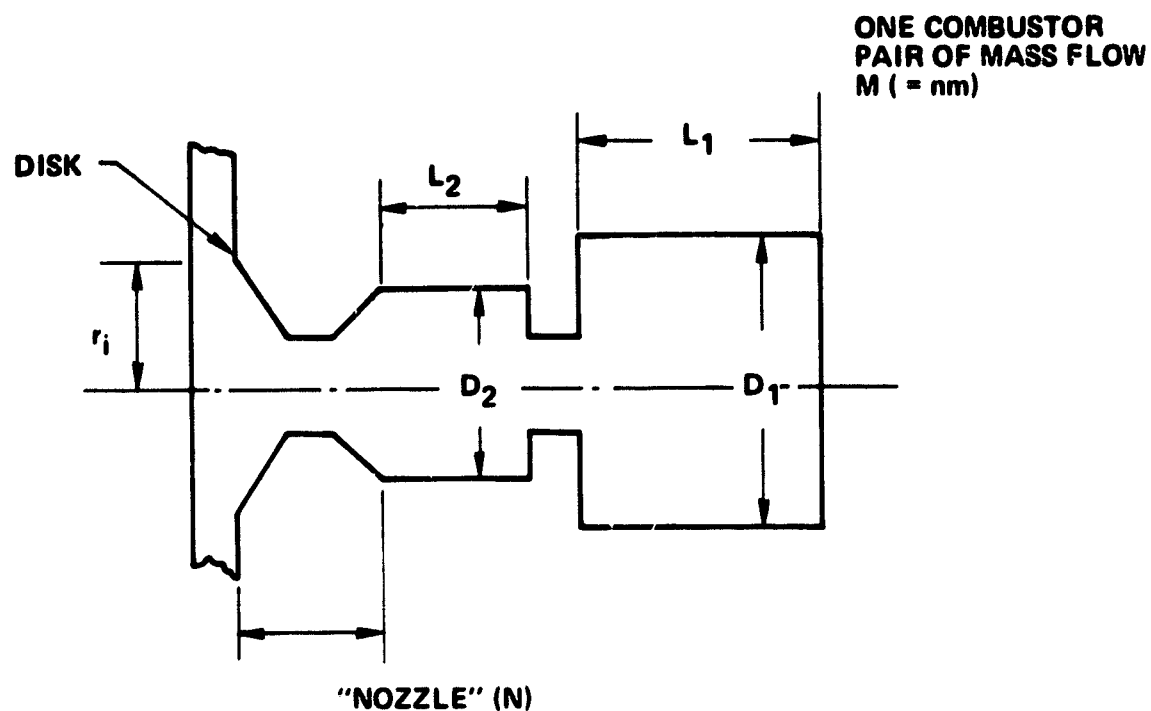
$$r_T/r_o \equiv \beta$$

$$d_T/d_2 \equiv \psi$$

$$\rho_1/\rho_2 \equiv \delta$$

705374-2A

Figure A-1. Inflow Geometry for Disk Generator Combustors



$$r_i/D_2 \equiv \epsilon$$

$$(L/D)_i \equiv \phi_i, i = 1, 2$$

WALL AREAS $A_i, i = 1, 2, N$

GAS RESIDENCE TIMES $t_i, i = 1, 2$

7-5374-3A

Figure A-2. Outflow Geometry for Disk Generator Combustors

First-stage scaling and heat loss

Use Wright's scaling of $\frac{m}{M} = \left(\frac{d_1}{D_1} \right)^{5/2}$

Now,

$$m = \frac{M}{n} \rightarrow \frac{1}{n} = \left(\frac{d_1}{D_1} \right)^{5/2}$$

$$\rightarrow n^{-2/5} = \frac{d_1}{D_1}$$

$$\rightarrow d_1 = D_1 n^{-2/5}$$

Wright also requires $\theta_1 = \phi_1$ (L/D constant). Thus the ratio of first-stage total wall areas is:

$$R_1 \equiv \frac{na_1}{A} = \frac{\pi n D_1^2 n^{-4/5} (\theta_1 + 1/2)}{\pi D_1^2 (\phi_1 + 1/2)} = n^{1/5}$$

n	R_1
2	1.149
4	1.320
6	1.431
8	1.516

If we assume that the heat transfer in the first stage is primarily convective, since the gas is optically thick, then the heat loss scales with the wall area, to a first approximation, i.e. $R_{H_1} = R_1$.

If the temperature of the first-stage combustion products is kept to a low value such that the walls can be run nearly at gas temperature, the heat loss magnitude will be small. A reasonable value might be 1% of the total enthalpy entering the entire combustion system.

Second-stage scaling and heat loss

We must assume $\tau_2 = t_2$ for these gas-gas combustors, then, from the earlier work,

$$d_2 = D_2 \left(\frac{\phi_2}{n\theta_2} \right)^{1/3}$$

and if we assume $\theta_2 = \phi_2 = \theta_{opt}$, then we obtain for the ratio of second-stage total wall areas,

$$R_2 \equiv \frac{na_2}{A_2} = n \left(\frac{d_2}{D_2} \right)^2 = n^{1/3}$$

Now suppose that the heat transfer is due to radiation and convection, such that for the large combustor the ratio $Q_r/Q_c \equiv F$. In general, we would expect $1 < F < 4$ for full-scale combustors for a variety of fuels. Then,

$$Q = h_G A_2 [T_p - T_w] + \epsilon_G \sigma A_2 [T_p^4 - T_w^4]$$

and

$$q = h_g a_2 [T_p - T_w] + \epsilon_g \sigma a_2 [T_p^4 - T_w^4]$$

and from Sarofim,⁽²⁾ for a gas which is neither optically thin nor optically thick,

$$\epsilon_g \approx K d^f$$

$$\epsilon_g \approx K D^f, \text{ where } 0.3 \leq f \leq 0.7, \text{ and } K \text{ is a constant.}$$

Let us adopt a representative mean value of $f = 0.5$, and take $h_g = h_g = h$, then,

$$q = h a_2 [T_p - T_w] + K' a_2 d_2^{1/2} [T_p^4 - T_w^4]$$

and

$$Q = h A_2 [T_p - T_w] + K' A_2 D_2^{1/2} [T_p^4 - T_w^4],$$

where

$$K' = Kd$$

By definition:

$$F = \frac{K' D_2^{1/2} [T_p^4 - T_w^4]}{h [T_p - T_w]} = \frac{K'' D_2^{1/2}}{h [T_p - T_w]}$$

where

$$K'' = K' [T_p^4 - T_w^4]$$

Thus, the total heat loss ratio for the second stages is

$$R_{H_2} = \frac{nq}{Q} = \frac{n[K'' D_2^{1/2} F^{-1} a_2 + K'' a_2 d_2^{1/2}]}{K'' D_2^{1/2} F^{-1} A_2 + K'' A_2 D_2^{1/2}} = \frac{n^{1/3} [1/F + (d_2/D_2)^{1/2}]}{1/F + 1}$$

$$\text{But, } (d_2/D_2)^{1/2} = n^{-1/6}$$

$$\text{Thus, } R_{H_2} = \frac{F n^{1/6} + n^{1/3}}{F + 1}$$

and tabulating:

F \ n	2	4	6	8
1	1.191	1.424	1.583	1.707
2	1.168	1.369	1.504	1.609
4	1.150	1.325	1.442	1.531

Ratio of heat loss between "Torus" and "Nozzle"

Again, let the ratio of radiative and convective flux be F for the nozzle of the outflow case. Then, from earlier work,

$$R_3 \equiv \frac{\text{Area torus}}{\text{Area nozzle}} \equiv \frac{a_T}{A_N} = \frac{2 \alpha \beta \epsilon n^{-1/3} \pi \psi}{\epsilon^2 (1 + \sqrt{2}) + \sqrt{2}/4}$$

As for the second-stage combustors,

$$Q_T = h a_T [T_p - T_w] + K' a_T d_T^{1/2} [T_p^4 - T_w^4]$$

and

$$Q_N = h A_N [T_p - T_w] + K' A_N L_N^{1/2} [T_p^4 - T_w^4]$$

where d_T and L_N are the characteristic length dimensions of the torus and nozzle, respectively, for radiative calculation purposes. In the spirit of the earlier calculations, we may identify $d_T \approx d_2$ (i.e. $\psi = 1$) and $L_N \approx D_2$;

Then, by definition

$$F = \frac{K'' D_2^{1/2}}{h [T_p - T_w]}$$

and the heat loss ratio becomes

$$R_{H_3} \equiv \frac{Q_T}{Q_N} = \frac{(D_2/F)^{1/2} + d_2^{1/2} a_T}{(D_2/F)^{1/2} + D_2^{1/2} A_N} = \frac{R_3 [1 + F n^{-1/6}]}{1 + F}$$

By way of example, let us make a reasonable choice of the geometrical and mean density ratios, i.e. $\tau_1/\tau_2 = t_1/t_2 = 5/2$; $\delta = 5/4$; $\epsilon = 2/3$; $\alpha = 3$; and $\beta = 5/4$. Then we find that, for $n = 4$, $R_3 = 6.937$, and tabulating:

F	R_{H_3}
1	6.221
2	5.983
4	5.792

We now need to make some estimate of the relative magnitudes 'P' of the total heat losses in the first stage, second stage and nozzle of the outflow case. From earlier work,

$$\frac{A_N}{A_2} = \frac{\sqrt{2}/4 + \epsilon (1 + \sqrt{2})}{\phi_2 + 1/4}$$

and for $\phi_2 = 1$, and $\epsilon = 2/3$,

$$\frac{A_N}{A_2} = \frac{.3535 + 1.07}{1.25} = 1.141$$

If the value of F is the same for the nozzle and the second stage, then the losses will be in the ratio A_N/A_2 .

If the total heat loss for the outflow case is 7%, which is a reasonable value for current cooling techniques with 1% debited to the first stage, then:

$$.07 = .01 + P_2 + P_N$$

and

$$P_N = 1.141 P_2$$

yielding

$$P_2 = .028 \text{ and } P_N = .032$$

Thus, for $n = 4$ and $F = 2$,

$$\frac{\text{Inflow heat loss}}{\text{Outflow heat loss}} = \frac{.0132 + .028 \times 1.369 + .032 \times 5.983}{.01 + .028 + .032} = 3.47$$

For $F = 4$, $n = 4$, the value drops slightly to 3.37.

By careful design, one could probably get this ratio down to between 2.5 and 3.0 but this must be a lower limit. The design goal for the inflow case would have to be the minimization of the torus wall area while still maintaining an acceptable degree of uniformity in the entry flowfield.

The situation will improve for $\theta_2 > 1$ and for $(d_T/d_2) \equiv \psi < 1$, since this reduces the torus wall area. For $\psi \neq 1$,

$$\begin{aligned} \frac{Q_T}{Q_N} &= \frac{a_T h [T_p - T_w] + K' d_2^{1/2} \psi^{1/2} [T_p^4 - T_w^4]}{A_N h [T_p - T_w] + K' L_N^{1/2} [T_p^4 - T_w^4]} \\ &= \frac{(a_T/A_N) [1 + F \psi^{1/2} n^{-1/6}]}{1 + F} \end{aligned}$$

and

$$\frac{a_T}{A_N} = \frac{2\pi\psi\alpha\beta\epsilon (\phi_2/n\theta_2)^{1/3}}{\sqrt{2}/4 + \epsilon^2 (1 + \sqrt{2})}$$

Thus, the radiative loss scales with $\psi^{3/2}$ and the convective loss with ψ . Then, with a reasonable geometry, i.e. $\alpha = 3$, $\beta = 5/4$, $\epsilon = 2/3$, and $\phi_2 = e_2$, we obtain:

$$\frac{Q_T}{Q_N} = \frac{11.01 \psi n^{-1/3} [1 + F \psi^{1/2} n^{-1/6}]}{1 + F}$$

Thus, tabulating values of R_{H_3} for credible ranges of values of n , ψ , and F :

		$n = 4$		$n = 8$	
$F \backslash \psi$		0.8	0.6	0.8	0.6
2		4.476	3.093	3.325	2.307
4		4.261	2.879	3.109	2.108

For the extreme credible case, i.e., radiative heat transfer four times convective; eight combustors; and a torus reduced in cross-sectional area to only 36% of the second stage combustor cross-sectional area, the value of R_{H_3} still exceeds 2.1.

We can thus conclude that for all practical choices of geometry, the heat loss of the "torus" will always be several times that of the "nozzle", and that the combustor-plus-nozzle heat loss for the inflow system must always be at least 2.5 times that of the equivalent outflow system, and that even this unfavorable ratio is to be obtained only at the expense of severe compromises of the desirable geometry.

REFERENCES FOR APPENDIX A

- (1) Wright, R. J., "Scaling MHD Cyclone Coal Combustors," Proc. 18th MHD Symposium, Stanford, 1979, p. K.6.8.
- (2) Sarofim, A. F. and H. C. Hottel, "Radiative Transfer in Combustion Chambers: Influence of Alternative Fuels," Proc. 6th International Heat Transfer Conf., Toronto, Aug. 1978.

APPENDIX B

APPENDIX B

CLOSED CYCLE DISK EQUATIONS AND SOLUTIONS

For all the cases examined in this study the relaxation length is negligibly small compared to the generator interaction length, and Saha equilibrium for the electrons prevails. This was verified using the finite-rate kinetics (and energetics) code described in Section 8.0. The system of equations used for the generator suboptimization and the method of solution is outlined below.

System of Equations (see Nomenclature)

Neutral gas momentum:

$$\frac{du_r}{dr} = C_1 \frac{dT}{dr} \gamma/(\gamma-1) + C_1 C_2 T/\rho + C_4$$

$$\frac{du_\theta}{dr} = -u_\theta/r - (j_r B + f_\theta) \rho u_r$$

Neutral gas energy:

$$\frac{d\rho}{dr} = C_2 + C_3 \frac{dT}{dr}$$

where

$$C_1 = -R/u_r$$

$$C_2 = -[\hat{v}k (T_e - T) + f_r u_r + f_\theta u_\theta]/(u_r RT)$$

$$C_3 = \rho/(\gamma - 1)T$$

$$C_4 = u_\theta^2/ru_r + (j_\theta B - f_r)/\rho u_r$$

Neutral gas continuity:

$$\dot{m} = \rho u_r 2\pi r z$$

Electron energy:

$$(j_r^2 + j_\theta^2)/\sigma_e = \hat{v} k (T_e - T) + Q_R$$

Saha equation:

$$N_e = f(\chi, p, T_e)$$

Ohm's law:

$$E = j_r (1 + \beta_e^2)/\sigma_e - (u_\theta + \beta_e u_r) B$$

$$j_\theta = -\sigma_e u_r B + \beta_e j_r$$

Current conservation:

$$I = 2\pi r z j_r$$

Constraint equation (for operation at maximum electrical efficiency):

$$j_r = \beta_1 \sigma_e (\beta_e + S) u_r B / (\beta_1 + S_1) (1 + \beta_e^2)$$

Additional relations:

(friction)

$$f_\theta = S f_r$$

$$f_r = \rho C_f u u_r / z, \text{ where } u^2 = u_r^2 + u_\theta^2$$

$$C_f = .058 R_e^{-0.2}$$

$$R_e = \rho u (r - r_0) / \mu, \text{ where } r_0 = .75 r_{\text{inlet}}$$

$$\mu = 2.02 \times 10^{-5} + 3.40 \times 10^{-8} T$$

(reduction formulae for effective plasma properties)

$$\beta = \frac{\beta^2}{1 + \beta^2} \hat{I}$$

$$\beta_e = \frac{1 + \beta^2}{1 + \frac{\beta^3}{1 + \beta^2} \hat{I}}$$

$$\frac{\sigma_e}{\sigma} = \frac{\left(\frac{\beta^2 \hat{I}}{1 + \beta^2} \right)^2}{\frac{\hat{I} \beta^3}{1 + \beta^2}}$$

where

$$\hat{I} = \frac{(\beta^2 - 1) \tan^{-1} \beta}{2\beta} - \frac{1}{2\beta}$$

and

$$\beta = \frac{eB}{m_e v}$$

(collision frequency and cross section)

$$\nu = c_e (nQ_g + N_e Q_{ei})$$

$$c_e^2 = \frac{8k T_e}{\pi m_e}$$

$$n = \rho/m$$

$$m = \frac{\tilde{m}}{L} = \frac{\overset{\text{CO}_2}{f_1(44)} + \overset{\text{CO or N}_2}{f_2(28)} + \overset{\text{Argon}}{40} + \overset{\text{Cs}}{x(133)}}{L}$$

$$Q_{ei} = (5.85 \times 10^{-10} \ln \Lambda) / T_e^2 \text{ mks units}$$

$$\Lambda = 1.24 \times 10^7 T_e^3 N_e$$

$$Q_g = f_1 Q_{g1} + f_2 Q_{g2} + Q_{gAr} + (n_{cs}/n) Q_{cs}$$

$$n_{cs} = n_x - N_e$$

$$Q_{g1} = 12 \times 10^{-20} m^2 \text{ (CO}_2 \text{, input)}$$

$$Q_{g2} = 10 \times 10^{-20} m^2 \text{ (N}_2 \text{, CO input)}$$

$$Q_{cs} = 1.0 \times 10^{-17} - (1.453 \times 10^{-19} T_e - 1000)$$

$$Q_{gAr} = 3.68 \times 10^{-24} (T_e - 1500) + .38 \times 10^{-20} \text{ for } T_e \geq 1500 \text{ K}$$

$$= .38 \times 10^{-20} \text{ for } T_e < 1500 \text{ K}$$

$$\sigma = \frac{N_e e^2}{m_e v}$$

$$\hat{v} = 3 m_e N_e c_e \left[n \left(\frac{f_1 \delta_1 Q_{g1}}{m_1} + \frac{f_2 \delta_2 Q_{g2}}{m_2} + \frac{Q_{gAr}}{m_{Ar}} \right) + \frac{n_{cs} Q_{cs}}{m_{cs}} + \frac{Q_e N_e}{m_{cs}} \right]$$

where

$$m_1 = 44/L$$

$$m_2 = 28/L$$

$$m_{Ar} = 40/L$$

$$m_{cs} = 133/L$$

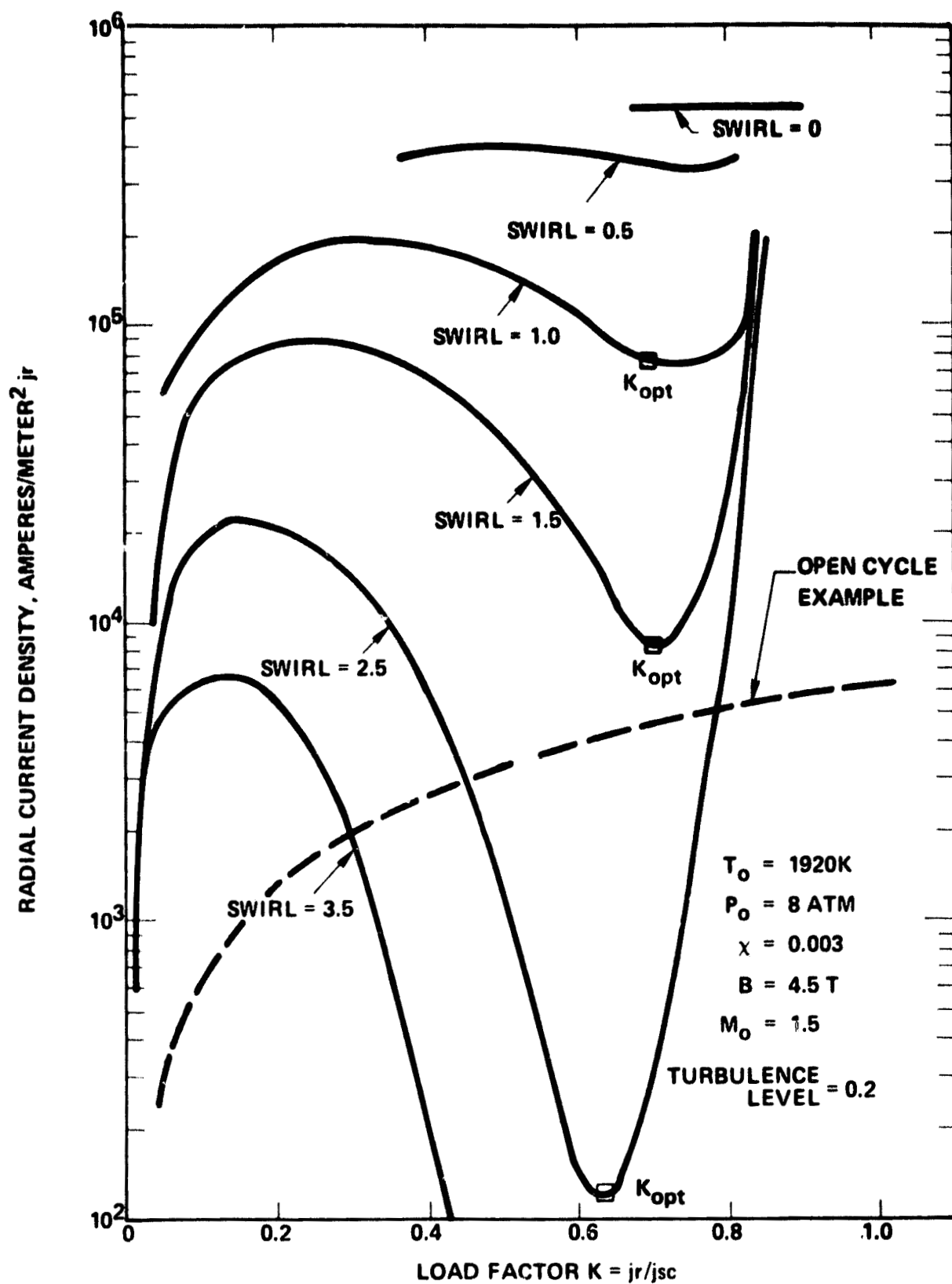
(radiation)

$$Q_r = f(z, n, T, T_e, N_e, n_{cs})$$

Method of Solution

The inputs for the channel calculation are the inlet stagnation conditions, Mach number, swirl, height, and radius. In addition, the B-field, turbulence level, seed fraction and impurity fraction and cross sections are required. The calculation begins at the inlet with a guess value for T_e . The plasma properties are computed and the electron energy equation is checked. Iteration on T_e is carried out until the energy equation is satisfied. This procedure is used for each integration step. The integration is carried-out by a standard Runge-Kutta technique with a variable grid size.

One draw-back of single electrode-pair devices is that controllability of loading must be accomplished entirely by the design of the local channel area (cross-section). In the open-cycle disk case, for given local stagnation conditions, swirl, magnetic field and total Mach number the short circuit current density is fixed (since the properties, σ , β are uniquely determined). Hence, the variation of area with loading (i.e., current load factor, K) is linear, as depicted in Figure B-1. In nonequilibrium disks the effective properties are coupled to the loading, and this coupling is not unique. For example, it can be seen in Figure B-1 that for certain specified areas (or radial current density, j_r) three possible loadings can exist. This presents some difficulty in the numerical analysis/integration of the channel design, particularly when operation at the optimum K (which occurs near the minimum of the j_r versus K curve) is desired. During an integration step the calculation can become unstable, with a jump to near open circuit conditions, if the current density (or area) is calculated prior to K and iteration is based on K approaching K_{opt} . The problem is resolved by first calculating $K = K_{opt}$ and iterating on the total current, I . That is, the gas temperature gradient is varied during each integration step until a value (of dT/dr) is found such that I (when calculated from the optimum load factor) remains constant (to within 0.1% of the value calculated at the previous step). This procedure can be applied to closed-cycle linear diagonal generator calculations as well.



705374-1A

Figure B-1. Load Map for Closed Cycle Disk Generator

NOMENCLATURE FOR APPENDIX B

B	Magnetic field strength
c_e	Electron thermal speed
C_f	Friction coefficient
E	Electric field strength
e	Electron charge
$f_{1,2}$	Mole fraction of impurities 1,2
f_r	Radial friction term
F_θ	Azimuthal friction term
I	Total/load current
j_r	Radial current density
j_θ	Azimuthal current density
k	Boltzmann's constant
K	Current load factor
K_{opt}	Optimum load factor
L	Avogadro's number
$m_{1,2}$	Mass of species 1,2
m_e	Electron mass
\bar{m}	Average molecular weight
\dot{m}	Mass flow rate
n	neutral gas number density
n_{cs}	Cesium number density
N_e	Electron density
p	Pressure
Q_{gAr}	Argon cross section

Nomenclature (cont'd)

$Q_{g1,2}$	Cross section of species 1,2
Q_{ei}	Coulomb cross section
Q_{cs}	Cesium cross section
Q_R	Radiation energy term
r	Radius
R	Gas constant
R_r	Reynold's number
S	Swirl ratio u_θ/u_r
S_1	$1 + S^2$
\hat{S}	Mean square of turbulence fluctuations
T	Gas temperature
T_e	Electron temperature
u_r	Radial gas velocity component
u_θ	Azimuthal gas velocity component
z	Channel height
β	Ideal/microscopic Hall parameter
β_e	Effective Hall parameter
β_1	$1 + \beta_e^2$
$\epsilon_{1,2}$	Collisional loss factor for species 1,2
γ	Specific heat ratio
μ	Plasma viscosity
ν	Collision frequency

$\hat{\nu}$	Energy averaged collision frequency
ρ	Neutral gas density
σ	Ideal plasma conductivity
σ_e	Effective plasma conductivity
x	Seed fraction of cesium

APPENDIX B

STATEPOINTS FOR CLOSED CYCLE DISK MHD/STEAM SYSTEM WITH COAL COMBUSTOR-FIRED ARGON REGENERATOR 33 CASE SUMMARY

NOTES

1. Plant efficiency (η_{plant}) does not include decrement for parasitic loads such as cooling tower, circulating pumps, SO_2 scrubber system.
2. Enthalpies rather than temperatures are reported for the following stations:
 - A. Economizer outlet (steam side)
 - B. Regenerator valve cooler outlet
 - C. Combustor cooling system outlet
3. System to operate at match point.

CCD/MHD/STEAM SYSTEMS PERFORMANCE SURVEY - CASE NO. 1

Assumed Coal Firing Rate = 784.2 MWt
MHD Gross Power Output: 375.7 MWe (V1)
Argon Compressor Pressure Ratio: 4.93
Disk/Diffuser Pressure Ratio: 4.33
 n_{HS} (calculated) = 88.9%; n_{Stm} (calculated) = 41.5%; n_{Plant} = 48.0%

A. ARGON LOOP (\dot{m} argon = 1060 kg/s)

Location	Temp, K	Power to Argon, MW
Compressor Inlet	330	-
Compressor Outlet	657.2	+ 178.8
Preheater Outlet	* 922	+ 144.7
Regenerator Outlet	*1920	+ 545.4
Disk Generator Outlet	1232	- 375.7
Radiant Furnace Outlet	1137	- 51.7
Reheater Outlet	*1000	- 75.0
ITAH Outlet	816.9	- 100.0
Economizer Outlet	* 471	- 189.1
LPFH Outlet	338.7	- 72.3
Precooler Outlet	330	- 4.78

B. STEAM LOOP (\dot{m} steam = 121.7 kg/s)

Location	Temp, K	Press, 10^5 Pa	Power, MW
Hotwell	*312	* (2" HgA)	-
Condensate Pump Discharge	*312.6	* 10.0	+ .16
LPFH	*451	* 9.53	+ 71.9
Main Feed Pump Discharge	*457.4	*273.9	+ 4.99
Economizer Out	(2.340 E6)	*265.7	+ 188.1
Valve Cooler Out	(2.434 E6)	*257.7	+ 11.4
Combustor Cooling Out	(2.883 E6)	*250.0	+ 54.6
Radiant Furnace Out	*811	*242.0	+ 51.5
HP Turbine Out	*564	*45.0	- 47.9
Reheater Out	*811	*40.0	+ 75.2
LP Turbine Out	"	-	- 145.8
Condenser Out	*312	* (2" HgA)	- 264.2

C. AIR SYSTEM (\dot{m} air = 242.4 kg/s)

Location	Temp, K	Power, MW
Compressor Inlet	* 288	-
Compressor Outlet	* 305	+ 4.09
ITAH 2 Outlet	* 479.8	+ 43.3
ITAH 1 Outlet	546.0	+ 16.8
ITAH Outlet	* 922	+ 99.5

D. COMBUSTION GAS SYSTEM

Location	Temp, K	\dot{m}_c , kg/s	Power, MW
Combustor	*2415	-	+ 893.0**
Regenerator Out	*1090	270.1	- 574.1
Argon Preheater Out	671.1	270.1	- 145.5
ITAH 1 Out	* 611	270.1	- 16.9
ITAH 2 Out	* 408	182.7	- 43.5
Coal Dryer Out	* 408	87.4	- 20.7
Stack	*(408)	(270.1)	- 60.5

*Denotes fixed quantities for all cases.

**Includes air and coal; deducts cooler losses.

MATCH POINT DEVIATION = + 5.72 MW

CCD/MHD/STEAM SYSTEMS PERFORMANCE SURVEY - CASE NO. 2

Assumed Coal Firing Rate = 949.0 MWt
MHD Gross Power Output: 459.1 MWe (V1)
Argon Compressor Pressure Ratio: 5.08
Disk/Diffuser Pressure Ratio: 4.46
 η_{HS} (calculated) = 89.5%; η_{Stm} (calculated) = 41.5%; η_{Plant} = 47.8%

A. ARGON LOOP (\dot{m}_{argon} = 1294 kg/s)

Location	Temp, K	Power to Argon, MW
Compressor Inlet	330	-
Compressor Outlet	665.7	+ 222.0
Preheater Outlet	* 922	+ 169.5
Regenerator Outlet	*1920	+ 660.0
Disk Generator Outlet	1225	- 459.1
Radiant Furnace Outlet	1138	- 57.7
Reheater Outlet	*1000	- 91.2
ITAH Outlet	825.5	- 115.4
Economizer Outlet	* 471	- 234.4
LPFH Outlet	338.5	- 87.6
Precooler Outlet	330	- 5.60

B. STEAM LOOP (\dot{m}_{steam} = 147.5 kg/s)

Location	Temp, K	Press, 10^5 Pa	Power, MW
Hotwell	*312	* (2" HgA)	-
Condensate Pump Discharge	*312.6	* 10.0	+ .20
LPFH	*451	* 9.53	+ 87.2
Main Feed Pump Discharge	*457.4	*273.9	+ 6.06
Economizer Out	(2.375 E6)	*265.7	+ 233.3
Valve Cooler Out	(2.469 E6)	*257.7	+ 13.8
Combustor Cooling Out	(2.917 E6)	*250.0	+ 66.1
Radiant Furnace Out	*811	*242.0	+ 57.4
HP Turbine Out	*564	*45.0	+ 58.1
Reheater Out	*811	*40.0	+ 91.1
LP Turbine Out	-	-	- 176.8
Condenser Out	*312	* (2" HgA)	- 320.4

C. AIR SYSTEM (\dot{m}_{air} = 293.3 kg/s)

Location	Temp, K	Power, MW
Compressor Inlet	* 288	-
Compressor Outlet	* 305	+ 4.95
ITAH 2 Outlet	* 479.8	+ 52.4
ITAH 1 Outlet	564.2	+ 25.9
ITAH Outlet	* 922	+ 114.8

D. COMBUSTION GAS SYSTEM

Location	Temp, K	\dot{m}_c , kg/s	Power, MW
Combustor	*2415	-	+ 1081.0**
Regenerator Out	*1090	326.9	- 694.8
Argon Preheater Out	686.8	326.9	- 170.4
ITAH 1 Out	* 611	326.9	- 26.0
ITAH 2 Out	* 408	221.0	- 52.7
Coal Dryer Out	* 408	105.9	- 25.1
Stack	*(408)	(326.9)	- 73.2

*Denotes fixed quantities for all cases.

**Includes air and coal; deducts cooler losses.

MATCH POINT DEVIATION = +1.82 MW

CCD/MHD/STEAM SYSTEMS PERFORMANCE SURVEY - CASE NO. 3

Assumed Coal Firing Rate = 866.4 MWt
MHD Gross Power Output: 415.8 MWe (VI)
Argon Compressor Pressure Ratio: 5.17
Disk/Diffuser Pressure Ratio: 4.50
 η_{HS} (calculated) = 88.4%; η_{Stm} (calculated) = 41.5%; η_{Plant} = 47.5%

A. ARGON LOOP (\dot{m}_{argon} = 1171 kg/s)

Location	Temp, K	Power to Argon, MW
Compressor Inlet	320	-
Compressor Outlet	650.3	+ 199.4
Preheater Outlet	* 922	+ 164.1
Regenerator Outlet	*1920	+ 602.6
Disk Generator Outlet	1231	- 415.8
Radiant Furnace Outlet	1136	- 57.3
Reheater Outlet	*1000	- 81.9
ITAH Outlet	810	- 114.7
Economizer Outlet	* 471	- 204.7
LPFH Outlet	340.3	- 78.9
Precooler Outlet	320	- 12.3

B. STEAM LOOP (\dot{m}_{steam} = 132.8 kg/s)

Location	Temp, K	Press, 10^5 Pa	Power, MW
Hotwell	*312	* (2" HgA)	-
Condensate Pump Discharge	*312.6	* 10.0	+ .18
LPFH	*451	* 9.53	+ 78.5
Main Feed Pump Discharge	*457.4	*273.9	+ 5.45
Economizer Out	(2.328 E6)	*265.7	+ 203.7
Valve Cooler Out	(2.423 E6)	*257.7	+ 12.6
Combustor Cooling Out	(2.877 E6)	*250.0	+ 60.3
Radiant Furnace Out	*811	*242.0	+ 57.0
HP Turbine Out	*564	*45.0	- 52.3
Reheater Out	*811	*40.0	+ 82.0
LP Turbine Out	-	-	- 159.2
Condenser Out	*312	* (2" HgA)	- 288.4

C. AIR SYSTEM (\dot{m}_{air} = 267.8 kg/s)

Location	Temp, K	Power, MW
Compressor Inlet	* 288	-
Compressor Outlet	* 305	+ 4.52
ITAH 2 Outlet	* 479.8	+ 47.8
ITAH 1 Outlet	531.3	+ 14.4
ITAH Outlet	* 922	+ 114.1

D. COMBUSTION GAS SYSTEM

Location	Temp, K	\dot{m}_c , kg/s	Power, MW
Combustor	*2415	-	+ 986.6**
Regenerator Out	*1090	298.4	- 634.3
Argon Preheater Out	658.4	298.4	- 164.9
ITAH 1 Out	* 611	298.4	- 14.5
ITAH 2 Out	* 408	201.1	- 48.1
Coal Dryer Out	* 408	96.6	- 22.9
Stack	*(408)	(298.4)	- 66.8

*Denotes fixed quantities for all cases.

**Includes air and coal; deducts cooler losses.

MATCH POINT DEVIATION = + 2.00 MW

CCD/MHD/STEAM SYSTEMS PERFORMANCE SURVEY - CASE NO. 4

Assumed Coal Firing Rate = 1610 MWt
MHD Gross Power Output: 763.3 MWe (VI)
Argon Compressor Pressure Ratio: 5.07
Disk/Diffuser Pressure Ratio: 4.42
 η_{HS} (calculated) = 88.9%; η_{Stm} (calculated) = 41.5%; η_{Plant} = 46.9%

A. ARGON LOOP (\dot{m}_{argon} = 2196 kg/s)

Location	Temp, K	Power to Argon, MW
Compressor Inlet	320	-
Compressor Outlet	657.2	+ 378.4
Preheater Outlet	* 922	+ 297.2
Regenerator Outlet	*1920	+ 1120
Disk Generator Outlet	1255	- 763.3
Radiant Furnace Outlet	1139	- 112.3
Reheater Outlet	*1000	- 155.6
ITAH Outlet	817	- 205.4
Economizer Outlet	* 471	- 388.3
LPFH Outlet	337.5	- 149.9
Precooler Outlet	320	- 19.6

B. STEAM LOOP (\dot{m}_{steam} = 252.3 kg/s)

Location	Temp, K	Press, 10^5 Pa	Power, MW
Hotwell	*312	* (2" HgA)	-
Condensate Pump Discharge	*312.6	* 10.0	+ .34
LPFH	*451	* 9.53	+ 149.1
Main Feed Pump Discharge	*457.4	*273.9	+ 10.4
Economizer Out	(2.326 E6)	*265.7	+ 386.3
Valve Cooler Out	(2.419 E6)	*257.7	+ 23.5
Combustor Cooling Out	(2.863 E6)	*250.0	+ 112.2
Radiant Furnace Out	*811	*242.0	+ 111.7
HP Turbine Out	*564	*45.0	- 99.3
Reheater Out	*811	*40.0	+ 155.8
LP Turbine Out	-	-	- 302.3
Condenser Out	*312	* (2" HgA)	- 547.8

C. AIR SYSTEM (\dot{m}_{air} = 497.8 kg/s)

Location	Temp, K	Power, MW
Compressor Inlet	* 288	-
Compressor Outlet	* 305	+ 8.41
ITAH 2 Outlet	* 479.8	+ 88.9
ITAH 1 Outlet	546	+ 34.4
ITAH Outlet	* 922	+ 204.4

D. COMBUSTION GAS SYSTEM

Location	Temp, K	\dot{m}_c , kg/s	Power, MW
Combustor	*2415	-	+ 1834 **
Regenerator Out	*1090	554.7	- 1179
Argon Preheater Out	671.1	554.7	- 298.7
ITAH 1 Out	* 611	554.7	- 34.6
ITAH 2 Out	* 408	375.1	- 89.4
Coal Dryer Out	* 408	179.6	- 42.6
Stack	*(408)	(554.7)	- 124.3

*Denotes fixed quantities for all cases.
**Includes air and coal; deducts cooler losses.

MATCH POINT DEVIATION = +4.33 MW

CCD/MHD/STEAM SYSTEMS PERFORMANCE SURVEY - CASE NO. 5

Assumed Coal Firing Rate = 1424 MWt
MHD Gross Power Output: 674.5 MWe (VI)
Argon Compressor Pressure Ratio: 5.44
Disk/Diffuser Pressure Ratio: 4.68
 η_{MS} (calculated) = 89.4%; η_{Stm} (calculated) = 41.5%; η_{Plant} = 46.7%

A. ARGON LOOP (\dot{m}_{argon} = 1922 kg/s)

Location	Temp, K	Power to Argon, MW
Compressor Inlet	320	-
Compressor Outlet	664.4	+ 341.8
Preheater Outlet	* 922	+ 255.6
Regenerator Outlet	* 1920	+ 990.4
Disk Generator Outlet	1239	- 674.5
Radiant Furnace Outlet	1140	- 98.2
Reheater Outlet	* 1000	- 139.1
ITAH Outlet	824.3	- 174.4
Economizer Outlet	* 471	- 350.5
LPFH Outlet	336	- 134.0
Precooler Outlet	320	- 15.9

B. STEAM LOOP (\dot{m}_{steam} = 225.5 kg/s)

Location	Temp, K	Press, 10^5 Pa	Power, MW
Hotwell	*312	* (2" Hg)	-
Condensate Pump Discharge	*312.6	* 10.0	+ .30
LPFH	*451	* 9	+ 133.3
Main Feed Pump Discharge	*457.4	*273.3	+ 9.25
Economizer Out	(2.341 E6)	*265.7	+ 348.8
Valve Cooler Out	(2.433 E6)	*257.7	+ 20.7
Combustor Cooling Out	(2.873 E6)	*250.0	+ 99.2
Radiant Furnace Out	*811	*242.0	+ 97.7
HP Turbine Out	*564	*45.0	- 88.7
Reheater Out	*811	*40.0	+ 139.3
LP Turbine Out	-	-	- 270.2
Condenser Out	*312	* (2" HgA)	- 489.6

C. AIR SYSTEM (\dot{m}_{air} = 440.1 kg/s)

Location	Temp, K	Power, MW
Compressor Inlet	* 288	-
Compressor Outlet	* 305	+ 7.43
ITAH 2 Outlet	* 479.8	+ 78.6
ITAH 1 Outlet	561.6	+ 37.7
ITAH Outlet	* 922	+ 173.5

D. COMBUSTION GAS SYSTEM

Location	Temp, K	\dot{m}_c , kg/s	Power, MW
Combustor	*2415	-	+ 1621 **
Regenerator Out	*1090	490.5	- 1042
Argon Preheater Out	684.6	490.5	- 256.9
ITAH 1 Out	* 611	490.5	- 37.8
ITAH 2 Out	* 408	331.7	- 79.0
Coal Dryer Out	* 408	158.8	- 37.7
Stack	*(408)	(490.5)	- 109.9

*Denotes fixed quantities for all cases.
**Includes air and coal; deducts cooler losses.

MATCH POINT DEVIATION = + 0.42 MW

CCD/MHD/STEAM SYSTEMS PERFORMANCE SURVEY - CASE NO. 6

Assumed Coal Firing Rate = 882.2 Mwt
MHD Gross Power Output: 419.7 MWe (VI)
Argon Compressor Pressure Ratio: 5.30
Disk/Diffuser Pressure Ratio: 4.66
 η_{HS} (calculated) = 88.9%; η_{Stm} (calculated) = 41.5%; η_{Plant} = 46.9%

A. ARGON LOOP (\dot{m} argon = 1196 kg/s)

Location	Temp, K	Power to Argon, MW
Compressor Inlet	320	-
Compressor Outlet	657.2	+ 208.7
Preheater Outlet	* 922	+ 163.9
Regenerator Outlet	* 1920	+ 617.8
Disk Generator Outlet	1241	- 419.7
Radiant Furnace Outlet	1139	- 63.2
Reheater Outlet	* 1000	- 86.2
ITAH Outlet	816.9	- 113.3
Economizer Outlet	* 471	- 214.1
LPFH Outlet	337	- 83.0
Precooler Outlet	320	- 10.5

B. STEAM LOOP (\dot{m} steam = 139.7 kg/s)

Location	Temp, K	Press, 10^5 Pa	Power, MW
Hotwell	*312	* (2" HgA)	-
Condensate Pump Discharge	*312.6	* 10.0	+ .19
LPFH	*451	* 9.53	+ 82.6
Main Feed Pump Discharge	*457.4	*273.9	+ 5.73
Economizer Out	(2.320 E6)	*265.7	+ 213.1
Valve Cooler Out	(2.413 E6)	*257.7	+ 12.9
Combustor Cooling Out	(2.856 E6)	*250.0	+ 61.9
Radiant Furnace Out	*811	*242.0	+ 62.9
HP Turbine Out	*564	*45.0	- 55.0
Reheater Out	*811	*40.0	+ 86.3
LP Turbine Out	-	-	- 167.3
Condenser Out	*312	* (2" HgA)	- 303.2

C. AIR SYSTEM (\dot{m} air = 274.6 kg/s)

Location	Temp, K	Power, MW
Compressor Inlet	* 288	-
Compressor Outlet	* 305	+ 4.64
ITAH 2 Outlet	* 479.8	+ 49.0
ITAH 1 Outlet	546.0	+ 19.0
ITAH Outlet	* 922	+ 112.8

D. COMBUSTION GAS SYSTEM

Location	Temp, K	\dot{m}_c , kg/s	Power, MW
Combustor	*2415	-	+ 1011 **
Regenerator Out	*1090	306.0	- 650.3
Argon Preheater Out	671.1	306.0	- 164.8
ITAH 1 Out	* 611	306.0	- 19.1
ITAH 2 Out	* 408	206.9	- 49.3
Coal Dryer Out	* 408	99.1	- 23.5
Stack	*(408)	(306.0)	- 68.5

*Denotes fixed quantities for all cases.

**Includes air and coal; deducts cooler losses.

MATCH POINT DEVIATION = + 3.18 MW

CCD/MHD/STEAM SYSTEMS PERFORMANCE SURVEY - CASE NO.7

Assumed Coal Firing Rate = 843.7 MWt
MHD Gross Power Output: 396.4 MWe (V1)
Argon Compressor Pressure Ratio: 5.26
Disk/Diffuser Pressure Ratio: 4.61
nHS (calculated) = 88.7%; nStm (calculated) = 41.5%; nPlant = 46.8%

A. ARGON LOOP (\dot{m} argon = 1136 kg/s)

Location	Temp, K	Power to Argon, MW
Compressor Inlet	320	-
Compressor Outlet	654.9	+ 196.9
Preheater Outlet	* 922	+ 157.0
Regenerator Outlet	* 1920	+ 586.8
Disk Generator Outlet	1245	- 396.4
Radiant Furnace Outlet	1140	- 61.9
Reheater Outlet	* 1000	- 82.2
ITAH Outlet	814.7	- 109.0
Economizer Outlet	* 471	- 202.1
LPFH Outlet	336.8	- 78.9
Precooler Outlet	320	- 9.85

B. STEAM LOOP (\dot{m} steam = 132.9 kg/s)

Location	Temp, K	Press, 10^5 Pa	Power, MW
Hotwell	*312	* (2" HgA)	-
Condensate Pump Discharge	*312.6	* 10.0	+ .18
LPHF	*451	* 9.53	+ 78.5
Main Feed Pump Discharge	*457.4	*273.9	+ 5.45
Economizer Out	(2.307 E6)	*265.7	+ 201.1
Valve Cooler Out	(2.400 E6)	*257.7	+ 12.3
Combustor Cooling Out	(2.842 E6)	*250.0	+ 58.8
Radiant Furnace Out	*811	*242.0	+ 61.6
HP Turbine Out	*564	*45.0	- 52.3
Reheater Out	*811	*40.0	+ 82.1
LP Turbine Out	-	-	- 159.2
Condenser Out	*312	* (2" HgA)	- 288.5

C. AIR SYSTEM (\dot{m} air = 260.8 kg/s)

Location	Temp, K	Power, MW
Compressor Inlet	* 288	-
Compressor Outlet	* 305	+ 4.40
ITAH 2 Outlet	* 479.8	+ 46.6
ITAH 1 Outlet	541.2	+ 16.7
ITAH Outlet	* 922	+ 108.4

D. COMBUSTION GAS SYSTEM

Location	Temp, K	\dot{m}_c , kg/s	Power, MW
Combustor	*2415	-	+ 960.7**
Regenerator Out	*1090	290.6	- 617.7
Argon Preheater Out	666.9	290.6	- 157.8
ITAH 1 Out	* 611	290.6	- 16.8
ITAH 2 Out	* 408	196.5	- 46.8
Coal Dryer Out	* 408	94.1	- 22.3
Stack	*(408)	(290.6)	- 65.1

*Denotes fixed quantities for all cases.
**Includes air and coal; deducts cooler losses.

MATCH POINT DEVIATION = + 4.67 MW

CCD/MHD/STEAM SYSTEMS PERFORMANCE SURVEY - CASE NO. 8

Assumed Coal Firing Rate = 1528 MWt
MHD Gross Power Output: 712 MWe (VI)
Argon Compressor Pressure Ratio: 5.08
Disk/Diffuser Pressure Ratio: 4.48
 η_{HS} (calculated) = 88.8%; η_{Stm} (calculated) = 41.5%; η_{Plant} = 47.0%

A. ARGON LOOP (\dot{m}_{argon} = 2059 kg/s)

Location	Temp, K	Power to Argon, MW
Compressor Inlet	325	-
Compressor Outlet	655.9	+ 352.4
Preheater Outlet	* 922	+ 283.3
Regenerator Outlet	* 1920	+ 1063
Disk Generator Outlet	1251	- 712.4
Radiant Furnace Outlet	1141	- 116.9
Reheater Outlet	* 1000	- 149.9
ITAH Outlet	815.7	- 196.3
Economizer Outlet	* 471	- 367.1
LPFH Outlet	335.5	- 144.3
Precooler Outlet	325	- 11.1

B. STEAM LOOP (\dot{m}_{steam} = 242.9 kg/s)

Location	Temp, K	Press, 10^5 Pa	Power, MW
Hotwell	*312	* (2" HgA)	-
Condensate Pump Discharge	*312.6	* 10.0	+ .33
LPFH	*451	* 9.53	+ 143.6
Main Feed Pump Discharge	*457.4	*273.9	+ 9.97
Economizer Out	(2.298 E6)	*265.7	+ 365.2
Valve Cooler Out	(2.389 E6)	*257.7	+ 22.3
Combustor Cooling Out	(2.827 E6)	*250.0	+ 106.4
Radiant Furnace Out	*811	*242.0	+ 116.3
HP Turbine Out	*564	*45.0	- 95.6
Reheater Out	*811	*40.0	+ 150.1
I ² Turbine Out	-	-	- 291.1
Condenser Out	*312	* (2" HgA)	- 527.5

C. AIR SYSTEM (\dot{m}_{air} = 472.3 kg/s)

Location	Temp, K	Power, MW
Compressor Inlet	* 288	-
Compressor Outlet	* 305	+ 7.98
ITAH 2 Outlet	* 479.0	+ 84.4
ITAH 1 Outlet	543.4	+ 31.4
ITAH Outlet	* 922	+ 195.3

D. COMBUSTION GAS SYSTEM

Location	Temp, K	\dot{m}_c , kg/s	Power, MW
Combustor	*2415	-	+ 1740 **
Regenerator Out	*1090	526.3	- 1119
Argon Preheater Out	668.8	526.3	- 284.8
ITAH 1 Out	* 611	526.3	- 31.5
ITAH 2 Out	* 408	355.9	- 84.8
Coal Dryer Out	* 408	170.4	- 40.4
Stack	*(408)	(526.3)	- 117.9

*Denotes fixed quantities for all cases.

**Includes air and coal; deducts cooler losses.

MATCH POINT DEVIATION = + 16.2 MW

CCD/MHD/STEAM SYSTEMS PERFORMANCE SURVEY - CASE NO. 9

Assumed Coal Firing Rate = 1471 MWt
MHD Gross Power Output: 703.8 MWe (VI)
Argon Compressor Pressure Ratio: 5.30
Disk/Diffuser Pressure Ratio: 4.66
 η_{HS} (calculated) = 88.9%; η_{Stm} (calculated) = 41.5%; η_{Plant} = 47.2%

A. ARGON LOOP (\dot{m}_{argon} = 1980 kg/s)

Location	Temp, K	Power to Argon, MW
Compressor Inlet	320	-
Compressor Outlet	657.4	+ 346.0
Preheater Outlet	* 922	+ 271.3
Regenerator Outlet	* 1920	+1023
Disk Generator Outlet	1233	- 703.8
Radiant Furnace Outlet	1138	- 98.1
Reheater Outlet	* 1000	- 141.0
ITAH Outlet	817.2	- 187.5
Economizer Outlet	* 471	- 355.0
LPFH Outlet	338.5	- 135.9
Precooler Outlet	320	- 18.9

B. STEAM LOOP (\dot{m}_{steam} = 228.8 kg/s)

Location	Temp, K	Press, 10^5 Pa	Power, MW
Hotwell	*312	* (2" HgA)	-
Condensate Pump Discharge	*312.6	* 10.0	+ .31
LPFH	*451	* 9.53	+ 135.2
Main Feed Pump Discharge	*457.4	*273.9	+ 9.39
Economizer Out	(2.338 E6)	*265.7	+ 353.2
Valve Cooler Out	(2.432 E6)	*257.7	+ 21.4
Combustor Cooling Out	(2.880 E6)	*250.0	+ 102.5
Radiant Furnace Out	*811	*242.0	+ 97.6
HP Turbine Out	*564	*45.0	- 90.0
Reheater Out	*811	*40.0	+ 141.3
LP Turbine Out	-	-	- 274.1
Condenser Out	*312	* (2" HgA)	- 496.8

C. AIR SYSTEM (\dot{m}_{air} = 454.8 kg/s)

Location	Temp, K	Power, MW
Compressor Inlet	* 288	-
Compressor Outlet	* 305	+ 7.68
ITAH 2 Outlet	* 479.8	+ 81.3
ITAH 1 Outlet	546.5	+ 31.7
ITAH Outlet	* 922	+ 186.5

D. COMBUSTION GAS SYSTEM

Location	Temp, K	\dot{m}_c , kg/s	Power, MW
Combustor	*2415	-	+ 1676 **
Regenerator Out	*1090	506.8	- 1077
Argon Preheater Out	671.5	506.8	- 272.7
ITAH 1 Out	* 611	506.8	- 31.8
ITAH 2 Out	* 408	342.7	- 81.7
Coal Dryer Out	* 408	164.1	- 38.9
Stack	*(408)	(506.8)	- 113.5

*Denotes fixed quantities for all cases.

**Includes air and coal; deducts cooler losses.

MATCH POINT DEVIATION = + 1.11 MW

CCD/MHD/STEAM SYSTEMS PERFORMANCE SURVEY - CASE NO. 10

Assumed Coal Firing Rate = 998.5 MWt
MHD Gross Power Output: 467.1 MWe (VI)
Argon Compressor Pressure Ratio: 5.50
Disk/Diffuser Pressure Ratio: 4.79
 η_{HS} (calculated) = 89.6%; η_{Stm} (calculated) = 41.5%; η_{Plant} = 46.3%

A. ARGON LOOP (\dot{m}_{argon} = 1344 kg/s)

Location	Temp, °C	Power to Argon, MW
Compressor Inlet	320	-
Compressor Outlet	667.6	+ 241.9
Preheater Outlet	* 922	+ 177.0
Regenerator Outlet	* 1920	+ 694.5
Disk Generator Outlet	1248	- 467.1
Radiant Furnace Outlet	1143	- 73.2
Reheater Outlet	* 1000	- 99.4
ITAH Outlet	827.5	- 120.1
Economizer Outlet	* 471	- 248.1
LPFH Outlet	333.8	- 95.5
Precooler Outlet	320	- 9.59

B. STEAM LOOP (\dot{m}_{steam} = 160.7 kg/s)

Location	Temp, K	Press, 10^5 Pa	Power, MW
Hotwell	*312	* (2" HgA)	-
Condensate Pump Discharge	*312.6	* 10.0	+ 0.22
LPFH	*451	* 9.53	+ 95.0
Main Feed Pump Discharge	*457.4	*273.9	+ 6.60
Economizer Out	(2.330 E6)	*265.7	+ 246.8
Valve Cooler Out	(2.420 E6)	*257.7	+ 14.6
Combustor Cooling Out	(2.853 E6)	*250.0	+ 69.6
Radiant Furnace Out	*811	*242.0	+ 72.8
HP Turbine Out	*564	*45.0	- 63.3
Reheater Out	*811	*40.0	+ 99.3
LP Turbine Out	-	-	- 192.6
Condenser Out	*312	* (2" HgA)	- 349.0

C. AIR SYSTEM (\dot{m}_{air} = 308.7 kg/s)

Location	Temp, K	Power, MW
Compressor Inlet	* 288	-
Compressor Outlet	* 305	+ 5.21
ITAH 2 Outlet	* 479.8	+ 55.2
ITAH 1 Outlet	568.4	+ 28.6
ITAH Outlet	* 922	+ 119.5

D. COMBUSTION GAS SYSTEM

Location	Temp, K	\dot{m}_c , kg/s	Power, MW
Combustor	*2415	-	+ 1137 **
Regenerator Out	*1090	344.0	- 731.1
Argon Preheater Out	690.5	344.0	- 177.9
ITAH 1 Out	* 611	344.0	- 28.8
ITAH 2 Out	* 408	232.6	- 55.4
Coal Dryer Out	* 408	111.4	- 26.4
Stack	*(408)	(344.0)	- 77.1

*Denotes fixed quantities for all cases.

**Includes air and coal; deducts cooler losses.

MATCH POINT DEVIATION = + 2.09 MW

CCD/MHD/STEAM SYSTEMS PERFORMANCE SURVEY - CASE NO. 11

Assumed Coal Firing Rate = 2293 MMt
MHD Gross Power Output: 10P5 MWe (VI)
Argon Compressor Pressure Ratio: 5.31
Disk/Diffuser Pressure Ratio: 4.66
 η_{HS} (calculated) = 88.9%; η_{Stm} (calculated) = 41.5%; η_{Plant} = 46.9%

A. ARGON LOOP (\dot{m} argon = 3089 kg/s)

Location	Temp, K	Power to Argon, MW
Compressor Inlet	320	-
Compressor Outlet	657.9	+ 540.0
Preheater Outlet	* 922	+ 422.2
Regenerator Outlet	* 1920	+ 1595
Disk Generator Outlet	1241	- 1085
Radiant Furnace Outlet	1139	- 162.1
Reheater Outlet	* 1000	- 222.5
ITAH Outlet	817.6	- 291.5
Economizer Outlet	* 471	- 554.0
LPFH Outlet	337	- 214.2
Precooler Outlet	320	- 27.1

B. STEAM LOOP (\dot{m} steam = 360.6 kg/s)

Location	Temp, K	Press, 10^5 Pa	Power, MW
Hotwell	*312	* (2" HgA)	-
Condensate Pump Discharge	*312.6	* 10.0	+ .48
LPFH	*451	* 9.53	+ 213.1
Main Feed Pump Discharge	*457.4	*273.9	+ 14.8
Economizer Out	(2.323 E6)	*265.7	+ 551.2
Valve Cooler Out	(2.416 E6)	*257.7	+ 33.4
Combustor Cooling Out	(2.859 E6)	*250.0	+ 159.7
Radiant Furnace Out	*811	*242.0	+ 161.3
HP Turbine Out	*564	*45.0	- 141.9
Reheater Out	*811	*40.0	+ 222.7
LP Turbine Out	-	-	- 432.0
Condenser Out	*312	* (2" HgA)	- 782.9

C. AIR SYSTEM (\dot{m} air = 708.9 kg/s)

Location	Temp, K	Power, MW
Compressor Inlet	* 288	-
Compressor Outlet	* 305	+ 12.0
ITAH 2 Outlet	* 479.8	+ 126.7
ITAH 1 Outlet	547.4	+ 50.1
ITAH Outlet	* 922	+ 290.0

D. COMBUSTION GAS SYSTEM

Location	Temp, K	\dot{m}_c , kg/s	Power, MW
Combustor	*2415	-	+ 2612 **
Regenerator Out	*1090	790.0	- 1679
Argon Preheater Out	672.4	790.0	- 424.3
ITAH 1 Out	* 611	790.0	- 50.4
ITAH 2 Out	* 408	534.2	- 127.3
Coal Dryer Out	* 408	255.8	- 60.6
Stack	*(408)	(790.0)	- 177.0

*Denotes fixed quantities for all cases.
**Includes air and coal; deducts cooler losses.

MATCH POINT DEVIATION = + 7.51 MW

CCD/MHD/STEAM SYSTEMS PERFORMANCE SURVEY - CASE NO. 12

Assumed Coal Firing Rate = 2220 Mwt
MHD Gross Power Output: 1057 MWe (VI)
Argon Compressor Pressure Ratio: 5.39
Disk/Diffuser Pressure Ratio: 4.72
 η_{HS} (calculated) = 89.2%; η_{Stm} (calculated) = 41.5%; η_{Plant} = 46.9%

A. ARGON LOOP (\dot{m} argon = 2989 kg/s)

Location	Temp, K	Power to Argon, MW
Compressor Inlet	320	-
Compressor Outlet	661.8	+ 528.9
Preheater Outlet	* 922	+ 402.7
Regenerator Outlet	* 1920	+ 1544
Disk Generator Outlet	1236	- 1057
Radiant Furnace Outlet	1139	- 150.7
Reheater Outlet	* 1000	- 215.1
ITAH Outlet	821.6	- 276.1
Economizer Outlet	* 471	- 542.5
LPFH Outlet	337	- 207.4
Precooler Outlet	320	- 26.3

B. STEAM LOOP (\dot{m} steam = 349.0 kg/s)

Location	Temp, K	Press, 10^5 Pa	Power, MW
Hotwell	*312	* (2" HgA)	-
Condensate Pump Discharge	*312.6	* 10.0	+ .47
LPFH	*451	* 9.53	+ 206.3
Main Feed Pump Discharge	*457.4	*273.9	+ 14.3
Economizer Out	(2.341 E6)	*265.7	+ 539.8
Valve Cooler Out	(2.433 E6)	*257.7	+ 32.4
Combustor Cooling Out	(2.877 E6)	*250.0	+ 154.7
Radiant Furnace Out	*811	*242.0	+ 149.9
HP Turbine Out	*564	*45.0	- 137.4
Reheater Out	*811	*40.0	+ 215.6
LP Turbine Out	-	-	- 418.2
Condenser Out	*312	* (2" HgA)	- 757.9

C. AIR SYSTEM (\dot{m} air = 686.4 kg/s)

Location	Temp, K	Power, MW
Compressor Inlet	* 288	-
Compressor Outlet	* 305	+ 11.6
ITAH 2 Outlet	* 479.8	+ 122.6
ITAH 1 Outlet	555.8	+ 54.6
ITAH Outlet	* 922	+ 274.8

D. COMBUSTION GAS SYSTEM

Location	Temp, K	\dot{m}_c , kg/s	Power, MW
Combustor	*2415	-	+ 2529 **
Regenerator Out	*1090	764.9	- 1626
Argon Preheater Out	679.6	764.9	- 404.8
ITAH 1 Out	* 611	764.9	- 54.9
ITAH 2 Out	* 408	517.2	- 123.3
Coal Dryer Out	* 408	147.7	- 58.7
Stack	*(408)	(764.9)	- 171.3

*Denotes fixed quantities for all cases.

**Includes air and coal; deducts cooler losses.

MATCH POINT DEVIATION = + 0.75 MW

CCD/MHD/STEAM SYSTEMS PERFORMANCE SURVEY - CASE NO. 13

Assumed Coal Firing Rate = 1298 MWt
MHD Gross Power Output: 603 MWe (VI)
Argon Compressor Pressure Ratio: 5.92
Disk/Diffuser Pressure Ratio: 4.87
 η_{MS} (calculated) = 89.9%; η_{Stm} (calculated) = 41.5%; η_{Plant} = 46.2%

A. ARGON LOOP (\dot{m} argon = 1749 kg/s)

Location	Temp, K	Power to Argon, MW
Compressor Inlet	320	-
Compressor Outlet	671.5	+ 318.1
Preheater Outlet	* 922	+ 226.7
Regenerator Outlet	* 1920	+ 903.1
Disk Generator Outlet	1247	- 608.3
Radiant Furnace Outlet	1143	- 93.8
Reheater Outlet	* 1000	- 129.5
ITAH Outlet	831.3	- 122.6
Economizer Outlet	* 471	- 326.
LPH Outlet	333.2	- 124.7
Precooler Outlet	320	- 11.9

B. STEAM LOOP (\dot{m} steam = 209.9 kg/s)

Location	Temp, K	Press, 10^5 Pa	Power, MW
Hotwell	*312	* (2" HgA)	-
Condensate Pump Discharge	*312.6	* 10.0	+ .28
LPHF	*451	* 9.53	+ 124.0
Main Feed Pump Discharge	*457.4	*273.9	+ 8.61
Economizer Out	(2.340 E6)	*265.7	+ 324.4
Valve Cooler Out	(2.430 E6)	*257.7	+ 18.9
Combustor Cooling Out	(2.861 E6)	*250.0	+ 90.4
Radiant Furnace Out	*811	*242.0	+ 93.3
HP Turbine Out	*564	*45.0	- 82.6
Reheater Out	*811	*40.0	+ 129.6
LP Turbine Out	-	-	- 251.4
Condenser Out	*312	* (2" HgA)	- 455.7

C. AIR SYSTEM (\dot{m} air = 401.4 kg/s)

Location	Temp, K	Power, MW
Compressor Inlet	* 288	-
Compressor Outlet	* 305	+ 6.78
ITAH 2 Outlet	* 479.8	+ 71.7
ITAH 1 Outlet	576.6	+ 40.7
ITAH Outlet	* 922	+ 151.9

D. COMBUSTION GAS SYSTEM

Location	Temp, K	\dot{m}_c , kg/s	Power, M
Combustor	*2415	-	+ 1479 **
Regenerator Out	*1090	447.3	- 950.6
Argon Preheater Out	697.6	447.3	- 227.8
ITAH 1 Out	* 611	447.3	- 40.9
ITAH 2 Out	* 408	302.4	- 72.1
Coal Dryer Out	* 408	144.9	- 34.3
Stack	*(408)	(447.3)	- 100.2

*Denotes fixed quantities for all cases.
**Includes air and coal; deducts cooler losses.

MATCH POINT DEVIATION = + 0.58 MW

CCD/MHD/STEAM SYSTEMS PERFORMANCE SURVEY - CASE NO. 14

Assumed Coal Firing Rate = 2267 MWt
MHD Gross Power Output: 1069 MWe (VI)
Argon Compressor Pressure Ratio: 5.47
Disk/Diffuser Pressure Ratio: 4.79
 η_{HS} (calculated) = 89.5%; η_{Stm} (calculated) = 41.5%; η_{Plant} = 46.5%

A. ARGON LOOP (\dot{m}_{argon} = 3054 kg/s)

Location	Temp, K	Power to Argon, MW
Compressor Inlet	320	-
Compressor Outlet	666.3	+ 547
Preheater Outlet	* 922	+ 404
Regenerator Outlet	* 1920	+ 1577
Disk Generator Outlet	1242	- 1069
Radiant Furnace Outlet	1141	- 159.8
Reheater Outlet	* 1000	- 222.9
ITAH Outlet	826.1	- 274.7
Economizer Outlet	* 471	- 561
LPH Outlet	335	- 214.8
Precooler Outlet	320	- 23.8

B. STEAM LOOP (\dot{m}_{steam} =

Location	Temp, K	Press, 10^5 Pa	Power, MW
Hotwell	*312	* (2" HgA)	-
Condensate Pump Discharge	*312.6	* 10.0	+ .49
LPHF	*451	* 9.53	+ 213.7
Main Feed Pump Discharge	*457.4	*273.9	+ 14.8
Economizer Out	(2.338 E6)	*265.7	+ 558.2
Valve Cooler Out	(2.430 E6)	*257.7	+ 33.0
Combustor Cooling Out	(2.866 E6)	*250.0	+ 157.9
Radiant Furnace Out	*811	*242.0	+ 159.0
HP Turbine Out	*564	*45.0	- 142.3
Reheater Out	*811	*40.0	- 223.3
LP Turbine Out	-	-	- 433.2
Condenser Out	*312	* (2" HgA)	- 785

C. AIR SYSTEM (\dot{m}_{air} = 700.7 kg/s)

Location	Temp, K	Power, MW
Compressor Inlet	* 288	-
Compressor Outlet	* 305	+ 11.0
ITAH 2 Outlet	* 479.8	+ 125.2
ITAH 1 Outlet	565.5	+ 62.9
ITAH Outlet	* 922	+ 273.3

D. COMBUSTION GAS SYSTEM

Location	Temp, K	\dot{m}_c , kg/s	Power, MW
Combustor	*2415	-	+ 2581 **
Regenerator Out	*1090	780.8	- 1660
Argon Preheater Out	688.0	780.8	- 406.0
ITAH 1 Out	* 611	780.8	- 63.2
ITAH 2 Out	* 408	528.0	- 125.8
Coal Dryer Out	* 408	252.8	- 60.0
Stack	*(408)	(780.8)	- 174.9

*Denotes fixed quantities for all cases.

**Includes air and coal; deducts cooler losses.

MATCH POINT DEVIATION = + 1.69 MW

CCD/MHD/STEAM SYSTEMS PERFORMANCE SURVEY - CASE NO. 15

Assumed Coal Firing Rate = 1457 MWt
MHD Gross Power Output: 677.3 MWe (VI)
Argon Compressor Pressure Ratio: 5.69
Disk/Diffuser Pressure Ratio: 4.95
 η_{MS} (calculated) = 89.0%; η_{Stm} (calculated) = 41.5%; η_{Plant} = 45.8%

A. ARGON LOOP (\dot{m}_{argon} = 1963 kg/s)

Location	Temp, K	Power to Argon, MW
Compressor Inlet	311	-
Compressor Outlet	658.2	+ 352.6
Preheater Outlet	* 922	+ 267.9
Regenerator Outlet	* 1920	+1014
Disk Generator Outlet	1252	- 677.3
Radiant Furnace Outlet	1142	- 112.1
Reheater Outlet	* 1000	- 143.8
ITAH Outlet	818	- 184.9
Economizer Outlet	* 471	- 352.4
LPFH Outlet	334.8	- 138.3
Precooler Outlet	311	- 24.2

B. STEAM LOOP (\dot{m}_{steam} = 232.8 kg/s)

Location	Temp, K	Press, 10^5 Pa	Power, MW
Hotwell	*312	* (2" HgA)	-
Condensate Pump Discharge	*312.6	* 10.0	+ .31
LPFH	*451	* 9.53	+ 137.6
Main Feed Pump Discharge	*457.4	*273.9	+ 9.55
Economizer Out	(2.300 E6)	*265.7	+ 350.6
Valve Cooler Out	(2.391 E6)	*257.7	+ 21.2
Combustor Cooling Out	(2.827 E6)	*250.0	+ 101.5
Radiant Furnace Out	*811	*242.0	+ 111.5
HP Turbine Out	*564	*45.0	- 91.6
Reheater Out	*811	*40.0	+ 143.8
LP Turbine Out	-	-	- 279.0
Condenser Out	*312	* (2" HgA)	- 505.5

C. AIR SYSTEM (\dot{m}_{air} = 450.4 kg/s)

Location	Temp, K	Power, MW
Compressor Inlet	* 288	-
Compressor Outlet	* 305	+ 7.61
ITAH 2 Outlet	* 479.8	+ 80.5
ITAH 1 Outlet	548.2	+ 32.2
ITAH Outlet	* 922	+ 183.9

D. COMBUSTION GAS SYSTEM

Location	Temp, K	\dot{m}_c , kg/s	Power, MW
Combustor	*2415	-	+ 1659 **
Regenerator Out	*1090	502.0	- 1067
Argon Preheater Out	673	502.0	- 269.3
ITAH 1 Out	* 611	502.0	- 32.4
ITAH 2 Out	* 408	339.4	- 80.9
Coal Dryer Out	* 408	162.6	- 38.5
Stack	*(408)	(502.0)	- 112.4

*Denotes fixed quantities for all cases.

**Includes air and coal; deducts cooler losses.

MATCH POINT DEVIATION = + 0.85 MW

CCD/MHD/STEAM SYSTEMS PERFORMANCE SURVEY - CASE NO. 16

Assumed Coal Firing Rate = 2210 MWt
MHD Gross Power Output: 1027 MWe (V1)
Argon Compressor Pressure Ratio: 5.54
Disk/Diffuser Pressure Ratio: 4.83
 η_{HS} (calculated) = 88.5%; η_{Stm} (calculated) = 41.5%; η_{Plant} = 46.1 %

A. ARGON LOOP (\dot{m} argon = 2978 kg/s)

Location	Temp, K	Power to Argon, MW
Compressor Inlet	311	-
Compressor Outlet	650.8	+ 523.3
Preheater Outlet	* 922	+ 417.8
Regenerator Outlet	*1920	+ 1537
Disk Generator Outlet	1252	- 1027
Radiant Furnace Outlet	1140	- 172.7
Reheater Outlet	*1000	- 215.6
ITAH Outlet	810.5	- 291.9
Economizer Outlet	* 471	- 523.0
LPFH Outlet	336.1	- 207.7
Precooler Outlet	311	- 38.7

B. STEAM LOOP (\dot{m} steam = 349.7 kg/s)

Location	Temp, K	Press, 10^5 Pa	Power, MW
Hotwell	*312	* (2" HgA)	-
Condensate Pump Discharge	*312.6	* 10.0	+ .47
LPHF	*451	* 9.53	+ 206.7
Main Feed Pump Discharge	*457.4	*273.9	+ 14.3
Economizer Out	(2.282 E6)	*265.7	+ 520.3
Valve Cooler Out	(2.374 E6)	*257.7	+ 32.2
Combustor Cooling Out	(2.815 E6)	*250.0	+ 153.9
Radiant Furnace Out	*811	*242.0	+ 171.9
HP Turbine Out	*564	*45.0	- 137.6
Reheater Out	*811	*40.0	+ 216.0
LP Turbine Out	-	-	- 419.0
Condenser Out	*312	* (2" HgA)	+ 759.3

C. AIR SYSTEM (\dot{m} air = 683.2 kg/s)

Location	Temp, K	Power, MW
Compressor Inlet	* 288	-
Compressor Outlet	* 305	+ 11.5
ITAH 2 Outlet	* 479.8	+ 122.1
ITAH 1 Outlet	532.3	+ 37.4
ITAH Outlet	* 922	+ 290.4

D. COMBUSTION GAS SYSTEM

Location	Temp, K	\dot{m}_c , kg/s	Power, MW
Combustor	*2415	-	+ 2517 **
Regenerator Out	*1090	761.3	- 1618
Argon Preheater Out	659.3	761.3	- 419.9
ITAH 1 Out	* 611	761.3	- 37.6
ITAH 2 Out	* 408	514.8	- 122.7
Coal Dryer Out	* 408	246.5	- 58.4
Stack	*(408)	(761.3)	- 170.5

*Denotes fixed quantities for all cases.
**Includes air and coal; deducts cooler losses.

MATCH POINT DEVIATION = +*7.28 MW

CCD/MHD/STEAM SYSTEMS PERFORMANCE SURVEY - CASE NO. 17

Assumed Coal Firing Rate = 2580 Mwt
MHD Gross Power Output: 1206 MWe (VI)
Argon Compressor Pressure Ratio: 5.56
Disk/Diffuser Pressure Ratio: 4.85
 η_{HS} (calculated) = 89.8%; η_{Stm} (calculated) = 41.5%; η_{Plant} = 46.2%

A. ARGON LOOP (\dot{m}_{argon} = 3476 kg/s)

Location	Temp, K	Power to Argon, MW
Compressor Inlet	320	-
Compressor Outlet	670.6	+ 630.2
Preheater Outlet	* 922	+ 452.0
Regenerator Outlet	* 1920	+ 1794
Disk Generator Outlet	1248	- 1206
Radiant Furnace Outlet	1143	- 188.5
Reheater Outlet	* 1000	- 257.2
ITAH Outlet	830.4	- 304.9
Economizer Outlet	* 471	- 646.2
LPFH Outlet	333.2	- 247.8
Precooler Outlet	320	- 23.7

B. STEAM LOOP (\dot{m}_{steam} = 417.1 kg/s)

Location	Temp, K	Press, 10^5 Pa	Power, MW
Hotwell	*312	* (2" HgA)	-
Condensate Pump Discharge	*312.6	* 10.0	+ .56
LPFH	*451	* 9.53	+ 246.5
Main Feed Pump Discharge	*457.4	*273.9	+ 17.1
Economizer Out	(2.336 E6)	*265.7	+ 642.9
Valve Cooler Out	(2.426 E6)	*257.7	+ 37.6
Combustor Cooling Out	(2.856 E6)	*250.0	+ 179.7
Radiant Furnace Out	*811	*242.0	+ 187.5
HP Turbine Out	*564	*45.0	- 164.1
Reheater Out	*811	*40.0	+ 257.6
LP Turbine Out	-	-	- 499.7
Condenser Out	*312	* (2" HgA)	- 905.6

C. AIR SYSTEM (\dot{m}_{air} = 797.4 kg/s)

Location	Temp, K	Power, MW
Compressor Inlet	* 288	-
Compressor Outlet	* 305	+ 13.5
ITAH 2 Outlet	* 479.8	+ 142.5
ITAH 1 Outlet	574.6	+ 79.3
ITAH Outlet	* 922	+ 303.3

D. COMBUSTION GAS SYSTEM

Location	Temp, K	\dot{m}_c , kg/s	Power, MW
Combustor	*2415	-	+ 2938 **
Regenerator Out	*1090	888.6	- 1889
Argon Preheater Out	695.9	888.6	- 439.4
ITAH 1 Out	* 611	888.6	- 94.6
ITAH 2 Out	* 408	600.9	- 143.2
Coal Dryer Out	* 408	287.7	- 68.2
Stack	*(408)	(888.6)	- 199.0

*Denotes fixed quantities for all cases.

**Includes air and coal; deducts cooler losses.

MATCH POINT DEVIATION = + 3.02 MW

CCD/MWD/STEAM SYSTEMS PERFORMANCE SURVEY - CASE NO. 18

Assumed Coal Firing Rate = 1559 MWt
MWD Gross Power Output: 715 MWe (VI)
Argon Compressor Pressure Ratio: 5.83
Disk/Diffuser Pressure Ratio: 5.14
 η_{HS} (calculated) = 89.4%; η_{Stm} (calculated) = 41.5%; η_{Plant} = 45.3%

A. ARGON LOOP (\dot{m}_{argon} = 2098 kg/s)

Location	Temp, K	Power to Argon, MW
Compressor Inlet	311	-
Compressor Outlet	664.9	+ 384.4
Preheater Outlet	* 922	+ 279.3
Regenerator Outlet	* 1920	+ 1085
Disk Generator Outlet	1260	- 715.6
Radiant Furnace Outlet	1144	- 125.9
Reheater Outlet	* 1000	- 157.0
ITAH Outlet	824.8	- 190.4
Economizer Outlet	* 471	- 384.4
LPFH Outlet	331.9	- 151.1
Precooler Outlet	311	- 22.7

B. STEAM LOOP (\dot{m}_{steam} = 254.4 kg/s)

Location	Temp, K	Press, 10^5 Pa	Power, MW
Hotwell	*312	* (2" HgA)	-
Condensate Pump Discharge	*312.6	* 10.0	+ .34
LPFH	*451	* 9.53	+ 150.4
Main Feed Pump Discharge	*457.4	*273.9	+ 10.5
Economizer Out	(2.298 E6)	*265.7	+ 382.5
Valve Cooler Out	(2.387 E6)	*257.7	+ 22.7
Combustor Cooling Out	(2.814 E6)	*250.0	+ 108.6
Radiant Furnace Out	*811	*242.0	+ 125.2
HP Turbine Out	*564	*45.0	- 100.1
Reheater Out	*811	*40.0	+ 157.1
LP Turbine Out	-	-	- 304.8
Condenser Out	*312	* (2" HgA)	- 552.4

C. AIR SYSTEM (\dot{m}_{air} = 482 kg/s)

Location	Temp, K	Power, MW
Compressor Inlet	* 288	-
Compressor Outlet	* 305	+ 8.14
ITAH 2 Outlet	* 479.8	+ 86.1
ITAH 1 Outlet	562.6	+ 41.8
ITAH Outlet	* 922	+ 189.5

D. COMBUSTION GAS SYSTEM

Location	Temp, K	\dot{m}_c , kg/s	Power, MW
Combustor	*2415	-	+ 1776 **
Regenerator Out	*1090	537.1	- 1142
Argon Preheater Out	685.5	537.1	- 280.7
ITAH 1 Out	* 611	537.1	- 42.0
ITAH 2 Out	* 408	363.2	- 86.6
Coal Dryer Out	* 408	173.9	- 41.2
Stack	*(408)	(537.1)	- 120.3

*Denotes fixed quantities for all cases.

**Includes air and coal; deducts cooler losses.

MATCH POINT DEVIATION = + 1.73 MW

CCD/MHD/STEAM SYSTEMS PERFORMANCE SURVEY - CASE NO. 19

Assumed Coal Firing Rate = 1895 MWt
MHD Gross Power Output: 875 MWe (VI)
Argon Compressor Pressure Ratio: 5.81
Disk/Diffuser Pressure Ratio: 5.12
 η_{HS} (calculated) = 89.4%; η_{Stm} (calculated) = 41.5%; η_{Plant} = 45.5%

A. ARGON LOOP (\dot{m}_{argon} = 2550 kg/s)

Location	Temp, K	Power to Argon, MW
Compressor Inlet	311	-
Compressor Outlet	663.9	+ 466.0
Preheater Outlet	* 922	+ 340.9
Regenerator Outlet	* 1920	+ 1318
Disk Generator Outlet	1257	- 875
Radiant Furnace Outlet	1144	- 149.5
Reheater Outlet	* 1000	- 189.5
ITAH Outlet	823.7	- 232.8
Economizer Outlet	* 471	- 465.7
LPFH Outlet	332.8	- 182.5
Precooler Outlet	311	- 28.8

B. STEAM LOOP (\dot{m}_{steam} = 307.2 kg/s)

Location	Temp, K	Press, 10^5 Pa	Power, MW
Hotwell	*312	* (2" HgA)	-
Condensate Pump Discharge	*312.6	* 10.0	+ .41
LPFH	*451	* 9.53	+ 181.6
Main Feed Pump Discharge	*457.4	*273.9	+ 12.6
Economizer Out	(2.303 E6)	*265.7	+ 463.4
Valve Cooler Out	(2.392 E6)	*257.7	+ 27.6
Combustor Cooling Out	(2.822 E6)	*250.0	+ 132.0
Radiant Furnace Out	*811	*242.0	+ 148.7
HP Turbine Out	*564	*45.0	- 120.9
Reheater Out	*811	*40.0	+ 189.8
LP Turbine Out	-	-	- 368.1
Condenser Out	*312	* (2" HgA)	- 667.1

C. AIR SYSTEM (\dot{m}_{air} = 585.7 kg/s)

Location	Temp, K	Power, MW
Compressor Inlet	* 288	-
Compressor Outlet	* 305	+ 9.89
ITAH 2 Outlet	* 479.8	+ 104.7
ITAH 1 Outlet	560.3	+ 49.4
ITAH Outlet	* 922	+ 231.7

D. COMBUSTION GAS SYSTEM

Location	Temp, K	\dot{m}_c , kg/s	Power, MW
Combustor	*2415	-	+ 2158 **
Regenerator Out	*1090	652.7	- 1387
Argon Preheater Out	683.5	652.7	- 354.7
ITAH 1 Out	* 611	652.7	- 37.5
ITAH 2 Out	* 408	441.4	- 105.2
Coal Dryer Out	* 408	211.3	- 50.1
Stack	*(408)	(652.7)	- 146.2

*Denotes fixed quantities for all cases.

**Includes air and coal; deducts cooler losses.

MATCH POINT DEVIATION = + 0.52 MW

CCD/MHD/STEAM SYSTEMS PERFORMANCE SURVEY - CASE NO. 20

Assumed Coal Firing Rate = 2345 Mwt
MHD Gross Power Output: 1085 MWe (VI)
Argon Compressor Pressure Ratio: 5.75
Disk/Diffuser Pressure Ratio: 5.07
 η_{HS} (calculated) = 89.2%; η_{Stm} (calculated) = 41.5%; η_{Plant} = 45.6%

A. ARGON LOOP (\dot{m}_{argon} = 3155 kg/s)

Location	Temp, K	Power to Argon, MW
Compressor Inlet	311	-
Compressor Outlet	661.1	+ 572.3
Preheater Outlet	* 922	+ 426.3
Regenerator Outlet	* 1920	+ 1631
Disk Generator Outlet	1255	- 1085
Radiant Furnace Outlet	1143	- 184.1
Reheater Outlet	* 1000	- 233.2
ITAH Outlet	820.9	- 292.6
Economizer Outlet	* 471	- 571.9
LPFH Outlet	333.6	- 224.6
Precooler Outlet	311	- 36.9

B. STEAM LOOP (\dot{m}_{steam} = 378.1 kg/s)

Location	Temp, K	Press, 10^5 Pa	Power, MW
Hotwell	*312	* (2" HgA)	-
Condensate Pump Discharge	*312.6	* 10.0	+ .51
LPFH	*451	* 9.53	+ 223.5
Main Feed Pump Discharge	*457.4	*273.9	+ 15.5
Economizer Out	(2.299 E6)	*265.7	+ 569.1
Valve Cooler Out	(2.390 E6)	*257.7	+ 34.2
Combustor Cooling Out	(2.822 E6)	*250.0	+ 163.3
Radiant Furnace Out	*811	*242.0	+ 183.1
HP Turbine Out	*564	*45.0	- 148.8
Reheater Out	*811	*40.0	+ 233.5
LP Turbine Out	-	-	- 453.0
Condenser Out	*312	* (2" HgA)	+ 821.0

C. AIR SYSTEM (\dot{m}_{air} = 724.9 kg/s)

Location	Temp, K	Power, MW
Compressor Inlet	* 288	-
Compressor Outlet	* 305	+ 12.2
ITAH 2 Outlet	* 479.8	+ 129.5
ITAH 1 Outlet	554.5	+ 56.7
ITAH Outlet	* 922	+ 291.2

D. COMBUSTION GAS SYSTEM

Location	Temp, K	\dot{m}_c , kg/s	Power, MW
Combustor	*2415	-	+ 2670 **
Regenerator Out	*1090	807.8	- 1717
Argon Preheater Out	678.5	807.8	- 428.5
ITAH 1 Out	* 611	807.8	- 56.9
ITAH 2 Out	* 408	546.2	- 130.2
Coal Dryer Out	* 408	261.0	- 62.0
Stack	*(408)	(807.8)	- 180.9

*Denotes fixed quantities for all cases.

**Includes air and coal; deducts cooler losses.

MATCH POINT DEVIATION = + 1.77 MW

CCD/MHD/STEAM SYSTEMS PERFORMANCE SURVEY - CASE NO.21

Assumed Coal Firing Rate = 1828 MWt
MHD Gross Power Output: 832.7 MW_e (V)
Argon Compressor Pressure Ratio: 5.92
Disk/Diffuser Pressure Ratio: 5.20
 η_{HS} (calculated) = 89.8%; η_{Stm} (calculated) = 41.5%; η_{Plant} = 45.0%

A. ARGON LOOP (\dot{m} argon = 2460 kg/s)

Location	Temp, K	Power to Argon, MW
Compressor Inlet	311	-
Compressor Outlet	669.3	+ 456.5
Preheater Outlet	* 922	+ 321.9
Regenerator Outlet	* 1000	+ 127.1
Disk Generator Outlet	1266	- 832.7
Radiant Furnace Outlet	1146	- 152.1
Reheater Outlet	* 1000	- 186.5
ITAH Outlet	829.2	- 217.6
Economizer Outlet	* 471	- 456.3
LPFH Outlet	330.0	- 179.6
Precooler Outlet	311	- 24.3

B. STEAM LOOP (\dot{m} steam = 302.3 kg/s)

Location	Temp, K	Press, 10^5 Pa	Power, MW
Hotwell	*312	* (2" HgA)	-
Condensate Pump Discharge	*312.6	* 10.0	+ .41
LPFH	*451	* 9.53	+ 178.7
Main Feed Pump Discharge	*457.4	*273.9	+ 12.4
Economizer Out	(2.296 E6)	*265.7	+ 454.0
Valve Cooler Out	(2.384 E6)	*257.7	+ 26.6
Combustor Cooling Out	(2.806 E6)	*250.0	+ 127.3
Radiant Furnace Out	*811	*242.0	+ 151.3
HP Turbine Out	*564	*45.0	- 119.0
Reheater Out	*811	*40.0	+ 186.7
LP Turbine Out	-	-	- 362.2
Condenser Out	*312	* (2" HgA)	- 656.3

C. AIR SYSTEM (\dot{m} air = 565.1 kg/s)

Location	Temp, K	Power, MW
Compressor Inlet	* 288	-
Compressor Outlet	* 305	+ 9.54
ITAH 2 Outlet	* 479.8	- 101.0
ITAH 1 Outlet	572.0	+ 54.6
ITAH Outlet	* 922	+ 216.6

D. COMBUSTION GAS SYSTEM

Location	Temp, K	\dot{m}_c , kg/s	Power, MW
Combustor	*2415	-	+ 2082 **
Regenerator Out	*1090	629.7	+ 1338
Argon Preheater Out	693.6	629.7	- 323.5
ITAH 1 Out	* 611	629.7	- 54.9
ITAH 2 Out	* 408	425.8	- 101.5
Coal Dryer Out	* 408	203.9	- 48.3
Stack	*(408)	(629.7)	- 141.3

*Denotes fixed quantities for all cases.

**Includes air and coal; deducts cooler losses.

MATCH POINT DEVIATION = + 2.64 MW

CCD/MHD/STEAM SYSTEMS PERFORMANCE SURVEY - CASE NO. 22

Assumed Coal Firing Rate = 2266 MWt
MHD Gross Power Output: 1039 MWe (VI)
Argon Compressor Pressure Ratio: 5.90
Disk/Diffuser Pressure Ratio: 5.19
 η_{HS} (calculated) = 89.7%; η_{Stm} (calculated) = 41.5%; η_{Plant} = 45.2%

A. ARGON LOOP (\dot{m}_{argon} = 3048 kg/s)

Location	Temp, K	Power to Argon, MW
Compressor Inlet	311	-
Compressor Outlet	668.5	+ 564.6
Preheater Outlet	* 922	+ 400.2
Regenerator Outlet	* 1920	+ 1576
Disk Generator Outlet	1261	- 1039
Radiant Furnace Outlet	1145	- 182.7
Reheater Outlet	* 1000	- 229.5
ITAH Outlet	828.4	- 271.0
Economizer Outlet	* 471	- 564.3
LPHF Outlet	331.1	- 220.9
Precooler Outlet	311	- 31.7

B. STEAM LOOP (\dot{m}_{steam} = 371.8 kg/s)

Location	Temp, K	Press, 10^5 Pa	Power, MW
Hotwell	*312	* (2" HgA)	-
Condensate Pump Discharge	*312.6	* 10.0	+ .50
LPHF	*451	* 9.53	+ 219.8
Main Feed Pump Discharge	*457.4	*273.9	+ 15.3
Economizer Out	(2.304 E6)	*265.7	+ 561.5
Valve Cooler Out	(2.393 E6)	*257.7	- 33.0
Combustor Cooling Out	(2.817 E6)	*250.0	+ 157.8
Radiant Furnace Out	*811	*242.0	+ 181.8
HP Turbine Out	*564	*45.0	- 146.3
Reheater Out	*811	*40.0	+ 229.7
LP Turbine Out	-	-	- 445.5
Condenser Out	*312	* (2" HgA)	+ 807.4

C. AIR SYSTEM (\dot{m}_{air} = 700.3 kg/s)

Location	Temp, K	Power, MW
Compressor Inlet	* 288	-
Compressor Outlet	* 305	+ 11.8
ITAH 2 Outlet	* 479.8	+ 125.1
ITAH 1 Outlet	570.3	+ 66.4
ITAH Outlet	* 922	+ 269.6

D. COMBUSTION GAS SYSTEM

Location	Temp, K	\dot{m}_c , kg/s	Power, MW
Combustor	*2415	-	+ 2580 **
Regenerator Out	*1090	780.4	- 1659
Argon Preheater Out	692.2	780.4	- 402.2
ITAH 1 Out	* 611	780.4	- 66.3
ITAH 2 Out	* 408	527.7	- 125.8
Coal Dryer Out	* 408	252.7	- 60.0
Stack	*(408)	(780.4)	- 174.8

*Denotes fixed quantities for all cases.

**Includes air and coal; deducts cooler losses.

MATCH POINT DEVIATION = + 0.23 MW

CCD/MHD/STEAM SYSTEMS PERFORMANCE SURVEY - CASE NO. 23

Assumed Coal Firing Rate = 2517 MWt
MHD Gross Power Output: 1146 MWe (VI)
Argon Compressor Pressure Ratio: 5.77
Disk/Diffuser Pressure Ratio: 5.07
 η_{HS} (calculated) = 89.2%; η_{Stm} (calculated) = 41.5%; η_{Plant} = 45.2%

A. ARGON LOOP (\dot{m}_{argon} = 3387 kg/s)

Location	Temp, K	Power to Argon, MW
Compressor Inlet	311	-
Compressor Outlet	662.0	+ 615.8
Preheater Outlet	* 922	+ 456.2
Regenerator Outlet	* 1920	+ 1751
Disk Generator Outlet	1266	- 1146
Radiant Furnace Outlet	1145	- 213.1
Reheater Outlet	* 1000	- 254.4
ITAH Outlet	821.8	- 312.7
Economizer Outlet	* 471	- 615.4
LPFH Outlet	331.3	- 245.1
Precooler Outlet	311	- 35.6

B. STEAM LOOP (\dot{m}_{steam} = 412.6 kg/s)

Location	Temp, K	Press, 10^5 Pa	Power, MW
Hotwell	*312	* (2" HgA)	-
Condensate Pump Discharge	*312.6	* 10.0	+ .55
LPFH	*451	* 9.53	+ 243.9
Main Feed Pump Discharge	*457.4	*273.9	+ 16.9
Economizer Out	(2.278 E6)	*265.7	+ 612.3
Valve Cooler Out	(2.367 E6)	*257.7	+ 36.7
Combustor Cooling Out	(2.792 E6)	*250.0	+ 175.3
Radiant Furnace Out	*811	*242.0	+ 212.0
HP Turbine Out	*564	*45.0	- 162.4
Reheater Out	*811	*40.0	+ 254.8
LP Turbine Out	-	-	- 494.3
Condenser Out	*312	* (2" HgA)	- 895.9

C. AIR SYSTEM (\dot{m}_{air} = 778.2 kg/s)

Location	Temp, K	Power, MW
Compressor Inlet	* 288	-
Compressor Outlet	* 305	+ 13.1
ITAH 2 Outlet	* 479.8	+ 139.0
ITAH 1 Outlet	556.3	+ 62.3
ITAH Outlet	* 922	+ 311.1

D. COMBUSTION GAS SYSTEM

Location	Temp, K	\dot{m}_c , kg/s	Power, MW
Combustor	*2415	-	+ 2867 **
Regenerator Out	*1090	867.1	- 1843
Argon Preheater Out	680	867.1	- 458.5
ITAH 1 Out	* 611	867.1	- 62.6
ITAH 2 Out	* 408	586.4	- 139.7
Coal Dryer Out	* 408	280.7	- 66.6
Stack	*(408)	(867.1)	- 194.2

*Denotes fixed quantities for all cases.

**Includes air and coal; deducts cooler losses.

MATCH POINT DEVIATION = + 10.8 MW

CCD/MHD/STEAM SYSTEMS PERFORMANCE SURVEY - CASE NO. 24

Assumed Coal Firing Rate = 2805 MWt
MHD Gross Power Output: 1284 MWe (VI)
Argon Compressor Pressure Ratio: 5.80
Disk/Diffuser Pressure Ratio: 5.10
 η_{MS} (calculated) = 89.3%; η_{Stm} (calculated) = 41.5%; η_{Plant} = 45.3%

A. ARGON LOOP (\dot{m} argon = 3774 kg/s)

<u>Location</u>	<u>Temp, K</u>	<u>Power to Argon, MW</u>
Compressor Inlet	311	-
Compressor Outlet	663.3	+ 688.5
Preheater Outlet	* 922	+ 505.8
Regenerator Outlet	* 1920	+ 1951
Disk Generator Outlet	1262	- 1284
Radiant Furnace Outlet	1744	- 230.7
Reheater Outlet	* 1000	- 282.4
ITAH Outlet	823.1	- 345.9
Economizer Outlet	* 471	- 688.2
LPFH Outlet	331.8	- 272.1
Precooler Outlet	311	- 40.6

B. STEAM LOOP (\dot{m} steam = 458.0 kg/s)

<u>Location</u>	<u>Temp, K</u>	<u>Press, 10⁵ Pa</u>	<u>Power, MW</u>
Hotwell	*312	* (2" HgA)	-
Condensate Pump Discharge	*312.6	* 10.0	+ .61
LPFH	*451	* 9.53	+ 270.7
Main Feed Pump Discharge	*457.4	*273.9	+ 18.8
Economizer Out	(2.289 E6)	*265.7	+ 684.7
Valve Cooler Out	(2.378 E6)	*257.7	+ 40.9
Combustor Cooling Out	(2.805 E6)	*250.0	+ 195.3
Radiant Furnace Out	*811	*242.0	+ 229.6
HP Turbine Out	*564	*45.0	- 180.2
Reheater Out	*811	*40.0	+ 282.9
LP Turbine Out	-	-	- 548.8
Condenser Out	*312	* (2" HgA)	- 994.5

C. AIR SYSTEM (\dot{m} air = 867 kg/s)

<u>Location</u>	<u>Temp, K</u>	<u>Power, MW</u>
Compressor Inlet	* 288	-
Compressor Outlet	* 305	+ 14.6
ITAH 2 Outlet	* 479.8	+ 154.9
ITAH 1 Outlet	559	+ 71.9
ITAH Outlet	* 922	+ 344.1

D. COMBUSTION GAS SYSTEM

<u>Location</u>	<u>Temp, K</u>	<u>\dot{m}_c, kg/s</u>	<u>Power, MW</u>
Combustor	*2415	-	+ 3194 **
Regenerator Out	*1090	966.1	- 2053
Argon Preheater Out	682.4	966.1	- 508.3
ITAH 1 Out	* 611	966.1	- 72.2
ITAH 2 Out	* 408	653.3	- 155.7
Coal Dryer Out	* 408	312.8	- 74.2
Stack	*(408)	(966.1)	- 216.4

*Denotes fixed quantities for all cases.

**Includes air and coal; deducts cooler losses.

MATCH POINT DEVIATION = + 6.99 MW

CCD/MHD/STEAM SYSTEMS PERFORMANCE SURVEY - CASE NO. 25

Assumed Coal Firing Rate = 3147 MWt
MHD Gross Power Output: 1449 MWe (VI)
Argon Compressor Pressure Ratio: 5.83
Disk/Diffuser Pressure Ratio: 5.13
 η_{HS} (calculated) = 89.4%; η_{Stm} (calculated) = 41.5%; η_{Plant} = 45.4%

A. ARGON LOOP (\dot{m}_{argon} = 4234 kg/s)

Location	Temp, K	Power to Argon, MW
Compressor Inlet	311	-
Compressor Outlet	664.8	+ 776.0
Preheater Outlet	* 922	+ 563.9
Regenerator Outlet	* 1920	+ 2189
Disk Generator Outlet	1259	- 1449
Radiant Furnace Outlet	1144	- 251.6
Reheater Outlet	* 1000	- 316.1
ITAH Outlet	824.7	- 384.5
Economizer Outlet	* 471	- 775.6
LPFH Outlet	332.2	- 304.4
Precooler Outlet	311	- 46.5

B. STEAM LOOP (\dot{m}_{steam} = 512.4 kg/s)

Location	Temp, K	Press, 10^5 Pa	Power, MW
Hotwell	*312	* (2" HgA)	-
Condensate Pump Discharge	*312.6	* 10.0	+ .69
LPHF	*451	* 9.53	+ 302.9
Main Feed Pump Discharge	*457.4	*273.9	+ 21.0
Economizer Out	(2.300 E6)	*265.7	+ 771.7
Valve Cooler Out	(2.390 E6)	*257.7	+ 45.8
Combustor Cooling Out	(2.817 E6)	*250.0	+ 219.1
Radiant Furnace Out	*811	*242.0	+ 250.3
HP Turbine Out	*564	*45.0	- 201.6
Reheater Out	*811	*40.0	+ 316.5
LP Turbine Out	-	-	- 613.9
Condenser Out	*312	" (2" HgA)	- 1113

C. AIR SYSTEM (\dot{m}_{air} = 972.7 kg/s)

Location	Temp, K	Power, MW
Compressor Inlet	* 288	-
Compressor Outlet	* 305	+ 16.4
ITAH 2 Outlet	* 479.8	+ 173.8
ITAH 1 Outlet	562.4	+ 84.1
ITAH Outlet	* 922	+ 382.6

D. COMBUSTION GAS SYSTEM

Location	Temp, K	\dot{m}_c , kg/s	Power, MW
Combustor	*2415	-	+ 3583 **
Regenerator Out	*1090	1084	- 2304
Argon Preheater Out	685.3	1084	- 566.8
ITAH 1 Out	* 611	1084	- 84.6
ITAH 2 Out	* 408	735	- 174.7
Coal Dryer Out	* 408	351	- 83.2
Stack	*(408)	(1084)	- 242.8

*Denotes fixed quantities for all cases.

**Includes air and coal; deducts cooler losses.

MATCH POINT DEVIATION = + 2.12 MW

CCD/MHD/STEAM SYSTEMS PERFORMANCE SURVEY - CASE NO. 26

Assumed Coal Firing Rate = 2123 MWt
MHD Gross Power Output: 962.2 MWe (VI)
Argon Compressor Pressure Ratio: 6.04
Disk/Diffuser Pressure Ratio: 5.29
 η_{HS} (calculated) = 91.5%; η_{Stm} (calculated) = 41.5%; η_{Plant} = 44.6%

A. ARGON LOOP (\dot{m}_{argon} = 2857 kg/s)

Location	Temp, K	Power to Argon, MW
Compressor Inlet	320	-
Compressor Outlet	694.4	+ 554.1
Preheater Outlet	* 922	+ 336.7
Regenerator Outlet	* 1920	+ 1477
Disk Generator Outlet	1269	- 962.2
Radiant Furnace Outlet	1152	- 173.2
Reheater Outlet	* 1000	- 225
ITAH Outlet	854.4	- 215.4
Economizer Outlet	* 471	- 567.4
LPFH Outlet	324.6	- 216.6
Precooler Outlet	320	- 6.88

B. STEAM LOOP (\dot{m}_{steam} = 364.5 kg/s)

Location	Temp, K	Press, 10^5 Pa	Power, MW
Hotwell	*312	* (2" HgA)	-
Condensate Pump Discharge	*312.6	* 10.0	+ .49
LPHF	*451	* 9.53	+ 215.5
Main Feed Pump Discharge	*457.4	*273.9	+ 15.0
Economizer Out	(2.343 E6)	*265.7	+ 564.5
Valve Cooler Out	(2.428 E6)	*257.7	+ 30.9
Combustor Cooling Out	(2.833 E6)	*250.0	+ 147.9
Radiant Furnace Out	*811	*242.0	+ 172.3
HP Turbine Out	*564	*45.0	- 143.5
Reheater Out	*811	*40.0	+ 225.2
LP Turbine Out	-	-	- 436.8
Condenser Out	*312	* (2" HgA)	- 791.5

C. AIR SYSTEM (\dot{m}_{air} = 656.4 kg/s)

Location	Temp, K	Power, MW
Compressor Inlet	* 288	-
Compressor Outlet	* 305	+ 11.1
ITAH 2 Outlet	* 479.8	+ 117.3
ITAH 1 Outlet	625.1	+ 100.6
ITAH Outlet	* 922	+ 214.4

D. COMBUSTION GAS SYSTEM

Location	Temp, K	\dot{m}_c , kg/s	Power, MW
Combustor	*2415	-	+ 2418 **
Regenerator Out	*1090	731.4	- 1555
Argon Preheater Out	740	731.4	- 338.4
ITAH 1 Out	* 611	731.4	- 101.1
ITAH 2 Out	* 408	494.6	- 117.9
Coal Dryer Out	* 408	236.8	- 56.2
Stack	*(408)	(731.4)	- 163.8

*Denotes fixed quantities for all cases.

**Includes air and coal; deducts cooler losses.

MATCH POINT DEVIATION = + 0.096 MW

CCO/MHD/STEAM SYSTEMS PERFORMANCE SURVEY - CASE NO. 27

Assumed Coal Firing Rate = 3728 MWt
MHD Gross Power Output: 1703 MWe (V1)
Argon Compressor Pressure Ratio: 5.88
Disk/Diffuser Pressure Ratio: 4.79
 η_{HS} (calculated) = 89.6%; η_{Stm} (calculated) = 41.5%; η_{Plant} = 45.1%

A. ARGON LOOP (\dot{m}_{argon} = 5016 kg/s)

Location	Temp, K	Power to Argon, MW
Compressor Inlet	312	-
Compressor Outlet	312.4	+ 925.8
Preheater Outlet	* 312	+ 661.5
Regenerator Outlet	* 312	+ 2593
Disk Generator Outlet	1264	- 1703
Radiant Furnace Outlet	1146	- 307.9
Reheater Outlet	* 1000	- 378.3
ITAH Outlet	827.2	- 448.9
Economizer Outlet	* 471	- 925.4
LPFH Outlet	330.7	- 364.5
Precooler Outlet	311	- 51.2

B. STEAM LOOP (\dot{m}_{steam} = 613.5 kg/s)

Location	Temp, K	Press, 10^5 Pa	Power, MW
Hotwell	* 312	* (2" HgA)	-
Condensate Pump Discharge	* 312.6	* 10.0	+ .82
LPFH	* 451	* 9.53	+ 362.7
Main Feed Pump Discharge	* 457.4	* 273.9	+ 25.2
Economizer Out	(2.295 E6)	* 265.7	+ 920.8
Valve Cooler Out	(2.384 E6)	* 257.7	+ 54.3
Combustor Cooling Out	(2.807 E6)	* 250.0	+ 259.6
Radiant Furnace Out	* 811	* 242.0	+ 306.3
HP Turbine Out	* 564	* 45.0	+ 241.4
Reheater Out	* 811	* 40.0	+ 378.9
LP Turbine Out	-	-	- 735.1
Condenser Out	* 312	* (2" HgA)	- 1332

C. AIR SYSTEM (\dot{m}_{air} = 1152 kg/s)

Location	Temp, K	Power, MW
Compressor Inlet	* 288	-
Compressor Outlet	* 305	+ 19.5
ITAH 2 Outlet	* 479.8	+ 205.9
ITAH 1 Outlet	567.8	+ 106.2
ITAH Outlet	* 922	+ 446.7

D. COMBUSTION GAS SYSTEM

Location	Temp, K	\dot{m}_c , kg/s	Power, MW
Combustor	* 2415	-	+ 4245 **
Regenerator Out	* 1090	1284	- 2729
Argon Preheater Out	690	1284	- 664.9
ITAH 1 Out	* 611	1284	- 106.8
ITAH 2 Out	* 408	868.3	- 206.9
Coal Dryer Out	* 408	415.7	- 98.6
Stack	*(408)	(1284)	- 287.6

*Denotes fixed quantities for all cases.

**Includes air and coal; deducts cooler losses.

MATCH POINT DEVIATION = + 5.98 MW

CCD/MHD/STEAM SYSTEMS PERFORMANCE SURVEY - CASE NO. 28

Assumed Coal Firing Rate = 340.8 MWt
MHD Gross Power Output: 161.9 MWe (VI)
Argon Compressor Pressure Ratio: 5.30
Disk/Diffuser Pressure Ratio: 4.60
 η_{MS} (calculated) = 88.9%; η_{Stm} (calculated) = 41.5%; η_{Plant} = 47.0%

A. ARGON LOOP (\dot{m}_{argon} = 463.0 kg/s)

Location	Temp, K	Power to Argon, MW
Compressor Inlet	320	-
Compressor Outlet	657.2	+ 80.1
Preheater Outlet	* 922	+ 69.9
Regenerator Outlet	* 1920	+ 237.0
Disk Generator Outlet	1237	- 161.9
Radiant Furnace Outlet	1138	- 23.4
Reheater Outlet	* 1000	- 32.8
ITAH Outlet	817	- 43.5
Economizer Outlet	* 471	- 82.2
LPFH Outlet	337.8	- 31.6
Precooler Outlet	320	- 4.22

B. STEAM LOOP (\dot{m}_{steam} = 53.3 kg/s)

Location	Temp, K	Press, 10^5 Pa	Power, MW
Hotwell	*312	* (2" HgA)	-
Condensate Pump Discharge	*312.6	* 10.0	+ .072
LPFH	*451	* 9.53	+ 31.5
Main Feed Pump Discharge	*457.4	*273.9	+ 2.19
Economizer Out	(2.329 E6)	*265.7	+ 81.8
Valve Cooler Out	(2.423 E6)	*257.7	+ 4.96
Combustor Cooling Out	(2.868 E6)	*250.0	+ 23.7
Radiant Furnace Out	*811	*242.0	+ 23.3
HP Turbine Out	*564	* 45.0	- 21.0
Reheater Out	*811	* 40.0	+ 32.9
LP Turbine Out	-	-	- 63.8
Condenser Out	*312	* (2" HgA)	- 115.7

C. AIR SYSTEM (\dot{m}_{air} = 105.3 kg/s)

Location	Temp, K	Power, MW
Compressor Inlet	* 288	-
Compressor Outlet	* 305	+ 1.78
ITAH 2 Outlet	* 479.8	+ 18.8
ITAH 1 Outlet	* 546.2	+ 7.31
ITAH Outlet	* 922	+ 43.2

D. COMBUSTION GAS SYSTEM

Location	Temp, K	\dot{m}_c , kg/s	Power, MW
Combustor	*2415	-	+ 388.1 **
Regenerator Out	*1090	117.4	- 249.5
Argon Preheater Out	671.3	117.4	- 63.2
ITAH 1 Out	* 611	117.4	- 7.34
ITAH 2 Out	* 408	79.4	- 18.9
Coal Dryer Out	* 408	38.0	- 9.01
Stack	*(408)	(117.4)	- 26.3

*Denotes fixed quantities for all cases.

**Includes air and coal; deducts cooler losses.

MATCH POINT DEVIATION = + 0.71 MW

CCD/MHD/STEAM SYSTEMS PERFORMANCE SURVEY - CASE NO. 29

Assumed Coal Firing Rate = 408.9 MWt
MHD Gross Power Output: 196.8 MWe (VI)
Argon Compressor Pressure Ratio: 5.40
Disk/Diffuser Pressure Ratio: 4.68
 η_{HS} (calculated) = 89.3%; η_{Stm} (calculated) = 41.4%; η_{Plant} = 47.1%

A. ARGON LOOP (\dot{m} argon = 555.7 kg/s)

Location	Temp, K	Power to Argon, MW
Compressor Inlet	320	-
Compressor Outlet	662.6	+ 97.6
Preheater Outlet	* 922	+ 73.9
Regenerator Outlet	* 1920	+ 284.4
Disk Generator Outlet	1228	- 196.8
Radiant Furnace Outlet	1139	- 25.5
Reheater Outlet	* 1000	- 39.6
ITAH Outlet	822.4	- 50.6
Economizer Outlet	* 471	- 100.2
LPFH Outlet	338.7	- 37.7
Precooler Outlet	320	- 5.32

B. STEAM LOOP (\dot{m} steam = 63.5 kg/s)

Location	Temp, K	Press, 10^5 Pa	Power, MW
Hotwell	*312	* (2" HgA)	-
Condensate Pump Discharge	*312.6	* 10.0	+ .085
LPFH	*451	* 9.53	+ 37.5
Main Feed Pump Discharge	*457.4	*273.9	+ 2.61
Economizer Out	(2.364 E6)	*265.7	+ 99.6
Valve Cooler Out	(2.453 E6)	*257.7	+ 5.96
Combustor Cooling Out	(2.906 E6)	*250.0	+ 28.5
Radiant Furnace Out	*811	*242.0	+ 25.4
HP Turbine Out	*564	* 45.0	- 25.0
Reheater Out	*811	* 40.0	+ 39.2
LP Turbine Out	-	-	- 76.1
Condenser Out	*312	* (2" HgA)	+ 137.8

C. AIR SYSTEM (\dot{m} air = 126.4 kg/s)

Location	Temp, K	Power, MW
Compressor Inlet	* 288	-
Compressor Outlet	* 305	+ 2.13
ITAH 2 Outlet	* 479.8	+ 22.6
ITAH 1 Outlet	557.6	+ 10.3
ITAH Outlet	* 922	+ 50.4

D. COMBUSTION GAS SYSTEM

Location	Temp, K	\dot{m}_c , kg/s	Power, MW
Combustor	*2415	-	+ 465.7**
Regenerator Out	*1090	140.9	- 299.4
Argon Preheater Out	681.2	140.9	- 74.3
ITAH 1 Out	* 611	140.9	- 10.3
ITAH 2 Out	* 408	95.3	- 22.7
Coal Dryer Out	* 408	45.6	- 10.8
Stack	*(408)	(140.9)	- 31.6

*Denotes fixed quantities for all cases.
**Includes air and coal; deducts cooler losses.

MATCH POINT DEVIATION = + 1.32 MW

CCD/MHD/STEAM SYSTEMS PERFORMANCE SURVEY - CASE NO. 30

Assumed Coal Firing Rate = 233.9 MWt
MHD Gross Power Output: 103.7 MWe (VI)
Argon Compressor Pressure Ratio: 5.22
Disk/Diffuser Pressure Ratio: 4.45
 η_{HS} (calculated) = 88.6%; η_{Stm} (calculated) = 41.5%; η_{Plant} = 45.5%

A. ARGON LOOP (\dot{m}_{argon} = 317.8 kg/s)

Location	Temp, K	Power to Argon, MW
Compressor Inlet	320	-
Compressor Outlet	653.3	+ 54.3
Preheater Outlet	* 922	+ 43.8
Regenerator Outlet	* 1920	+ 162.7
Disk Generator Outlet	1282	- 103.7
Radiant Furnace Outlet	1146	- 22.1
Reheater Outlet	* 1000	- 23.9
ITAH Outlet	813	- 30.5
Economizer Outlet	* 471	- 55.7
LPFH Outlet	330	- 23.0
Precooler Outlet	320	- 1.63

B. STEAM LOOP (\dot{m}_{steam} = 36.7 kg/s)

Location	Temp, K	Press, 10^5 Pa	Power, MW
Hotwell	*312	* (2" HgA)	-
Condensate Pump Discharge	*312.6	* 10.0	+ .052
LPHF	*451	* 9.53	+ 22.9
Main Feed Pump Discharge	*457.4	*273.9	+ 1.59
Economizer Out (2.228 E6)		*265.7	+ 55.5
Valve Cooler Out (2.316 E6)		*257.7	+ 3.41
Combustor Cooling Out (2.737 E6)		*250.0	+ 16.3
Radiant Furnace Out	*811	*242.0	+ 22.0
HP Turbine Out	*564	* 45.0	- 15.2
Reheater Out	*811	* 40.0	+ 23.9
LP Turbine Out	-	-	- 46.4
Condenser Out	*312	* (2" HgA)	- 84.0

C. AIR SYSTEM (\dot{m}_{air} = 72.3 kg/s)

Location	Temp, K	Power, MW
Compressor Inlet	* 288	-
Compressor Outlet	* 305	+ 1.22
ITAH 2 Outlet	* 479.8	+ 12.9
ITAH 1 Outlet	* 537.6	+ 4.37
ITAH Outlet	* 922	+ 30.3

D. COMBUSTION GAS SYSTEM

Location	Temp, K	\dot{m}_c , kg/s	Power, MW
Combustor	*2415	-	+ 266.3 **
Regenerator Out	*1090	80.6	- 171.2
Argon Preheater Out	663.9	80.6	- 44.0
ITAH 1 Out	* 611	80.6	- 4.39
ITAH 2 Out	* 408	54.5	- 13.0
Coal Dryer Out	* 408	26.1	- 6.19
Stack	*(408)	(80.6)	- 18.1

*Denotes fixed quantities for all cases.
**Includes air and coal; deducts cooler losses.

MATCH POINT DEVIATION = + 4.40 MW

CCD/MHD/STEAM SYSTEMS PERFORMANCE SURVEY - CASE NO. 31

Assumed Coal Firing Rate = 274 MWt
MHD Gross Power Output: 125 MWe (VI)
Argon Compressor Pressure Ratio: 5.89
Disk/Diffuser Pressure Ratio: 4.98
 η_{HS} (calculated) = 89.6%; η_{Stm} (calculated) = 41.5%; η_{Plant} = 45.0%

A. ARGON LOOP (\dot{m}_{argon} = 369.3 kg/s)

Location	Temp, K	Power to Argon, MW
Compressor Inlet	311	-
Compressor Outlet	667.8	+ 68.0
Preheater Outlet	* 922	+ 48.5
Regenerator Outlet	* 1920	+ 190.3
Disk Generator Outlet	1263	- 124.8
Radiant Furnace Outlet	1146	- 22.3
Reheater Outlet	* 1000	- 27.9
ITAH Outlet	827.6	- 32.9
Economizer Outlet	* 471	- 68.0
LPFH Outlet	330.9	- 26.7
Precooler Outlet	311	- 3.8

B. STEAM LOOP (\dot{m}_{steam} = 44.9 kg/s)

Location	Temp, K	Press, 10^5 Pa	Power, MW
Hotwell:	*312	* (2" HgA)	-
Condensate Pump Discharge	*312.6	* 10.0	+ .06
LPFH	*451	* 9.53	+ 26.6
Main Feed Pump Discharge	*457.4	*273.9	+ 1.85
Economizer Out	(2.299 E6)	*265.7	+ 67.7
Valve Cooler Out	(2.388 E6)	*257.7	+ 3.99
Combustor Cooling Out	(2.812 E6)	*250.0	+ 19.0
Radiant Furnace Out	*811	*242.0	+ 22.2
HP Turbine Out	*564	* 45.0	- 17.7
Reheater Out	*811	* 40.0	+ 27.8
LP Turbine Out	-	-	- 53.9
Condenser Out	*312	* (2" HgA)	- 97.6

C. AIR SYSTEM (\dot{m}_{air} = 84.6 kg/s)

Location	Temp, K	Power, MW
Compressor Inlet	* 288	-
Compressor Outlet	* 305	+ 1.43
ITAH 2 Outlet	* 479.8	+ 15.1
ITAH 1 Outlet	568.7	+ 7.88
ITAH Outlet	* 922	+ 32.7

D. COMBUSTION GAS SYSTEM

Location	Temp, K	\dot{m}_c , kg/s	Power, MW
Combustor	*2415	-	+ 311.5 **
Regenerator Out	*1090	94.2	- 200.3
Argon Preheater Out	690.8	94.2	- 48.7
ITAH 1 Out	* 611	94.2	- 7.91
ITAH 2 Out	* 408	63.7	- 15.2
Coal Dryer Out	* 408	30.5	- 7.23
Stack	*(408)	(94.2)	- 21.1

*Denotes fixed quantities for all cases.

**Includes air and coal; deducts cooler losses.

MATCH POINT DEVIATION = + 0.25 MW

CCD/MHD/STEAM SYSTEMS PERFORMANCE SURVEY - CASE NO. 32

Assumed Coal Firing Rate = 544.0 MWt
MHD Gross Power Output: 246.2 MWe (VI)
Argon Compressor Pressure Ratio: 6.06
Disk/Diffuser Pressure Ratio: 5.10
 η_{HS} (calculated) = 90.2%; η_{Stm} (calculated) = 41.5%; η_{Plant} = 44.6%

A. ARGON LOOP (\dot{m}_{argon} = 734.3 kg/s)

Location	Temp, K	Power to Argon, MW
Compressor Inlet	311	-
Compressor Outlet	675.9	+ 138.3
Preheater Outlet	* 922	+ 93.3
Regenerator Outlet	* 1920	+ 378.4
Disk Generator Outlet	1269	- 246.2
Radiant Furnace Outlet	1148	- 45.6
Reheater Outlet	* 1000	- 56.2
ITAH Outlet	835.8	- 62.3
Economizer Outlet	* 471	- 138.3
LPFH Outlet	328.3	- 54.1
Precooler Outlet	311	- 6.55

B. STEAM LOOP (\dot{m}_{steam} = 91.1 kg/s)

Location	Temp, K	Press, 10^5 Pa	Power, MW
Hotwell	*312	* (2" HgA)	-
Condensate Pump Discharge	*312.6	* 10.0	+ .12
LPFH	*451	* 9.53	+ 53.8
Main Feed Pump Discharge	*457.4	*273.9	+ 3.74
Economizer Out	(2.305 E6)	*265.7	+ 137.6
Valve Cooler Out	(2.392 E6)	*257.7	+ 7.93
Combustor Cooling Out	(2.808 E6)	*250.0	+ 37.9
Radiant Furnace Out	*811	*242.0	+ 45.4
HP Turbine Out	*564	* 45.0	- 35.8
Reheater Out	*811	* 40.0	+ 56.3
LP Turbine Out	-	-	- 109.1
Condenser Out	*312	* (2" HgA)	- 197.8

C. AIR SYSTEM (\dot{m}_{air} = 168.2 kg/s)

Location	Temp, K	Power, MW
Compressor Inlet	* 288	-
Compressor Outlet	* 305	+ 2.84
ITAH 2 Outlet	* 479.8	+ 30.0
ITAH 1 Outlet	586.0	+ 18.7
ITAH Outlet	* 922	+ 61.9

D. COMBUSTION GAS SYSTEM

Location	Temp, K	\dot{m}_c , kg/s	Power, MW
Combustor	*2415	-	+ 619.5 **
Regenerator Out	*1090	187.4	- 398.3
Argon Preheater Out	705.8	187.4	- 93.8
ITAH 1 Out	* 611	187.4	- 18.8
ITAH 2 Out	* 408	126.7	- 30.2
Coal Dryer Out	* 408	60.7	- 14.4
Stack	*(408)	(187.4)	- 42.0

*Denotes fixed quantities for all cases.

**Includes air and coal; deducts cooler losses.

MATCH POINT-DEVIATION = + 0.059 MW

CCD/MHD/STEAM SYSTEMS PERFORMANCE SURVEY - CASE NO. 33

Assumed Coal Firing Rate = 1133 MWt
MHD Gross Power Output: 530.7 MWe (V1)
Argon Compressor Pressure Ratio: 5.48
Disk/Diffuser Pressure Ratio: 4.73
 η_{HS} (calculated) = 89.6%; η_{Stm} (calculated) = 41.5%; η_{Plant} = 46.3%

A. ARGON LOOP (\dot{m}_{argon} = 1545 kg/s)

Location	Temp, K	Power to Argon, MW
Compressor Inlet	320	-
Compressor Outlet	666.5	+ 273.7
Preheater Outlet	* 922	+ 201.8
Regenerator Outlet	* 1920	+ 788.3
Disk Generator Outlet	1247	- 530.7
Radiant Furnace Outlet	1142	- 82.6
Reheater Outlet	* 1000	- 112.1
ITAH Outlet	826.3	- 137.2
Economizer Outlet	* 471	- 280.7
LPFH Outlet	334.2	- 108.1
Precooler Outlet	320	- 11.2

B. STEAM LOOP (\dot{m}_{steam} = 181.9 kg/s)

Location	Temp, K	Press, 10^5 Pa	Power, MW
Hotwell	*312	* (2" HgA)	-
Condensate Pump Discharge	*312.6	* 10.0	+ .24
LPFH	*451	* 9.53	+ 107.5
Main Feed Pump Discharge	*457.4	*273.9	+ 7.47
Economizer Out	(2.329 E6)	*265.7	+ 279.3
Valve Cooler Out	(2.420 E6)	*257.7	+ 16.5
Combustor Cooling Out	(2.854 E6)	*250.0	+ 78.9
Radiant Furnace Out	*811	*242.0	+ 82.2
HP Turbine Out	*564	* 45.0	- 71.6
Reheater Out	*811	* 40.0	+ 112.4
LP Turbine Out	-	-	- 217.9
Condenser Out	*312	* (2" HgA)	- 395.0

C. AIR SYSTEM (\dot{m}_{air} = 350.3 kg/s)

Location	Temp, K	Power, MW
Compressor Inlet	* 288	-
Compressor Outlet	* 305	+ 5.92
ITAH 2 Outlet	* 479.8	+ 62.6
ITAH 1 Outlet	566.0	+ 31.6
ITAH Outlet	* 922	+ 136.5

D. COMBUSTION GAS SYSTEM

Location	Temp, K	\dot{m}_c , kg/s	Power, MW
Combustor	*2415	-	+ 1291 **
Regenerator Out	*1090	390.4	- 829.8
Argon Preheater Out	688.4	390.4	- 202.8
ITAH 1 Out	* 611	390.4	- 31.8
ITAH 2 Out	* 408	264.0	- 62.9
Coal Dryer Out	* 408	126.4	- 30.0
Stack	*(408)	(390.4)	- 87.4

*Denotes fixed quantities for all cases.
**Includes air and coal; deducts cooler losses.

MATCH POINT DEVIATION = + 2.43 MW

APPENDIX C

**APPENDIX C - NATURAL RESOURCE REQUIREMENTS
AND EMISSIONS LEVELS FOR OCD PLANTS**

Disk MHD Systems Design Case	Net Electrical Power Output (MWe)	Gross Thermal Input (MMt)	Flue Gas Emissions (ng/J)						Heat Rejected (MM)		Materials and Resource Requirements kg/kWhr		
			NO _x	SO ₂	Partic.	HC	CO	CO ₂	Cooling Tower	Stack and Other Losses	Coal*	Water**	Other
CASE 1A OCD - Directly Fired 1920 K Preheat	963.0	2118.6	210	247	13	nil	nil	92,088	826	330	0.381	2.04	Ammonia - 0.034
CASE 1B OCD - Directly Fired 1650 K Preheat	1012.0	2330.5	210	247	13	nil	nil	92,088	973	346	0.399	2.29	
CASE 2 OCD - Separately Fired 1920 K Preheat	983.8	2522.4	210	247	13	nil	nil	92,088	956	582	0.443	2.34	
CASE 3 OCD with O ₂ Augmentation	978.0	2115.2	210	247	13	nil	nil	92,088	1058	379	0.428	2.57	

* As received

** Losses: Cooling tower evaporation, drift, and blowdown on design day.
Other makeup and seed regeneration water requirements not included.

APPENDIX D

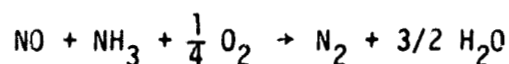
APPENDIX D

NO_x CONTROL IN 1920 K DIRECTLY-FIRED DISK GENERATOR SYSTEM

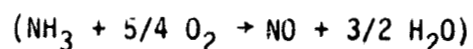
For the OCD directly-fired case at 1920 K preheat (Case 1A), the use of radiant furnace residence time within the critical 2200 K-1800 K temperature range to provide NO_x removal from the flue gas is not possible. The restrictions imposed by the high preheat temperature requirement and the matrix material environments have been discussed in the body of the report. In order to achieve NO_x levels in the flue gas that meet the NSPS requirements (Section 4.2) it is necessary to introduce an auxiliary flue gas NO_x removal scheme.

The NO_x removal process chosen for evaluation was the thermal DeNO_x Process of the EXXON Research and Engineering Company, described in Reference D-1. While no application to large-scale coal-fired power plants (1000 MW_e range) has been demonstrated, the process has been introduced into industrial plants and small gas-and oil-fired power plants. Operating with retrofit installations of the thermal DeNO_x process, such plants have achieved reductions in NO_x emissions of up to 70 percent, with initial low NO_x levels. As adapted to a coal-fired power generating facility, where it is installed as a component of the original power plant systems, NO_x reductions approaching 95 percent for high initial NO_x levels can be predicted. The actual performance in a coal-fired unit has yet to be determined.

The process involves the injection of ammonia into the hot flue gas in the presence of a slight excess of oxygen. For critical removal of the NO_x in the gas, the injection temperature must be controlled to within strict limits. The NO_x reduction reaction is:



at T = 1225 K. Higher temperatures will cause the NO production reaction



to occur. Below 1125 K, the reaction rate decreases rapidly and the injected ammonia remains unreacted with the flue gas constituents. Laboratory tests have also shown that minimizing the excess air tends to enhance the NO_x reduction reaction. Minor flue gas species such as SO_2 , water, and ash apparently have negligible effects on the reduction reaction.

One important caveat regarding the use of the Thermal De NO_x process is the necessity for achieving rapid and complete mixing of the ammonia and flue gas to prevent the breakthrough of unreacted ammonia to the stack, and to achieve maximum reduction fractions. For the purposes of this study, it is assumed that a mixing system design can be developed to provide the requisite performance of the process; the details of such a system are not within the scope of the study.

An additional consideration in the use of this process for MHD NO_x reduction is the potential set of reactions between the injected ammonia and seed remaining in the flue gas. These would be limited to surface reactions between the condensed and/or frozen seed fractions remaining in the flue gas at the point of NH_3 injection, since the required injection temperature is below the vaporization temperature of the seed and sulfur-reacted seed materials.

NO_x Levels in OCD Combustion Gas

For the Case 1A combustion gas system, the equilibrium NO_x level in the combustor with the chosen stoichiometric ratio ($\Phi = 0.95$) is 1100 PPM. The elapsed time from acceleration of the combustion products through the supersonic nozzle until, fully diffused, they enter the radiant furnace is less than 100 milliseconds. For these conditions, the NO_x level in the combustion gas can be considered to be frozen at the combustor level even though the static temperature drops rapidly to the 2200 K range within the disk generator and thereafter recovers to about 2450 K at the radiant furnace inlet. The residence time in the radiant furnace is approximately 700 milliseconds, but the final gas temperature is only within the range where NO_x decomposition becomes significant (i.e., 2200 K or less) for approximately a quarter of this

time period. Thus, the radiant furnace outlet NO_x concentration will be on the order of 1000 PPM, just prior to the introduction of air for the secondary combustion. (The equilibrium concentration of NO_x at the temperature and pressure representative of the radiant furnace outlet ducts is 920 PPM for $\Phi = 0.95$).

Secondary combustion of the flue gas occurs at 2150 K; for this condition, if the combustion results in a final stoichiometric ratio of 1.05, the expected equilibrium NO_x concentration would be approximately 2500 PPM. The actual NO_x concentration in the combustion products, which will be frozen in by the rapid cooling of the gas through the regenerative air heaters, will be expected to be in the 2000 PPM range. The final value depends upon the design of the hot gas mains and headers, and the specific location of the secondary air injection points with respect to the hot gas inlets to the regenerative air heater vessels.

For evaluation purposes, the final frozen value of NO_x in the reheat gas exiting the air preheater system will be assumed to be 2000 PPM. For the directly-fired OCD system burning Montana Rosebud coal, the NO_x emissions limit is approximately 390 PPM in the stack gas. Assuming that NH_3 injection and mixing must occur near the 1225 K temperature point, as recommended by the De NO_x process literature, this means that the injection point is located between the reheater and superheater modules in the bottoming plant heat recovery equipment. In the actual plant design, this could most probably be achieved by locating the injector and mixing sections at the outlet of the seed recovery (radiant) furnace which furnishes most of the reheater heat transfer requirement. The introduction of the additional sections requires a larger induced draft fan; to represent the increased fan power requirements and pumping power requirements for the ammonia systems, a power charge to the plant of 2% of gross steam plant output was taken.

AMMONIA REQUIREMENTS

The required NO_x reduction is 81% for a 390 PPM limit in the stack gas. The available reference material for the EXXON De NO_x process indicates that such

reductions are potentially possible with an NH_3/NO_x molar ratio of about 0.8 to 1 (based upon the initial NO_x concentration). For the OCD directly-fired system, this requires an ammonia injection rate of approximately 53 moles/sec or 0.91 kg/s (86.5 tons/day). At a supplied price of \$200/ton, the additional charge incurred for the ammonia is \$6.3 millions per year.

APPENDIX E

APPENDIX E

COMPONENT DIMENSIONS AND WEIGHTS FOR REFERENCE 500 MW DISK POWER MANAGEMENT SYSTEM

(The items A-R below are keyed to Figure 6-4-3)

- A: DC Switchgear
3 rows, each 32 cabinets stacked 2 high. Each cabinet 56.5" wide x 42" deep x 53" high, 3500 #. 5' lateral separation, 4' between rows and fence and between rows.
- B: DC Capacitor Banks
Each 12' x 7 1/2' x 21' overall height, 13200 #.
- C: DC Inductors for 11880V and 10800V Converters
Each 7 1/2' diameter x 17' overall height, 8 (@) 11840 # and 8 (@) 10920 #.
- D: DC Inductors for 6120V and 5760V Converters
Each 6' diameter x 14' overall height 8 (@) 7560 # and 8 (@) 7290 #.
- E: Controls Building
108' x 18' x 10' to roof beams
Houses 32 cabinets each 6' x 3' 8' high, 2 rows back to back butted and side to side butted. Each cabinet 3600 #.
- F: Valve Hall
124' x 48' x 32' to roof beams. Houses all active devices (with room for addition of VAR control if needed) and device cooling system.
- G: Converter Transformers for 11880V and 10800V Converters
19' 7" x 14' 2" x 17' 11" to top of bushings, 16' 3" to tank cover, each 180,000 #.
- H: 34.5 kV Breakers Throat Mounted to Transformers
Each 46.25" x 75" x 127.5" to top of bushings, 5000 #.
- I: Converter Transformers for 6120V and 5760V Converters
Each 17' 1" x 12' 1" x 15' 10" to top of bushings, 14' 2" to tank cover, 120,000 #.
- J: 11th Harmonic Filter Capacitor Banks
Each 13' x 7 1/2' x 21' overall height, 14800 #.
- K: 11th Harmonic Filter Inductors
Rack mounted, rack dimensions 19' x 6', 20' overall height, 8400 #.
- L: 13th Harmonic Filter Inductors
Rack mounted, rack 17' x 6' x 20' overall height, 7200#.

- M: 13th Harmonic Filter Capacitor Banks
Each 19' x 7 1/2' x 21' overall height, 21120 #.
- N: Broadband Filter Damping Resistors
3 racks, each 12' x 6' x 21' overall height, 52500 #.
- O: Broadband Filter Inductors
Rack 14' x 4' x 17' overall height, 3600 #.
- P: Broadband Filter Capacitor Banks
Each 15' x 7 1/2' x 21' overall height, 15840 #.
- Q: Main Transformer
37 1/2' x 28 1/3' x 40' to top of bushings, 23 3/4' to tank cover,
1,050,000 #.
- R: 500 kV SF6 Breaker
36' x 56' x 26' to top of bushings, 107,040 #.
- (The following items S - X are keyed to Figure 6-4-4)
- S: Control Cabinet, 6' x 3' x 8'H, 3600 #.
- T: Converter Values, 13' x 5' x 26' H, 14000 #.
- U: Bypass Values, 13' x 5' x 12' H, 7000 #.
- V: Freewheel Values, 13' x 5' x 12' H, 7000 #.
- W: Water Cooling System, 26' x 16' x 10' H, 42,000 #.
- X: VAR Values (if required), 13' x 5' x 19' H, 10500 #.
- VAR Passive Components (if required):
- o Capacitor Banks (18); (@) 16' x 7 1/2 x 21' H, 19000 #.
 - o Reactors (18); (@) 8' diameter x 18' H, 18330 #.